SPECTROCHEMICAL ANALYSIS OF WHOLE POWDERED COAL

H. G. M. PARRY

Ph. D.   1987

A thesis entitled

SPECTROCHEMICAL ANALYSIS OF WHOLE

POWDERED COAL

presented by

HUW GARETH MICHAEL PARRY, B.Sc.

In part fulfilment of the
requirements for the degree of

DOCTOR OF PHILOSOPHY
of the
COUNCIL FOR NATIONAL ACADEMIC AWARDS

Department of Environmental Sciences
Plymouth Polytechnic
Drake Circus
PLYMOUTH
PL4 8AA

Collaborating establishment:
Headquarters Scientific Control
National Coal Board
Coal House
Lyon Road
HARROW
Middlesex

ABSTRACT

The analysis of coal without sample dissolution was investigated by introducing coal slurries, into a variety of atom cells including electrothermal atomisation atomic absorption spectroscopy (ETA-AAS), inductively coupled plasmas and direct current plasmas for atomic emission spectroscopy (ICP-AES, DCP-AES) and inductively coupled mass spectroscopy (ICP-MS). All the analyses were calibrated using aqueous standards.

Slurries were injected into an electrothermal atomiser. The effects of furnace programme, background correction and air ashing were investigated. As, Se, Cd and Sb were successfully determined in a variety of certified reference material coals. For As the coal was slurried in nickel nitrate, magnesium nitrate, nitric acid and ethanol. Continuum source and Smith-Hieftje background correction were compared for correction of a broadened Al line interference at the As (193.7 nm) line. Only the latter was effective. Smaller Se signals were obtained from coal compared to aqueous solutions. Iron coal produced structured background and hence overcorrection. The successful method introduced air into the ash stage.

Both DCP and ICP techniques yielded good agreement with certificate values provided that the particle size was reduced to below 16 μm and 10 μm respectively. Simplex optimisation identified the critical parameters for aluminium determinations as being high injector flow rate and low observation height.

Preliminary investigations of slurry atomisation using ICP-MS and 0.2% m/v slurried coal gave no blocking. Contamination from zirconia grinding elements used to comminute coal was investigated using laser ablation ICP-MS.

Excitation temperature (T_{exc}), ionisation temperature (T_{ion}) rotational temperature (T_{rot}) and electron number density (n_e), were measured for different slurry concentrations (1-30% m/v) in the ICP. Depending on themometric species used, T_{exc} may decrease with slurry concentration, but there were no similar decreases in T_{ion}, $T_{(rot)}$ and n_e. Observed decreases in analyte emission with increased sample loadings (> 10%) were shown to be caused by transport effects.

ACKNOWLEDGEMENTS

CONTENTS

LIST OF FIGURES

LIST OF TABLES

- x -

CHAPTER 1

INTRODUCTION

1.1 INTRODUCTION

1.1.1 The need for coal analysis

There is an increasing demand for trace element information on coal because of concerns such as quality control, corrosion and contamination, catalyst poisoning and environment pollution. Recently, there has been an increasing awareness of the problems that arise in the environment due to concentration of elements normally present in only trace amounts. As reserves of coal far exceed those of any other fossil fuel (1), it seems likely that coal will be the major source of energy in the foreseeable future. Therefore coal combustion will be under scrutiny as a potential source of trace element pollution (2). It is known that a variety of trace elements, some of which are toxic to plant and animal life in other chemical combinations, occur in coal (3). The very high tonnages of coal used, around 120 million tonnes per year for Britain (4), and the possibilities of concentration during conversion processes, mean that even ngg^{-1} levels may be significant. It has therefore become imperative to develop accurate and reliable techniques, which can determine the amount of these trace elements present in coal as highlighted in the literature. (5-9).

1.1.2 Coal Analysis

Coal is a notoriously difficult matrix to bring into solution. A comprehensive discussion of the historical development of various analytical methods published by the British Standard Institution (BSI) is given by Pearce (10). Some methods are slow and only produce incomplete dissolution, while other more rapid digestions e.g. using perchloric and hydro-fluoric acid (11-13) are potentially hazardous. Additionally there is a likelihood that volatile elements such as As and Se may be lost on dissolution. Therefore any techniques which avoid this stage would be highly favourable.

One of the aims of the work described in this thesis was the development of methods which eliminated sample preparation, be easily calibrated, accurate and use existing instrumentation which offer comparable precision to those described in the British Standard 1016 (14).

1.2 SOLID ANALYSIS

1.2.1 Instruments available for coal analysis

Several analytical techniques are available for the analysis of solid samples.

X-ray fluorescence (XRF) is a well established and powerful method for multi element analysis. It offers uniform detection limits across a large portion of the periodic table and allows direct analysis of solid samples without the need for pretreatment. In a recent book, Tertian and Claisse (15) have comprehensively described the principles of quantitative X-ray fluorescence. However, XRF does suffer from several disadvantages. It is suited for rapid elemental determinations when their concentrations are greater than 10-100 μgg^{-1}, but lacks sensitivity for low trace element analysis in the ngg^{-1} region. The technique also suffers from matrix effects and difficulty in converting measured intensities to concentrations. Many methods have been proposed to correct for these effects and can be found in the literature (16-18).

Sample heterogeneity gives rise to erroneous results in XRF analysis and several authors have attributed particle size of the samples as a contributing factor to sample heterogeneity. Preparation of matching standards for all elements of interest and matrix effect correction make any quantitative XRF procedure time consuming and expensive. Problems encountered in XRF analysis of whole coal, which includes sample thickness, X-ray absorption, volatile element and mineralogical effect have been discussed by Willis (19).

Spark Source Mass Spectrometry (SSMS) (20) on the other hand is capable of the determination of most elements at concentrations down to 0.01-1 μgg^{-1} (21). The idea of SSMS as an analytical technique for element analysis was first introduced by Dempster 50 years ago. Successive innovation and developments have meant that the whole periodic table can be covered in one analysis by SSMS irrespective of sample type or element concentration with minimal sample preparation. The technique has declined in popularity due to instrument complexity, expense, poor precision and particularly long analysis time. Perhaps only 3 or 4 samples per day may be analysed. This technique has however been used for multi element analysis of whole coal, as reported by several authors (22-26) and other applications are listed in a comprehensive review by Bacon and Ure (27).

Neutron Activation Analysis (NAA) has the sensitivity to perform these determinations, but is confined to those elements which, upon activation produce a radioactive isotope giving statistically significant decay signals. The technique allows direct analysis thereby reducing the probability of sample contamination and loss of volatile elements. Large quantities (several grams) of each sample are analysed by NAA, thus minimising inhomogeneity effects. Several papers describe this technique in relation to coal analysis (28-30), but certain toxic elements such as Cd, Cu, Hg, Ni, Pb and Zn (24) are not easily determined by NAA. Unfortunately the equipment is not readily available to most laboratories and results are not available for several days due to the initial decay of the samples.

Atomic Absorption Spectrometry (AAS) is conventionally regarded as a solution based technique, but over the last ten years significant developments in solid sampling have occurred, thus making atomic absorption using electrothermal atomisation (ETA-AAS) both a promising and attractive technique, especially as the necessary instrumentation is found in many laboratories. The technique is extremely sensitive with detection limits in the pgg^{-1} region

and offers adequate precision. With the advent of more efficient background correction systems such as those based on the Zeeman and Smith-Hieftje effects, it has become possible to consider direct solid analysis by ETA-AAS.

Inductively-coupled plasma atomic emission spectroscopy (ICP-AES) is a technique which is growing in popularity since its introduction for the determination of trace elements by Greenfield et al. (31) and Wendt and Fassel (32). Unlike ETA-AAS, ICP-AES relies on the ICP as an excitation source from which excitation and emission occur. Though not as sensitive as ETA-AAS it has multi-element capability and allows rapid determinations in the ngg^{-1} region. The technique has been applied successfully by Pearce et al. (33) for the determination of 11 major and minor elements following a hydrofluoric acid digest of coal ash whilst Ebdon and Wilkinson (34, 35) have used the technique to directly analyse coal slurries.

A second source for emission spectroscopy is the direct current plasma (DCP) and though the plasma is cooler than the ICP, it still offers a powerful and rapid technique. In a publication by Decker (36), he concluded that: the source was stable over long periods of time; both atomic and ionic spectral lines were enhanced in the presence of easily ionizable elements and the detection limits in general are less than 1 order of magnitude higher than for ICP-AES. Due to the rugged construction of the nebulizer and also due to the wide (8mm i.d.) injector tip, DCP-AES is well suited for the introduction of slurries. This was illustrated by McCurdy et al. (37) who introduced coal slurries for the successful determination of Cr, Cu, Mg, Mn, Ni and Pb.

Inductively coupled plasma-mass spectrometry (ICP-MS) is a recently introduced technique which offers high sensitivity and good selectivity and is thus well suited for the quantitative analysis of trace elements. Detection limits are lower than for ICP-AES and are in the pg ml^{-1} region for the rare earth elements. Date and Gray (38) have used this technique to determine 13 trace elements in standard reference water samples and 14 rare earth elements

in reference silicate rocks. Until recently sample introduction has been via nebulization of solution, but recently it has been shown that it is possible to introduce samples in the slurry form for ICP-MS analysis (39). The analysis of coal slurries by ICP-MS has not however been reported. A first report of such works is described in detail in Chapter 7.

1.3 SLURRY ATOMISATION

A slurry contains particulate matter suspended in a liquid medium. This suspension, or slurry, has many properties of a liquid. It is an aim of this work to use slurries for solid sampling together with calibration using simple aqueous standards, minimal sample pretreatment, and the use of the conventional instrumentation without the need for major modification.

The pioneering study of Gilbert demonstrated the direct flame spectroscopic analysis of solid samples (40). He observed emission lines for major elements when soil slurries were aspirated into a total consumption burner, but no attempt was made to make the method quantitative. A comprehensive review of the direct analysis of solids by atomic absorption spectrometry has been given by Langmyhr (41) who described the advantages and possibilities of such solid analysis by flame and electrothermal atomic absorption. The main reason why this solid sampling has not been universally accepted is the need for repeated microweighings, the slow rate of analysis and problems with calibration.

Several authors have reported direct slurry atomisation into flame AAS (FAAS). Fagioli et al. (42, 43) introduced carbonaceous slurries for the determination of Ca, Fe, K, Mg, Mn and Zn in different vegetable and plant material. Willis (44) outlined that the greatest limitation to slurry atomisation in FAAS was the particle size of the slurry. Fuller et al. (45, 46) alleviated this problem by pulse nebulization of 100 µl aliquots and the removal of the flow spoiler from the nebulizer spray-chamber. Fry and co-workers re-designed the spray chamber, burner and used a Babington-type 'clog-free' nebulizer for the successful

determination of Cu, Mn and Zn in beef and liver slurries (47). They also successfully

determined levels of Cu and Zn in whole blood, urine, seawater, evaporated milk concentrate

and tomato sauce (48). O'Reilly et al. (49,50) developed a direct method for atomising

several coal slurries in acetylene flames, but more recent work by Mohamed et al. (51) has

concluded the reason for low recoveries for coal slurries was due to incomplete particle

vaporisation in the relatively low temperature nitrous oxide/acetylene flames and suggested the

use of a hotter atomisation source (e.g. plasma) to achieve complete atomisation.

Headridge (52) reviewed methods of introduction of samples into a furnace but similarly to

FAAS, most techniques suffer from repetitive microweighings of the sample. Langmyhr (53)

recently reviewed methods for direct sampling solids by AAS and lists the matrices and

elements determined to date.

Effects from particle size are seen to a lesser extent in ETA-AAS and in a study (46), where

FAAS, ETA-AAS and ICP-AES were compared, significant effects were only observed if the

particle size was greater than 25 μm. Fuller and Thompson (54) used thixotropic thickening

agents to achieve a stabilized slurry for injection into a graphite furnace, whilst Ebdon and

Pearce (55) achieved stabilisation by magnetically stirring the slurry prior to injection. Other

applications of slurry analysis by ETA-AAS include the determination of chromium and

vanadium in Ilmenite and Rutile (46), copper, nickel and vanadium in coal and coke (56),

arsenic in coal (55, 57), selenium in coal (58) lead and cadmium in soil (59) various trace

elements in titanium (IV) oxide (45), lead in spinach (60) and lead and cadmium in

environmental samples (61, 62). This technique, though successful for many elements, is

limited by the temperature the furnace can attain, therefore more refractory matrices and

elements may suffer from incomplete atomisation.

Plasma sources have been used as atomisers for slurry atomisation and successful applications continue to be reported in the literature. The two commonly used sources are, the inductively coupled plasma (ICP) and direct current plasma (DCP). They are well suited as atomisation sources due to their high temperatures (about 8000 and 6000K respectively) but problems may be encountered owing to the nebulisation - sample introduction process. Applications reported include those for rocks (46), mineral (63, 64), pre-concentrated ion exchange resins (65) sediments and plant tissue (66), coals (35, 37, 67, 68) animal tissue (69) and soils (70). Therefore slurry atomisation is an attractive and promising technique due to its speed of analysis, simplicity and applicability to ETA-AAS, DCP-AES, ICP-AES and ICP-MS. Problems which are encountered in ICP-AES due to sample introduction problems are eliminated in ETA-AAS due to direct insertion of the slurry into the furnace. However the use of the plasma as an atom cell with its high temperature, means that complete matrix decomposition may be achieved, thereby avoiding problems associated with electrothermal atomisation.

1.4 ELECTROTHERMAL ATOMISATION ATOMIC ABSORPTION SPECTROSCOPY (ETA-AAS)

Atomic absorption spectroscopy (AAS) was first developed by the British born physicist Walsh (71) in Australia in 1955. He applied the observations of Bunsen and Kirchhoff a hundred years previously to deduce that atomic absorption and atomic emission could be used for elemental determination. In 1929 Lundegardh described a technique of flame emission spectrography for the analysis of agricultural materials in which a sample solution was nebulized into an air/acetylene flame. Walsh used the Lundegardh burner to atomise the sample and since then AAS has become one of the most versatile techniques in analytical chemistry as published in several reviews (72-75).

Atomic absorption spectroscopy (AAS) based on flame atomisation is well established and during the last decade alternative methods of atomisation have been studied. The most promising of the new techniques is electrothermal atomisation (ETA) in which the sample is atomised from an electrically heated carbon tube furnace. The earliest description was given by L'vov (76) and recently translated into English (77). The theory of atomic absorption, a description of the furnace and applications can be found in L'vov's textbook (78). Since then there have been numerous publications on the advances of ETA-AAS from its infancy to the present day.

As outlined by Ottaway (79), ETA-AAS has the sensitivity for direct determination of trace elements, but it suffers problems from interferences. These can often be overcome by the addition of specific compounds such as ascorbic acid (80), citric acid (81), ammonium phosphate (82) and magnesium chloride (83), thus modifying the matrix. In a recent paper published by Egila et al. (84) a comparison of various interferences and matrix modifiers in the determination of gold by ETA-AAS was made. A second, more effective method for the elimination of chemical interferences was proposed by L'vov (85), so called iso-thermal atomisation, most practically exhibited by platform atomisation. When a platform, which is a small piece of graphite and sits within the cuvette, is heated, partly by radiative and convective means, the analyte atoms upon atomisation are released into a hotter environment and thus recombination into molecular forms is less likely (86, 87).

The third method for eliminating the effects of chemical interference is that of probe atomisation as described by L'vov (88) and Manning et al. (89), originally devised for the introduction of the sample on the end of a tungsten wire into a pre-heated furnace and since modified and refined (90). Graphite probes are used and near complete removal of chemical interference has been reported as the analyte atoms are introduced into a furnace atmosphere at much higher temperatures than achieved with platform atomisation. Further work on both platform and probe atomisation has been performed by many authors, of note Frech and

Jonsson (91), Chakrabarti et al. (92), who used captacitive discharge heating to obtain isothermal conditions, Giri (90) and Slavin and Manning (93). A theoretical review by Sturgeon (94) examined the formation of atoms, vaporization equilibria and attempted to throw light on some of the less well understood parameters in ETA-AAS.

The use of background correction is imperative with real samples and is well documented for ETA-AAS. Problems due to light scattering are caused by the sample matrix condensing, after vaporisation, to form smoke or mist or from particulate carbon from the tube walls. Molecular absorption is caused through the broad absorption bands of molecular species present in the atomizer. Failure to correct for these absorbances, which may be high, will result in an overestimation of the element concentration. Background absorption is much greater in the U.V. range than in the visible range, so the determination of arsenic at 193.7nm and selenium 196.0nm already require background correction. The continuum source, as described by Koirtyohann and Picket (95), is the most common type of background corrector used today. With ETA-AAS however positive errors are noticed with certain elements, which are attributed to 'structured background'. The variation in background within the band pass of the spectrometer, known as 'structured background' is caused by the fine structure of molecular electronic spectra or the broadened edges of other elemental atomic-adsorption lines, especially if the element is present in high concentrations. This type of background cannot be corrected for by continuum source background correction systems which by definition assumes the background is unstructured across the band pass of the spectrometer. The problem of 'structured background' may be overcome by the use of a system based upon the Zeeman effect (96) or the system described by Smith and Hieftje (97) of pulsed hollow-cathode lamps.

Even though a continuum source produces very good correction for most cases, there are certain disadvantages, such as incorrect results in the presence of structured background and different geometries and optical paths lead to errors if optical alignment is not correct. The

Zeeman and pulsed hollow cathode systems overcome the weaknesses of the continuum source system such as correction of structured background and alignment problems are eliminated. However problems are encountered with Zeeman, such as analytical curves can be double-valued, i.e. they "roll-over", and in the pulsed hollow cathode lamp system, of failure to correct for rapidly increasing backgrounds due to a low modulation frequency.

Diffusion of the analyte through the tube walls leads to insensitivity and imprecision and improvements can be made by the use of pyrolytically coated graphite. This also has the advantage of eliminating unwanted reactions between the analyte and graphite substrate, which otherwise might lead to carbide formation. However as the pyrolytic layer was removed from the tube wall, so the sensitivity tended towards that of an uncoated graphite cuvette. Recent advances have made it possible to construct a cuvette made entirely of pyrolytic graphite and this has been shown (98) to be superior to either pyro-coated or uncoated graphite. Therefore within the last decade advances in ETA-AAS mean that the technique can offer extremely low limits of detection, requires smaller samples and is thus better suited for analysis of solid materials by slurry atomisation, thereby eliminating the need for lengthy decomposition steps and when sample destruction is performed in situ, the loss of volatilized elements can be restricted.

1.5 INDUCTIVELY-COUPLED PLASMA ATOMIC EMISSION SPECTROSCOPY

A plasma is described as "any luminous volume of gas having a fraction of its atoms or molecules ionized" (99). In recent years the inductively coupled plasma along with the direct current plasma have become widely used as excitation sources. Theoretical considerations of emission spectrometry can be found in the review by Sharp (99).

In 1962 Reed (100) descibed the induction-coupled plasma and this was the first flowing plasma to be described. The plasma was sustained on argon or an argon mixture containing 20% air, helium or hydrogen or 50% oxygen and was used to grow refractory oxide crystals.

In 1963, Greenfield et al. (31) recognised the analytical potential of the plasma as an excitation source and so began the evolution of ICP-AES into a powerful technique for the determination of trace metals in solution. Original and later designs of the torch can be found in the literature (31, 32, 100, 101, 102) and today the Fassel version is mainly used owing to its lower power and argon requirements.

Sample introduction into the ICP has been described as its 'Achilles heel' (103). In conventional solution analysis the sample is introduced via a nebuliser-spray chamber arrangement. The sample aerosol formed is carried by an argon flow along the injector tube which guides the aerosol to the central channel punching the plasma. This method of sample introduction has several limitations in the analysis of solids. For solids, there are two methods of introduction: discrete and continuous. Discrete introduction relies on the injection of a pulse of material derived from the samples, to produce a transient signal which is measured in a similar way to ETA-AAS measurements. Volatilisation methods include laser ablation (104-105), arc/spark vapour generation (106) and electrothermal vaporisation (107-112). Graphite rods or cups have also been used successfully to insert a solid sample into the base of the plasma (113-116). Continuous introduction of solids into the plasma has been attempted by methods such as fluidized beds (117-118) and spark elutriation (119), but these methods have not yet proved practical for routine analysis. Of the solid techniques mentioned most suffer from problems arising from either the matrix or standards.

The most successful method of solid introduction is nebulisation of slurries by means of a Babington-type nebuliser as previously used in this research group (120 - 123) which has the advantage of retaining the normal introduction system with calibration using aqueous standards.

- 11 -

1.6 DIRECT CURRENT PLASMA ATOMIC EMISSION SPECTROSCOPY

The direct current plasma (DCP) is a widely used source, but this is not reflected in the literature. The present three-electrode argon plasma, which evolved from the original two-electrode DCP, is a suitably stable source. The plasma is sustained between a single tungsten cathode and two graphite anodes which results in an inverted 'Y' shaped plasma.

The high temperature and stability of the DCP may enable the atomisation of powdered samples in the form of slurry, thus gaining all the advantages of solid sampling, such as elimination of lengthy sample preparation steps and contamination. The use of electrothermal atomisation for solid sample introduction into a DCP has been described by Wirz et al. (124) and Mohamed et al. (69) have studied the possibility of slurry atomisation of a bovine liver sample.

Recently McCurdy (37) has successfully determined trace levels in 1632(a) NBS bituminous coal slurry by nebulisation into a three electrode DCP. The three important parameters were described as:

(i)   extremely small particle size;

(ii)   spray chamber conditions which favour efficient aerosol mass transfer;

(iii)   high particle atomisation efficiencies characteristic of the hot DCP.

The potential advantages of slurry atomisation are that calibration can be achieved using aqueous standards and due to the continuous nature of the signal produced, a series of integrations may be performed. Thus solid sampling would enjoy the sensitivity, precision and convenience which is normally associated with aqueous samples and together with atomisation and excitation characteristics of the DCP and result in a technique which would be suited for the rapid analysis of coal slurries.

1.7 INDUCTIVELY COUPLED PLASMA MASS SPECTROMETRY

Inductively coupled plasma mass spectrometry (ICP-MS) is a growing technique for multi-element analysis. Its attractiveness stems from its excellent detection limits, simple spectra and similar sensitivity for most elements (125, 126). Much of the work published in ICP-MS concerns the introduction of solution samples. However, lately, much has been published on the direct analysis of solids, which therefore avoid acid dissolution and resulting polyatomic ion peaks such as ClO^+ or SO^+ (125, 126).

The various methods for introducing solids into ICP-MS directly, include laser ablation (127), electrothermal vaporisation (128), arc nebulisation (129, 130) and the direct insertion of a wire loop containing the sample into the ICP (131). To date there is one paper (39), which describes slurry nebulisation into ICP-MS and this concluded that it is a viable method of sample introduction with excellent agreement with certified values for major, minor and trace elements in soils, zeolites and catalysts.

Slurry nebulisation ICP-MS offers several advantages over other forms of solid sampling. It is a rapid multi-element technique, from which isotope data can be obtained and this means that sample preparation is the major time-consuming factor. Sample preparation is cut down considerably with slurry atomisation due to the ease with which samples may be prepared.

1.8 OBJECTIVES OF THIS WORK

Greenfield et al. (71) stated that there was a "golden opportunity for someone to make considerable advances in ICP-AES by devising a rapid method of transporting solid samples into a plasma which is of general applicability". The main object of this work was the development of successful methods for the analysis of coals using either ETA-AAS, ICP-AES, DCP-AES or ICP-MS by introduction of the solid in a slurry form using simple aqueous calibration.

Electrothermal atomisation atomic absorption spectroscopy is an extremely sensitive technique, which is readily available in most laboratories and is well suited to the determination of difficult volatile trace elements such as arsenic and selenium. A method was developed for the routine determinations of these elements, taking advantage of the novel Smith-Hieftje background correction system, thereby enabling their successful determination by ETA-AAS which previously was fraught with problems due to structured background.

A successful method for the direct introduction of solid samples via slurry atomisation was developed for the determination of major and minor elements in coal by ICP-AES and DCP-AES and encouraging results were obtained also for ICP-MS using this technique. Careful attention was paid to particle size which is a critical parameter for successful analysis by slurry atomisation. For this technique to be practical in the routine analysis of coal, calibration should be achieved using aqueous standards, since in slurry atomisation the sample matrix loading is changed. It has therefore become necessary to elucidate any temperature changes within the plasma during slurry nebulisation, thereby enabling a deeper understanding of the technique.

There still exists uncertainty on the fundamental mechanism of these plasmas and as they are an excellent excitation source for emission and ionisation source for mass spectrometry, it is a necessary requirement to understand the mechanism involved. Slurry atomisation potentially provides a diagnostic tool which is suitable for the elucidation of plasma mechanisms. Of special interest as diagnostic indicators are electron temperature (T_e), electron density (n_e), excitation temperature (T_{ext}) and rotational temperature (T_{rot}) as these can give an indication to the extent of and changes in thermodynamic equilibrium which exists in a plasma and thus provide information on plasma mechanisms.

CHAPTER 2

DETERMINATION OF ARSENIC IN COAL SLURRIES BY ELECTROTHERMAL ATOMISATION ATOMIC ABSORPTION SPECTROSCOPY

2.1 INTRODUCTION

The toxicity of arsenic and its compounds is well documented and therefore there is a need for a rapid method that allows the levels of arsenic in coal to be monitored. Arsenic is present in coal in trace amounts and monitoring is essential, e.g. for the food industry and where there is concern over quality control, catalyst poisoning and environmental pollution. The very high tonnages of coal used and the possibilities of concentration during conversion processes mean that even ngg^{-1} levels may be significant.

Traditionally arsenic determinations have been performed using variations of the Grutzeit method after a wet or dry oxidation stage. The Case method (132) has been modified to give a simple and rapid procedure for the estimation of small amounts of arsenic in coal. After ashing the coal, the ash is dissolved in a sulphuric/oxalic acid mix, thereby reducing the arsenic to the trivalent state. Conversion to arsine is completed by treatment with zinc and sulphuric acid. The evolved arsine is passed through mercuric bromide impregnated paper and the resulting stain is compared with stains obtained from standard arsenic solutions. A more precise and superior method is the spectrophotometric procedure based on the measurement of arsenic diethyl dithiocarbamate (133) or arsenomolybdate complexes (134), the latter being similar to the method adopted by the British Standards (135) for the determination of arsenic in coal and coke. However the limit of detection is insufficient for trace level determinations.

Other methods which exist for the determination of arsenic include gas-liquid chromatography (136), ion-exchange chromatography, atomic emission and atomic absorption of which the latter two are the most popular techniques.

Arsenic determinations by ICP-AES (137,138), FAAS (139), heated quartz tube (140) and ETA-AAS (141), have encountered problems from interferences caused by various complex matrixes (141, 142). In order to minimise these interferences several procedures are available whereby the arsenic can be isolated from the matrix, such as complexation and solvent extraction (143, 144), co-precipitation (145, 146) and arsine generation (147-151). Arsine generation involves the reduction of arsenic to arsine by either zinc metal or sodium borohydride. The gaseous As H_3 is passed directly into the atom cell for atomisation and subsequent analysis by atomic absorption or emission spectroscopy. Unfortunately hydride generation suffers from a number of interferences (148, 152) and all the above mentioned techniques are primarily applicable to solution samples.

As coal is a notoriously difficult matrix to bring into solution there are advantages to be gained by the direct instrumental determination of arsenic in coal, such as the elimination of the complex error prone sample preparation stage. X-ray fluorescence spectrometry is a rapid technique but does not possess the required sensitivity for direct trace element analysis of coal. Spark-source mass spectrometry and neutron activation analysis (NAA), on the other other hand, are both capable of determinations of elements at concentrations down to 0.1-1ugg^{-1}, but these techniques are slow, and, in NAA, the equipment is not readily available to most laboratories.

2.1.2. Determination of Arsenic by Electrothermal Atomisation Atomic Absorption Spectroscopy

Atomic absorption spectrometry is conventionally regarded as a solution-based technique, but recent developments in solid sampling have made atomic absorption using electrothermal atomisation (ETA-AAS) a promising approach, especially as the necessary instrumentation is available in most laboratories.

Methods whereby coal can be introduced directly into a furnace atomiser, in a slurry form, without the need for lengthy ashing or digestion stages, appear preferable. Such a slurry method has been described by Ebdon and Pearce (55), who used nickel nitrate (as a matrix modifier), magnesium nitrate (as an ashing aid), nitric acid (to provide an acid environment) and ethanol (wetting agent) to prepare the slurries. Positive errors were noticed at the more sensitive analytical resonance arsenic line, 193.7nm, however, this was later attributed to a broadened aluminium - line spectral interference (10), first reported by Riley (153). This type of interference remains uncorrected by continuum-source correction systems, but it has been reported that such problems can be alleviated by using a background correction system as described by Smith and Hieftje (97).

2.2 BACKGROUND CORRECTION

As previously mentioned, the need for background correction in atomic absorption spectroscopy is well documented, especially for electrothermal atomizers. Three methods of background correction are currently available commercially and the two systems available in this laboratory are described below.

2.2.1 Continuum Source Method

The continuum source method is the most common type of background corrector used today. To correct for background effects, light from a deuterium arc or D_2 hollow cathode lamp continuum source and from an elemental hollow cathode lamp is alternated rapidly, through the atom cell. The light from the hollow cathode lamp is absorbed by the analyte and background. The absorbance by atoms of the continuum source is negligible, but that absorbed by the background is the same percentage as for the line source (154). Therefore differences between the hollow cathode absorbance and continuum absorbance is the absorbance due to the analyte. However positive errors such as those noticed with arsenic at 193.7 nm line due to broadened aluminium line remain uncorrected as described by Riley (153). He concluded that the emission lines of Al^{2+} at 193.47 and 193.45 nm were

responsible for the spectral interferences as they were in close proximity to and overlapped the resonance line of arsenic. This is due to the high concentration of aluminium in coal which results in considerable broadening of the line and thus leads to inaccurate correction by the continuum source corrector. Depending upon the shape of the background, when its averaged absorption is subtracted from the atomic-absorption signal it can result in under or over compensation (Figure 1).

2.2.2 Smith-Hieftje Method

The problem of 'structured background' may be overcome by the use of Smith-Hieftje background correction, which was first described in 1982 (155). The phenomenon of self-reversal has been known for the last 20 years. It occurs when an excessive current is passed through a hollow cathode lamp, which results in broadening of the emission line and atomic absorption from the analyte is greatly reduced. The unexcited atoms in the lamp absorb the radiation of the atomic spectral line, so the output resembles that shown in Figure 2.

Smith and Hieftje (97) applied this phenomenon to background correction. The lamp is first run at low current, and its light is absorbed by the analyte as well as the background. Then a very brief pulse of a much higher current is passed through the lamp, causing self-reversal. Atomic absorption by the sample is much reduced, but the background absorbs the same proportion of light as before. Background correction is obtained by taking the difference of the two signals.

2.2.3 Comparisons Between the Two Background Correction Systems

Even though a continuum source produces very good correction for most cases, there are certain disadvantages, such as:

1. incorrect results in the presence of structured background;

2. different geometries and optical paths lead to errors if optical alignment is not correct;

FIGURE 1

Illustration of structured background resulting in over correction using a deuterium arc background corrector
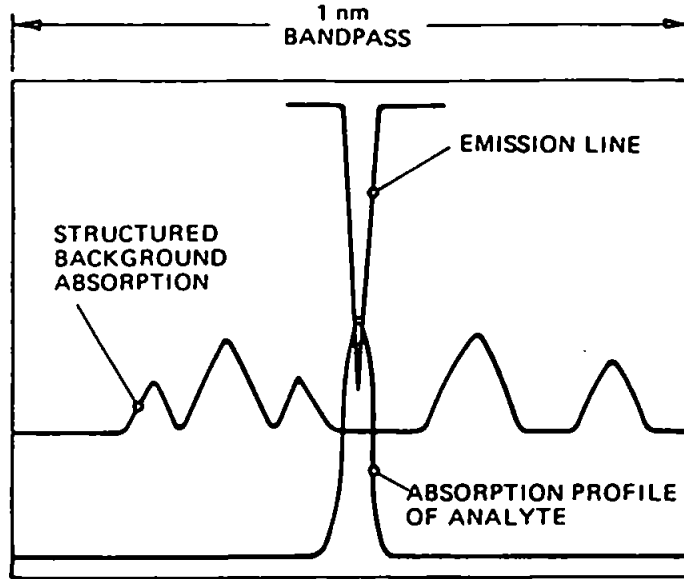
FIGURE 2

Schematic diagram of emission line profile of a hollow cathode lamp as a function of lamp current
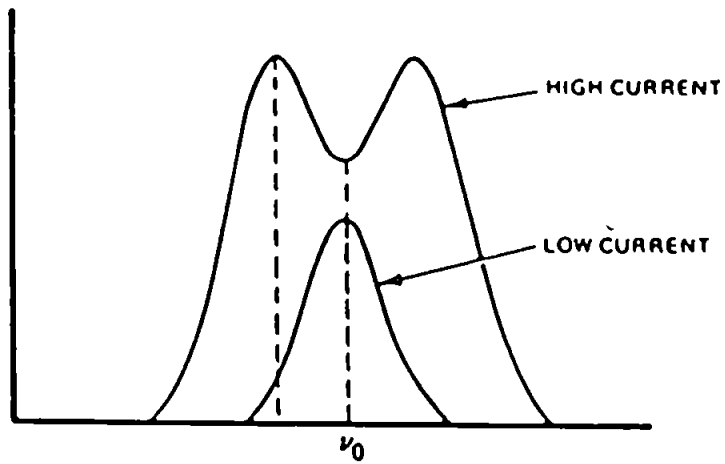
3.   loss of light if a 50% beam splitter is used, or cumbersome optics if rotating mirrors are used;

The Smith-Hieftje overcomes many weaknesses of the continuum source system such as (i) Smith-Hieftje may correct for structured background, (ii) estimated distance of background from analytical wavelength for successful correction is 0.005nm, (iii) alignment problems are eliminated.

However the Smith-Hieftje system suffers from reduced sensitivity. Self reversal in the hollow cathode is rarely complete, so there is some atomic absorption even during the light current phase and the loss in sensitivity can range between 10% to 75%. The system also suffers from a failure to correct for rapidly increasing backgrounds owing to the low modulation frequency of the current pulse. The problem can be alleviated by . complete sample destruction during the ashing stage.

2.3 EXPERIMENTAL

An instrument fitted with both deuterium-arc and Smith-Hietfje background correction systems (IL 655 furnace fitted to a Video 12 spectrometer; Thermo-Electron Warrington, UK) or an instrument fitted with deuterium hollow-cathode lamp, continuum source, background correction,(SP-9 furnace fitted to an SP-9 spectrometer with PU9095 video furnace programmer and SP-9 computer; Pye Unicam, Cambridge, UK) were used. Full operating details are given in Table 1. Slurry samples were injected into the graphite furnace using precision micropipettes (Gilson Pipetman P; Anachem, Luton, Bedfordshire, UK).

2.4 CHEMICAL REAGENTS

Three certified reference material coals were analysed: sub-bituminous coal (NBS SRM 1632a; National Bureau of Standards, Washington, DC, USA), bituminous coal (NBS SRM 1635) and European coal (BCR No. 40; Community of Bureau of Reference, Brussels, Belgium).

All reagents used were of analytical-reagent grade (BDH Chemicals, Poole, Dorset, UK) and all solutions were prepared with doubly distilled, de-ionised water.

2.4.1 Stock standard arsenic solution

1000 mg l^{-1} prepared by the addition of As_2O_3 (1.3200 g) to water (24 ml) and nitric acid (50 ml) and heating until dissolved. After dilution with water to 1000 ml, the solution was stored in previously acid-washed polyethylene bottles.

2.4.2 Working standard arsenic solutions

Prepared by taking various aliquots of the stock standard solution and matching with the slurry reagent.

2.5 SAMPLE PREPARATION

Coal (0.5-1 g) was weighed accurately into a 50-ml polypropylene screw-capped bottle, to which 10 ml of slurry reagent (containing 10 g l^{-1} of $Ni(NO_3)_2.6H_2O$, 10 g l^{-1} of $Mg(NO_3)_2.6H_2O$, 50 ml l^{-1} of concentrated nitric acid and 100 ml l^{-1} of ethanol) were added. A magnetic stirrer bar was inserted, the bottle was sealed and the contents were stirred until the coal was a homogeneous mixture (typically 5 min). Aliquots of the suspension slurry (10-30 µl) were taken using a micropipette, whilst stirring continuously.

When extra grinding was required, this was achieved in a vibrating agate ball mill (Mark 2 Vibrating Mill; Beckman-RIIC, Glenrothes, UK). Particle size measurements were made by the electrical zone-sensing method (Coulter Counter TA II; Coulter Electronics, Luton, Befordshire, UK).

In order to prepare a thixotropic slurry, 1 g of sample was added to 50 ml of distilled water. The mixture was stirred and 3.0 ml of 0.1% m/V sodium hexametaphosphate solution were added. This was followed by the addition of 0.1 ml of H2 antifoam agent (Allied Colloids, Bradford, UK) and 1 ml of Viscalex HV30 thixotropic thickening agent (Allied Colloids). The pH was adjusted to 7.5 by addition of ammonia solution, and, once settled, the gel was transferred to a 100-ml calibrated flask and diluted to the mark. Standards were prepared using the same method.

2.6 RESULTS AND DISCUSSION

The initial ETA-AAS results for arsenic in NBS SRM 1632a and 1635 using a deuterium arc as a background corrector did not show good agreement with the certified value as reported by Ebdon and Pearce (55). This, however, was in agreement with Riley (153) who attributed the positive errors at the 193.7-nm arsenic line to the broadened aluminium-line, so-called structured background.

With this in mind, a furnace programme was developed (Table 1) that included an atomisation step ramped over 5 s, thereby enabling the volatile arsenic to be atomised before the more refractory aluminium. The resulting printout from the instrument (Fig. 3) shows temporal separation of the arsenic and aluminium peaks. However, despite this separation, the continuum background corrector failed to correct for the aluminium interference (Table 2) and large positive errors were observed.

TABLE 1

Spectrometer and furnace operating parameters used in the
determination of arsenic

Video 12 instrument: furnace programme using pyrolytically coated cuvettes						
	Dry		Ash		Atomise	
Time/s	30	40	30	45	5	5
Temperature/°C	80	180	900	1200	2200	2200
Internal N$_2$ gas flow-rate (SCFH)*	20	20	20	5	5	5
Spectrometer parameters:						
Wavelength	193.7 and 197.2 nm					
Bandpass	1.0 nm					

SP-9 instrument: furnace programme using pyrolytically coated cuvettes			
	Temperature/°C	Hold time/s	Ramp
1. Dry	200	20	8
2. Ash	900	30	7
3. Ash	1200	5	5
4. Atomise	2300	10	0
5. Clean	2800	3	0
Gas flow-rate	3 l min^{-1} during dry and ash stages		
	0.5 l min^{-1} during atomisation stage		
Spectrometer parameters:			
Wavelength	193.7 and 197.2 nm		
Band pass	1.0 nm		

* Standard cubic feet per hour

FIGURE 3

Plot of signal versus time for arsenic atomisation using deuterium-arc background correction at 193.7nm
A, corrected signal; B, total signal; C, arsenic absorption peak; and D, interfering peak
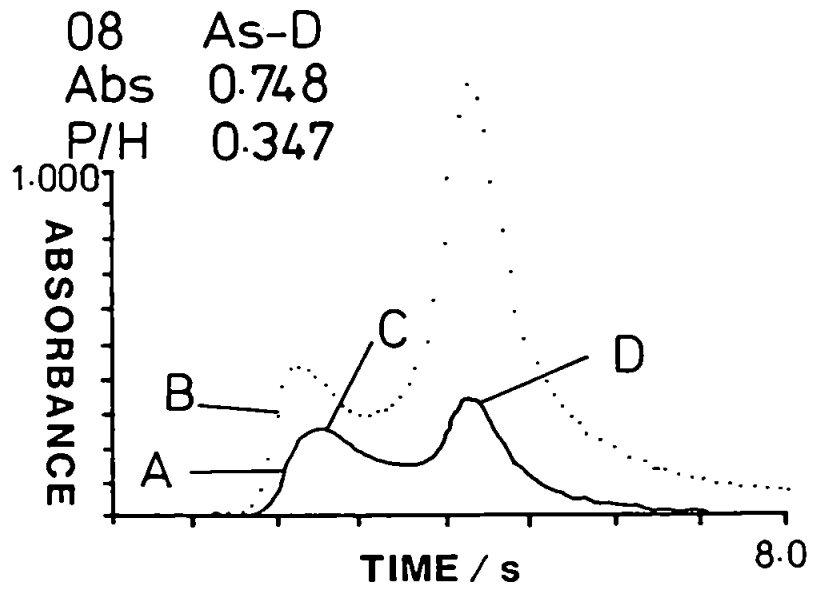
TABLE 2

Determination of As in reference coals by direct slurry atomisation
using deuterium-arc background correction

Wavelength/nm	Sample	As/µg g^{-1}	
		NBS SRM 1635	NBS SRM 1632a
193.7	Slurry	1.1 ± 0.5	20.0 ± 0.8
197.2	Slurry	0.38 ± 0.10	5.0 ± 0.60
-	Certificate value	0.32 ± 0.13	9.3 ± 1.0

When the analysis was repeated using the less sensitive 197.2 nm line, the results for NBS SRM 1635 were within the limits of the certificate value (Table 2). This is not unexpected as the 197.2 nm line is free from any spectral interference from aluminium, thereby illustrating that both background correctors are capable of correcting for the background at this wavelength.

The values obtained for NBS SRM 1632a were low, so a new slurry was prepared in which the coal had been ground in a vibrating ball mill for 35 min to reduce the particle size from 100 to 30 um. When the above experiments were repeated with the ground coal, the recovery of arsenic from the coal matrix was enhanced and at 197.2 nm acceptable accuracy was obtained (see Table 3). This is in agreement with the findings of Fuller (45) who studied slurry atomisation by ETA-AAS, and suggests that arsenic was not fully released from large particles in the brief atomisation stage.

The possibility of correcting for structured background by the use of the correction system developed by Smith and Hieftje (97) was then investigated because, whereas the 197.2 nm line appeared to be interference free, the 193.7 nm line is about twice as sensitive. The above work was repeated using the Smith-Hieftje background correction system in place of the deuterium arc. The results, shown in Table 4, show that with this background corrector, even at the 193.7 nm line good agreement with the certified values is obtained. This demonstrates the effectiveness of this correction system in compensating for the structured background at 193.7 nm. The effective correction of the aluminium peak can be clearly observed in the atomisation printout (Fig. 4) where the background (broken line) still shows the interfering line but the solid line shows that the corrected signal is not affected. Similar results were observed at the 197.2 nm line, which was free of spectral interference. Again, the arsenic recoveries were enhanced by grinding the coal. The slow atomisation ramp proved advantageous at both lines because the relatively slow modulation frequency of the Smith-Hieftje corrector caused problems with rapidly changing high levels of background.

TABLE 3

Effect of particle size on arsenic determination at 197.2 nm

Sample	As in NBS SRM 1632a/µg g^{-1}
Slurry of coal as received	5.0 ± 0.60
Slurry of ground coal	9.2 ± 1.0
Certificate value	9.3 ± 1.0

TABLE 4

Determination of arsenic in reference coals by direct slurry atomisation using Smith-Hieftje background correction

Wavelength/ nm	Sample	As/µg g^{-1}		
		NBS SRM 1635	NBS SRM 1632a	NBS SRM 1632a (ground)
193.7	Slurry	0.4 ± 0.1	8.2 ± 1.1	9.5 ± 0.7
197.2	Slurry	0.39 ± 0.1	6.0 ± 0.8	9.2 ± 1.0
	Certificate value	0.32 ± 0.13	9.3 ± 1.0	9.3 ± 1.0

FIGURE 4

Plot of signal versus time for arsenic atomisation using Smith-Hieftje background correction at 193.7nm
A, corrected signal; B, total signal; C, arsenic absorption peak; and D, corrected interfering peak
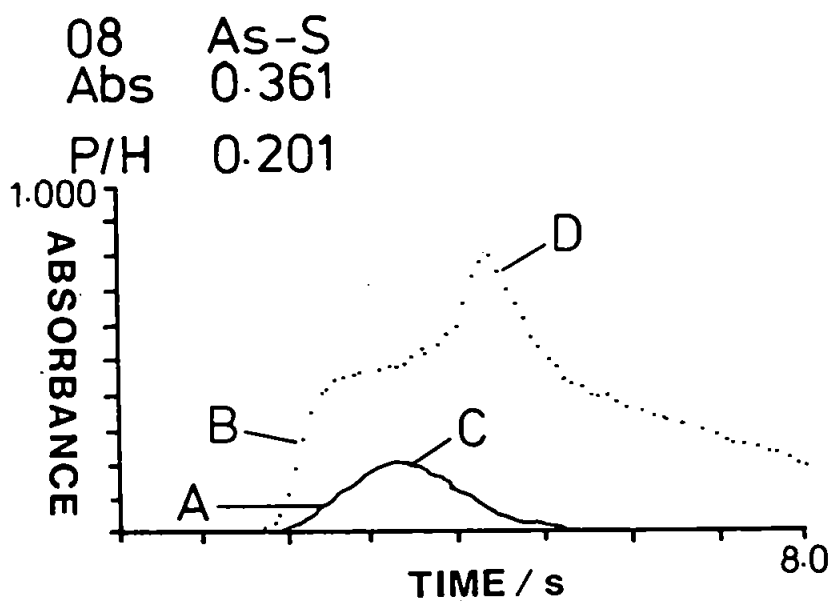
This work was repeated on the SP-9 instrumentation fitted with continuum-source background correction. Errors were observed at the primary resonance line (193.7 nm) whereas the correct value was achieved at the "interference free" line (197.2 nm). Table 1 lists the operating parameters and Table 5 gives the results obtained.

2.6.1 Analysis of Reference Coal BCR No. 40

The levels of arsenic in BCR No. 40 were determined. The particle size was reduced to below 25 μm and the coal was suspended in the slurry reagent as previously described. The conventional cuvettes previously used in the IL furnace were now replaced by the delayed atomisation cuvettes (DAC), (Figure 5), in which the centre of the cuvette is thicker than the edges, which leads to slower heating of the centre compared with the ends. In effect, atomisation occurs into a hotter environment, which should reduce the level of non-specific absorption, which is important when considering slurry loading and the determination of volatile elements. The furnace programme was re-optimised, which resulted in a higher atomisation temperature (see Table 6). The results with these new cuvettes and using both background correctors are shown in Table 7. It is obvious that both background correctors produce results that are in excellent agreement with the certified values. This implies that the structured background due to aluminium, observed with the previous coals, does not present a significant problem in BCR No. 40. The aluminium interference still persisted for the other coals in the new cuvettes and therefore the reduced interference seems to be due to the higher As:Al ratio in BCR No. 40 compared with the other coals.

2.6.2 Thixotropic Slurries

Another method by which slurries have been analysed is by preparing the slurry in a thixotropic medium as described by Fuller and Thompson (54). Although this does not improve the dispersion of the coal, it may be more suitable for certain auto-samplers as a thixotropic slurry remains homogeneous without constant agitation. The resulting slurries were stable for up to 24 h, but the results were not as reproducible owing to the

TABLE 5

Determination of arsenic in NBS SRM 1632(a) using deuterium hollow-cathode lamp backgrnd correction (SP-9 spectrometer)

Wavelength/nm	Sample	As/μg g^{-1}
197.2	Slurry	9.8 $\pm$ 0.8
193.7	Slurry	21.5 $\pm$ 0.9
	Certificate value	9.3 $\pm$ 1.0

FIGURE 5

Diagram of a delayed atomisation cuvette (DAC)
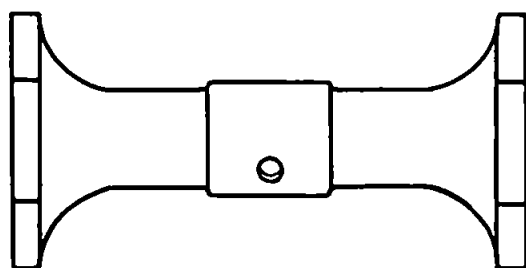
TABLE 6

Furnace programme for delayed atomisation cuvettes

	Dry		Ash		Atomise	
Time/s	30	40	35	40	5	5
Temperature/$^{\circ}$C	70	110	550	1000	2300	2300
N_2 flow-rate (SCFH)*	20	20	20	5	5	5

* Standard cubic feet per hour

TABLE 7

Determination of arsenic in BCR No. 40 coal with different forms of background correction at 193.7 nm

Sample	As/μg g^{-1}		
	Smith-Hieftje		Deuterium arc
Slurry	12.3 $\pm$ 1.0		12.8 $\pm$ 0.8
Certificate value		13.2 $\pm$ 1.1	

hydrophobic - hydrophilic interaction between the slurry and the pipette tip, whereby not all the slurry was expelled. It is expected that a pneumatically operated auto-sampler would improve the reproducibility.

2.7 CONCLUSION

The results illustrate how the problem of structured background, encountered by other workers, can be overcome in the determination of arsenic in whole coal by use of a Smith-Hieftje background correction system. The slurry injection technique described offers a simple and rapid form of analysis, eliminating the need for lengthy contamination-prone sample preparation stages, thereby increasing the speed of analysis, and is readily adaptable to existing instrumentation. Although there was some decrease in sensitivity using Smith-Hieftje background correction for arsenic (a factor of 1.3 compared with continuum-source correction), the limit of detection at 193.7 nm was still superior by a factor of 2 to that obtained at 197.2 nm using deuterium-arc background correction. The limit of detection using a 10% m/V coal slurry was 0.03 µg g^{-1} of arsenic in coal, which is adequate for all practical purposes. Slurry atomisation has been shown to be more rapid than dissolution approaches, accurate, provided that care is taken over background correction procedures and the furnace programme is optimised, and to offer excellent sensitivity.

CHAPTER 3

DETERMINATION OF SELENIUM IN COAL SLURRIES BY ELECTROTHERMAL ATOMISATION ATOMIC ABSORPTION SPECTROSCOPY

3.1 INTRODUCTION

The importance of selenium within the environment has been well reviewed, with respect to its occurrence, distribution, toxicity and essential levels required by both man and animals and analytical methodology for the element (156, 157). The combustion of fossil fuel can introduce selenium into the biosphere. Additionally selenium can act as a catalytic inhibitor, therefore information on selenium levels in coal used in conversion processes is important. The most common analytical technique for the determination of selenium is · a fluorimetric procedure following sample digestion. The problems associated with this technique include, loss of analyte through volatilization during the digestion step (158) and the carcinogenic properties of the fluorescing agent (159). Other techniques for the determination of selenium in coal include spark source mass spectrometry (25) and neutron activation methods (160, 161) with good agreement being reported for the latter with certified values. However with SSMS, poor accuracy resulted due to spectral and matrix interferences, whilst · NAA suffers.·long analysis time so as to allow the sample activity to decay.

Atomic absorption spectroscopy is by far the most widely used technique for the determination of selenium (157) incorporating either flame, electrothermal or heated quartz cell atomization (162). Determination by direct flame techniques have lost popularity due to the greater sensitivity offered by hydride generation and electrothermal atomisation, the latter offering the best sensitivity and detection limits.

Hydride generation AAS has been used Nadkarni (163) and Agterdenbos et al. (164) for the determination of selenium in coal, but the technique suffers many interferences owing to variation in valency states, other metals (165, 139) and anions (165). Methods proposed to eliminate such interferences include the use of masking agents, such as acetate and citrate (166) or 1,10-phenanthroline (167), or separation of the analytes from the interfering species by coprecipitation on metal hydroxides (168).

3.1.1 Determination of Selenium by ETA-AAS

Although electrothermal atomic absorption is a sensitive technique, it is affected by spectral interferences, analyte volatilization problems and vapour phase interferences during the ashing and atomisation stage (169, 170, 41). In the determination of selenium the need for matrix modification is imperative, so as to minimise the loss of the analyte during the ash stage as reported by several authors (171-178, 169). Manning (179) found spectral interferences from iron when selenium was determined at 196.0nm, the primary resonance line, using continuum source background correction. This interference was apparently more pronounced at the 204.0nm line. Coal contains large quantities of iron and only small amounts of selenium. Thus while ETA-AAS is required to provide the necessary sensitivity, spectral interference may be expected when using continuum source background correction.

The volatility of selenium creates further problems in its analytical determination owing to losses which may be encountered during ashing and digestion procedures (180). Coal is a particularly difficult matrix to digest and many digestion procedures involve elevated temperatures for lengthy periods, which can be detrimental due to the loss of selenium at temperatures above 300°C. Thus to overcome the problems of coal digestion in the determination of selenium a method which uses solid samples directly would be advantageous.

Selenium is not presently measured by British Coal on a routine basis as there is no BS method. There is a need therefore for a method which incorporates speed, sensitivity and precision for the determination of selenium in coal. The performance of continuum source background correction and a Smith-Heftje correction system which can eliminate certain spectral interferences was compared and the results assessed. Sample pretreatment was kept to a minimum and increased sample destruction was achieved by using air during the ashing stage. The effect of various matrix modifiers was also investigated. The method was calibrated using aqueous standards and validated using certified reference material coals.

3.2 EXPERIMENTAL

An Instrumentation Laboratory Video 12 atomic absorption spectrometer fitted with an IL655 graphite furnace (Thermo-Electron, Warrington, UK) was used throughout for selenium determination. A selenium hollow cathode lamp operated at 2.5 mA was used as the primary source of radiation. A spectral bandpass of 2nm was selected to isolate the 196.0nm line. Either Smith-Hieftje or deuterium arc background correction were employed throughout. Both pyrolytic coated and uncoated tubes and pyrolitic coated microboats were used. The furnace conditions found optimum for the determinations of selenium in coal slurry are summarised in Table 8. Slurry samples were injected into the graphite furnace using precision micropipettes (Gilson Pipetteman P; Anachem Ltd, Luton, Bedfordshire, UK).

3.3 CHEMICALS AND REAGENTS

Five certified reference material coals were analysed: bituminous coal (NBS SRM 1632(a) National Bureau of Standards, Washington, DC, USA), sub-bituminous coal (NBS SRM 1635), gas coal (BCR, No 180, Community Bureau of Reference, Brussels, Belgium), coking coal (BCR No. 181) and steam coal (BCR No. 182).

TABLE 8

Spectrometer and furnace operating parameters used in the determination of selenium

Furnace programme using pyrolytically coated delayed atomisation cuvettes

	DRY		ASH		ATOMISE	
Time (s)	30	40	30	45	5	5
Temperature (^{o}C)	80	120	600	800	2200	2350
Gas Flow	AIR	AIR	AIR	N_2	N_2	N_2
Rate (SCFH)	20	20	20	5	5	5
l/min	7.0	7.0	7.0	2.5	2.5	2.5

Spectrometer Parameters using Smith-Hieftje background correction	
Wavelength (nm)	196.0
Lamp (mA)	2.5
Bandpass (nm)	2

All reagents used were of analytical reagent grade ("AnalaR", BDH Chemicals Ltd, Poole, Dorset, UK) and all solutions were prepared with doubly distilled, deionized water.

3.3.1 Stock Standard Solutions

Stock 1000mg l^{-1} selenium solution was prepared by the addition of selenium metal (1.000 g) to nitric acid (25 ml) with heating until dissolution was complete. After dilution with water to 1000ml the solution was stored in acid washed polyethylene bottles.

Working standards were prepared by taking various aliquots of the standard stock solution and diluting with the slurry reagent solution. Suitable precautions were taken when handling standards given the known toxicity of selenium.

3.3.2 Sample Preparation

Coal was ground for 15-30 minutes so as to reduce the particle size. A McCrone micronising mill (McCrone RA Ltd, Belsize Lane, London) was used. Particle size measurements were made by the electrical zone sensing method (Coulter Counter TAII, Coulter Electronics, Luton, Bed). A typical particle size distribution is shown in Figure 6.

The ground coal (0.4 - 2.0 g) was weighed accurately into a 50 ml polypropylene screw cap bottle, to which 10 ml of slurry reagent (containing 10 g l^{-1} of $Ni(NO_3)_2.6H_2O$, 10 g l^{-1} $Mg(NO_3)_2.6H_2O$, 5 ml l^{-1} concentrated nitric acid and 100 ml l^{-1} ethanol) were added. A magnetic stirrer bar was inserted, the bottle sealed and stirred until the coal was a homogenous mixture (typically 5 mins). Aliquots of this slurry (10 - 30 μl) were taken using a micropipette whilst stirring continuously and introduced into the graphite furnace. In the final stages of the work and in the successful method the magnesium nitrate was omitted from the slurry reagent solution.

FIGURE 6

By volume particle size distribution of coal NBS SRM 1632(a) after 30 minutes grinding in a micronising mill
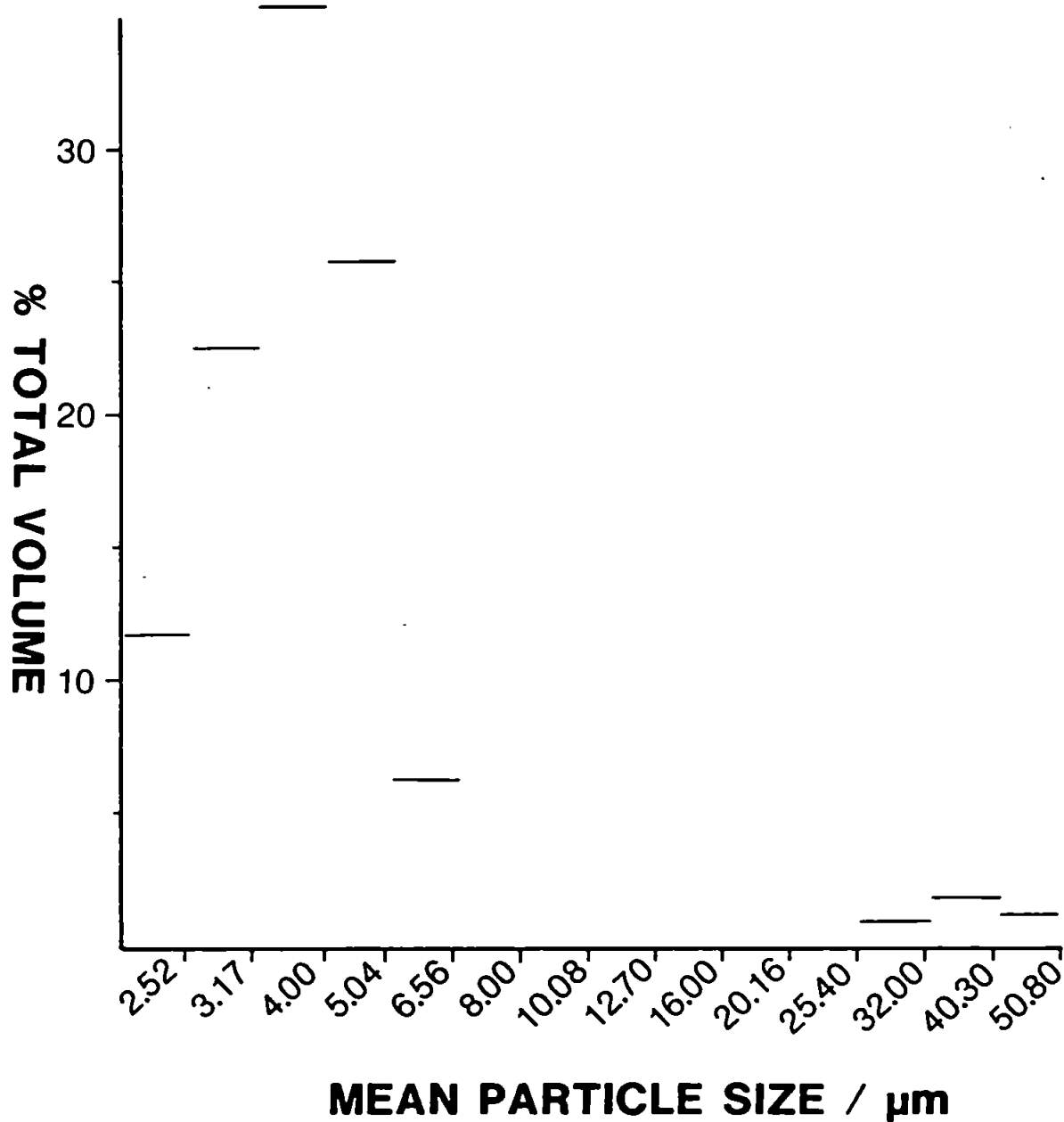
3.4 RESULTS AND DISCUSSION

3.4.1 Preliminary Experiments

Initial experiments were performed using a deuterium arc background corrector. Using the 196.0 nm line large positive interferences were observed when analysing coal slurries. This was attributed to the failure of the correction system to correct for the interference of a broadened iron line on the selenium absorption line. Both iron and selenium were atomised simultaneously within the graphite furnace and thus an overestimation of the selenium content in the coal was obtained.

The above experiments, in which nickel nitrate acted as a matrix modifier, were repeated with the Smith-Hieftje background corrector. The results proved unreproducible. Initially a signal resulted, but upon further experiments, no signal was evident. Experiments were devised to elucidate the problem of the diminished selenium signal. Several variables were considered. Reduction of the ashing temperature to minimise the possible loss of volatile selenium during the ashing stage yielded an erratic signal. This was attributed to smoke formed during the atomisation stage due to incomplete matrix destruction during the ash stage. The acid concentration of the slurry was altered so as to minimise the possible generation of gaseous hydrogen selenide, but again no signal resulted. The major problem was considered to be the quantity of iron (at the 3% m/m level) which was masking the small amount of analyte. Measurement of both iron and selenium atomisation profiles suggested both elements were atomised at similar times under the furnace programme used and indeed over a wide range of such programmes, e.g. increased atomisation temperature, increased and decreased rate of atomisation.

The use of other modifiers was examined in the hope of separating the iron and selenium atomisation profiles. Nickel nitrate was replaced by copper nitrate in the reagent and ash atomise plots constructed using both copper nitrate and nickel nitrate in coated and uncoated tubes. It was evident that pyrolytically coated tubes and nickel nitrate modifier

were preferable as higher atomisation temperatures could be tolerated. No signal for selenium in coal was observed when a palladium nitrate matrix modifier was used. Having established that nickel nitrate was the preferred modifier, hydrogen peroxide was added to the slurry reagent in the hope that this would produce a more oxidising environment in the ashing stage. No selenium signal was obtained from coals although various concentrations of hydrogen peroxide together with differing furnace conditions were applied.

A series of experiments were devised using aqueous selenium, nickel nitrate and iron oxide. As expected a low signal resulted when nickel nitrate was omitted due to loss of analyte during the ashing stage. However, the signal was enhanced when the nickel nitrate was included. This was attributed to the formation of nickel selenide which is stable at more elevated temperatures, which is indicative of successful modification of the analyte. The addition of both nickel nitrate and iron oxide (1%) caused the signal to be depressed. Omission of nickel nitrate, but inclusion of both the iron and selenium, produced and enhanced signal compared to using nickel nitrate as the modifier. The conclusion drawn from these experiments was that iron oxide acted as a matrix modifier in the absence of nickel nitrate, but in the presence of both nickel nitrate and iron oxide, the analyte signal was supressed due to spectral interference.

Ash-atomise plots were constructed for selenium in solution in a slurry of iron oxide particles and compared with similar plots for a solution of selenium in nickel nitrate. It was apparent that higher temperature was required to atomise the selenium from the iron oxide slurry and a higher ashing temperature could also be tolerated. A third ash-atomise plot was constructed using two slurries of iron oxide only one of which contained selenium solution. All measurements were made at the selenium 196.0 nm resonance line. It was possible to construct ash-atomise curves for both slurries. On comparison of both plots, the apparent atomisation temperature for the pure iron oxide slurry was higher than the atomisation temperature observed using the iron oxide slurry containing selenium. This

suggested that with careful control and manipulation of furnace temperature and ramping of the furnace programme, it might be possible to separate the selenium signal from the iron interference. In practice this was not possible and it is suggested that iron and selenium form a condensed phase selenide which ensures co-evolution of atoms in mixtures.

Hydrogen sulphide was bubbled through the selenium in iron oxide slurry in an attempt to liberate the selenium from the iron. Varying quantities of hydrogen sulphide gas were bubbled through the slurry which was observed to change colour. When the ash-atomise curves were repeated erratic results were obtained. This, together with the unpleasant nature of hydrogen sulphide, caused the termination of this work. Ammonium sulphide solution was also used but little advantage was observed.

Further experiments were conducted to determine the level of iron (as iron oxide in slurry form) that Smith-Hieftje background correction could tolerate at both the primary and secondary selenium wavelengths (196.0 and 204.0 nm). At the 196.0 nm line addition of iron oxide to 50 ng ml^{-1} selenium solution caused an initial enhancement of the signal up to 0.8% m/v iron oxide in the slurry, thereafter the signal decreased. The experiments were repeated at the less sensitive 204.0 nm wavelength and due to the lack of sensitivity, the selenium standard concentration was increased to 150 ng ml^{-1}, and various amounts of iron oxide added. The results indicated no interference from iron was observed at this wavelength, unfortunately this line is 5 times less sensitive and problems remained in coal analysis.

3.4.2 Use of air ashing

When dry powdered coal on a microboat, Figure 7, without the addition of any form of matrix modifiers was introduced into the graphite furnace, selenium absorption signals were observed. Not all the coals studied produced a signal. By introducing air, supplied by a cylinder, at the ashing stage a selenium signal was obtained from all the coals investigated.

FIGURE 7

Diagram showing sample boat in a rectangle cuvette
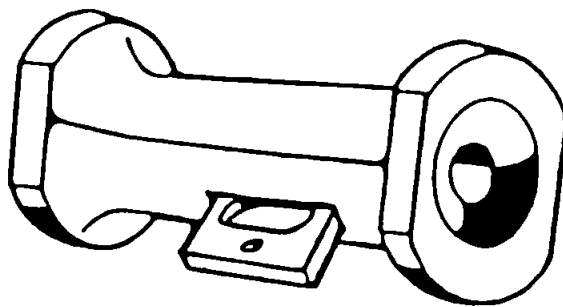
A simple procedure was employed using an air cylinder and a nitrogen cylinder connected to the gas supply of the furnace via a two-way switching valve. Using a flow of air during the ashing stage promoted more efficient ashing and markedly reduced the background levels observed in coal analysis, see Figures 8 and 9. Attempts were then made to convert this solid sampling technique to a slurry analysis procedure as slurries are simple to handle and can be micropipetted, which is more rapid than the use of a microbalance as required by the boat technique. Additionally it was intended to develop an aqueous solution calibration which is more suited to slurry analysis. Initially a slurry reagent was used which omitted nickel nitrate as this had seemed to aggravate the iron interferences observed above. Without nickel nitrate in the slurry no signals were obtained and this was attributed to premature loss of the selenium presumably as hydrogen selenide. When nickel nitrate was added to the slurry usable selenium signals were obtained.

3.5   OPTIMISATION STUDIES

The method was optimised principally by careful study of ash-atomise curves and the most successful programme is given in Table 8. The most significant advance achieved in the method development was considered to have been obtained by using air during the dry and ash stages. The compressed air was introduced into the furnace gas line via a switching valve. The programme commenced with air flowing through the furnace head and at the end of the ash stage the gas flow was switched manually to nitrogen. It became apparent that switching from one gas to another was a critical parameter. If air was present during the atomisation stage, a dramatically increased temperature in the furnace tube resulted, which led to rapid tube destruction. In order to avoid this situation, the nitrogen flow was always introduced before the atomisation cycle commenced. It would be possible to readily automate this switching using a pneumatic valve for routine analysis. It is believed that the air ashing confers two benefits. Firstly, the organic matrix of the coal is more readily

FIGURE 8

Atomisation profile of selenium in coal NBS SRM 1632(a) without air ashing
.... total signal; _____ corrected signal

Se-S
Abs 0.023
P/H 0.023
1.000

ABSORBANCE

TIME/s   ·8
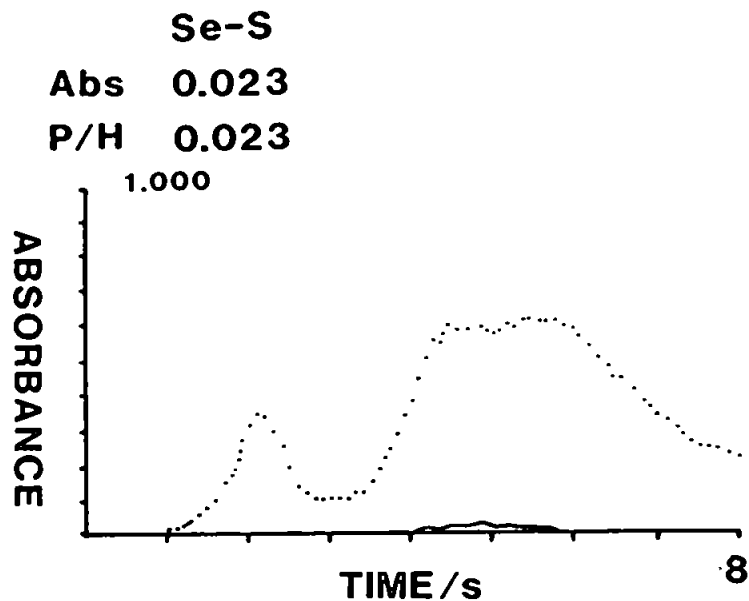
FIGURE 9

Atomisation profile of selenium in coal NBS SRM 1632(a) with air-ashing
.... total signal; _____ corrected signal

Se-S
Abs 0.103
P/H 0.062
1.000

ABSORBANCE

TIME/s   8
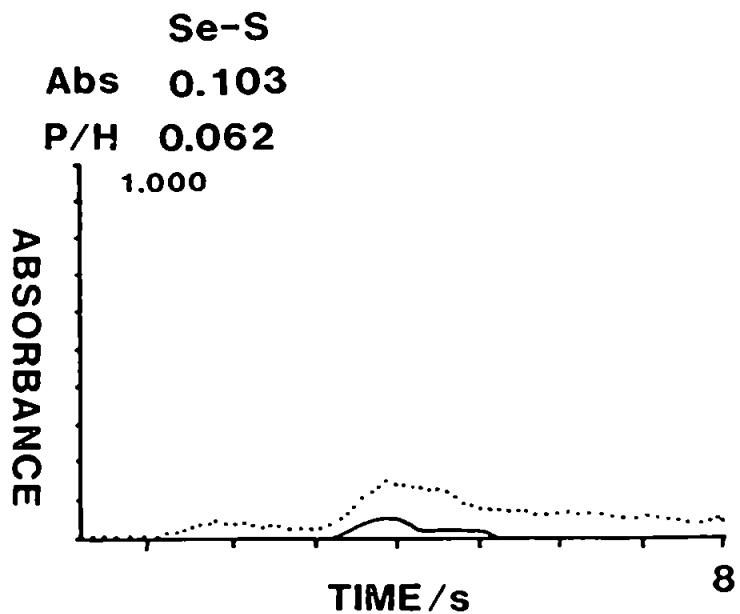
destroyed thereby lowering the overall background. Secondly, as the spectral interference is due to iron conversion of iron to iron oxide reduces the extent of the interference to a tolerable level for the Smith-Hieftje correction system.

3.6 EVALUATION OF METHOD

Varying amounts of coal were taken (0.5 - 2.0 g) and suspended with nickel nitrate, ethanol and water. The slurry was agitated to ensure homogenuity before introduction into the furnace. A detection limit (2σ) of 0.05 μg g^{-1} of selenium in coal was obtained using a 15% m/v slurry.

Selenium was determined in five certified reference material coals. The results are given in Table 9. For four of the coals good agreement was obtained with certified values. The exception being NBS SRM 1635, from which no signal was observed. The reason for this was unclear, especially as the Se:Fe ratio is similar to that for the other coals. More work is required to elucidate this problem fully. Meanwhile NBS SRM 1635 can be analysed using solid sampling and microboats as described above. In the proposed slurry method the furnace cycle time is in the order of three minutes which includes furnace cool time.

This method offers the advantages of slurry atomisation along with simple calibration using aqueous standards. The relative standard deviation is typically 5% at the 1 μg g^{-1} level.

3.7 CONCLUSION

Major problems may be encountered in the determination of selenium in coal slurries due to interference from iron. The use of continuum source background correction or the less sensitive 204.0 nm selenium line did not successfully eliminate problems. At the 204.0 nm line, there was reduced interference using Smith-Hieftje background correction, but this line did not prove sufficiently sensitive for coal analysis. Attempts to temporally separate the selenium and iron atomisation by means of matrix modification, addition of H_2O_2, H_2S and

TABLE 9

Determination of Se ($\mu g \ g^{-1}$) in reference coals by direct slurry
atomisation using Smith-Hieftje background correction at 196.0 nm

	Slurry ($\mu g \ g^{-1}$)	Cert Value ($\mu g \ g^{-1}$)
NBS SRM 1632(a)	2.1 $\pm$ 1.2	2.6 $\pm$ 0.7
NBS SRM 1635	<0.05	0.9 $\pm$ 0.3
BCR No 180	0.92 $\pm$ 0.10	1.32 $\pm$ 0.06
BCR No 181	1.14 $\pm$ 0.09	1.15 $\pm$ 0.05
BCR No 182	0.59 $\pm$ 0.06	0.68 $\pm$ 0.07

modification of furnace programme, proved unsuccessful. The introduction of air ashing in conjunction with Smith-Hieftje background correction and a carefully optimised furnace programme allowed the successful determination of selenium in coal slurries. This method offers the well known advantages of slurry atomisation which, in comparison to dissolution techniques, eliminates lengthy and contamination prone, sample preparation stages, thereby increasing the speed and accuracy of analysis.

CHAPTER 4

DETERMINATION OF CADMIUM AND ANTIMONY IN COAL SLURRIES BY ELECTROTHERMAL ATOMISATION ATOMIC ABSORPTION SPECTROSCOPY

4.1 INTRODUCTION

Cadmium is extremely toxic and accumulates in humans mainly in the kidneys and liver. Prolonged intake causes kidney disfunction and bone demineralisation and inhalation causes fibrosis of the lungs. Cadmium inhibits -SH containing enzymes by binding onto the -SH group of cystine residues as well as inhibiting the action of zinc enzymes by displacing the zinc. The major use of cadmium is as a protective coating in the electroplating industry, but this has been limited due to environmental concerns. It is also used in small quantities in alloys and batteries and can be used as a stabilizer in PVC to prevent degradation by heat or ultra violet radiation. Cadmium may reach the atmosphere through smelting, reclamation of steel scrap and incineration of plastics. The principle human intake of cadmium is either through the inhalation of dusty soils or through the food chain as a result of its uptake by edible plants (59). Typical amounts of cadmium ingested daily are between 20 and 50 µg of which 2 µg is retained. This is not excreted due to the extremely long half-life of cadmium in the body.

Antimony, found primarily in mineral ores, is derived principally from stibnite Sb_2S_3. The major use of antimony is in the production of antimonial lead for ⁝ use in storage batteries. The antimony content is usually 5% and imparts fluidity, creep resistance, fatigue strength, electrochemical stability and the minimisation of self-discharging of the negative electrode. Antimony enters the food chain as a result of leaching into surface and drinking waters, where the maximum admissible level is 10 ng ml^{-1} (181). Similarly to cadmium, antimony enters the environment through the smelting reclamation of scrap metal.

Both elements are present at trace levels in coal, typically less than 1 µgg^{-1}, and may be concentrated during energy conversion processes. There is therefore a need to establish methodologies for the routine monitoring of these volatile elements at trace levels in coal.

- 51 -

Antimony and cadmium in low concentrations have been frequently determined by spectrophotometric methods, but such methods are sometimes complicated by the need for extraction procedures to avoid interferences from other trace metals. The Rhodamine S method has been used for antimony in the 0.2 to 10 µg range (182) but is unsuitable for trace levels. Electrothermal atomisation atomic absorption spectroscopy is the technique routinely employed in modern laboratories for the determination of such elements owing to its sensitivity. Antimony has been determined by hydride generation atomic absorption or emission spectroscopy (183, 168, 139, 184) after reduction of antimony to stibine by sodium tetrahydroborate (111).

However, in order to generate the hydride, the coal must first be brought into solution, thus increasing the possible loss of the analyte during the dissolution procedure. This technique is limited to those elements which on reduction, form a volatile hydride to which group cadmium does not belong.

As with arsenic and selenium, the successful determination of antimony and cadmium depends on the prevention of analyte volatilization during the ash stage by the addition of matrix modifiers. Haynes (185) and Hamner et al. (186) used nickel nitrate as a volatilization suppressant for antimony. The resulting antimonide is more refractory and thus retained until the atomisation stage. Ediger (171) reported that cadmium in 1% nitric acid was stable below temperatures of 500°C and in order to utilise higher ashing temperatures, a matrix modifier would have to be used to render the cadmium less volatile. Ediger showed the effect by adding $(NH_4)_2S$, NH_4F, $(NH_4)_2 SO_4$ and $(NH_4)_2 HPO_4$ upon the cadmium volatility and concluded that ammonium phosphate was the most effective. He concluded that the ammonium salts of the desired anions seemed to have a greater stabilising effect than the addition of the corresponding acid.

The volatility of both antimony and cadmium create problems in their determination owing to losses encountered during ashing and digestion procedures. Thus the successful method described in CH2 and 3 for the determination of arsenic and selenium by the introduction of coal slurries into the electrothermal atomizer, has been developed further to enable determinations of antimony and cadmium, thereby eliminating problems of analyte loss associated with coal digestions.

4.2 EXPERIMENTAL

The IL Video 12 fitted with Smith Hieftje and deuterium-arc background correction systems and the Pye Unicam, SP-9 spectrometers were used for the determinations as previously described in section 2.3. Full operating details are given in Table 10 and Table 11.

4.3 CHEMICALS AND REAGENTS

Three certified reference material coals were analysed: sub-bituminous coal (NBS SRM 1632(a); National Bureau of Standards, Washington, DC, USA) and bituminous coal (NBS SRM 1635) and European coal (BCR No. 40; Community of Bureau of Reference, Brussels, Belgium).

All reagents used were of analytical-reagent grade (BDH Chemicals, Poole, Dorset, UK) and all solutions were prepared with doubly distilled, de-ionized water.

4.3.1 Stock Standard Solution

Stock 1000 mg l^{-1} cadmium solution was prepared by dissolving 2.7444g of cadmium nitrate $(Cd(NO_3)_2.4H_2O$ AnalaR grade) in 20 ml of concentrated nitric acid and then diluting to 1.000 l with deionized doubly distilled water, where upon the solution was stored in acid washed polyethylene bottles. Antimony solution (1000 mg l^{-1}) was obtained from BDH.

TABLE 10

Spectrometer and furnace operating conditions for cadmium

Video 12 instrument: furnace programme using pyrolytically coated cuvettes

	Dry		Ash		Atomise	
Time/s	10	35	40	40	0	10
Temperature/^{o}C	80	120	300	500	1300	1400
Gas flow-rate/l min^{-1}	7.0	7.0	7.0	2.5	2.5	2.5
Spectrometer parameters:						
Wavelength	228.8 nm					
Bandpass	1.0 nm					
Lamp current	2.5 mA					

SP-9 instrument: furnace programme using pyrolytically coated cuvettes

	Temperature/^{o}C	Hold time/s	Ramp
1. Dry	70	10	9
2. Dry	130	10	9
3. Ash	400	5	7
4. Ash	500	12	7
5. Atomise	1800	10	0
6. Clean	2500	2	0
Gas flow-rate	3 l min^{-1} during dry and ash stages		
	0.5 l min^{-1} during atomisation stage		
Spectrometer parameters:			
Wavelength	228.8 nm		
Band pass	1.0 nm		
Lamp current	6 mA		

TABLE 11

Spectrometer and furnace operating conditions for antimony

Video 12 instrument: furnace programme using pyrolytically coated cuvettes

	Dry		Ash		Atomise	
Time/s	5	30	30	40	5	10
Temperature/^{o}C	80	120	300	680	2100	2200
Gas flow-rate/l min^{-1}	7.0	7.0	7.0	2.5	2.5	2.5
Spectrometer parameters:						
Wavelength	217.6, 206.8 and 231.2					
Bandpass	1.0 nm					
Lamp current	2.5 mA					

Working standard solutions were prepared by taking various aliquots of the standard solutions and diluting with the slurry reagent solution.

4.4 SAMPLE PREPARATION

Coal was ground for 15-30 minutes so as to reduce the particle size. A McCrone micronising mill (McCrone RA Ltd., Belsize Lane, London) was used. Particle size measurements were made by the electrical zone sensing method (Coulter Counter TA II, Coulter Electronics, Luton, Beds).

Slurries for ETA-AAS were prepared by weighing an appropriate amount of finely ground coal into a 50 ml polyethylene screw-top container, adding 10 ml of slurry reagent (as described in section 2.5) omitting the $Ni(NO_3)_2$ for cadmium determinations and stirring magnetically for 5 minutes. For the analysis of antimony, $Ni(NO_3)_2$ was included as a matrix modifier. The amount of coal was chosen to give a concentration in the linear range of the appropriate calibration graph. Stirred slurry (10 μl) was pipetted into the furnace and absorption peak height or area was measured on each analysis which was performed in triplicate. The heating programme shown in Tables 10 and 11 were used for the IL 655 graphite furnace. Standardisation was achieved using aqueous calibrations.

4.5 RESULTS AND DISCUSSION FOR CADMIUM

Lengthy drying stages ensured even evaporation of the sample with no sputtering of the sample onto the walls of the cuvette.

The ash temperatures are higher than recommended in the IL handbook (187). This is due to the fact that at lower ash temperatures there is incomplete pyrolysis of the coal, but on increasing the temperature, complete pyrolysis is achieved. Ash atomise plots were performed with aqueous cadmium, which showed that cadmium was not lost at the slightly

higher ash temperature. The atomisation temperature 1300°C was chosen since it gave the highest peak height for both standards and sample. There was no apparent improvements in precision with peak area measurements in comparison to peak height measurements.

Successful determinations of cadmium were achieved using both deuterium arc and Smith-Hieftje background correction systems, with good agreement with the certified values in both cases, Table 12.

The above work was repeated on the SP-9 graphite furnace atomic absorption spectrometer (Pye Unicam), which has a more versatile deuterium background corrector as its modulation frequency is higher than that of the Video 12 (150 Hz cf 25 Hz). The furnace programme is described in Table 10. Again there was good correlation with the certified values, Table 13. There was improved precision using the SP-9 in comparison with the V.12. This was attributed to superior background correction for rapidly rising backgrounds. A significance test was conducted to determine whether the results from the V.12 were from a different population to those achieved from the SP-9. The test was performed using the means and concluded that at the 10% significance level, both sets of results originated from the same population.

4.6   RESULTS AND DISCUSSION FOR ANTIMONY

Initial slurries were prepared as for cadmium with the omission of nickel nitrate and the results were not in agreement with the certified values. As antimony is a relatively volatile element its loss can be expected during the ashing stage unless prevented by the addition of a matrix modifier. On the addition of nickel nitrate the results improved, see Table 14, owing to the prevention of early volatilisation of antimony during the dry and ash stages.

TABLE 12

Measured Cadmium Concentration (V.12)

	Cadmium/µg g^{-1}		
	1632(a)	1635	BCR 40
D_2	0.17 ± 0.02	0.03 ± 0.02	0.17 ± 0.03
S-H	0.19 ± 0.01	0.04 ± 0.01	0.11 ± 0.03
Certificate Value	0.17 ± 0.02	0.04 ± 0.01	0.11 ± 0.02

D_2 - Deuterium arc background correction

S-H - Smith-Hieftje background correction

TABLE 13

Measured Cadmium Concentrations (SP-9)

	Cadmium/µg g^{-1}	
	1632(a)	1635
Slurry	0.18 ± 0.01	0.03 ± 0.01
Certificate Value	0.17 ± 0.02	0.03 ± 0.01

TABLE 14

Determination of antimony (results in µg g^{-1}) in reference coal with nickel nitrate as matrix modifier

	1632(a) S-H	1632(a) D_2	1635 S-H
/nm			
217.6	0.9 ± 0.2	Negative peaks	0.14 ± 0.06
206.8	3.1 ± 0.2	4.5 ± 0.2	0.16 ± 0.04
231.2	Negative peaks	Negative peaks	0.08 ± 0.04
Certificate Value	(0.6)		(0.14)

S-H - Smith-Hieftje background corrector

D_2 - Deuterium background corrector

( ) - Uncertified results

Three different resonance lines were studied with the conclusion that the 217.6 nm line gave the best results. Interferences were present at the other two lines which led to overcorrection with the deuterium background corrector and at the 231.2 nm line overcorrection also occurred with the Smith-Hieftje system for NBS 1632(a). An example of overcorrection with the deuterium system is shown in Figure 10 whilst Figure 11 shows how Smith-Hieftje corrects for the same situation. Koizumi (188) has shown the existence of a direct spectral overlap interference of nickel upon the 231.2 nm antimony line. The nickel line is 0.05 nm away and the interferences were alleviated upon the use of Zeeman background correction.

In order to elucidate the cause of the interferences, standard solutions of antimony were spiked with nickel, aluminium and iron. These elements were selected as they are among the major constituents of the coal slurry. The results obtained showed that the most significant suppression of the antimony signal was caused by iron interference, Figure 12. Slavin and Carnrick (189) have listed some potential background overcorrection situations in ETA-AAS and they have included lead, copper, cobalt and iron as possible interferents at the 217.6 nm antimony line.

In a 10% slurry of 1632(a) the levels of Cu, Pb and Co are less than 2 μgg^{-1}, whereas the concentration of Fe in the same slurry, would exceed 1000 μgg^{-1}.

As iron is the most probable interferent, antimony solutions were spiked with 1% iron and analysed using the 217.6 nm line along with the alternative lines at 208.6 and 231.2 nm with both deuterium and Smith-Hieftje background correction systems.

Suppression, similar to Figure 12 was observed at all three wavelengths, regardless of which background correction system was employed. Niskavaara et al. (190) reported that when antimony was determined using the line at 217.6 nm, spectral interference caused by iron

FIGURE 10

Atomisation profile of antimony in coal NBS SRM 1632(a) using deuterium arc background correction at 208.6 nm

Sb-D

Abs -0.128

P/H -0.015
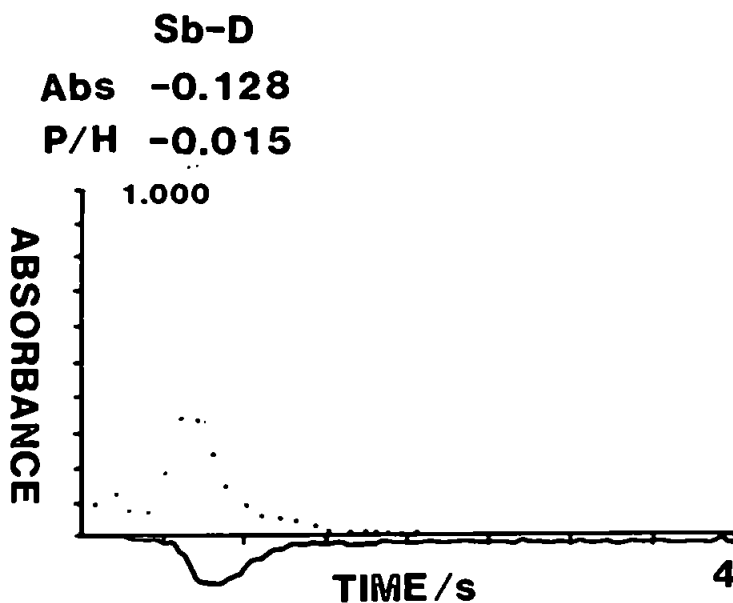
FIGURE 11

Atomisation profile of antimony in coal NBS SRM 1632(a) illustrating the successful use of Smith-Hieftje background correction at 208.6 nm

Sb-S

Abs 0.018

P/H 0.076
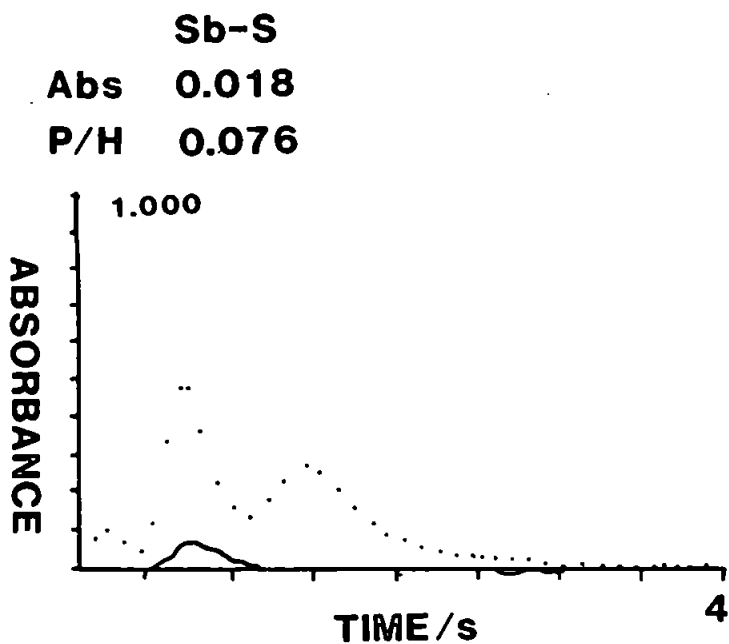
FIGURE 12

Diagrams illustrating the effect of 1% iron upon the atomisation profile of antimony

Sb-D

Abs   0.089

P/H   0.076
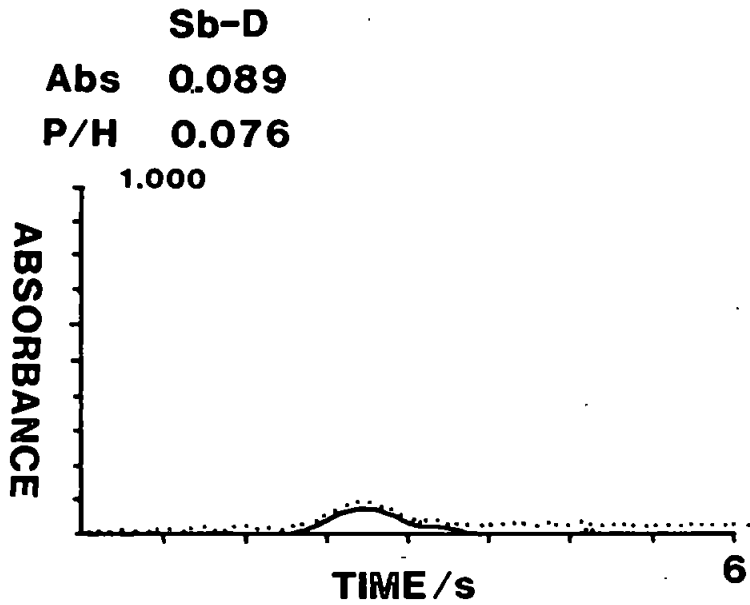
(a) Aqueous antimony (30 ng ml^{-1})

Sb-S

Abs   0.001

P/H   0.016
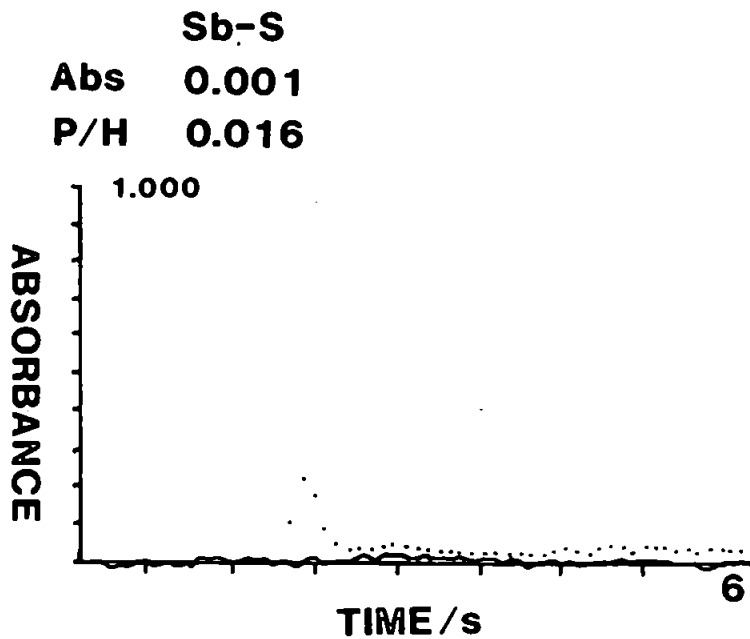
(b) Suppression due to addition of 1% iron with aqueous antimony (30 ng ml^{-1})

can be expected, which can be seen as an over-correction with a deuterium background corrector. This is in agreement with this work, where negative peaks were observed caused by over-correction of the deuterium corrector in the analysis of 1632(a) at the 217.6 nm line. However this interference is apparently eliminated with the use of Zeeman background correction (191) and the use of Smith-Hieftje background corrector in this study alleviated the problem, but the problem of slight under correction existed.

At the 231.2 nm wavelength there is a reported spectral interference by nickel (188) which although seen in this work, was not as significant as that caused by iron. However over-correction occurred producing negative peaks at this wavelength using both correction systems which rendered the 231.2 nm line unfavourable for antimony determinations.

The determination at 206.8 nm using both background correctors resulted in a high value for antimony in 1632(a) suggesting that both background correctors were under correcting for the interference which was present under the analytical conditions found at the 206.8 nm line. It is therefore recommended that for antimony determinations the 217.6 nm line be used as the interferences present at this line are corrected by Smith-Hieftje background correction.

4.7 CONCLUSION

The results obtained for cadmium determinations in 1632(a) and 1635, Tables 12 and 13, show good agreement with the certificate values. Despite reports that cadmium is lost above 400°C, ash-atomise plots showed that no cadmium was lost during the ashing stage up to 500°C and aqueous calibration yielded excellent results for the three certified coals.

Cadmium nitrate in 2% nitric acid was used to evaluate the ash-atomise plots and the results were in agreement with Ediger (171) and showed that up to 500°C no loss of cadmium was observed. Sturgeon et al. (192) have proposed that temperatures at which

cadmium vaporises is dependent on whether the metal is taken as the chloride or the nitrate. When taken as the nitrate, Cd $O_{(s)}$ is formed at the appearance temperature of the signal, 720 K, as a result of the thermal decomposition of the nitrate at 617 K. It may be preferable for routine analysis when the coal matrix may vary to add ammonium phosphate as matrix modifier as recommended by Ebdon and Lechotychi for slurry analysis (62).

The results obtained for antimony determinations in 1635, Table 14, show good agreement with the certified values with Smith-Hieftje background correction. This can be attributed to the lower levels of iron present in this sub-bituminous, lower ash coal, which enable the successful determination of antimony due to the tolerable amount of background which can be corrected for using the Smith-Hieftje correction system. Results were obtained for the analysis of 1632(a), but were not in such close agreement with the indicated value. This is presumably due to either the high ash content of this bituminous coal together with higher levels of iron and other major elements in comparison to 1635 or errors in the indicated, rather than certified, value.

Consequently antimony determinations were more successful in 1635 and would prove possible in coals with a low iron content.

CHAPTER 5

DETERMINATION OF MAJOR, MINOR AND TRACE ELEMENTS IN COAL

SLURRIES BY DIRECT CURRENT

PLASMA ATOMIC EMISSION SPECTROSCOPY

5.1 INTRODUCTION

The direct current plasma (DCP) is currently a popular and versatile source for excitation in atomic emission spectroscopy. It allows the introduction of sample into the base of the plasma via a 8mm i.d. injector tube. On expulsion from the injector, the sample is carried towards the high temperature plasma which offers a line-rich source with the capability of simultaneous multi-element determination. The long residence time of the sample in the excitation zone ensures sample matrix decomposition and thus avoids many of the problems associated with flame and electrothermal atomisation. The above mentioned advantages indicate that the DCP is a good source for the introduction of solid samples ie slurry atomisation and successful application of this technique using DCP have been shown by several workers (37, 125, 200).

This work describes the determination of major, minor and trace elements by slurry atomisation using DCP with its inherent advantages such as ease of sample introduction, high temperature source and long residence time.

5.2 DESCRIPTION OF EXCITATION SOURCE

The present configuration of the inverted 'Y'-shaped plasma has evolved from the d.c. plasma arcs and jets. A criterion of a plasma is to have a fraction of its atoms or molecules ionized and this is achieved in the DCP by a three electrode argon plasma, sustained between a single tungsten cathode and two graphite anodes (Figure 13). The result is an inverted 'Y', shaped plasma formed by argon flowing through the ceramic sleeves and around

- 65 -

FIGURE 13

Diagram of direct current plasma source
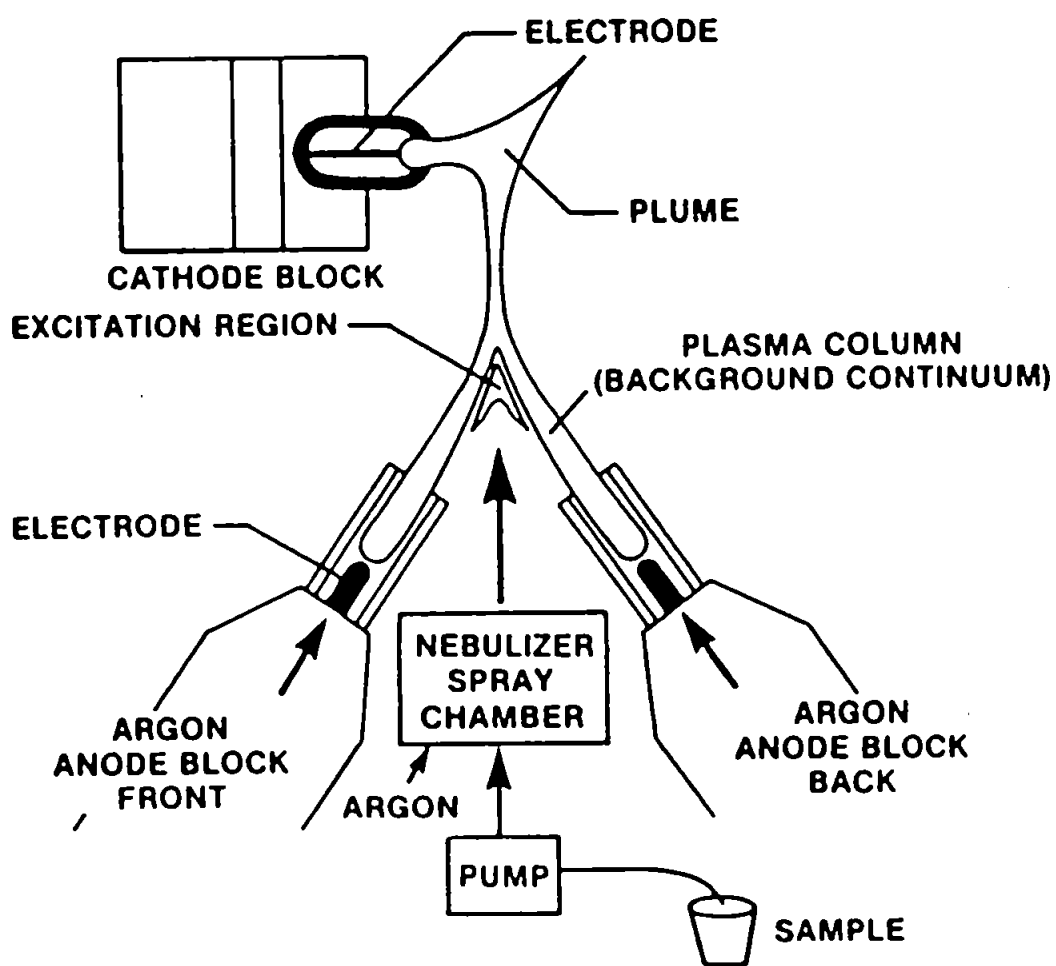
the electrodes. Once the plasma has been ignited, the electrodes withdraw into their normal analytical configuration thereby allowing sample introduction into the base of the inverted "Y". Sample introduction is via a ceramic nebulizer Figure 14, where argon acts as a carrier gas and sample is introduced via a peristatic pump normally at a rate of 1.5 ml min^{-1}.

The use of a high resolution Echelle monochromator in combination with the DCP offers precision and accuracy probably better or similar to flame emission along with improved detection limits for difficult to excite elements.

5.3 INSTRUMENTATION

The standard plasma jet from a Spectraspan III A DCP spectrometer, (ARL, Luton, Beds, UK) was used with the standard cross flow ceramic nebuliser together with a 0.75 m Echelle grating monochromator for wavelength separation. Instrument specification and typical operating conditions are given in Table 15 whilst plasma and nebuliser details are shown in Figure 13 and 14. Data collection was via the 0-10 V output from the dedicated on-board computer to a chart recorder (Lloyd Instruments, Brook Lane, Warsash, Southampton).

Particle size measurements were made using a Coulter counter TAII particle size analyzer (Coulter Electronics Ltd., Luton Bed., UK) fitted with a 140 μm sampling tube and a Malvern particle sizer (Malvern Instruments, Spring Lane, Malvern, UK). A practical and theoretical review of the former technique is given by Allen (193).

5.4 EMISSION ENHANCEMENT BY EASILY IONIZED ELEMENTS

Emission enhancement by easily ionized elements (EIE) is an inherent characteristic of the DCP, which has been reported by many workers (194-196). Models have been constructed in an attempt to explain why small concentrations of EIE can induce analyte emission enhancement. The early models all assumed that the plasma is in a state of local

FIGURE 14

Diagram of direct current plasma nebuliser
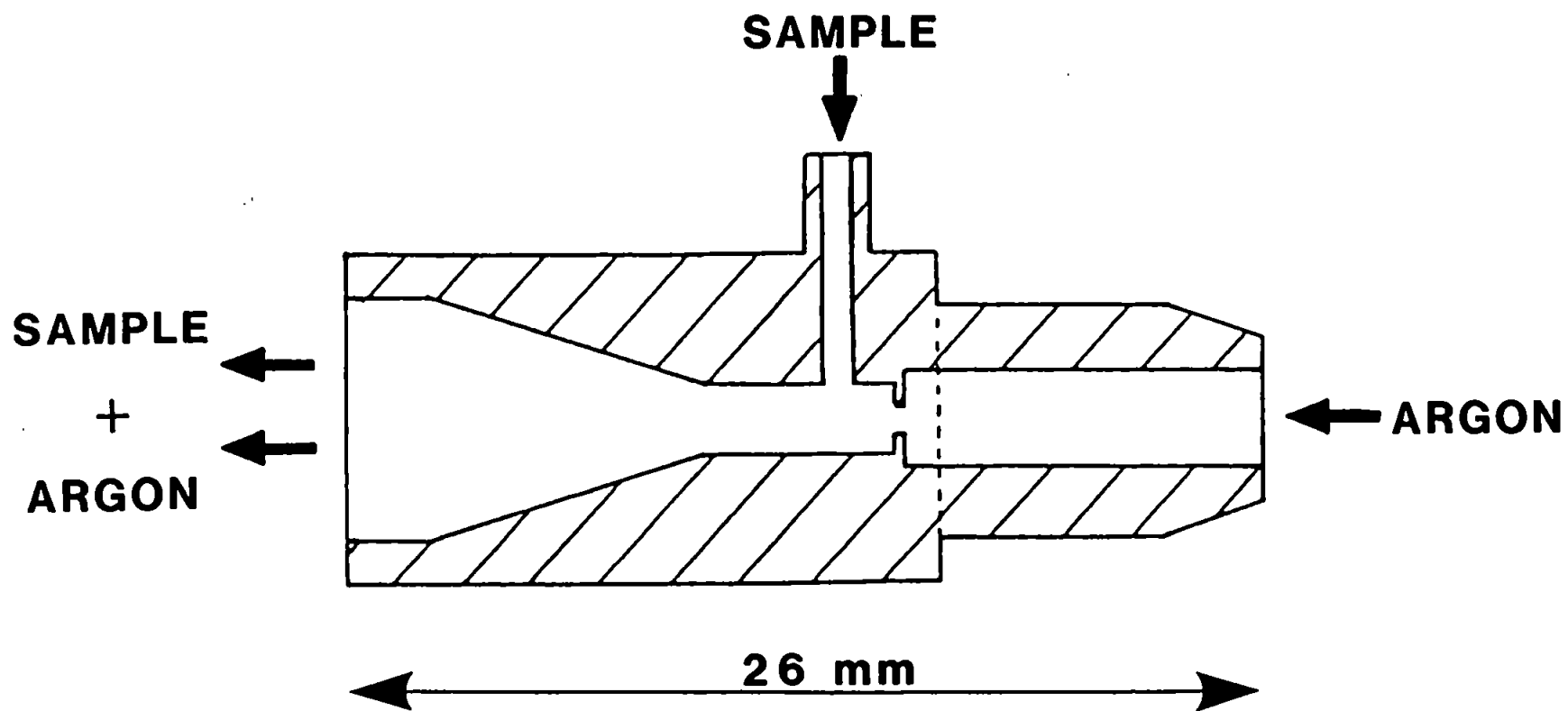
TABLE 15

Instrument specifications and Experimental Conditions

Excitation Source	Three-electrode direct current plasma. Two standard graphite electrodes and tungsten cathode
Running current/A	7
Gas supply	Argon
Nebuliser flow rate/l min^{-1}	4
Sleeve flow rate/l min^{-1}	4
Nebuliser pressure/psi	25
Sleeve pressure/psi	50
Nebuliser type	Cross flow
Sample pump rate/ml min^{-1}	1.6
Spectrometer	SpectraSpan IIIA (ARL, Luton, Beds, UK) high resolution echelle grating spectrometer (79 grooves/mm) with 30° prism for order separation. Spectral range 190-800 nm
Entrance slits/µm	Width: 50; Height: 200
Exit slits/µm	Width: 100; Height: 300
Detector	Hamamatsu R292
Integration time/s	10
No. of replicate readings	3

thermodynamic equilibrium (LTE). However this does not seem to be the case and theory predicts that the DCP analytical zone is a recombining plasma in a state of partial thermodynamic equilibrium (PTE).

The model proposed by Miller et al. (197), does not assume that the plasma is in a state of LTE. In their critical review, they proposed an excitation model based on radiative transfer and collisional redistribution/which argon resonance lines radiatively transferred away from high current, analyte poor, zones of the LTE plasma, to low-current sample rich areas of the PTE plasma and which was followed by collisional redistribution to analytes from radiatively-inverted first excited state argon populations. Additional features include the blanketing effect of the absorption lines in the analytical zone upon the resonance line emitted by the core of the plasma controlled by Stark broadening and proportional to the electron density (n_e). The n_e is dependant upon local radiation density and plasma composition.

Easily ionized elements (EIE) induced emission enhancement occurs via several methods. Firstly by creating additional channels for radiative transfer. Secondly the EIE acts as electron donors in the sample rich region and owing to the increased n_e, so the Stark broadening is increased as is the net energy flow to the outer zones. Thirdly the addition of EIE causes reduction in background emission owing to accelerated cooling of the plasma core, thereby reducing emission from the core, which at low EIE concentrations is offset by the improved outer zone absorption cross-sections, resulting in a net enhancement of the analyte line. Finally the excited EIE have a large cross-section thus allowing resonant collisional interaction with analyte species.

By spiking sample and standard matrices with EIE, such as lithium (5 gl^{-1}), two processes results:

1)   enhancement of atomic and ionic analyte lines, whilst molecular background is
     quenched;

2)   the lithium acts as a buffer against analyte enhancement by EIE naturally present in
     the samples.

In recent years an insight into analyte excitation and emission enhancement in the DCP has
been gained and methods for its control such as buffering with lithium have been
successfully applied.

5.5   IMPORTANCE OF PARTICLE SIZE IN SAMPLE PREPARATION

In a recent study, Gray (120) has shown that successful analysis of clays by slurry
atomisation ICP-AES, is dependant upon the size of the particles in suspension. It was
concluded that in order to avoid losses of material along the sample introduction system i.e.
spray chamber and injector tube, the size of the particles should not exceed 7 μm for
successful analysis using slurries with a 3.0 mm injector tube. Mohamed et al. (69) and
McCurdy et al. (37) working with DCP's have agreed that particle size is a critical
parameter in slurry atomisation. Sparkes (198) also using a DCP has confirmed that
reference soil particles of size > 8μm will not pass through the sample introduction system.
Therefore for successful slurry atomisation, the particle size of the coal should fall below 8
μm when using the DCP.

For a successful slurry, it is necessary to suspend powders in a liquid medium which is
achieved by the use of dispersants. A detailed theory of dispersion of powders is given by
Allen (193) who outlined three stages in the dispersion process. Initially there is a surface
wetting of the solid material, which is followed by a process of disaggregation of clusters of
particles and is finally followed by the stability of the resulting dispersion. Initial work used
alcohol as the wetting agent, but this did not result in evenly dispersed slurries. However
this problem was overcome by the use of Aerosol OT.

5.5.1 Grinding Procedure

The grinding method employed has been previously described (199, 200) and was achieved by weighing 1 g of coal into a 30 ml Nalgene bottle together with 10 g of zirconia beads (Glen Creston Ltd., Stanmore, Middlesex). An aqueous solution of Aerosol OT (BDH Chemicals Ltd., Poole, Dorset, UK) was added until the beads were just covered, typically 4 ml. The sealed bottle was shaken using a laboratory flask shaker (Gallenkamp, Loughborough, Leicestershire, U.K.), until such time that particle size had been sufficiently reduced. The slurries were washed into a volumetric flask through a Buchner funnel which separated grinding elements and allowed the slurry to be made up to the mark.

As small particles are required for successful atomisation, the grinding technique was investigated. In order to ascertain the optimum conditions for grinding, coals were ground for varying times, with differing concentrations of surfactant and were measured using a Malvern 2200/3300 particle sizer. The results are shown in Figure 15.

The graphical representation of the decrease in particle size with grinding time is shown in Figures 15a and 15b which indicate that a concentration of 0.1% Aerosol OT was preferred and that after three hours, no marked reduction in particle size was observed. It is often, however, convenient to grind the coals over night and depending upon the composition of the coal particle size of 2 µm or less can be achieved.

5.6 EXPERIMENTAL

The conditions for the direct current plasma and cross flow nebulizer are described in Table 15. Coal slurries were prepared as described in section 5.5.1. Aerosol OT was used as a surfactant in all slurry preparations at a concentration of 0.1% m/v so as to stabilise the suspension. Each slurry contained 10 ml lithium nitrate solution as 5 g l^{-1} Li enhancement

FIGURE 15a
GRAPH SHOWING THE EFFECT OF GRINDING TIME
UPON PARTICLE SIZE USING 1.0% AEROSOL OT

- 73 -
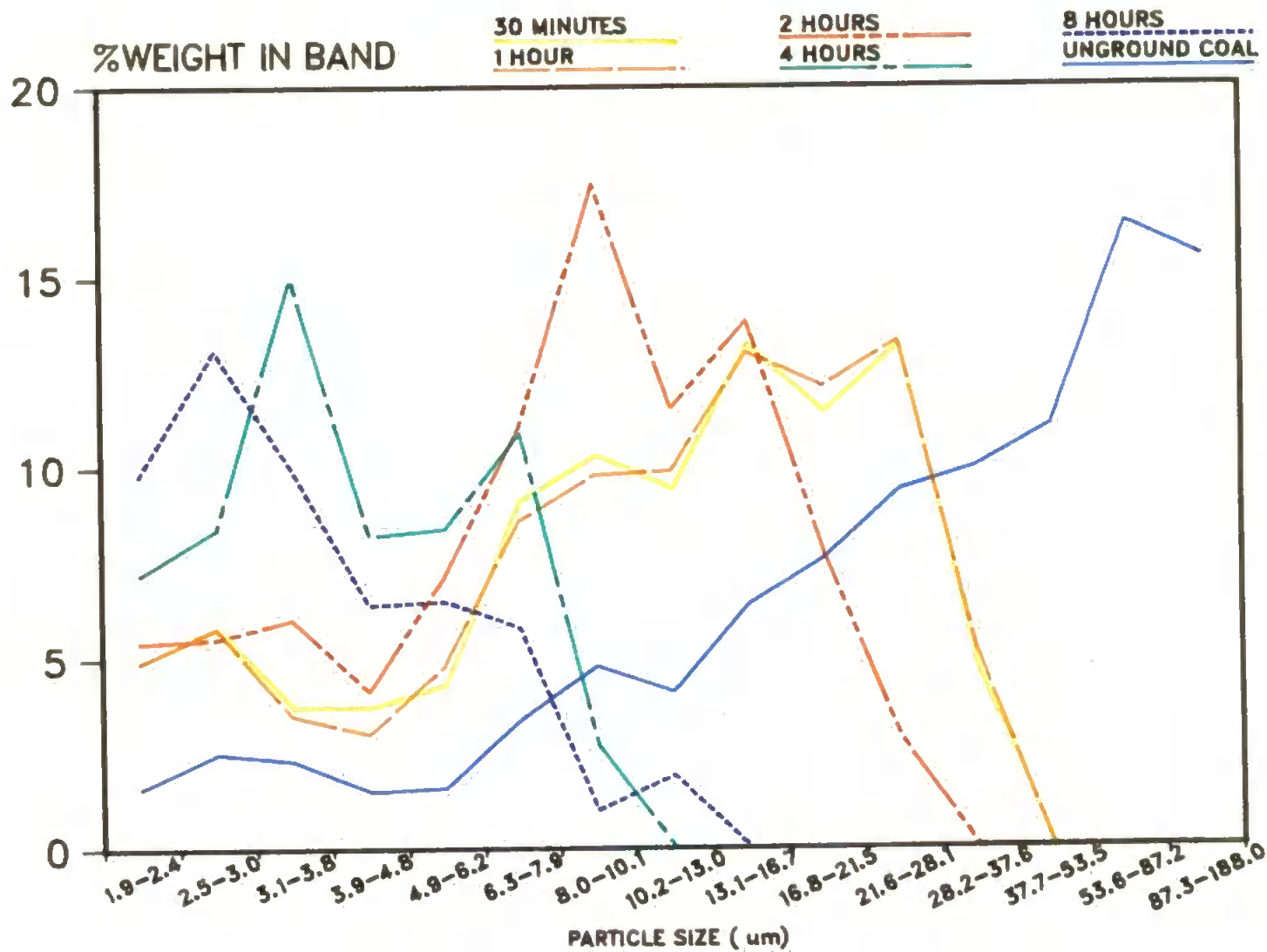
FIGURE 15b
GRAPH SHOWING THE EFFECT OF GRINDING TIME
UPON PARTICLE SIZE USING 0.1% AEROSOL OT
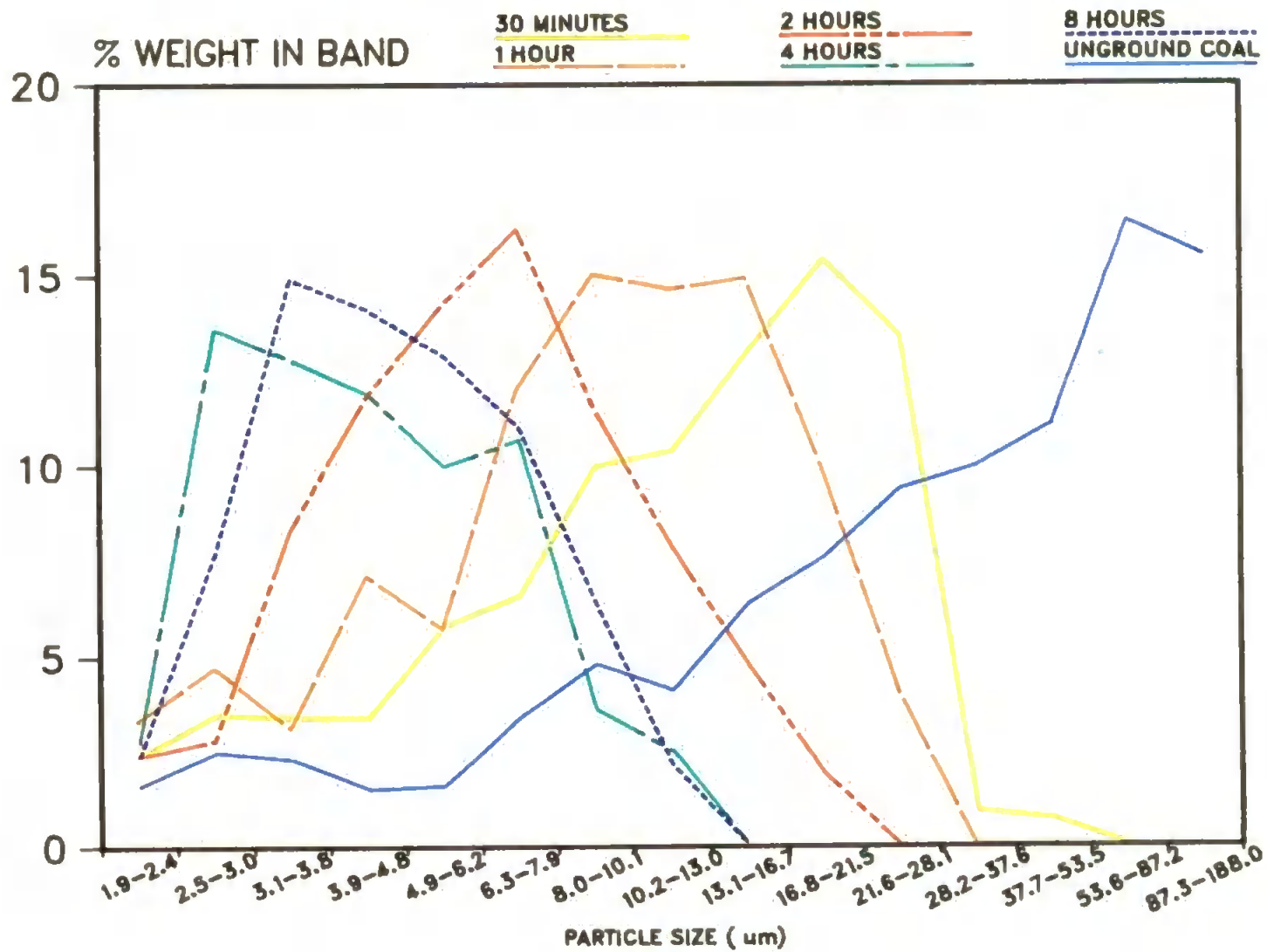
buffer. This was prepared from a stock Li solution (40 g litre Li) by dissolving 213 g of lithium carbonate (BDH Chemicals, Poole, Dorset, UK) in 250 ml of concentrated nitric acid and diluting this to 1 litre.

Five certified reference material coals were analysed: bituminous coal (NBS 1632(a) National Bureau of Standards, Washington, DC, USA), sub-bituminous coal (NBS SRM 1635), gas coal (BCR No. 180, Community Bureau of Reference, Brussels, Belgium), coking coal (BCR No. 181) and steam coal (BCR No. 182). Aliquots of all slurries were reserved for laser diffraction particle size analysis.

5.7   RESULTS AND DISCUSSION

Particle size distribution for slurries of reference coals NBS 1632(a) and 1635 and BCR 180, 181 and 182 prepared as described above are shown in Figures 16-20. For 1632(a), 100% of the particles were less than 21 μm, whilst 70% were less than 10 μm. The particles in 1635 slurry were 100% below 10 μm for the same grinding conditions, while for BCR 180, 181 and 182, 100% of the particles fell below 16 μm.

Table 16 shows the preliminary values obtained for the analysis of bituminous and sub-bitumous coals by the slurry atomisation DCP-AES method. Calibration was by aqueous standards, matched with 5 g l^{-1} lithium and the results obtained show excellent agreement with the certificate values.

The results show atomisation efficiency approaching 100% using the definition of atomisation of efficiency proposed by Willis (44) as "the ratio of the concentration of free atoms of the analyte in the flame (plasma) when a suspension of particles is sprayed to the concentration in the same part of the flame (plasma) when the same amount of analyte is sprayed as solution". Simplified it refers to the net slurry signal compared to the net signal obtained from a solution of equivalent concentration.

FIGURE 16

Particle size distribution of coal NBS SRM 1632(a)
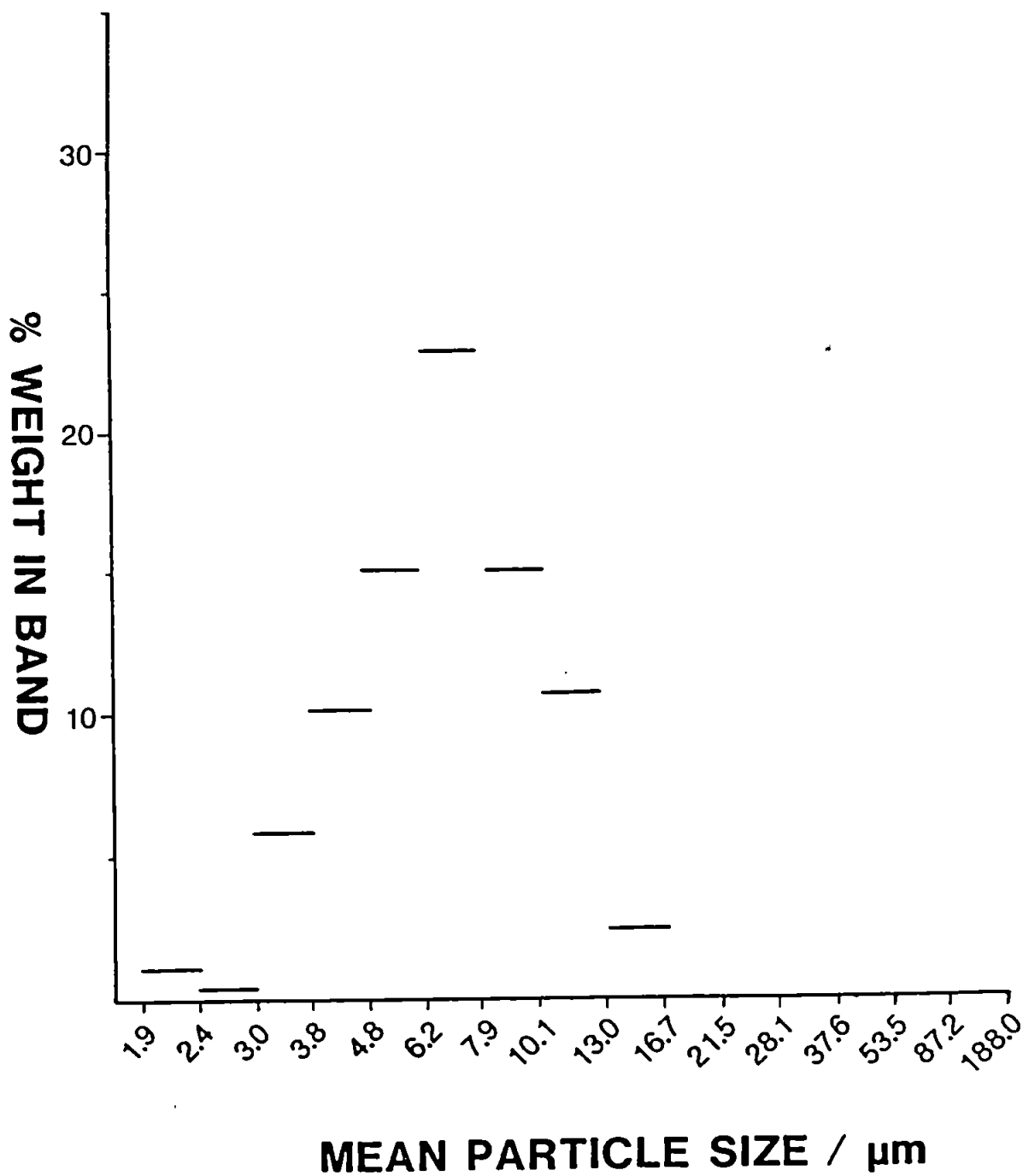
FIGURE 17

Particle size distribution of coal NBS SRM 1635

MEAN PARTICLE SIZE / μm
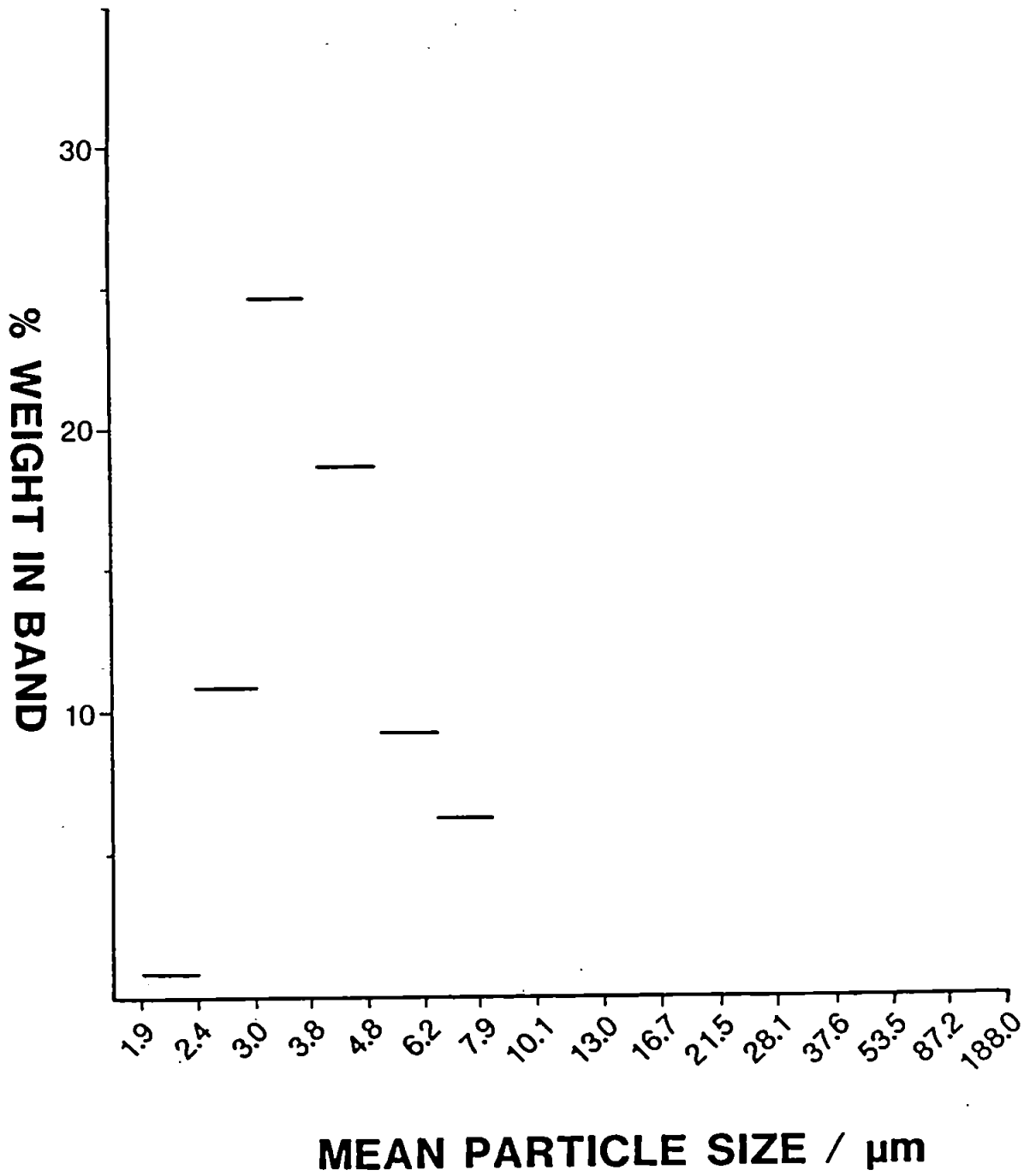
FIGURE 18

Particle size distribution of coal BCR 180
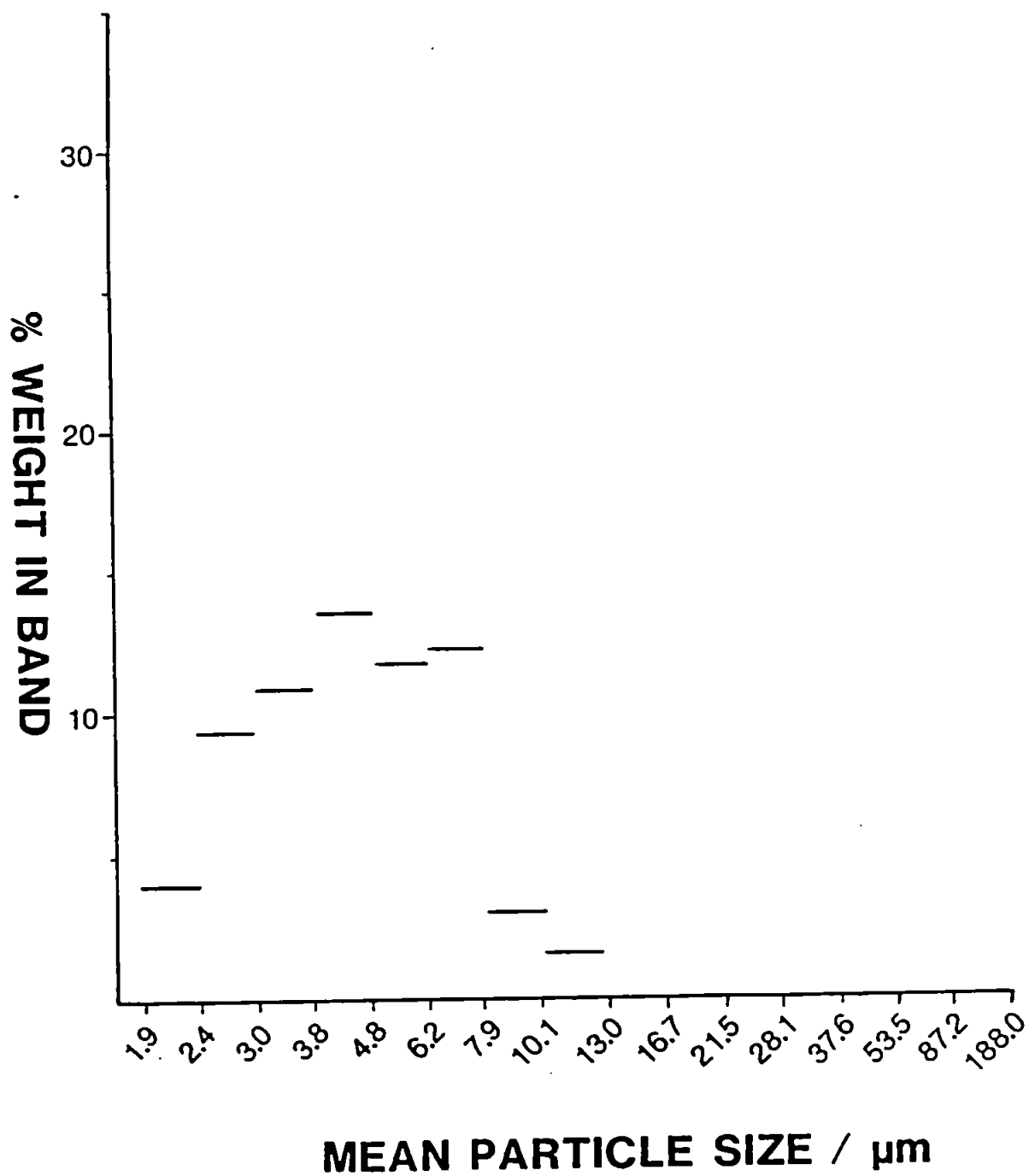
FIGURE 19

Particle size distribution of coal BCR 181
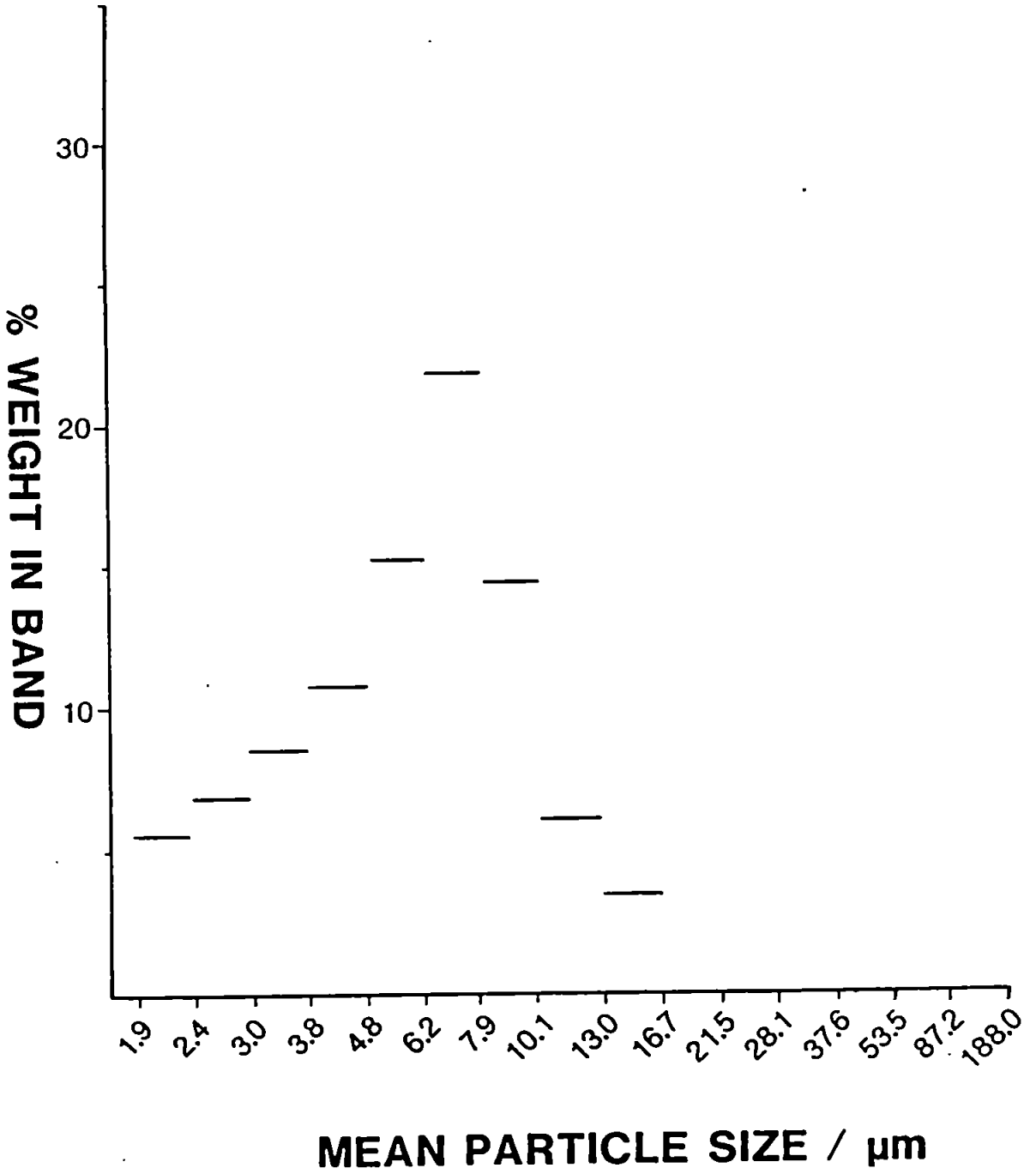
FIGURE 20

Particle size distribution of coal BCR 182

MEAN PARTICLE SIZE / µm
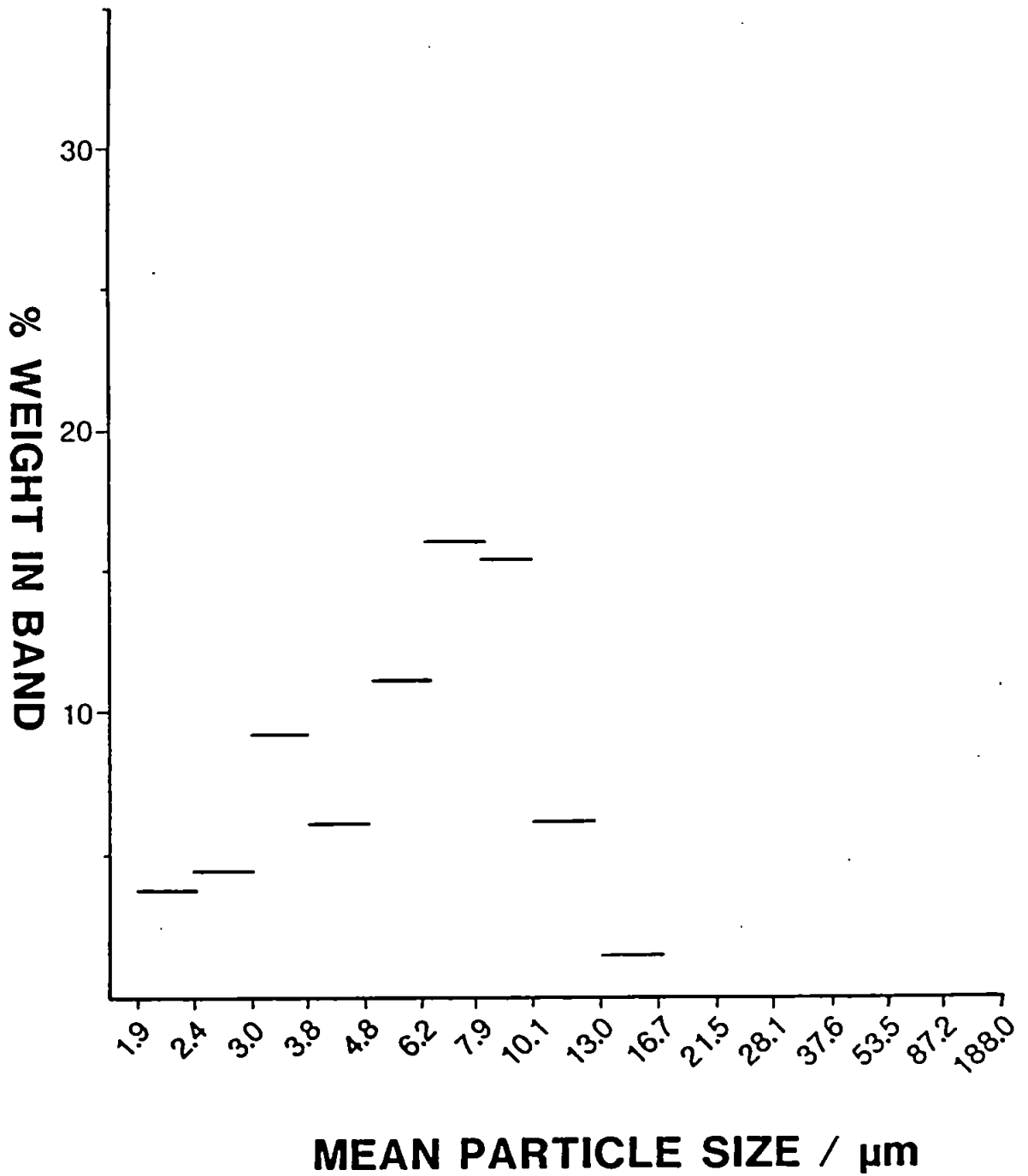
TABLE 16

Determination of trace elements in ground NBS 1632(a) and NBS 1635 coals by slurry atomisation.

NBS SRM 1632(a)		
Element	Slurry atomisation $\mu g\ g^{-1}$	Certificate Value $\mu g\ g^{-1}$
Cr	37.7 $\pm$ 2.0	34.4 $\pm$ 1.5
Cu	17.2 $\pm$ 1.5	16.5 $\pm$ 1.0
Zn	27.5 $\pm$ 2.0	28.0 $\pm$ 2

NBS SRM 1635		
Element	Slurry atomisation $\mu g\ g^{-1}$	Certificate Value $\mu g\ g^{-1}$
Cr	2.3 $\pm$ 0.3	2.5 $\pm$ 0.3
Cu	3.5 $\pm$ 0.5	3.6 $\pm$ 0.3
Zn	3.9 $\pm$ 0.2	4.7 $\pm$ 0.5

Following these initial experiments, major, minor and trace elements in both coals were determined, once again using aqueous calibration and as can be seen from Tables 17 and 18 good agreement exists between the slurry results and the certified values.

The atomisation of the major elements fall between 80 and 103% with the exception for aluminium. The atomisation efficiency for aluminium is 72% which can be explained by the incomplete decomposition by the plasma of thermally stable aluminium - oxygen species. Complete decomposition of the coal matrix can be assumed by the high atomisation and other elements, which suggests efficiency of silicon that the DCP temperature is insufficiently high to completely destroy the aluminium oxide matrix. The results for the determination of B, Si, Ni and Mn are shown in Tables 19 and 20 but with the exception of Mn for BCR 180 and 182 certified values of these elements do not exist.

5.8 CONCLUSION

Thirteen major, minor and trace elements have been successfully determined by slurry atomisation using the DCP and the results are generally in excellent agreement with the certificate values. Particle size analysis has shown all particles are below 21 μm with the majority below 16 μm and in the case of 1635 below 10 μm. McCurdy (37) reported that particles as large as 23 μm were able to pass through the spray chamber and into the plasma yielding results by slurry atomisation with a relative standard deviation (RSD) of 6%. Results obtained in this study are in agreement with his conclusion. Thus the rugged design of the spray chamber and nebuliser appears to enable coal particles between 21 μm and 23 μm to reach the plasma for successful atomisation.

TABLE 17

Major, minor and trace elements in ground NBS 1632(a) coal.

NBS SRM 1632(a)		
Element	Slurry atomisation % m/v	Certificate Value % m/v
Al	2.23 + 0.02	(3.1)
Fe	1.08 + 0.01	1.11 + 0.02
Ti	0.15 + 0.01	(0.18)
Ca	0.22 + 0.01	0.23 + 0.03
Si	6.10 + 0.06	5.9 + 0.2
Mg	0.08 + 0.01	(0.1)

Element	Slurry atomisation $\mu g\ g^{-1}$	Certificate Value $\mu g\ g^{-1}$
Na	1078 + 30	840 + 40
Ba	130 + 8	130[*]
V	41.4 + 1.5	44 + 3

values indicated by ( ) represent uncertified values.

[*] values reported by Gladney. (201)

TABLE 18

Major, minor and trace levels in ground NBS 1635 coal.

NBS SRM 1635		
Element	Slurry atomisation % m/v	Certificate Value % m/v
Al	0.900 ± 0.003	(0.32)
Fe	0.200 ± 0.007	0.239 ± 0.005
Ca	0.43 ± 0.04	0.56 ± 0.02
Si	0.54 ± 0.01	0.64 ± 0.13
Mg	0.08 ± 0.01	0.09*

Element	Slurry atomisation $\mu g\ g^{-1}$	Certificate Value $\mu g\ g^{-1}$
Na	2200 ± 20	(2400)
Ba	88 ± 11	84*
Ti	190 ± 10	(200)
V	5.9 ± 0.4	5.2 ± 0.5

Values indicated by ( ) represent uncertified values.

* Values reported by Gladney (201).

TABLE 19

Determination of boron, manganese, strontium, titanium and nickel in reference coals BCR 180, BCR 181 and BCR 182 by slurry atomisation.

Element	BCR 180		BCR 181		BCR 182	
	Slurry $\mu g\ g^{-1}$	Certificate $\mu g\ g^{-1}$	Slurry $\mu g\ g^{-1}$	Certificate $\mu g\ g^{-1}$	Slurry $\mu g\ g^{-1}$	Certificate $\mu g\ g^{-1}$
B	75.00		15.00		45.00	
Mn	20.3	34.3 ± 1.1	2.3		97.2	195 ± 6
Sr	50.0		6.3		14.2	
Ni	50.0		96.7		36.8	

TABLE 20

Determination of boron, manganese, strontium & nickel in reference cards NBS 1632(a) and NBS 1635.

Element	NBS 1632(a)		NBS 1635	
	Slurry $\mu g\ g^{-1}$	Certificate $\mu g\ g^{-1}$	Slurry $\mu g\ g^{-1}$	Certificate $\mu g\ g^{-1}$
B	111 $\pm$ 3	53[*]	135 $\pm$ 5	105[*]
Mn	28.0 $\pm$ 1	28 $\pm$ 2	20.5 $\pm$ 1	21.4 $\pm$ 1.5
Sr	72.5 $\pm$ 4	88[*]	96.6 $\pm$ 1	140[*]
Ni	125.2 $\pm$ 7	19.4 $\pm$ 1	104.6 $\pm$ 5	1.74 $\pm$ 0.1

*   Values reported by Gladney (201).

These preliminary results have shown the DCP to be an excellent excitation source for coal analysis and highlights the advantages of minimal sample preparation and aqueous calibration which enable successful slurry analysis with precision 2% (RSD) or less. This form of solid sampling can be seen to enjoy the sensitivity, precision and convenience normally associated with aqueous samples.

CHAPTER 6

DETERMINATION OF MAJOR, MINOR AND TRACE ELEMENTS

IN COAL SLURRIES BY INDUCTIVELY COUPLED PLASMA -

ATOMIC EMISSION SPECTROSCOPY

6.1 INTRODUCTION

Inductively coupled plasma atomic emission spectroscopy (ICP-AES) has grown rapidly in its

popularity since its conception as a spectroscopic source in the early 1960's as first reported

by Greenfield et al. (31). Its advantages of high temperature, long linear working range and

detection limits in the ngg^{-1} region have led to the various applications of ICP-AES in the

determinations of major, minor and trace elements in a variety of matrices including rocks

(46) sediments (202) and coal ash (33).

The potential of ICP-AES has been recognised for solids analysis and one method of

introducing solids into the ICP is slurry nebulisation where the solid is suspended in a liquid

medium. Ebdon and Wilkinson (35) have used this technique to analyse coal slurry directly

sprayed into the plasma, whilst McCurdy and Fry (203) have determined sulphur in coal

slurries by ICP-AES.

This work describes the development of methodology for the analysis of coal samples using

direct slurry atomisation into an inductively coupled plasma. A brief description of the ICP-

AES is presented here, but more theoretical and detailed reviews have been presented by

Sharp (99) and Thompson and Walsh (204).

6.1.1 Plasma description

The ICP is a hot ionized gas with a temperature of 4000-10,000K. It is sustained in a quartz tube which consists of three accurately aligned concentric tubes of silica glass, the outermost being encircled by a three turn water-cooled induction coil. A schematic diagram of the plasma torch showing the three separate gas flows is shown in Figure 21. The outer or coolant gas flow is introduced tangentially and prevents the plasma from melting the torch. The plasma gas which is also introduced tangentially, sustains and propagates the plasma, whilst the nebulizer gas transports the sample aerosol to the plasma.

The induction coil is coupled to a r.f. generator typically producing a few kilowatts at 27.12 MHz thus producing an alternating magnetic field in the coil. To initiate a plasma, the gas is ionized so as to make it electrically conductive, by providing a "seed" of electrons from a Tesla spark. The alternating magnetic field accelerates these electrons in a torroidal path enabling them to gain sufficient energy to ionize the argon, thus creating more electrons. Due to the continual application of the radio frequency, the plasma becomes self-sustaining.

The sample once introduced into the plasma is confined to the cooler central channel which is heated by the surrounding plasma. The background continuum in the plasma fireball is intense and for analytical purposes it is necessary to view the spectrum at some point in the tail flame where the background is low but the temperatures are high enough to prevent recombination of atoms. Owing to the cooler nature of the axial channel in comparison with the surrounding plasma problems such as self-absorption and self-reversal, which are characteristic of arcs and flames, are avoided as the plasma behaves as an optically thin source. This phenomenon results in the large linear dynamic working ranges observed as well as freedom from chemical interference.

The sample is normally introduced via a nebuliser which generates an aerosol of fine droplets. The aerosol then enters a spray chamber whose primary function is to remove large droplets to prevent them entering the plasma. Once in the plasma the sample is atomised and the emitted light is resolved into its component radiation by means of a diffraction grating, then measured with a photomultiplier tube, which converts the electromagnetic radiation into electrical signals that can be measured quantitatively.

Depending on the type of spectrometer installed in the instrumentation, two modes of analysis can be performed i.e. simultaneous or sequential. The former relies on a polychromator, whilst the latter requires a scanning monochromator. The basic difference between the two systems is that the polychromator measures all the lines simultaneously, whilst the scanning monochromator measures one element after another, thus allowing an unrestricted choice of wavelengths to be measured, but requiring more time for analysis. Scanning monochromators were introduced so as to reduce the cost of the ICP instrumentation in comparison with a polychromator system. The monochomator system also gives increased flexibility, as unlimited lines may be used, which allow problems such as matrix effects and spectral overlap to be alleviated.

6.2 INSTRUMENTION

In this study two commercially available plasma emission spectrometers were used. The two instruments Plasmakon S-35, (Konton Spectroanalytic, Eching, West Germany) and ARL 3520, (ARL, Luton, Beds, UK) both of sequential design are briefly described in Section 6.2.1. and 6.2.2. respectively.

6.2.1 Kontron Plasmakon S-35

A schematic diagram of this instrumentation is shown in Figure 21.

Interface
(analog – digital)

Computer with
associated software

VDU

Teletype

PM
Tube

Mirrors

Plasma

Czerny – Turner Monochromator

Grating fixed
to angle encoder

Periscopic
arrangement

RF
Generator

Argon

Massflow
Controllers

Pump , nebuliser
and double – pass
spray chamber

Sample

Drain
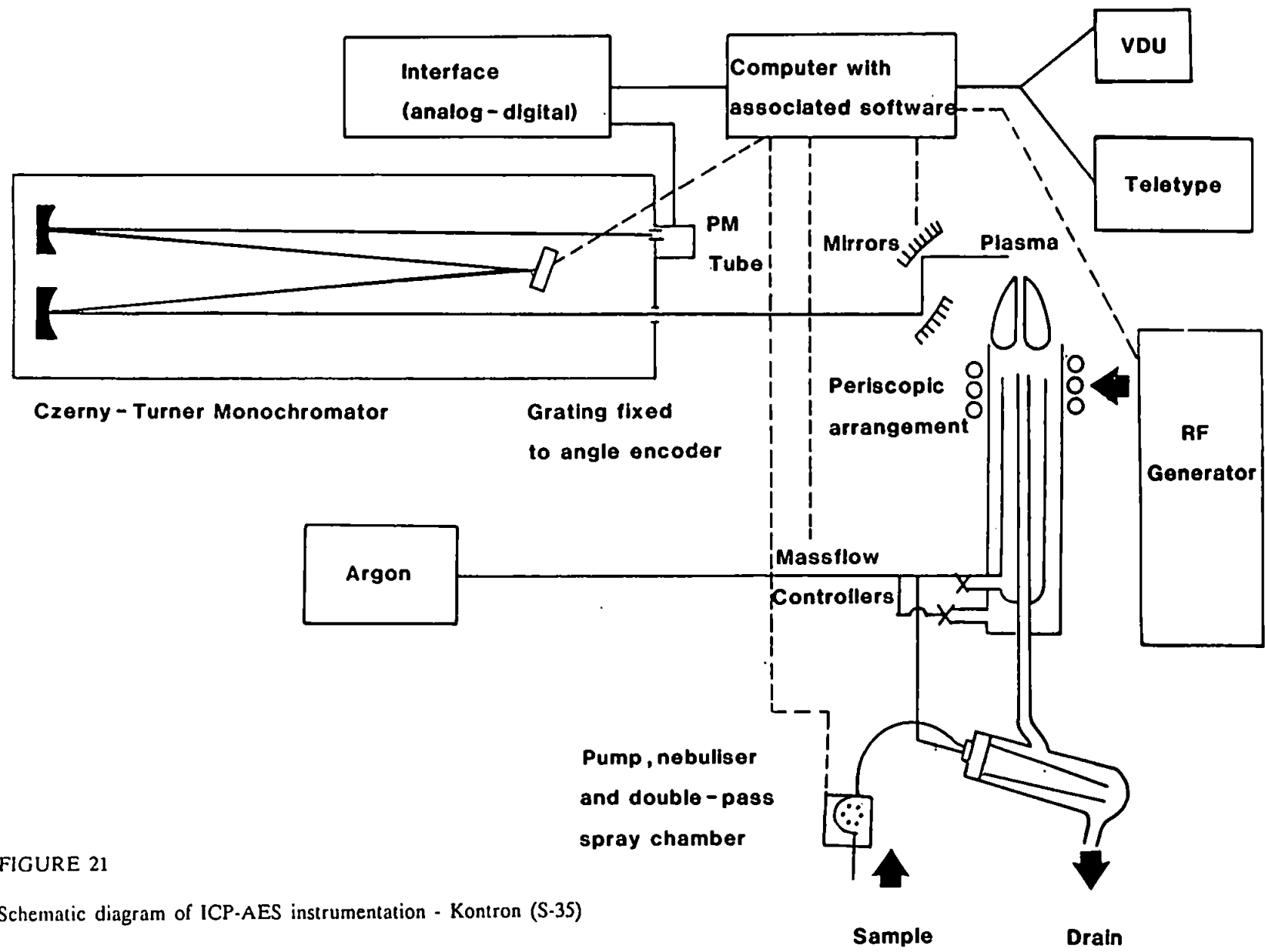
FIGURE 21

Schematic diagram of ICP-AES instrumentation - Kontron (S-35)

The 27.12 MHz crystal controlled radio frequency generator supplies a maximum power of 3.5 kW to the four turn water cooled induction coil via a motor-driven automatic tuning circuit. The semi-demountable torch which is of the Greenfield type is concentrically mounted in a PTFE/glass fibre (60:40) base, Figure 22. The dimensions of the one-piece quartz coolant and auxiliary body are 29 mm OD and 25 mm OD respectively. The separate 3 mm injector is located in the removable two- part base.

The sample is introduced as an aerosol generated from a Babington-type high solids nebuliser and is carried to the plasma, via an in-house constructed double pass spray chamber by the argon injector gas. The argon flow is regulated by three mass flow controllers, which once the automatic start-up procedure has been initiated, come under manual control along with the r.f. power generator.

Emission from the plasma enters the entrance slit of the monochomator via a computer controlled periscope arrangement which allows the accurate adjustment of the viewing zone, which extends 60 mm above the top of the induction coil. The 0.6 metre Czerny-Turner monochromator is under computer control, this ensures the precise selection of wavelengths to within 0.0015 nm by use of an angle encoder. The selected wavelength passes through the exit slit where its intensity is measured by a photomultiplier (Thorne-EMI 9781A). A wide range of intensities can be measured by stepping the supply voltage to the photomultiplier.

Signals from the photomultiplier are collected and processed by the Z-80A on-board microprocessor which also controls the monochromator drive, periscope viewing position and photomultiplier voltage. It also performs mathematical and statistical calculations of the data collected from the photomultiplier which allow line calibration etc. The information is provided either visually on a monitor or on a dot-matrix printer.

FIGURE 22

Diagram of Greenfield type inductively coupled plasma torch

COOLANT
GAS

AUXILIARY
GAS

INJECTOR GAS
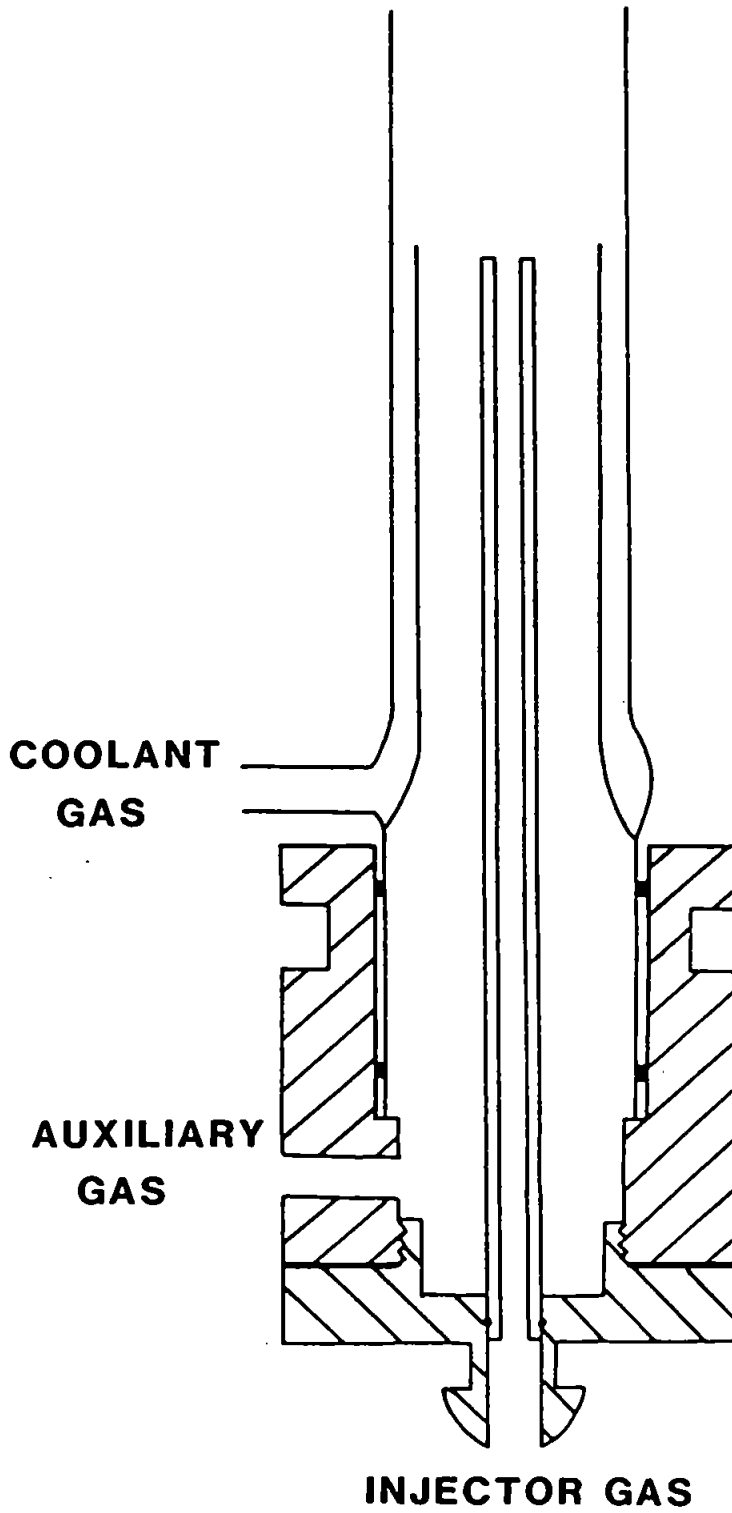
6.2.2 ARL 3520 ICP

The ARL 3520 is also a sequential instrument. A schematic diagram is shown in Figure 23. The 2.5 kW maximum, 27.12 MHz r.f. generator (Henry Radio, California, USA) supplies power to the three turn water cooled load coil. The torch, which is of the "Fassel" type is constructed in quartz with a coolant tube of 20 mm OD and a 'tulip' design auxiliary tube. The one piece torch includes a 1.8 mm i.d. injector. The injector bore can be increased by using a two piece demountable torch.

The instrument is fitted as standard with a glass concentric pneumatic nebuliser (J.E. Meinhard Associates, California, USA) which was replaced for this work by a high-solids nebuliser (Ebdon Nebuliser, P.S. Analytical, Arthur House, Orpington, Kent, UK). The generated aerosol passed to the injector via a single pass spray chamber fitted with an impactor bead, which not only removes the larger droplets, but may also generate more smaller droplets by secondary fragmentation.

Wavelength selection is achieved with a 1 metre grating monochromator based on the Paschen-Runge geometry. Both the primary slit which is 20 μm wide and 4 mm high, and grating (1080 lines mm^{-1}) lie on the "Rowland Circle" which causes the diffracted spectral lines also to come to a focus on the circle for detection by a scanning photomultiplier behind the secondary slits (Figure 23). The dispersion for this monochromator is 0.92 nm mm^{-1} in first order. The collected signals from the photomultiplier are processed by a PDP 11/23 digital processor unit.

6.2.3 Nebulisers

A nebuliser is a device for transforming a solution into an aerosol. The so-called Ebdon nebuliser, used in this work, is a V-groove nebuliser based on the Babington design, as reported by Cave and Ebdon (205) shown in Figure 24 which is ideally suited for the analysis of slurries owing to its main advantage of being unblockable. The main body of the

FIGURE 23

Schematic diagram of ICP-AES instrumentation - ARL 3520
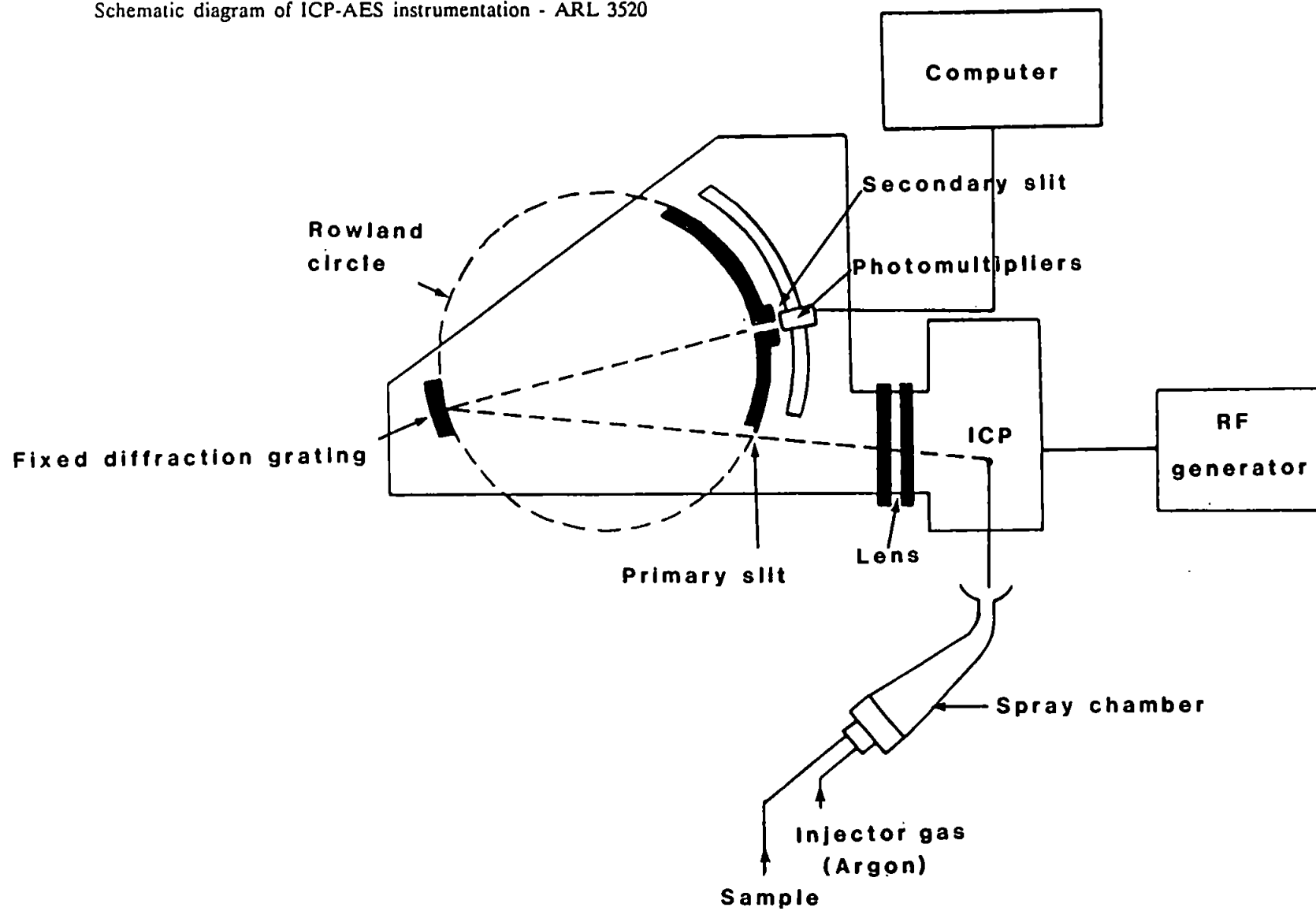
FIGURE 24

Diagram of the Babington type Ebdon nebuliser
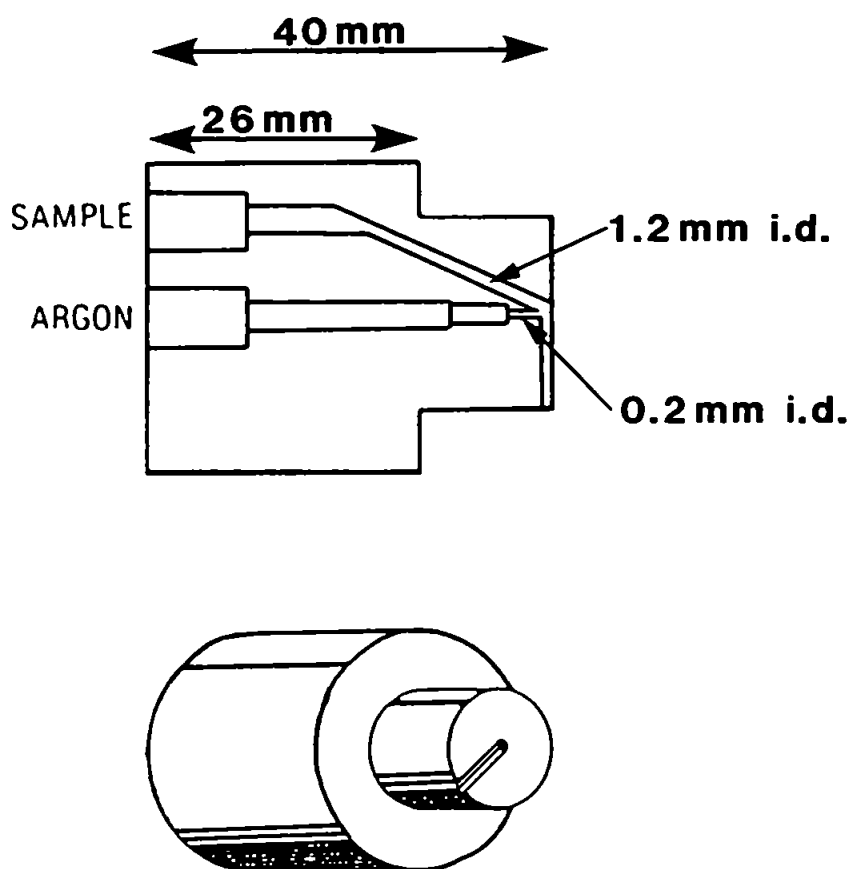
nebuliser is constructed from either PTFE or KEL-F and contains two threaded holes both ending in orifi. The slurry is pumped along the uppermost channel through the sample orifice (1.2 mm diameter) into a V-groove which is cut into the face of the nebuliser. In flowing down the groove, the slurry flows over the gas orifice (0.2mm diameter) from which the argon gas emerges at a high velocity thereby producing an aerosol which is swept into the plasma.

6.2.4 Simplex Optimisation

Simplex optimisation is a method of optimising all operating parameters simultaneously. The technique was first described by Spendly et al. (206) and since modified by Nelder and Mead (207) to incorporate a variable step size thereby speeding-up optimisation, improving precision, and correct identification of optima. Yarbro and Deming (208) have identified the advantage of initiating the optimisation with a large stepsize, allowing the majority of factor space to be explored, before the simplex contracts onto the optimum.

Cave (209) provides an excellent account of the practice of simplex optimisation. A simplex is a geometric figure in space which has vertices in number equal to one plus the number of parameters accounted for in the optimisation (n + 1). Therefore for a two parameter optimisation, the simplex is a triangle. The optimisation proceeds by rejecting the point with the worst response and forming a new simplex by reflecting that worse point away from itself in the mirror image of the other two points. The modified simplex method of Nelder and Mead accommodates a variable stepsize, thus allowing contraction or expansion thereby accelerating the rate at which the optimum is found. Wilkinson (121) applied the simplex procedure for the optimisation of ICP-AES for the analysis of coal slurries.

In this work the simplex procedure was applied for the optimisation of aluminium determinations in slurries because of the low recoveries normally experienced in its determination. Signal to background ratio (SBR), was initially used as the response factor,

but this was later substituted for a ratio of net signal of slurry signal to solution signal. The
simplex programme, based upon Nelder and Meads modified version, has been written in
BASIC for the Apple IIe microcomputer (210) and was used in this work.

6.3   COAL ANALYSIS USING THE ARL 3520

The instrument described in Section 6.2.2 was used for the determination of major, minor
and trace elements in coal. The objective of the study was to determine the optimal
conditions for slurry atomisation by altering the injector gas, spray chamber design and
injector size, so as to achieve 100% recovery. Initial experiments were performed using the
reference coal NBS 1635 which was ground using the bottle and bead method described in
Section 5.5.1. The experimental conditions are shown in Table 21.

Before commencing, spectral lines were selected on the basis of signal to background ratio
and freedom from spectral interferences. This was achieved by scanning a slurry of 1635
(2.0%) and selecting the spectral lines of interest in comparison to aqueous solutions. Two
integrations were performed for each element in the standard and sample.

6.4   RESULTS AND DISCUSSION

6.4.1 Variation of injector size, flow rate and spray chamber design

Initial work was performed using the standard conical ARL spray chamber, which included a
spoiler so as to prevent the passage of large drops to the plasma, see Figure 25. The
standard one piece Fassel torch was replaced by a two-piece demountable torch, which
allowed the use of a 3 mm i.d. injector. The instrument was calibrated using the 3 mm i.d.
injector together with an Ebdon nebuliser operated with an injector flow rate of 1.0 l min^{-1}.
The flow rate was subsequently increased to 1.5 l min^{-1} and the results obtained at both
flow rates are shown in Table 22. The recovery increased with the increased flow rates, but
problems arose from blockage of the dead volume beneath the injector. Owing to these

TABLE 21

Operating conditions for ARL 3520 ICP.

Power / kW	1.2
Gas flows / l min^{-1}	
Coolant	12
Auxiliary	2
Injector	0.5 - 1.5
Injector diameter / mm	1.8, 3.0
Viewing height / mm	15
Nebuliser types	Ebdon (V - groove)
Torch	Fassel

FIGURE 25

Diagram of single pass ARL spray chamber

TO PLASMA

SPOILER

NEBULISER

TO DRAIN
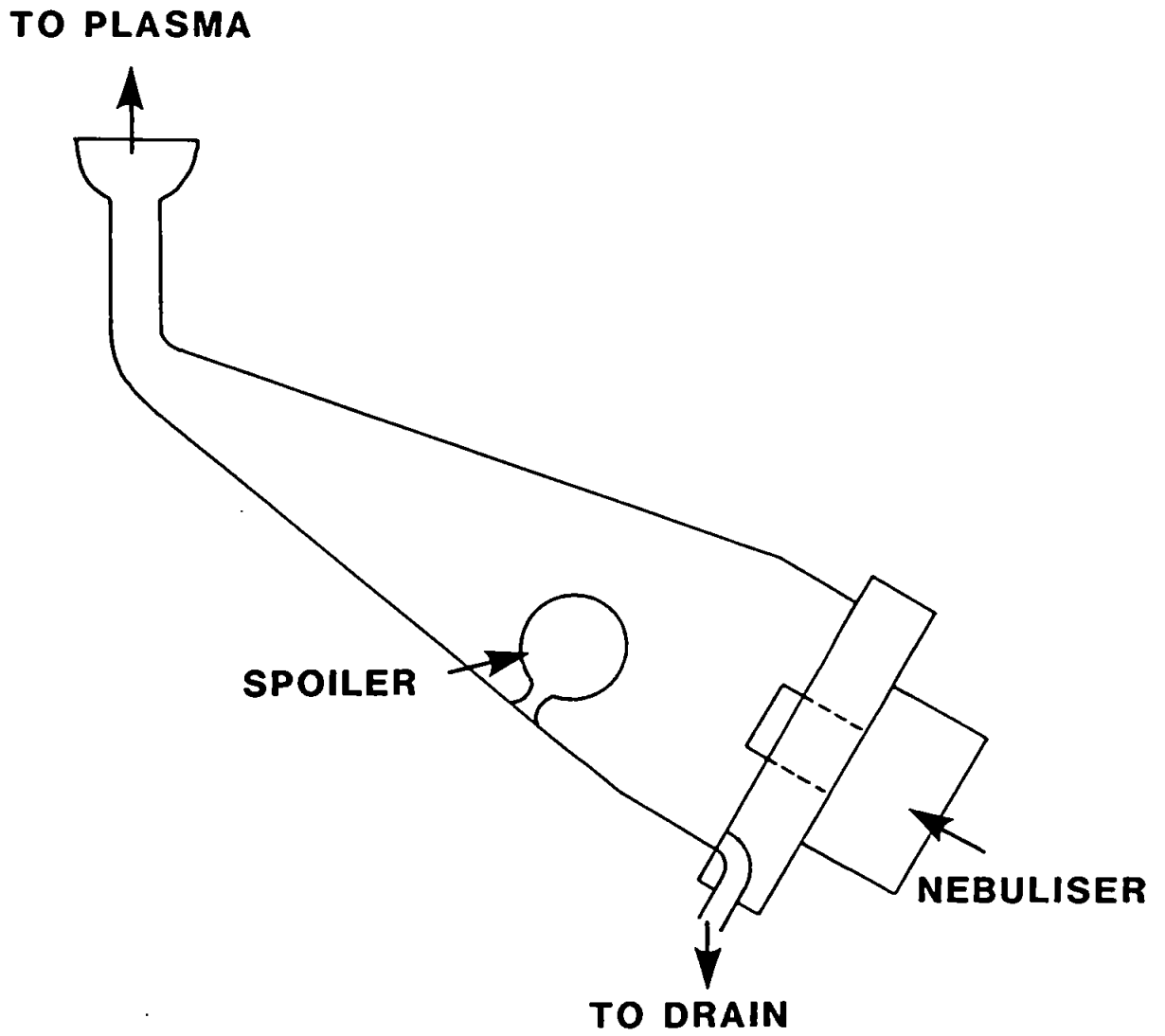
TABLE 22

Effect of increased injector flow rate using Ebdon nebuliser with 3.0 mm injector and standard ARL spray chamber.

3 mm i.d. Injector using 1.0 lmin^{-1} Flow with Spoiler			
Element	NBS 1635 Certificate Value µg g^{-1}	Slurry Value µg g^{-1}	Atomisation efficiency %
Cr	2.5 + 0.3	1.87 + 0.13	75
Mn	21.4 + 1.5	15.30 + 0.14	71
Fe	2390 + 50	1505 + 53	63
Co	(0.65)	0.54 + 0.08	83
Ni	1.74 + 0.10	1.24 + 0.2	71
Al	(3200)	2312 + 91	72
Cu	3.6 + 0.3	3.07 + 0.04	85

3 mm i.d. Injector using 1.5 lmin^{-1} Flow with Spoiler			
Element	NBS 1635 Certificate Value µg g^{-1}	Slurry Value µg g^{-1}	Atomisation efficiency %
Cr	2.5 + 0.3	2.81 + 0.15	112
Mn	21.4 + 1.5	15.1 + 0.15	71
Fe	2390 + 50	1631 + 22	68
Co	(0.65)	0.86 + 0.09	132
Ni	1.74 + 0.10	1.24 + 0.19	71
Al	(3200)	2221 + 120	69
Cu	3.6 + 0.3	3.68 + 0.05	102

sample delivery problems, the 3 mm injector was replaced by the standard torch which contained a 1.8 mm injector. The flow rate was reduced to 1.0 l min⁻¹ and the results obtained are shown in Table 23 where the recovery varied between 70% - 140%.

Following the work of McCurdy and Fry (211), who reported the successful determination of sulphur in coal by using reduced injector flow rates and eliminating any obstruction into the spray chamber, it was decided to remove the spoiler from the ARL spray chamber. Once removed, the injector flow rates were further decreased to 0.95, 0.75 and finally 0.61 l min⁻¹. The improved results obtained are shown in Table 24. By decreasing the flow rate, the residence time spent in the plasma is increased and constriction occurs of the cooler central axial channel of the plasma. This in effect forces the coal particles into a higher temperature region of the plasma than normally experienced at the same viewing height at 1.0 l min⁻¹.

Subsequent determinations of certified coals and British Coal "in-house" standards were performed using the 1.8 mm injector and the low flow rate of 0.61 l min⁻¹, having determined that these were the favourable conditions for slurry atomisation. The results of the analysis of reference coals NBS 1632(a) and NBS 1635 are shown in Table 25, whilst Table 26 shows the results of the analysis for reference coals BCR 40, BCR 181 and BCR 182. From these two tables it can be seen that the slurry atomisation results are in excellent agreement with those of the certificate values, which is encouraging considering that the particles size of some of the coals were larger than 10 μm, see Figures 26-30. This is in contradiction to previous work which has stated that particles larger than 6-7 μm (120) do not reach the plasma when using a 3 mm injector. However these results were obtained using a double pass spray chamber which includes many tortuous bends and hence only the smaller particles have the ability to negotiate those bends en route to the plasma. It would seem reasonable to suggest that larger particles can reach the plasma using the modified ARL spray chamber owing to the removal of the spoiler thus providing a relatively

TABLE 23

Effect of decreasing the flow using a 1.8 mm injector with Ebdon nebuliser and standard ARL spray chamber.

1.8 mm Injector using 1.0 lmin^{-1} Flow With Spoiler			
Element	Certificate Value $\mu g\ g^{-1}$	Slurry Value $\mu g\ g^{-1}$	Atomisation efficiency %
Cr	2.5 ± 0.3	3.01 ± 0.02	120
Mn	21.4 ± 1.5	16.8 ± 0.12	79
Fe	2390 ± 50	1660 ± 20	69
Co	(0.65)	0.91 ± 0.02	140
Ni	1.74 ± 0.10	1.56 ± 0.03	90
Al	(3200)	2484 ± 50	78
Cu	3.6 ± 0.3	4.21 ± 0.04	117

TABLE 24

Effect of removing the spoiler and decreasing injector flow rate using
1.8 mm i.d. injector.

0.95 lmin^{-1} Flow		NO SPOILER	
Element	Certificate 1632(a)	Slurry μg g^{-1}	% Recovery
Ti	(1750)	1367 + 7	78%
V	44 + 3	35.1 + 0.5	80%
Ca	(2300)	1841 + 125	80%
Ba	(130)	101.3 + 2.5	78%
Sr	(88)	81.3 + 1.1	92%
Zn	28 + 2	21.7 + 0.48	78%
Pb	12.4 + 0.6	0.53 + 0.22	4·3%
P	(280)	229.1 + 3.3	82%
K	(4100)	4026 + 500	98%

0.75 lmin^{-1} Flow		NO SPOILER	
Element	Certificate 1632(a)	Slurry μg g^{-1}	% Recovery
Ti	(1750)	1567+ 40	90%
V	44 + 3	41.1 + 1.1	95%
Ca	(2300)	2463 + 15	107%
Ba	(130)	110 + 1.8	85%
Sr	(88)	85.1 + 1.3	97%
Zn	28 + 2	27.4 + 0.2	98%
Pb	12.4 + 0.6	0.77 + 0.07	6·2%
P	(280)	235.3 + 2.1	84%
K	(4100)	3788 + 7	92%

0.61 lmin^{-1} Flow		NO SPOILER	
Element	Certificate 1632(a)	Slurry μg g^{-1}	% Recovery
Ti	(1750)	1652 + 17	94%
V	44 + 3	41.5 + 0.3	94%
Ca	(2300)	2381 + 22	104%
Ba	(130)	109 + 0.5	84%
Sr	(88)	82.2 + 0.3	93%
Zn	28 + 2	27.3 + 0.05	98%
Pb	12.4 + 0.6	0.25 + 0.02	20%
P	(280)	238·0 + 1.4	85%
K	(4100)	4004 + 11	98%

TABLE 25

Determination of major, minor and trace elements in NBS 1632(a) and 1635 coals using a 1.8 mm i.d. injector together with a flow rate of 0.61 lmin^{-1}.

Element	1632(a) Slurry % m/v	Certified % m/v	% Recovery
Ti	0.165 ± 0.006	(0.18)	92
Mg	0.096 ± 0.004	(0.1)	96
Ca	0.238 ± 0.009	0.23	103
K	0.400 ± 0.04	0.42	95
Al	2.606 ± 0.09	(3.1)	84
Fe	0.916 ± 0.004	1.11	83
	µg g^{-1}	µg g^{-1}	
V	41.5 ± 1.2	44	94
Ba	109 ± 2.0	(130)	84
Sr	82.1 ± 1.1	(88)	93
Zn	27.3 ± 2.3	28	98
Pb	2.5 ± 1.8	12.4	20
P	224 ± 4.5	(280)	80
Cr	29.2 ± 1.8	34.4	85
Mn	21.5 ± 1.8	28	77
Co	8.7 ± 0.9	(6.8)	127
Ni	16.5 ± 0.09	19.4	85
Cu	14.1 ± 0.04	16.5	85

Element	1635 Slurry % m/v	Certified % m/v	% Recovery
Al	0.295 ± 0.07	0.320	92
Fe	0.194 ± 0.002	0.239	81
	µg g^{-1}	µg g^{-1}	
V	-	-	-
Ba	-	-	-
Sr	-	-	-
Zn	-	-	-
Pb	-	-	-
P	-	-	-
Cr	2.7 ± 0.1	2.5	108
Mn	13.6 ± 0.8	21.4	64
Co	0.7 ± 0.3	0.65	107
Ni	1.1 ± 0.1	1.74	63
Cu	4.0 ± 0.2	3.6	111

TABLE 26

Determination of major, minor and trace elements in BCR 40, BCR 181, and BCR 182 using a 1.8 mm injector together with a flow rate of 0.6 l min⁻¹.

Element	BCR 40 Slurry % m/v	Certified % m/v	% Recovery
Ti	0.105 ± 0.002	–	–
Mg	0.146 ± 0.004	–	–
Ca	0.173 ± 0.001	–	–
K	0.577 ± 0.03	–	–
Al	2.039 ± 0.07	–	–
Fe	0.933 ± 0.004	–	–
	$\mu g\ g^{-1}$	$\mu g\ g^{-1}$	
V	58.9 ± 2.6	–	–
Sr	430 ± 3.0		
Zn	300 ± 4.0	30.2 ± 2	99
Pb	21.1 ± 4.0	24.2	87
P	64.2 ± 3.9		
Cr	24.9 ± 2.4	31.2 ± 2	80
Mn	98.8 ± 8.0	139 ± 5	71
Co	8.4 ± 0.3		
Ni	20.1 ± 0.9	25.4 ± 1.7	79
Cu	29.2 ± 1.4		

Element	BCR 181 Slurry % m/v	Certified % m/v	% Recovery
Ti	0.010 ± 0.001	–	–
Mg	0.004 ± 0.001	–	–
Ca	0.013 ± 0.001	–	–
K	0.010 ± 0.003	–	–
Al	0.217 ± 0.006	–	–
Fe	0.207 ± 0.003	–	–
	$\mu g\ g^{-1}$	$\mu g\ g^{-1}$	
V	9.1 ± 1.2	12.0 ± 0.4	75
Ba	14.4 ± 0.8		–
Sr	7.2 ± 0.1		–
Zn	8.1 ± 0.3	8.4 ± 0.6	96
Pb	3.2 ± 0.4	2.6	123
P	11.7 ± 0.3	–	–
Cr	2.7 ± 0.1	–	–
Mn	1.9 ± 0.1	–	–
Co	1.4 ± 0.1	–	–
Ni	2.4 ± 0.1	–	–
Cu	8.9 ± 0.4	–	–

Element	BCR 182 Slurry % m/v	Certified % m/v	% Recovery
Ti	0.066 ± 0.007	–	–
Mg	0.122 ± 0.003	–	–
Ca	0.223 ± 0.005	–	–
K	0.400 ± 0.02	–	–
Al	1.533 ± 0.04	–	–
Fe	0.680 ± 0.004	–	–
	$\mu g\ g^{-1}$	$\mu g\ g^{-1}$	
V	22.3 ± 0.2	24.3 ±	92
Ba	94.6 ± 2.6		–
Sr	33.2 ± 1.1		–
Zn	30.1 ± 0.8	33.3 ± 1.5	90
Pb	11.1 ± 0.1		–
P	164 ± 5.0	–	–
Cr	19.2 ± 0.3		–
Mn	146 ± 7.0	195 ±	75
Co	9.0 ± 0.1		–
Ni	24.8 ± 2.0	–	–
Cu	13.6 ± 1.1	–	–

FIGURE 26

By volume particle size distribution of coal NBS SRM 1632(a)

MEAN PARTICLE SIZE / μm
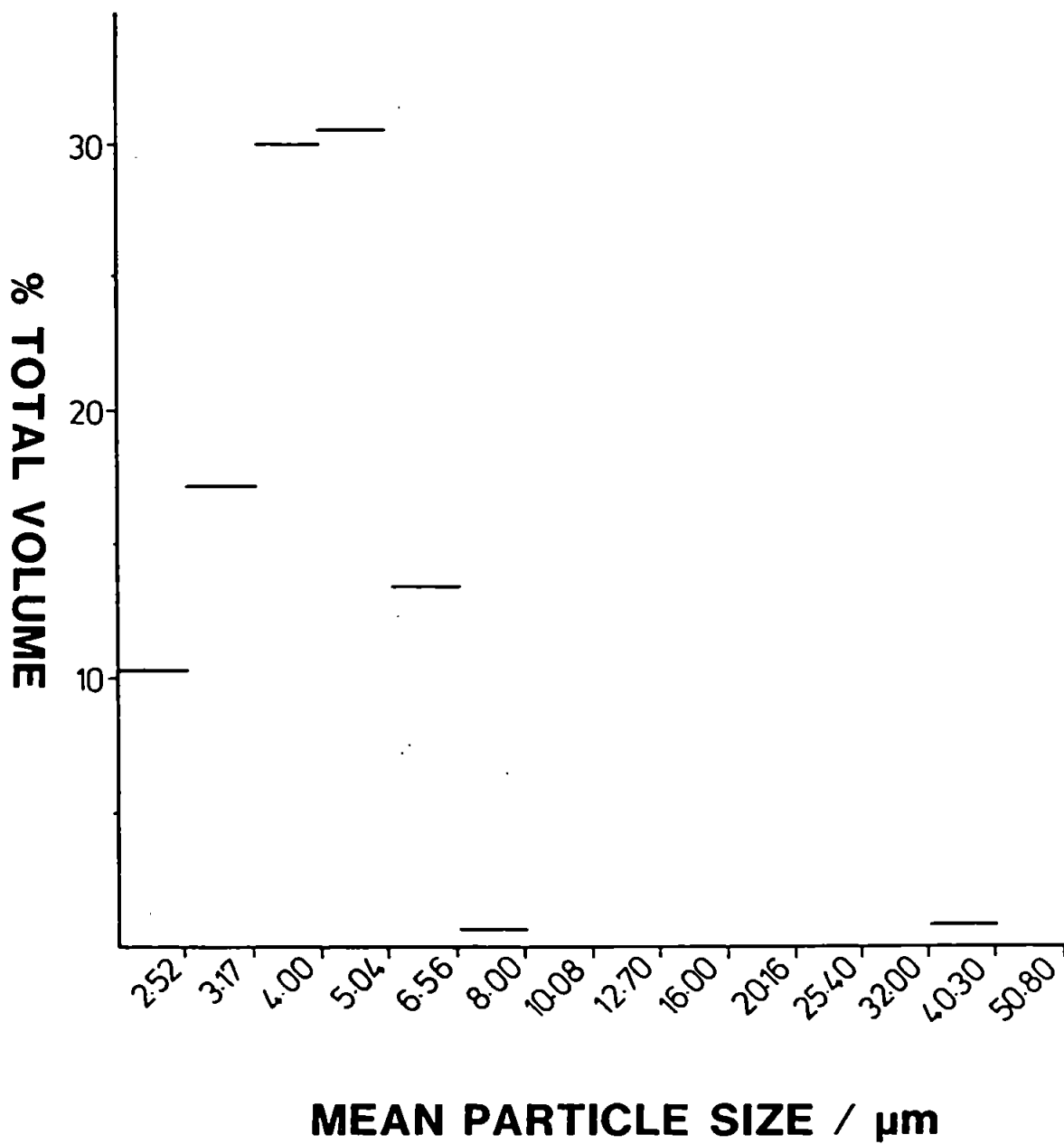
FIGURE 27

By volume particle size distribution of finely ground coal NBS SRM 1635

MEAN PARTICLE SIZE / µm
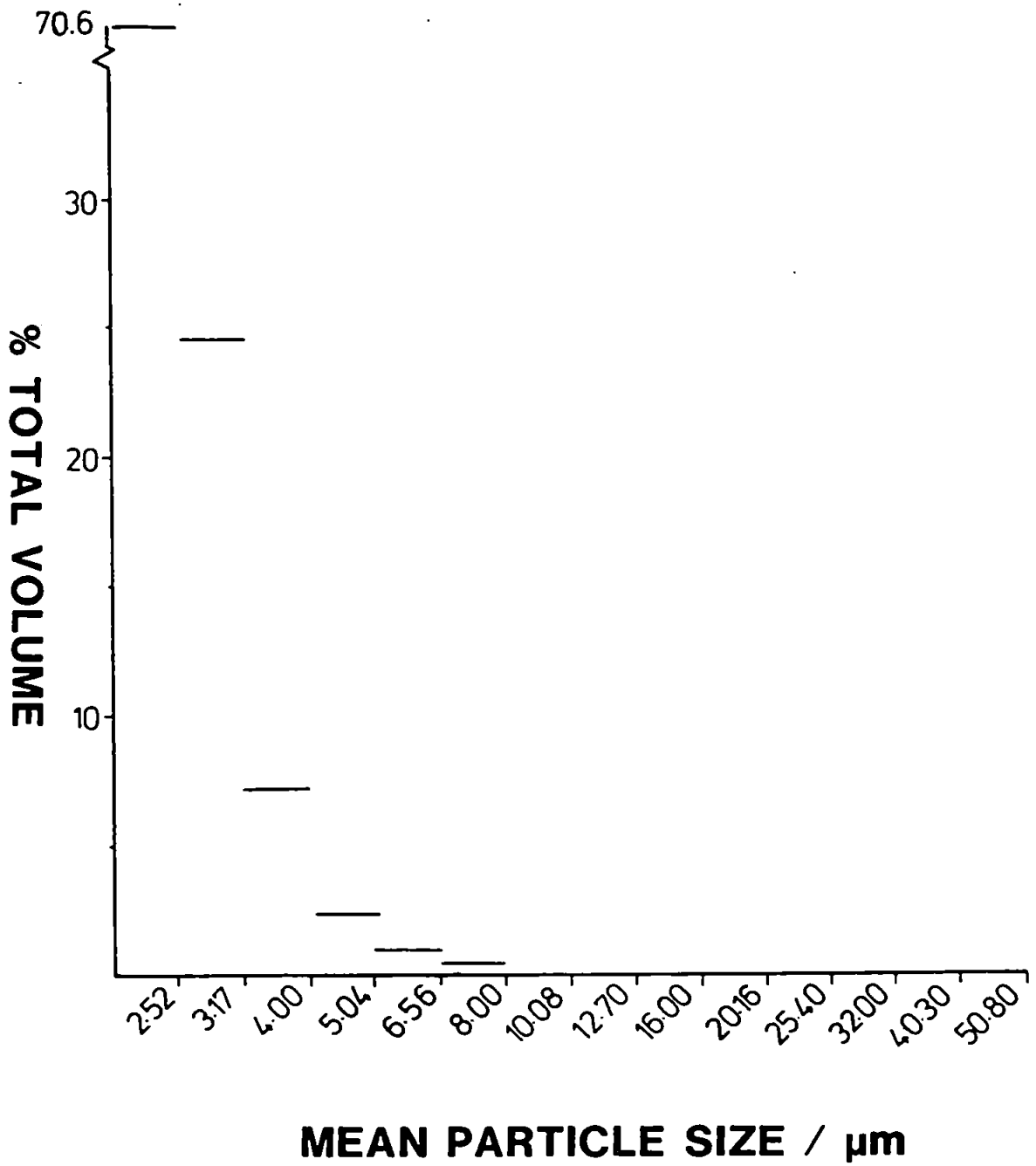
FIGURE 28

By volume particle size distribution of coal BCR 40

MEAN PARTICLE SIZE / µm
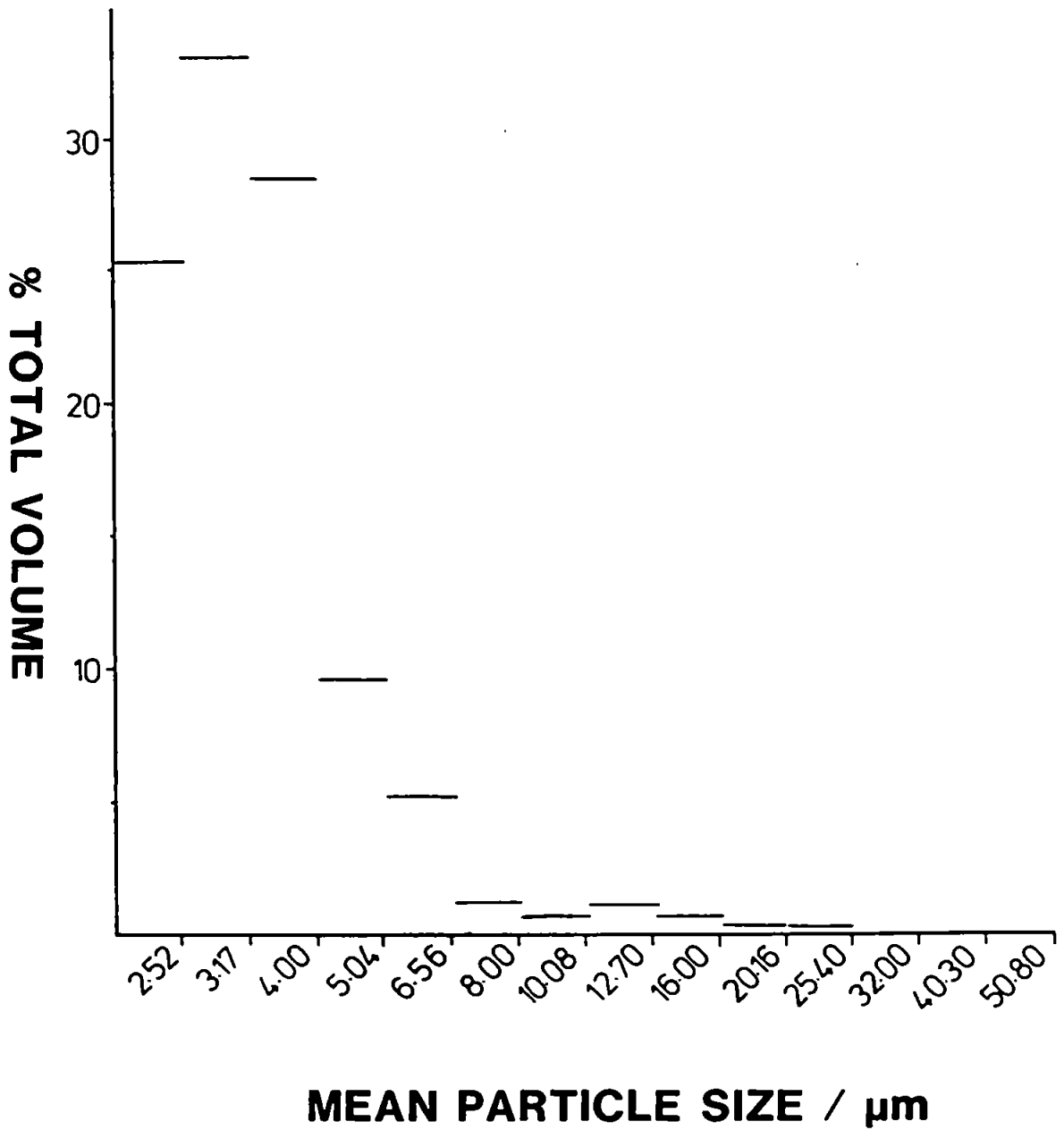
FIGURE 29

By volume particle size distribution of coal BCR 181
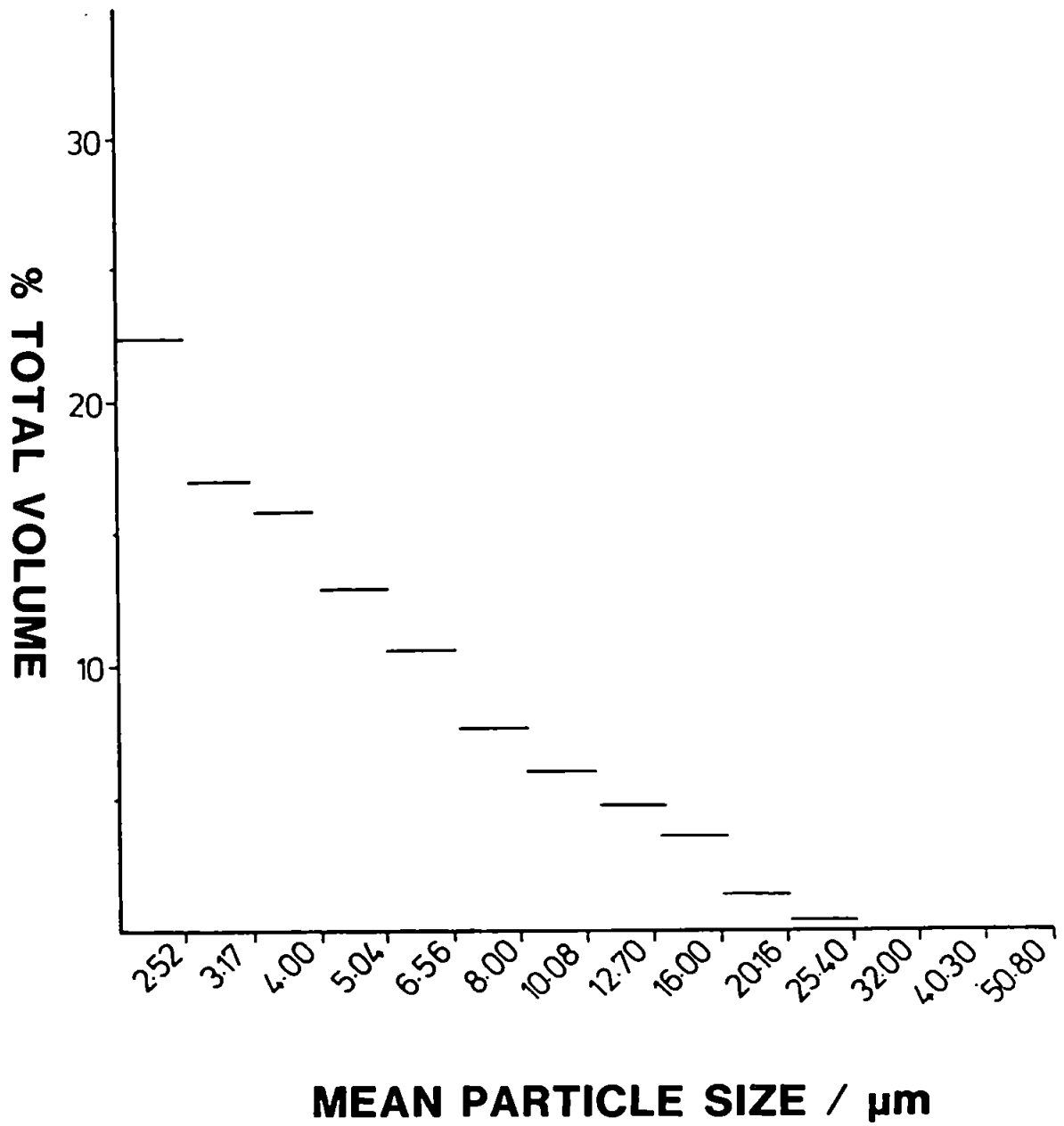
FIGURE 30

By volume particle size distribution of coal BCR 182
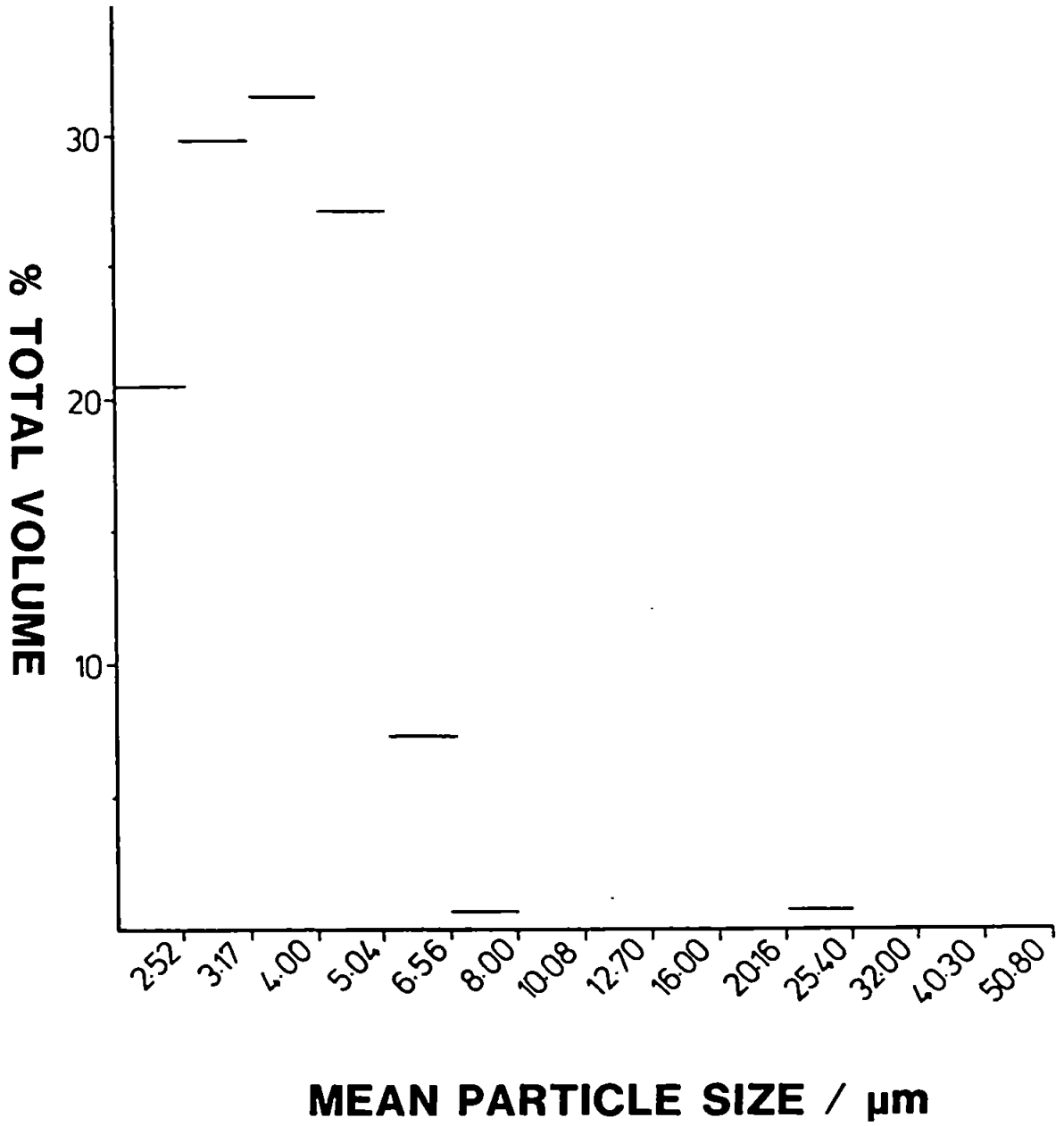
unobstructed aerosol path. This is in agreement with recent work (212) which has shown particles in the region of 20-25 µm reached the injector tip when the modified ARL spray chamber was used with 1.0 l min^{-1} flow rate. Using these conditions, the analysis of the British Coal "in-house" standards was performed and the slurry results compared directly with results obtained by dissolution techniques in BC laboratories, Table 27. A wide range of coals with increasing ash content were analysed to determine whether the ash content would have any affect upon the analysis of the coals. Certain elements such as aluminium and silicon are associated in the ash content, therefore one might expect that for coals with a high ash content the recovery of these elements would be improved. This in fact was not the case, as there was not much variation in recovery for each element regardless of which coal was analysed.

6.4.2 Analysis of coal using single pass spray chamber and ARL 3520 ICP

The modified ARL spray chamber was replaced by a single pass version which is shown in Figure 31. The injector gas flow rate was increased to 1.0 l min^{-1} using the 1.8 mm injector and a stable plasma was sustained. The flow rate was increased until the recovery approached 100%. The increased flow rate is necessary owing to the path in the single pass spray chamber not being as direct to the plasma as in the ARL chamber. The results are shown in Table 28 and are in excellent agreement with the certified values. The same conditions were retained for the analysis of the British Coal "in-house" standards, Table 29, and the results are in reasonable agreement with those that are obtained by British Coal using ICP following dissolution. The results from Table 29 are lower in comparison with Table 27, which is difficult to explain considering the excellent agreement with the certified values. However, on examining the particle size diagrams Figures 32-39 it is evident that grinding of these particular coals was not complete as indicated by the presence of particles in the 30 µm region. The low recoveries compared to aqueous solutions are explained by the inability of the larger particles to negotiate the final right angled bend of the spray

FIGURE 31

Diagram of single pass spray chamber

TO PLASMA

NEBULISER

TO DRAIN
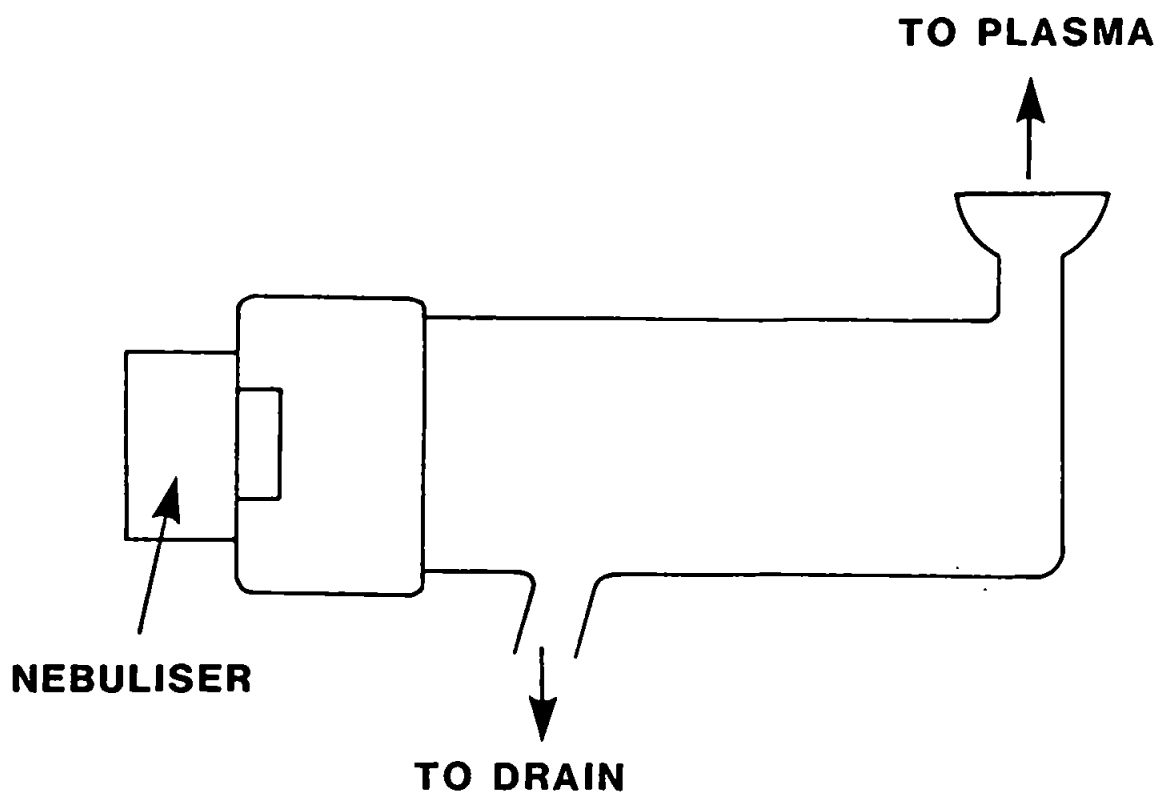
TABLE 27

Analysis by slurry atomisation ICP of British Coal 'in house' standards$(\%m/v)$ using the modified ARL pass spray chamber and 0.61 lmin^{-1} injector flow rate.

Range of NCB "In House" Standards								
E5 (3% ASH)			**E9 (5% ASH)**			**E7 (10% ASH)**		
ICP	XRF	%R	ICP	XRF	%R	ICP	XRF	%R
Ti	0.007	0.009	78	0.032	0.029	110	0.052	0.054	96
Mg	0.034	0.039	87	0.028	0.032	88	0.120	0.140	86
Ca	0.121	0.135	90	0.200	0.209	96	0.214	0.223	96
K	0.021	0.030	70	0.085	0.089	96	0.302	0.317	95
Al	0.238	0.292	82	0.547	0.637	86	1.257	1.424	88
Fe	0.444	0.563	79	0.561	0.664	84	0.729	0.872	84

E10 (11% ASH)			**E14 (15% ASH)**			**E23 (15% ASH)**		
ICP	XRF	%R	ICP	XRF	%R	ICP	XRF	%R
Ti	0.072	0.061	118	0.081	0.082	99	0.082	0.081	101
Mg	0.077	0.090	86	0.095	0.110	86	0.104	0.135	77
Ca	0.247	0.255	97	0.092	0.109	84	0.389	0.438	89
K	0.299	0.311	96	0.463	0.498	93	0.353	0.397	90
Al	1.361	1.518	90	1.922	2.172	88	1.697	2.051	83
Fe	0.785	0.907	87	1.411	1.669	85	0.934	1.193	78

E30 (20% ASH)			**E38 (20% ASH)**			**E46 (25% ASH)**		
ICP	XRF	%R	ICP	XRF	%R	ICP	XRF	%R
Ti	0.129	0.112	115	0.106	0.093	114	0.162	0.143	113
Mg	0.178	0.200	89	0.172	0.200	86	0.211	0.242	87
Ca	0.272	0.304	89	0.434	0.501	87	0.230	0.251	92
K	0.669	0.688	97	0.505	0.503	95	0.701	0.696	101
Al	2.851	3.098	92	2.212	2.468	90	3.453	3.697	93
Fe	0.825	0.964	86	1.156	1.403	82	1.247	1.436	87

E4 (31% ASH)								
ICP	XRF	%R						
Ti	0.214	0.168	127					
Mg	0.234	0.262	89					
Ca	0.560	0.611	92					
K	0.865	0.877	97					
Al	3.754	4.038	93					
Fe	1.225	1.402	87					

TABLE 28

Determination of major amd minor elements by slurry atomisation using a single pass spray chamber with Ebdon nebuliser.

1.0 1 min^{-1} Flow 1.8 mm i.d. Injector.			
Element	1632(a) Slurry µg g^{-1}	Cert µg g^{-1}	% Recovery
Ca	2300	2300	100
K	3860	4100	94
Al	22790	31000	90
Fe	9830	11.100	86
Mn	30.2	28	108
Ni	19.6	19.4	101
Cu	17.6	16.5	107
Element	BCR 40 Slurry µg g^{-1}	Cert µg g^{-1}	% Recovery
Ca	1750	–	–
K	5830	–	–
Al	21200	–	–
Fe	6690	–	–
Mn	142	139	102
Ni	36.3	–	–
Cu	24.8	–	–
Element	BCR 181 Slurry µg g^{-1}	Cert µg g^{-1}	% Recovery
Ca	130	–	–
K	140	–	–
Al	2500	–	–
Fe	2770	–	–
Mn	2.8	–	–
Ni	3.8	–	–
Cu	13.8	–	–
Element	BCR 182 Slurry µg g^{-1}	Cert µg g^{-1}	% Recovery
Ca	2120	–	–
K	3510	–	–
Al	14500	–	–
Fe	6690	–	–
Mn	182	195	93
Ni	28	–	–
Cu	16.4	–	–
Element	BCR 182 Slurry µg g^{-1}	Cert µg g^{-1}	% Recovery
Ca	5470	5600	98
K	1700	90	188
Al	3980	(3200)	124
Fe	2430	2390	101
Mn	22.3	21.4	104
Ni	2.60	1.74	150
Cu	7.2	3.6	200

( ) = not certified values   * = values reported by Gladney (201).

TABLE 29

Analysis by slurry atomisation ICP of British Coal 'in house' standards(%m/v) using single pass spray chamber and 1.0 lmin^{-1} injector flow rate.

	E5 (3% ASH)			E9 (5% ASH)			E7 (10% ASH)		
	ICP	XRF	%R	ICP	XRF	%R	ICP	XRF	%R
Ca	0.108	0.135	80	0.177	0.209	85	0.191	0.223	86
K	0.027	0.030	90	0.058	0.089	65	0.153	0.317	48
Al	0.216	0.292	74	0.519	0.637	81	1.223	1.424	86
Fe	0.411	0.563	73	0.549	0.664	83	0.754	0.872	86

	E10 (11% ASH)			E14 (15% ASH)			E23 (15% ASH)		
	ICP	XRF	%R	ICP	XRF	%R	ICP	XRF	%R
Ca	0.215	0.255	84	0.083	0.109	76	0.193	0.438	44
K	0.239	0.311	77	0.398	0.498	80	0.163	0.397	41
Al	1.268	1.518	84	1.775	2.172	81	1.547	2.051	75
Fe	0.784	0.907	86	1.411	1.669	85	0.925	1.193	78

	E30 (20% ASH)			E38 (20% ASH)			E46 (25% ASH)		
	ICP	XRF	%R	ICP	XRF	%R	ICP	XRF	%R
Ca	0.228	0.304	75	0.398	0.501	80	0.215	0.251	86
K	0.342	0.688	49	0.460	0.533	86	0.679	0.696	98
Al	2.662	3.098	85	2.096	2.468	85	3.173	3.697	86
Fe	0.864	0.964	90	1.151	1.403	82	1.244	1.436	87

	E4 (31% ASH)								
	ICP	XRF	%R						
Ca	0.484	0.611	78						
K	0.746	0.877	85						
Al	3.304	4.038	82						
Fe	1.162	1.402	83						

FIGURE 32

Particle size distribution of British Coal in house standard coal E 38
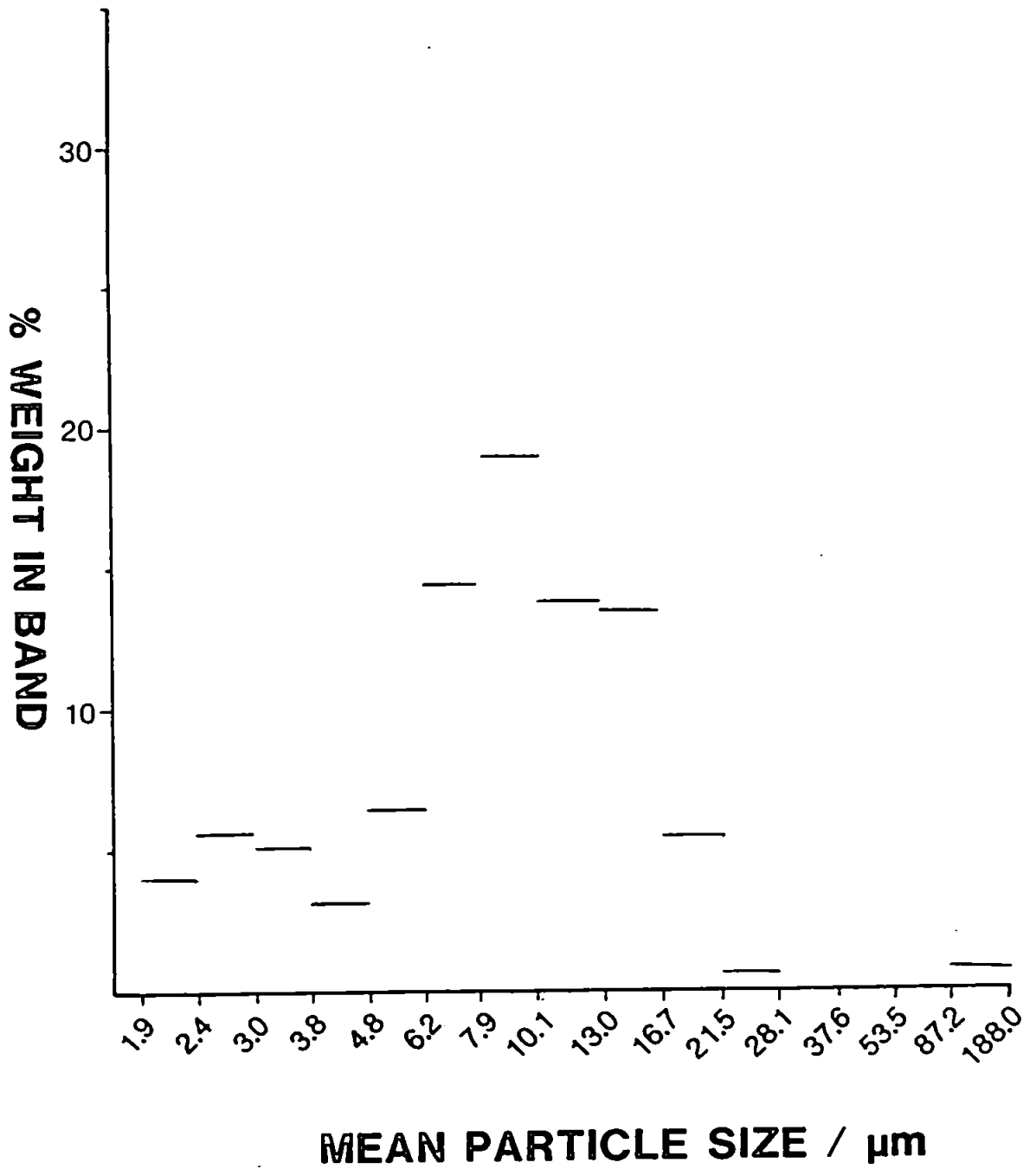
FIGURE 33

Particle size distribution of British Coal in house standard coal E 14
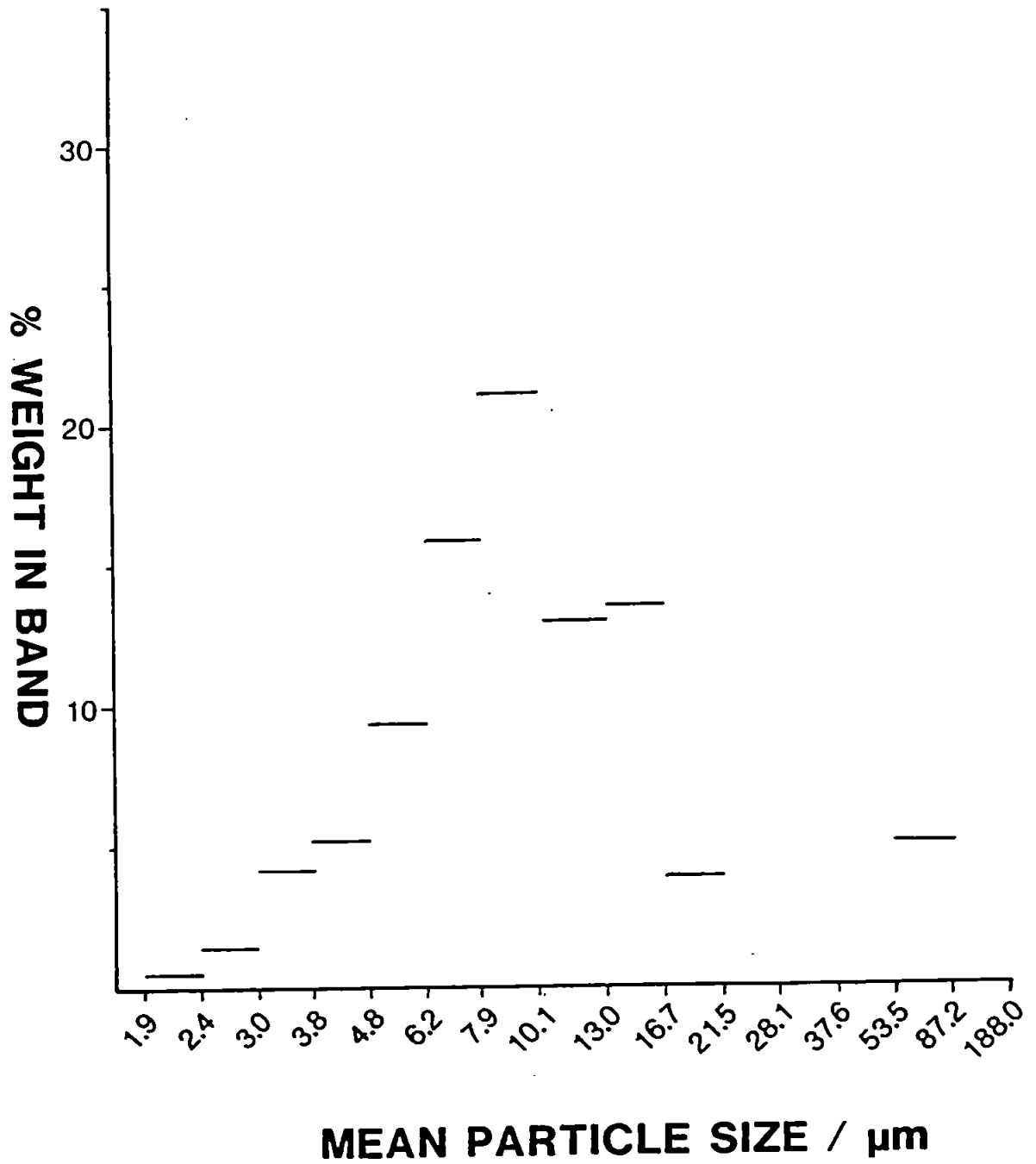
FIGURE 34

Particle size distribution of British Coal in house standard coal E 30
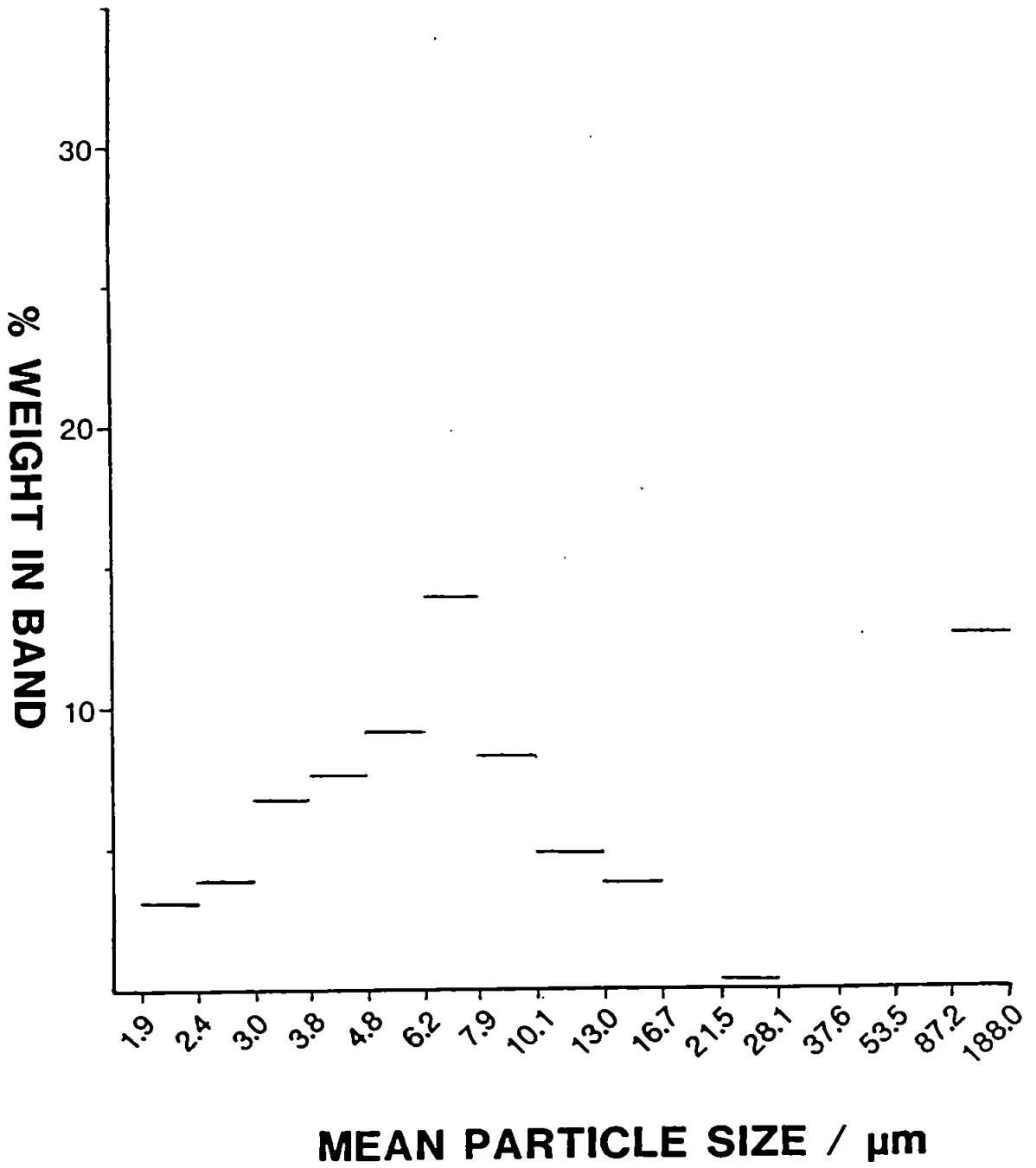
FIGURE 35

Particle size distribution of British Coal in house standard coal E 23
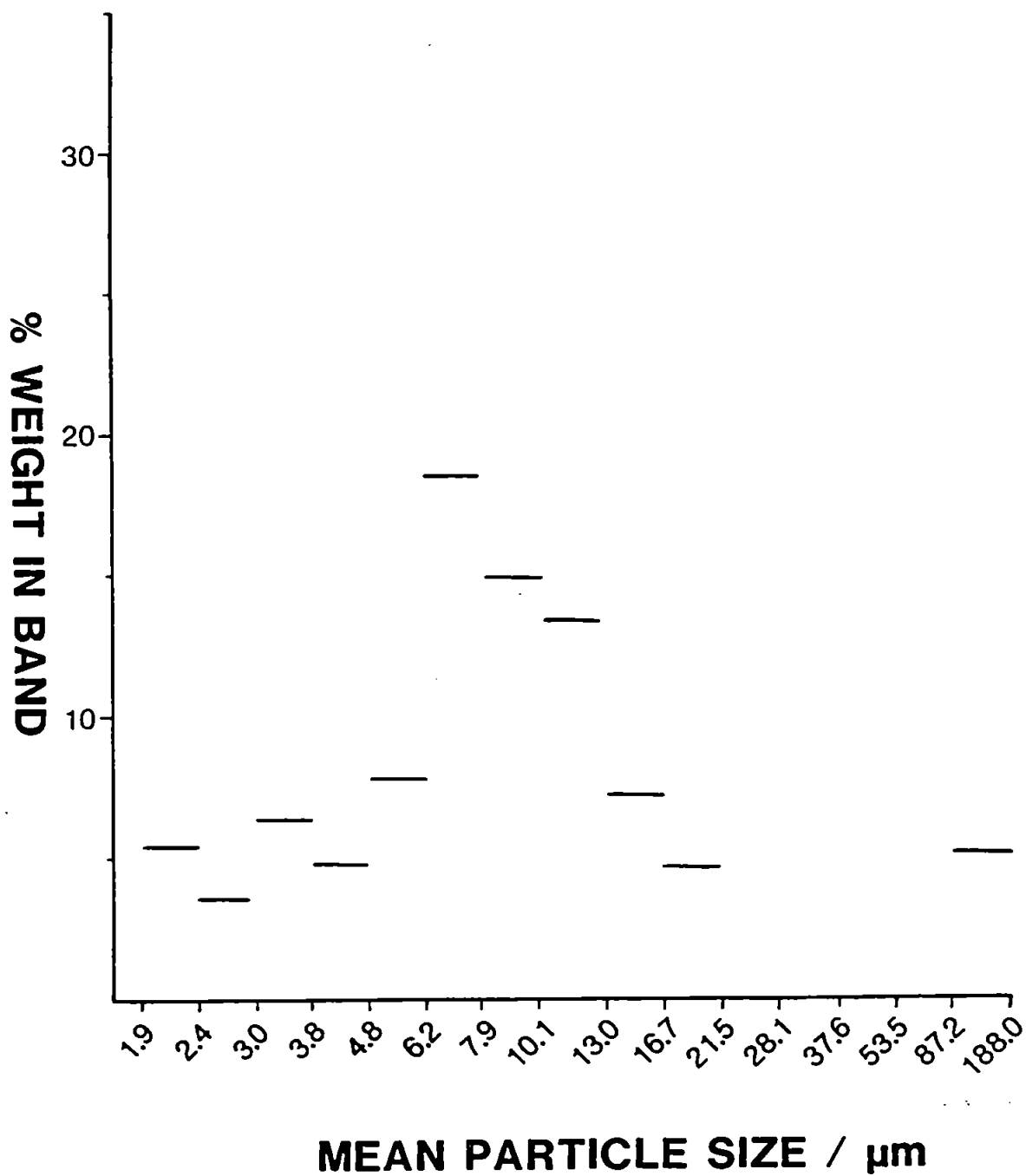
FIGURE 36

Particle size distribution of British Coal in house standard coal E 9
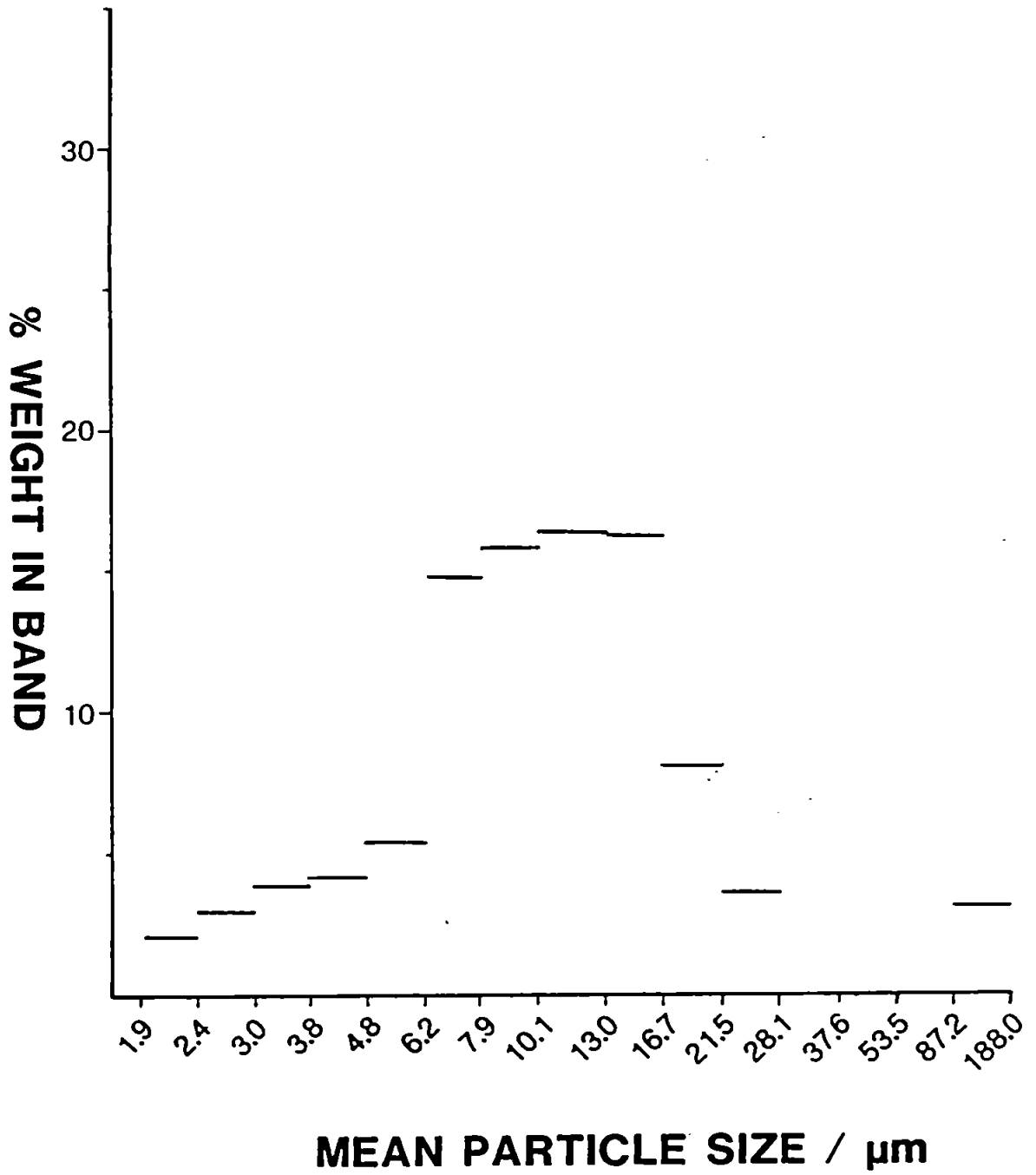
FIGURE 37

Particle size distribution of British Coal in house standard coal E 46
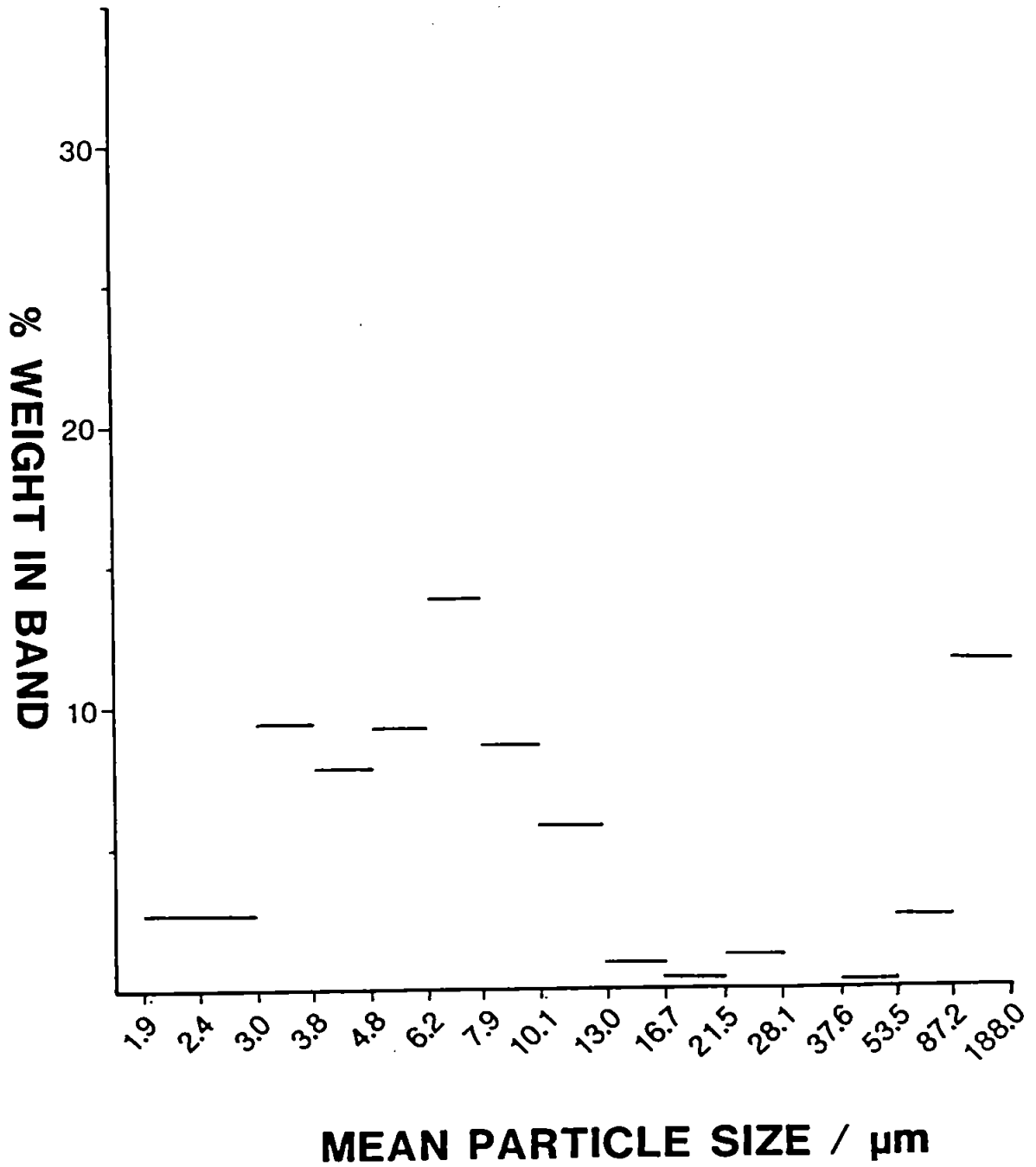
FIGURE 38

Particle size distribution of British Coal in house standard coal E 4
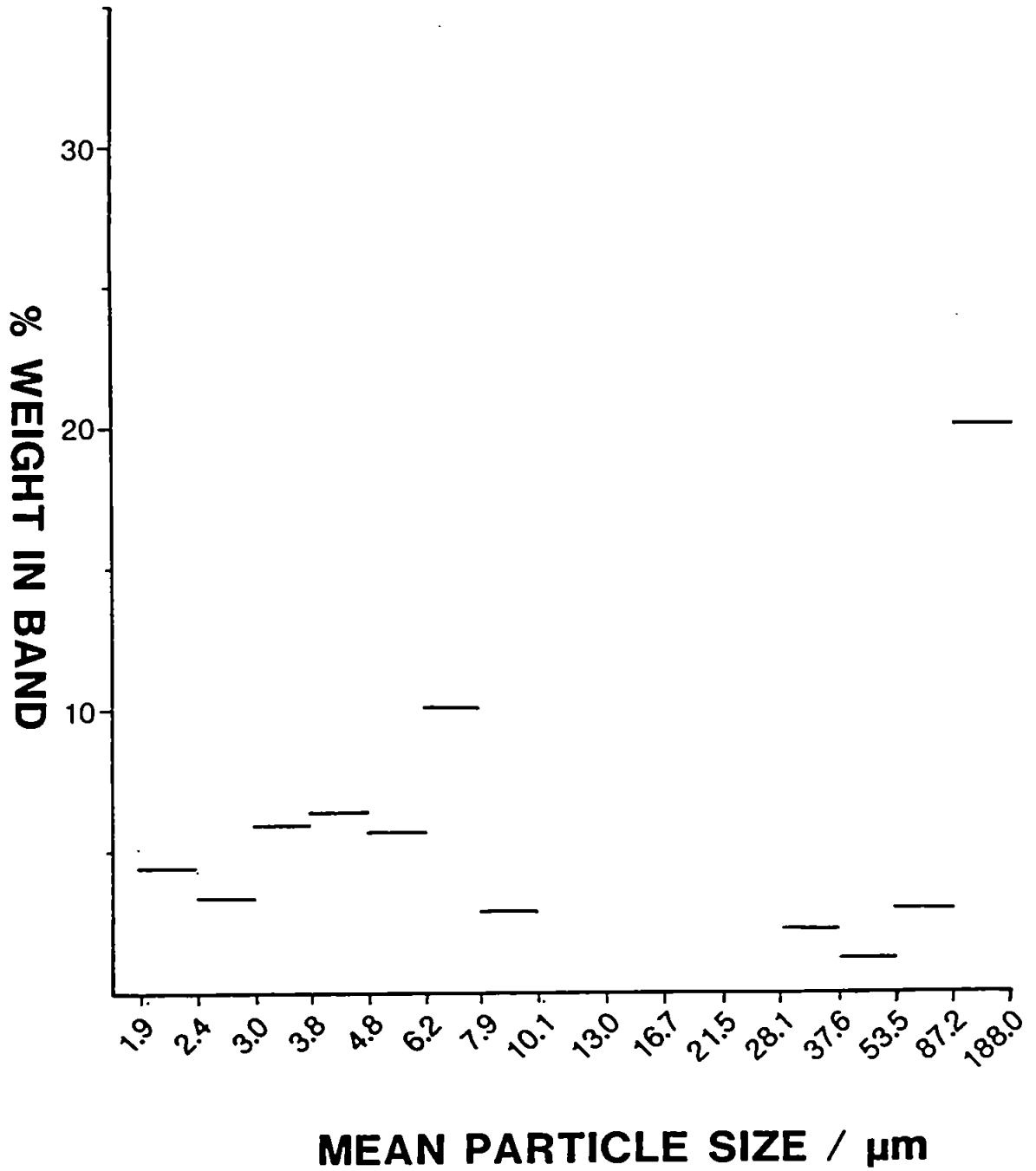
FIGURE 39

Particle size distribution of British Coal in house standard coal E 5
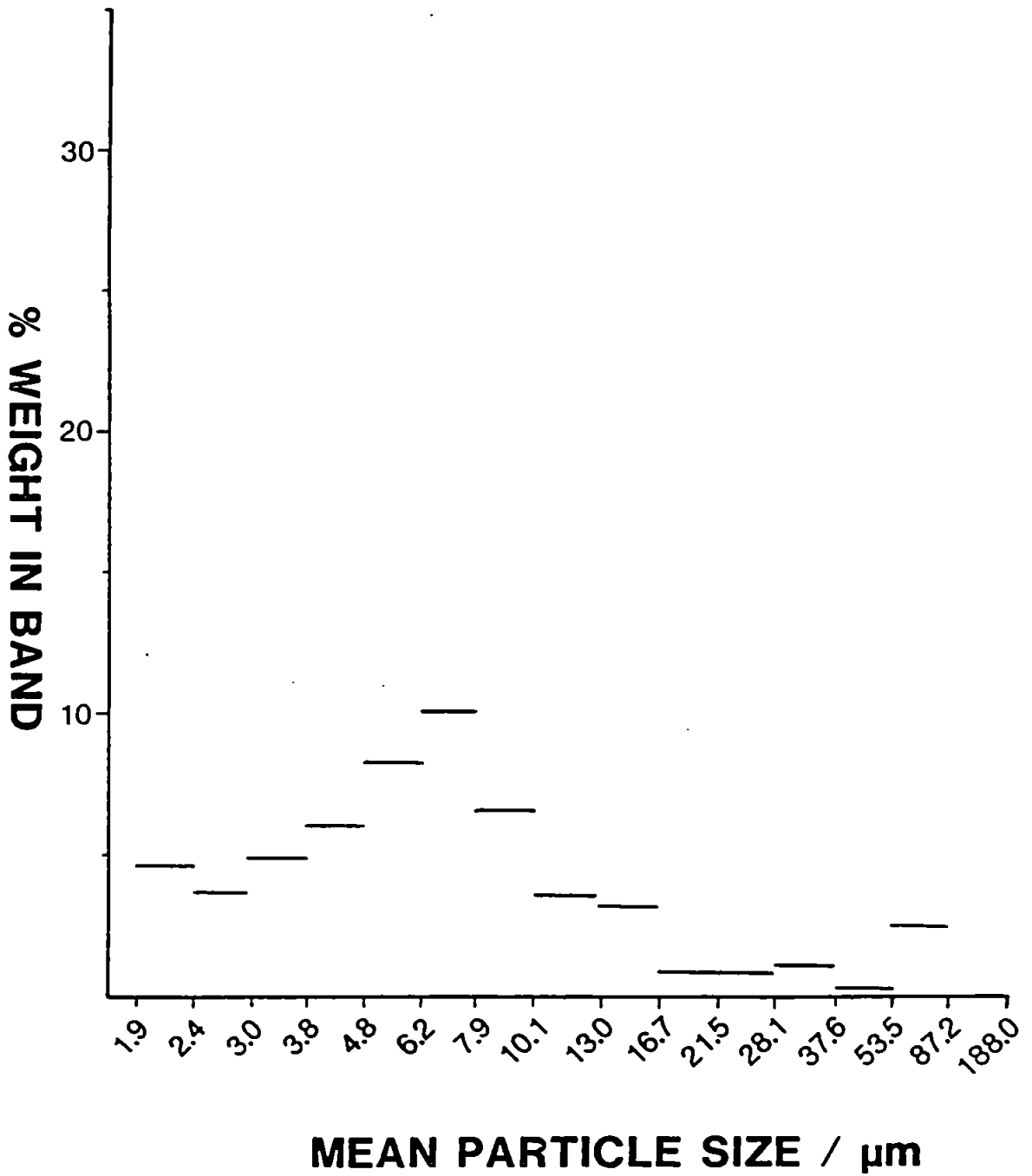
chamber where sample was deposited and thus the single pass spray chamber only allows the passage of the smaller particles, unlike the modified ARL chamber which seems to accept larger particles.

6.5 CONCLUSION TO ARL STUDIES

The results clearly demonstrate that by decreasing the injector flow the successful determinations of major, minor and trace elements is achieved when using an ARL spray chamber from which the spoiler has been removed. Flow rates above 1.0 l min^{-1} cannot be tolerated by this system as this results in plasma instability. The ARL chamber yield better results than the single pass chamber. The low flow rates through the plasma causes increased residence times, which in turn force the coal particles into the hotter regions of the plasma due to constriction of the central cooler channel. This gives rise to complete matrix destruction and hence excellent agreement with the certificate values was achieved.

6.6 OPTIMISATION OF PLASMA PERFORMANCE FOR THE DETERMINATION OF ALUMINIUM

As aluminium consistently yielded low recoveries, a simplex optimisation was undertaken in an attempt to improve recovery.

The criterion of merit used in the simplex procedure was that of the ratio of corrected slurry signal over the corrected solution signal for a aqueous solution of equivalent aluminium concentration to that expected in the slurry. This is expressed in the following equation:

$$\text{Criterion of Merit} = \frac{\text{Signal}_{\text{(slurry)}} - \text{Signal}_{\text{(Slurry background)}}}{\text{Signal}_{\text{(Solution)}} - \text{Signal}_{\text{(Solution background)}}}$$

- 125 -

The aluminium 308.215 nm atom line was used for the determination using the modified ARL spray chamber. The optimum values obtained for the various flow rates and power setting are given in Table 30 and yielded between 95 to 99% aluminium recovery. However, the optimal conditions require slightly less power and a higher injector flow rate than previously used in the analysis of the coals see Table 21. The conditions found by the simplex optimisation for aluminium in reference coal NBS 1635 seem at first difficult to explain. By increasing the flow rate, the residence time in the plasma is decreased and the cooler central channel is once again elongated. Also the lower power equates to a plasma of slightly less excitation capability. The problem of low aluminium recoveries has been attributed to the inability of the plasma to break the aluminium-oxygen species. One might expect that by increasing both the power to the plasma and the residence time, that this would result in a more efficient matrix destruction and atomisation of the aluminium oxide. However in essence, the optimal conditions have decreased both the power and observation height in the plasma, the latter by increasing the injector flow rate.

The conditions described in Table 30 were utilised in the determination of major, minor and trace elements for 8 certified reference coals at the wavelengths shown in Table 31. Results for 5 coals are shown in Tables 32-36.

These results clearly show that the aluminium recoveries have been improved, such that typical atomisation efficiency of between 90-115% was achieved. The exception to this was 1632(b) which showed an atomisation efficiency of 84%. However the recoveries for iron show some variation, the reason for this being unclear. One possibility for the low recovery of iron is that the iron is present in coal as relatively large inclusions of oxides and sulphides as suggested by Wilkinson (35) thus proving more refractory in the plasma. A second possibility is that the magnetic stirrer which was used to keep the coals in suspension, may cause migration of some of the magnetic iron mineral particles to the bottom of the volumetric flask. The recovery for calcium was consistent at about 80%, the

TABLE 30

Simplex optimised operating conditions for the recovery of aluminium coal using the 308.215 nm line and the ARL 3520 with modified spraychamber.

Power / kW	1.14
Gas flows / 1 min^{-1}	
Coolant	12.4
Auxiliary	0.8
Injector	1.0
Injector Diameter/mm	1.8
Viewing height/mm	15
Nebuliser type	Ebdon V-Groove
Torch	Fassel

TABLE 31

Wavelength for elemental analysis.

Element	Wavelength/nm	Order
Al	308.215	2
Fe	259.940	2
Ca	317.933	2
Ti	337.280	2
Mg	279.080	2
K	766.490	1
Mn	275.610	2
Cu	324.754	2
Ba	455.403	1
Sr	407.771	1
V	292.402	2
Zn	213.856	3

TABLE 32

Major and minor elements in reference coal 1635 by slurry atomisation using optimised conditions.

Element	Slurry Atomisation % m/v	Certificate Value % m/v	Recovery (slurry/ref) %
Al	0.289	(0.32)	90
Fe	0.187	0.239 ± 0.005	78
Ca	0.447	$0.5600 \pm 0.020^*$	80
Ti	0.018	(0.02)	90
Mg	0.070	0.098^*	71
	$\mu g\ g^{-1}$	$\mu g\ g^{-1}$	
K	108.7	95 ± 16	113
Mn	20.7	21.4 ± 1.5	95
Cu	3.1	3.6 ± 0.3	86
Ba	70	83^*	84
Sr	93.8	140^*	67
V	4.1	5.2 ± 0.5	80
Zn	6.24	4.7 ± 0.5	127

( ) = Non certified values.

* = Values reported by Gladney (201).

TABLE 33

Major and minor elements in reference coal 1632(b) by slurry

atomisation using optimised conditions.

Element	Slurry Atomisation % m/v	Certificate Value % m/v	Recovery (slurry/ref) %
Al	0.717	0.855 $\pm$ 0.019	84
Fe	0.560	0.759 $\pm$ 0.045	74
Ca	0.195	0.204 $\pm$ 0.006	98
Ti	0.033	0.0454 $\pm$ 0.0017	73
Mg	0.033	0.0383 $\pm$ 0.0008	87
	$\mu g\ g^{-1}$	$\mu g\ g^{-1}$	
K	688	748 $\pm$ 28	92
Mn	10.4	12.4 $\pm$ 1	84
Cu	4.4	6.28 $\pm$ 0.3	70
Ba	56.6	67.5 $\pm$ 2.1	84
Sr	66.5	(102)	65
V	13.3	(14)	95
Zn	13.2	11.89 $\pm$ 0.78	111

TABLE 34

Major and minor elements in reference coal SARM 18 by slurry atomisation using optimised conditions.

Element	Slurry Atomisation % m/v	Certificate Value % m/v	Recovery % (slurry/ref)
Al_2O_3	2.54	2.57 (2.54 - 2.61)	99
Fe_2O_3	0.22	0.29 (0.28 - 0.29)	76
CaO	0.16	0.18 (0.17 - 0.19)	87
TiO_2	0.096	0.114 (0.111 - 0.116)	84
MgO	0.09	0.11 (0.10 - 0.11)	84
K_2O	0.147	0.145 (0.140 - 0.150)	101
	$\mu g \ g^{-1}$	$\mu g \ g^{-1}$	
Mn	19.1	22 (21 - 23)	86
Cu	5.0	5.9 (5.2 - 6.4)	85
Ba	76.5	78 (71 - 82)	98
Sr	31.0	44 (42 - 45)	70
V	18.2	23 (21 - 25)	79
Zn	10.2	5.5 (5.2 - 6.8)	185

TABLE 35

Major and minor elements in reference coal SARM 19 by slurry atomisation using optimised conditions.

Element	Slurry Atomisation % m/v	Certificate Value % m/v	Recovery (slurry/ref) %
Al_2O_3	9.26	8.01 (7.86 - 8.15)	115
Fe_2O_3	1.60	1.75 (1.73 - 1.76)	92
CaO	1.12	1.39 (1.37 - 1.41)	80
TiO_2	0.300	0.341 (0.324 - 0.356)	88
MgO	0.23	0.20 (0.20 - 0.22)	115
K_2O	0.31	0.24 (0.24 - 0.25)	130
	$\mu g\ g^{-1}$	$\mu g\ g^{-1}$	
Mn	130.3	157 (143 - 168)	83
Cu	15.9	13 (11 - 14)	120
Ba	353.0	304 (295 - 318)	116
Sr	117.3	126 (125 - 141)	93
V	29.9	35 (33 - 37)	85

TABLE 36

Major and minor elements in reference coal SARM 20 by slurry

atomisation using optimised conditions.

Element	Slurry atomisation % m/v	Certificate value % m/v	Recovery (slurry/ref) %
Al_2O_3	12.50	11.27 (11.16 - 11.73)	106
Fe_2O_3	1.07	1.17 (1.15 - 1.19)	92
CaO	1.49	1.87 (1.85 - 1.89)	80
TiO_2	0.54	0.63 (0.61 - 0.65)	86
MgO	0.46	0.43 (0.41 - 0.45)	109
K_2O	0.19	0.14 (0.14 - 0.15)	138
	$\mu g\ g^{-1}$	$\mu g\ g^{-1}$	
Mn	68.4	80 (77 - 82)	86
Cu	22.9	18 (18 - 19)	127
Ba	322.1	372 (363 - 384)	87
Sr	286.5	330 (318 - 338)	87
V	41.4	47 (45 - 50)	90

exception being 1632(b) where recovery was 98%. The values obtained for potassium were in good agreement with those of the certificates, the exception being SARM 19 and 20, where values exceeded those given on the certificate.

6.6.1 Conclusion to optimisation studies and subsequent coal analysis.

Slurry atomisation ICP-AES shows promise as a technique for the rapid determination of major, minor and trace elements in coal. The plasma was optimised for aluminium and consequently its recoveries improved as shown in Tables 32-36. Using the conditions which were optimal for aluminium, levels of Ca, Ti, Mg, K, Mn, Cu, Ba, Sr, V and Zn were determined and showed reasonable agreement with the certificate values. The agreement with certificate values would presumably improve if a more typical element was optimised, one which did not show such peculiar behaviour as aluminium.

Unfortunately, direct comparison with the results achieved in section 6.4.1, Tables 22-26 is not possible as the certified coals examined in the latter section, were not available at the time of analysis. The uniformity to which the samples were ground contributes to the accuracy and precision, often better than 2% RSD, which accompanies this technique. This should be acceptable for routine monitoring of trace elements in coal.

Preliminary investigations show that the ARL spray chamber, with the spoiler removed together with the low injector flow rates, yielded results which are in excellent agreement with the certified values. However, the object of the aluminium simplex was to attempt to improve the recovery of aluminium typically 70-80% under normal analytical conditions, to 100%, which come to fruition as shown in Tables 32-36.

Hence the technique of slurry atomisation has been successfully adapted to the ARL 3520 with minimum instrumental modifications. The determination of major, minor and trace elements, together with careful control of the instrumental conditions have allowed the successful determination of elements such as aluminium, which have in the past proved difficult to determine using slurry atomisation.

The technique has the benefits of rapidity, owing to elimination of digestion procedures and the ability to perform elemental analysis on solid samples using aqueous calibration.

6.7   COAL ANALYSIS USING THE PLASMAKON

The instrument was described in section 6.2.1 and is shown schematically in Figure 22. The objective of the study was to observe the effect of a larger diameter injector tube 3 mm i.d. in comparison to the 1.8 mm i.d. injector used in the earlier studies with the ARL instrumentation.

The three elements determined initially were aluminium, iron and zinc, the operating conditions used for these determinations are shown in Table 37. The coal slurries were ground and prepared as previously described in section 5.5.1. Ten integrations were performed for each element in the standard and the sample.

TABLE 37

Operating conditions for Plasmakon S - 35 ICP

Power / kW	1.7
Gas flows / $lmin^{-1}$	
Coolant	16
Auxiliary	0.8
Injector	1.7
Injector diameter i.d. /mm	3
Nebuliser type	Ebdon (V - Groove)
Torch	Greenfield

Element	Wavelength/nm
Al	308.215
Fe	258.588
Zn	213.856

6.7.1 Results and discussion

Table 38 shows the results of the determination of Al, Fe and Zn in four certified coals, namely NBS 1632(a), NBS 1635, BCR 181 and BCR 182. The iron results for 1632(a) and 1635 show reasonable agreement with the certificate values, whilst the only comparative values for BCR 181 and 182 are the results obtained from the work performed on the ARL 3520 ICP, which are lower in comparison to the Plasmakon S-35 results. The aluminium results are low in comparison for both 1632(a) and 1635. There is good agreement for zinc, the exception being 1635 where the value is elevated.

Clearly the problem of low aluminium recovery was again apparent from these results, therefore a simplex optimisation was performed to elucidate the optimum conditions for aluminium recovery using the Plasmakon S-35.

6.8 SIMPLEX OPTIMISATION OF PLASMA PERFORMANCE FOR THE DETERMINATION OF ALUMINIUM

As previously mentioned recoveries of aluminium were consistently low. Therefore following the success of the optimisation of the ARL 3520 for aluminium recovery, the same technique was applied to the Plasmakon S-35. The ratio of corrected signal for slurry over the corrected signal for solution was used as a criterion of merit on aqueous solution of equivalent aluminium concentration to that expected in the slurry. The aluminium 308.215 nm line was used for the optimisation in NBS 1635 which had been ground using the bottle and bead method, so as to reduce the particle size to 100% below 1.9 μm.

6.8.1 Results and Discussion

The five optimal conditions found by the simplex search for the various flow rates, power settings and observation heights are shown in Table 39. Aluminium recoveries were increased to between 97 and 107%. The conditions show a high injector flow rate, which in effect decreases the residence time in the plasma. The auxiliary flows are slightly higher

TABLE 38

Determination of aluminium, iron and zinc in NBS 1632(a), NBS 1635, BCR 181 and BCR 182 reference coals using Plasamakon S-35.

	1632(a)			NBS 1635	
Element	Slurry atomisation % m/v	Certificate Value % m/v	Element	Slurry atomisation % m/v	Certificate Value % m/v
Fe	1.08 ± 0.02	1.11 ± 0.02	Fe	0.217 ± 0.001	0.239 ± 0.005
Al	2.28 ± 0.04	[3.1]	Al	0.268 ± 0.011	[0.32]
	$\mu g\ g^{-1}$	$\mu g\ g^{-1}$		$\mu g\ g^{-1}$	$\mu g\ g^{-1}$
Zn	25.2 ± 1.4	28 ± 2	Zn	7.5 ± 0.5	4.7 ± 0.5

	BCR 181			BCR 182	
Element	Slurry atomisation % m/v	Certificate Value % m/v	Element	Slurry atomisation % m/v	Certificate Value % m/v
Fe	0.32 ± 0.01	(0.27)[1]	Fe	0.75 ± 0.02	(0.67)[1]
Al	0.225 ± 0.07	(0.217 ± 0.06)[2]	Al	1.25 ± 0.06	(1.53 ± 0.04)[2]
	$\mu g\ g^{-1}$	$\mu g\ g^{-1}$		$\mu g\ g^{-1}$	$\mu g\ g^{-1}$
Zn	8.0 ± 0.4	(8.1 ± 0.3)[2]	Zn	26.2 ± 2	33.3 ± 1.5

[ ] = non certified values   (1)   = Values from TABLE 28 (ARL)

(2)   = Values from TABLE 26 (ARL)

TABLE 39

Final simplex vertices for optimisation of operating conditions for Plasmakon S-35.

Injector / lmin^{-1}	Auxilary / lmin^{-1}	Coolant / lmin^{-1}	r.f. Power / kW	Height /mm	Response
2.69	1.69	22.29	1.33	14.3	101.5
2.69	0.77	17.00	1.24	12.2	102.5
2.95	1.55	22.56	1.38	5.5	97.1
3.00	1.75	22.79	1.30	9.7	107.3
2.59	1.54	20.05	1.50	8.8	104.3

than normal, whilst there is no increase in the coolant flow. Not much variation in the power is evident although this has been optimised to run at slightly lower power than would normally be used routinely. The greatest variation is noticed with the height of observation. The first two responses of the final simplex are 14 mm and 12 mm respectively, whilst the last vertex has a height as low as 5 mm. In essence a similar trend to that seen on the ARL 3520 has emerged where the optimisation favours a high injector flow rate, slightly lower power and reduced observation height, which contribute to a short residence time in the plasma. A comparison of plasma conditions before and after the simplex optimisation are shown in Table 40. Confirmation that this corresponded to optimal conditions was obtained using the method of univariate searches (101). In this method one parameter is altered whilst the other parameters are held constant at the optimum value defined by the simplex method. This provided information on the influence of each individual parameter on the operation and performance of the plasma. The univariate searches are shown in Figures 40 - 42 inclusive. On each plot a graph of signal ratios of slurry and solution is plotted against the parameter of interest. This in effect shows that the simplex optimisation successfully identified the local optima in the plasma as a region where the signal from the solution and slurry are similar.

There seems to exist some uncertainty about the actual optimum identified by the simplex method on this occasion. One must take into consideration the complex criterion of merit used which consisted of a ratio which under optimisation may become distorted by errors. Secondly the contours of factor space as defined by the criterion of merit, are very flat and this does not assist the simplex procedure, which prefers sharp peaks created by well defined contours.

With regards to the aluminium optimisation, there seems to be two potential regions which have been identified by the optimisation procedure. From Table 39, it is evident that the preferred viewing height is low in the plasma, between 5 and 14 mm above the load coil.

TABLE 40

Conditions used prior to and after simplex optimisation for determination of aluminium in coal.

	Pre-simplex	Post simplex
Al Recovery / %	75 - 80	97 - 120
Injector gas / $lmin^{-1}$	1.5	2.7
Plasma gas / $lmin^{-1}$	0.8	0.9
Coolant gas / $lmin^{-1}$	15.0	18.0
Power / kW	1.5	1.3
Height / mm	20.0	11.0

FIGURE 40

Univariate search of vertical viewing height for aluminium

FIGURE 41

Univariate search of plasma power for aluminium
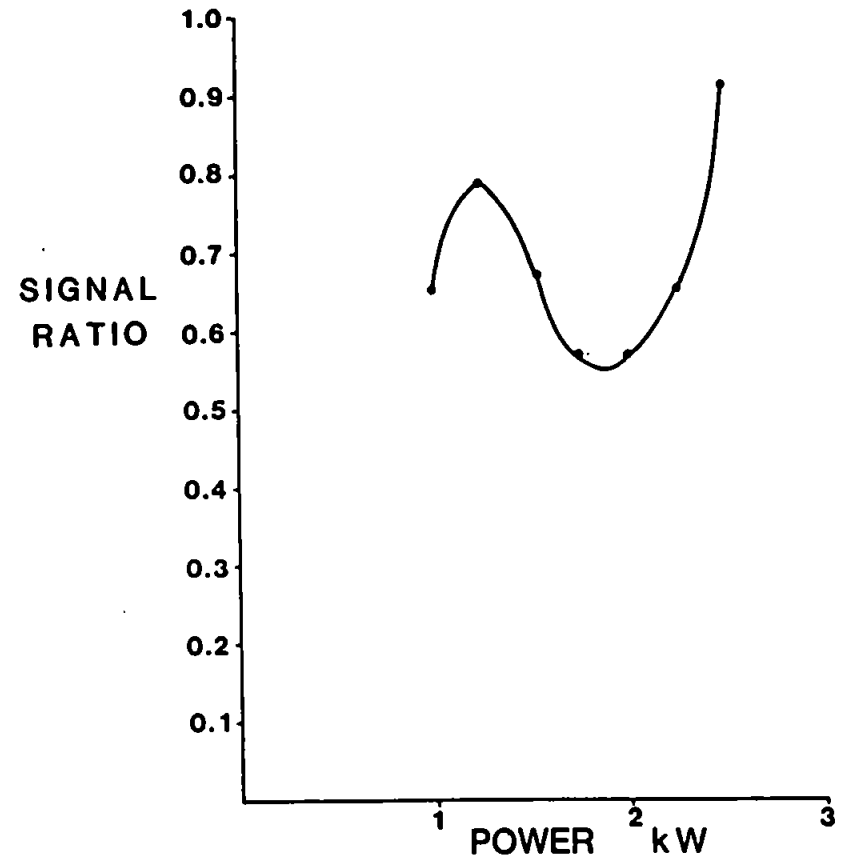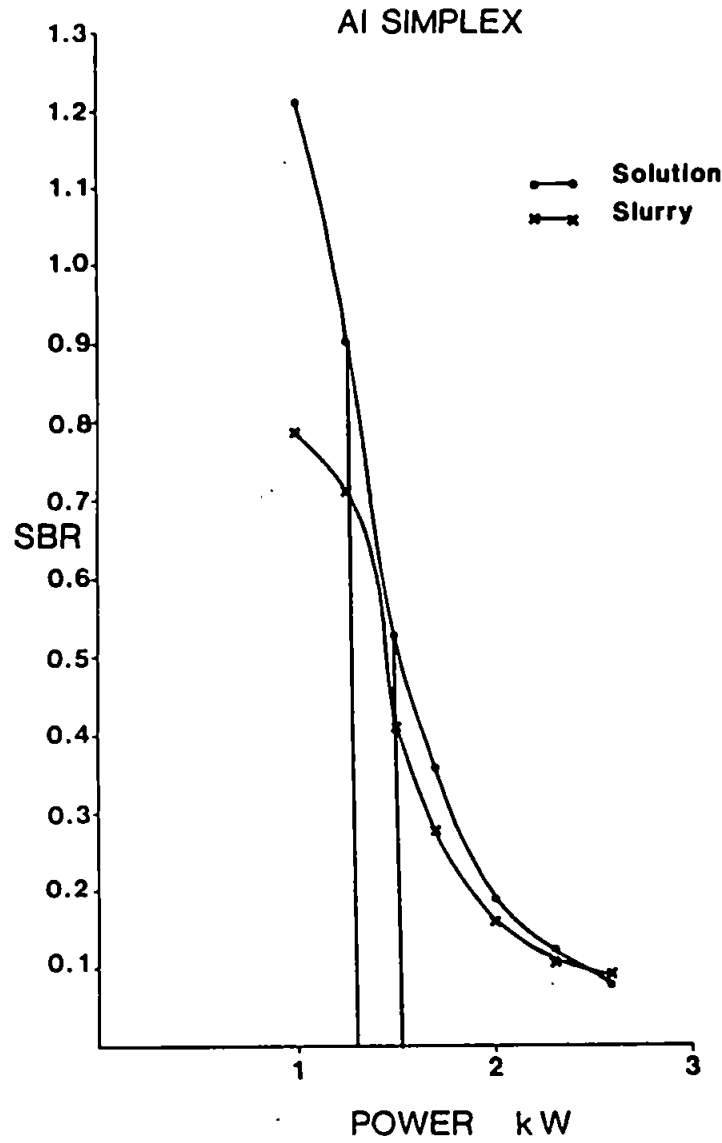
FIGURE 42

Univariate search of carrier gas flow rate for aluminium

AI SIMPLEX
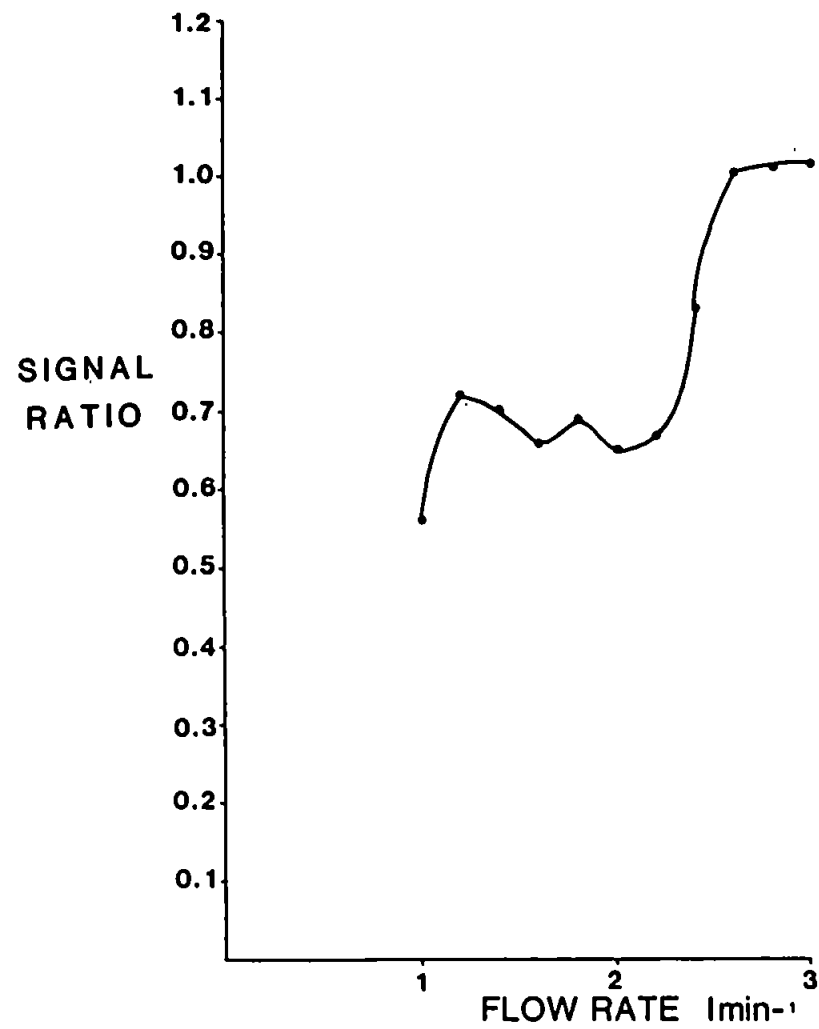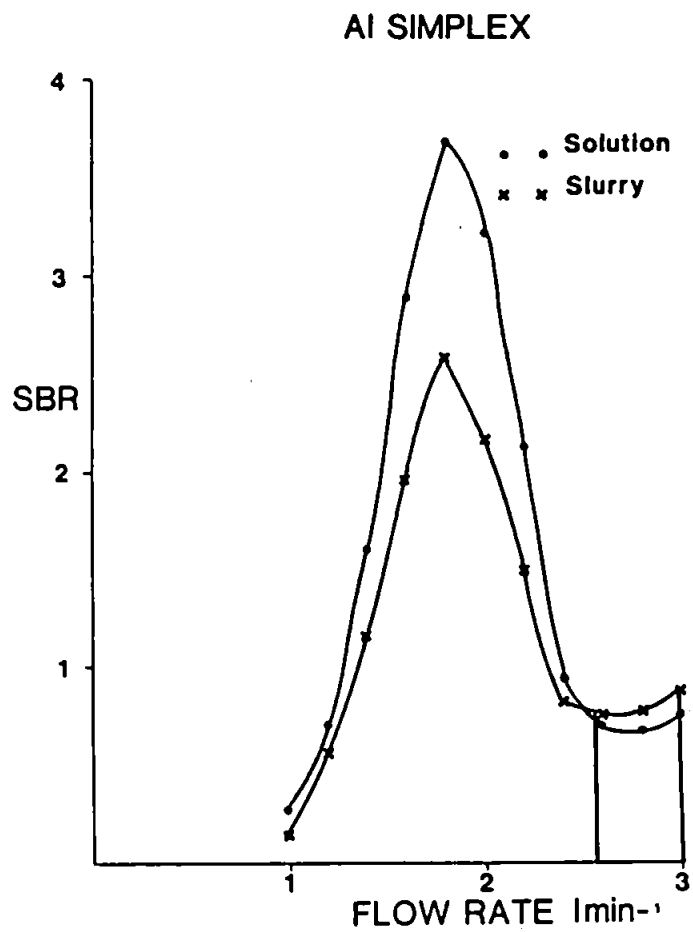
Examination of Figure 40 confirms this as the maximum signal to background ratio (SBR) peak for both slurry and solution is at a height of 10 mm. However the plot of signal ratio of slurry and solution against observation in height Figure 40, show that the optimal conditions as regards the ratio of the two signals is higher in the plasma than indicated by the univariate search. This is possibly explained by the presence of two potential regions in the plasma where the atomisation of aluminium occurs and which corresponds to the conditions laid down by the criterion of merit. The first region is low in the plasma, below the normal analytical zone (NAZ) as identified by the simplex procedure. This is a high energy region and allows the destruction of the aluminium-oxygen species, thereby enhancing the recovery of aluminium. However in this region the plasma temperature is high, but also the argon continuum background is intense and thus not favoured for normal analytical emission observations. The second region is high up in the plasma as identified in Figure 40 where the signal ratios plot identified a maximum peak 40 mm above the load coil. Although this region is cooler, the increased residence time of the plasma would contribute to the complete atomisation of the aluminium species.

Clearly it can be seen that the simplex optimisation has identified the two local optima where increased aluminium atomisation is possible. Of these two local optima it seems likely that the former possibility low down in the plasma is unpredictable and therefore there is a need for the assurance that the optimisation procedure has identified the correct optima. This could be achieved by commencing the optimisation in a different orientation, i.e. with new starting conditions, thereby allowing the optimisation to approach the optima from a new direction.

Figure 41 illustrates how the slurry/solution signal ratio/against power has identified a optimal power of 1.3 kW. However on examination of Figure 41, it is possible to see two optima, the first corresponding to 1.3 kW, the second to 2.5 kW. The latter seems more realistic as it is where the slurry and solutions exhibit the same magnitude of signal.

Thus the invariate searches allow a better understanding of simplex optimisation for the results of observation height and power. The simplex defines these optima as low viewing height and power whereas the univariate search suggests a higher observation height and power might be more practical. There is agreement between the simplex and invariate search that a high carrier gas flow rate is optimal, although here again there is a second sub-optimal condition at very low carrier gas flow rate, Figure 42.

Calibration of each of the five simplex conditions was achieved using aqueous standards and subsequent determinations of aluminium in coal NBS 1635 at each suggested condition all resulted in recoveries between 97 and 120%. A comparison of plasma conditions before and after the simplex optimisation are shown in Table 40.

6.9   DETERMINATION OF Ca, Mn, Ni and Cu in 1632(a) and 1635 REFERENCE COALS

The Plasmakon S-35, described in Section 6.2.1 was used for the determination of Ca, Mn, Ni and Cu in reference coals 1635 and 1632(a). The instrument was calibrated using aqueous standards and conditions described in Table 41. The coals were ground and prepared as described in Section 5.5.1.

6.9.1. Results and discussion

The results obtained for the analysis of 1635 and 1632(a) are shown in Tables 42 and 43 respectively. The value for Ca in 1635 is low by comparison with the value reported by Gladney (201) and also the value obtained using the ARL ICP which had a injector of 1.8 mm i.d. The reason for this is unclear as the particle size of 1635 is 100%, below 10 μm. The agreement between 1632(a) and the certificate is better, though not as good as the results achieved using the ARL 3520, see Table 43. The particle size of this coal as shown in Figure 43 was larger than the 8 μm cut off which has been found to be critical in the sample transport system of this instrument (120). As previously mentioned, the use of a

- 145 -

TABLE 4 1

Operating conditions for plasmakon S-35 ICP for the determination of calcium, manganese, nickel and copper.

Power / kW	1.7
Gas flows / 1 min^{-1}	
Coolant	16
Auxiliary	0.4
Injector	1.7
Injector diameter/ mm	3
Element	Wavelength / nm
Ca	317.933
Mn	293.936
Ni	361.939
Cu	324.754

TABLE 42

Determination of calcium, nickel and copper in reference coal 1635.

Element	Slurry Atomisation $\mu g \ g^{-1}$	Certificate Value $\mu g \ g^{-1}$
Ca	3100 + 30	5600 + 200[*]
Mn	16.3 + 2.2	21.5 + 1.5
Ni	43.5 + 0.9	1.74 + 0.1
Cu	6.4 + 0.4	3.6 + 0.3

* = Values reported by Gladney (201).

TABLE 43

Determination of calcium, manganese, nickel and copper in reference coal 1632(a).

Element	Slurry Atomisation $\mu g \ g^{-1}$	Certificate Value $\mu g \ g^{-1}$
Ca	2200 + 21	2300 + 300
Mn	25.2 + 1.4	28 + 2
Ni	640 + 8	19.4 + 1.0
Cu	16.1 + 0.1	16.5 + 1.0

FIGURE 43

Particle size distribution of coal NBS SRM 1632(a)
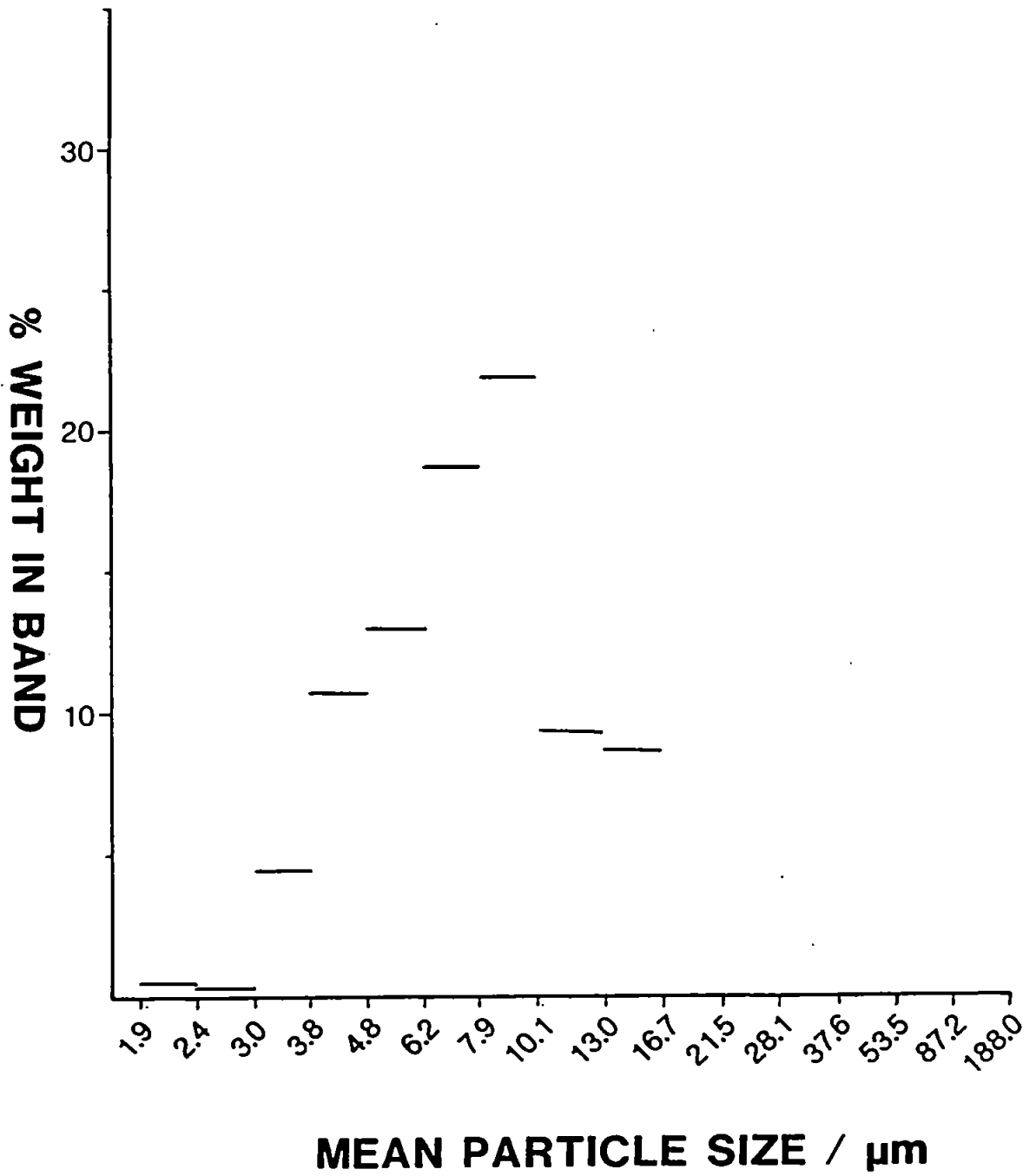
double pass spray chamber with its tortuous bends limits the size of particle reaching the plasma, and this could be a possible explanation why using the ARL system higher recoveries were achieved, due to the fact that larger particles can reach the plasma.

The values for manganese are low for both coals in comparison to the certificate value, again unlike the values reported using the ARL instrument which show complete recovery see Table 28. However the values obtained for nickel in both reference coals varied drastically in comparison to the certificate value. The most probably cause was contamination of the sample and this is discussed in Section 6.10. Finally the results for copper were in good agreement for 1632(a), however the 1635, the result from slurry atomisation is higher than the certified value.

Only reasonable results were obtained using the plasma with a 3 mm injector and were slightly disappointing considering the good recoveries achieved using a system with a smaller injector.

6.10 ANALYSIS OF ZIRCONIA GRINDING ELEMENTS

As previously mentioned, results for nickel were abnormally high, which indicated sample contamination. The most likely stage for contamination is in the grinding step, where the coals are ground using zirconia balls as grinding elements. It was noticed that after prolonged grinding, the surface of the balls were pitted and thus would cause concern as a possible source of contamination of the sample.

Therefore analysis of the grinding elements was undertaken to establish their composition on solution samples obtained using a sodium peroxide fusion and using ICP-AES for the determination.

6.10.1 Experimental procedure for Sodium Perioxide fusion

The zirconia balls (50 g) were ground using a Teamer mill with tungsten carbide grinding elements, which reduced the particle size so that the sample passed through a 125 μm sieve after 3 minutes grinding. The ground material (0.1 g) was weighed accurately into a zirconium crucible and Na_2O_2 (1 g) was added. The powders were mixed thoroughly and covered by a layer of Na_2O_2 (0.5 g). The powders were fused in a muffle furnace at 700° for 1 hour. The fused mixture was swirled frequently to ensure a even dispersion of the flux. The crucible was allowed to cool to room temperature and then placed in a 250 ml glass beaker covered with a watch glass. From under the lid water was added together with concentrated nitric acid (5 ml) and swirled until a further amount of nitric acid was added (5 ml). The beaker was turned on its side and emptied of its contents, which were brought to the boil and then allowed to cool and made up to 100 ml.

The analytical system used in this study was the Plasmakon S-35 which has been previously described in Section 6.2.1.

6.10.2 Results of zirconia ball analysis and discussion

The results of the grinding element analysis are given in Table 44. It is evident that there is a high proportion of nickel present in the grinding elements and it is feasible that contamination of the coal could occur if pitted zirconia grinding balls were used owing to the fragments of the balls entering the sample. Minor constituents in the zirconia balls include Fe, Ti, B and Mg, whilst levels of Cr, Zn, Cd, Pb, Co, Mn, V, Cu and Sc were below the limit of detection.

As a result of this analysis and to ensure no further contamination of coal samples, new grinding elements were used with each grinding preparation of the coals.

TABLE 44

Determination of major and minor elements in a sodium peroxide fusion of zirconia grinding elements.

Element	Wavelength nm	Fusion analysis by ICP - AES % m/v
Ni	221.647	2.0
Al	309.278	0.1
		ug g^{-1}
Fe	238.204	300
Ti	334.941	270
B	249.773	60
Mg	279.553	27
Cr	205.552	<20
Zn	213.856	<20
Cd	214.438	<20
Pb	220.353	<20
Co	238.892	<20
Mn	257.610	<20
V	309.311	<20
Cu	324.754	<20
Sc	361.384	<20

6.11 COAL ANALYSIS AT BRITISH COAL LABORATORIES

The purpose of the visit to the British Coal laboratories was to adapt existing instrumentation for the successful analysis of coals by ICP-AES slurry atomisation.

Conventional analysis of coal ash was performed in solution after a hydrofluoric dissolution procedure as described by Pearce et al. (33). The instrumentation used was similar to that previously described in Section 6.2.2 and minor modifications were implemented. These modifications included the replacement of the Meinhard nebulizer with a Ebdon V-groove nebulizer and pump, as well as replacing the standard ARL spray chamber (Figure 25), with a double pass spray chamber which is commercially available (PS Analytical) and shown in Figure 44.

6.11.1 Results and discussion

The spectral lines were selected on the appraisal of signal to background ratio and freedom from spectral interferences. This was achieved by scanning the spectrum of a 2% m/m slurry of 1635 and selecting the spectral lines of interest having established that no interferences existed, and that the background was not elevated. The spectral lines used in the analysis of various coals are shown in Table 45. Calibration was achieved using aqueous standards and the instrument was operated using similar conditions to those described previously (10) in routine laboratory use.

Duplicate samples were taken from certified reference coals NBS 1632(b), SARM 18, 19 and 20 and their moisture content determined as described in BS 1016 (14): Part 1 total moisture of coal. A known mass of coal is heated to constant mass in a current of nitrogen in an oven maintained at 105°C to 110°C from which the percentage moisture is calculated from the

FIGURE 44

Commercially available double pass spray chamber

TO PLASMA

AEROSOL

TO DRAIN
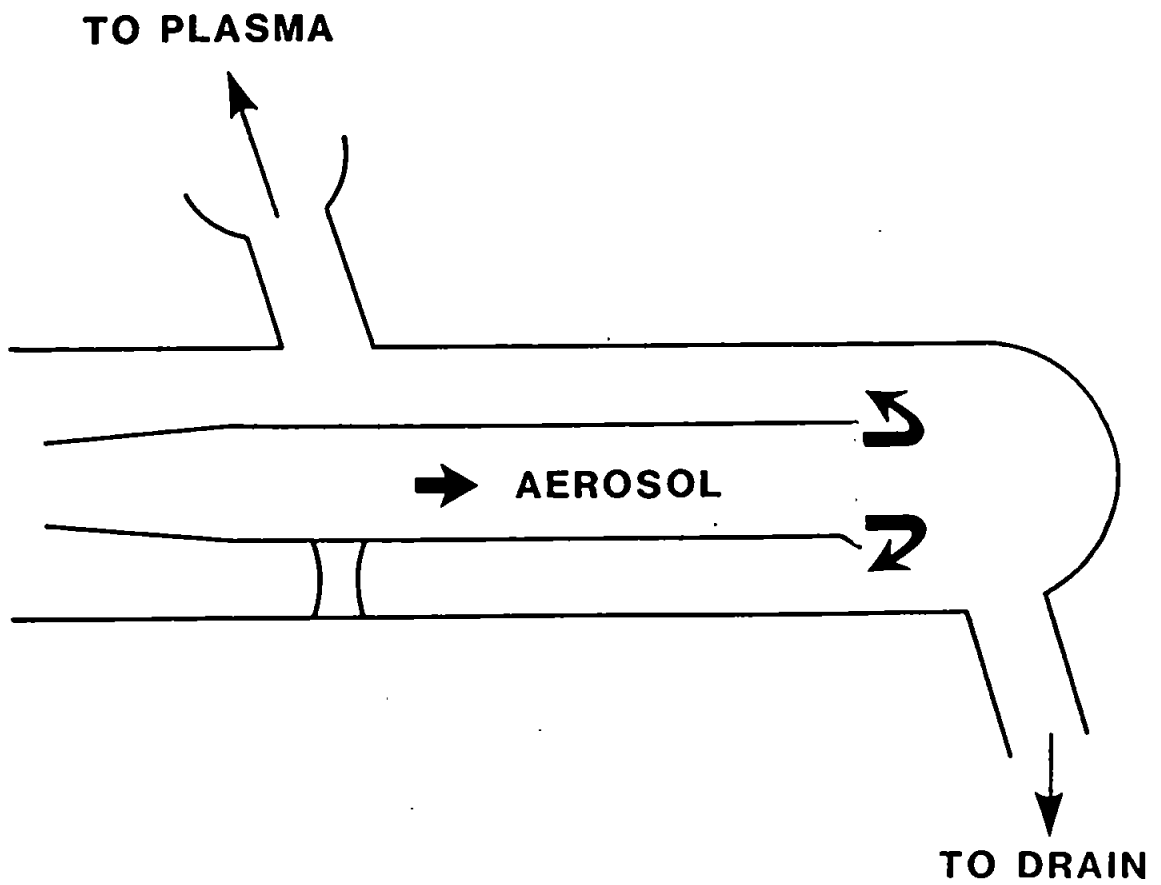
TABLE 45

Spectral lines used for the analysis of coals.

Element	Wavelength nm	Order
Cr	267.716	2
Mn	257.610	2
Al	308.215	2
Fe	259.940	2
Cu	324.754	2
Ca	317.933	2
Sr	407.771	1
Ti	337.280	2
V	292.402	2
Mg	279.080	2
Zn	213.856	3
Co	228.616	3
Ni	231.604	2
Mg	383.826	2

TABLE 46

Moisture content (%) of NBS 1632(b) SARM 18, 19 and 20.

Sample	Moisture % m/m
NBS 1632(b)	1.6
SARM 18	3.5
SARM 19	5.4
SARM 20	6.2

loss in the mass of coal. The results of this analysis are shown in Table 46 and were taken into account when the determination of major, minor and trace elements was performed on these coals.

Having modified the instrumentation for the analysis of coals by slurry atomisation, preliminary investigations were performed to elucidate the optimum conditions using the commercially available spray chamber. This was achieved by the determination of various elements in coal at different instrument settings and comparing the achieved results to those of the certified value. Power, injector flow rate and spray chamber design were the parameters which were varied. When instrumentation conditions which achieved 90-100% recovery was found, analysis of reference coals was performed. However on examination, the results proved disappointing owing to low recoveries and poor relative standard deviations. These poor results were attributed to a design fault in the spray chamber. It was apparent that the central tube did not fit flush with the face of the nebulizer, therefore instead of the produced aerosol travelling along its length, as designed, the generated aerosol flowed into the outer cavity and straight into the injector outlet. This had the effect of allowing excessively large water particles to pass into the plasma, and transmission of pulses from the peristatic pump due to inefficient damping. These two factors contributed to the poor precision and accuracy obtained in the initial analysis.

In order to overcome this problem, the central tube was extended so as to become flush with the nebulizer. This was achieved by placing some stiff polyethylene tubing over the central tube, which was cut to length so that the nebulizer fitted tightly against it.

The analysis was repeated and the results for the certified coals are shown in Table 47-55. It is clear to see that the obtained results show excellent agreement with the certified values using the instrument conditions shown in Table 56. Table 47 shows good correlation between results obtained by slurry atomisation for NBS 1632(b) and the certified value.

TABLE 47

Determination of major, minor and trace elements in NBS 1632(b) reference coal by ICP – AES slurry atomisation using double pass spray chamber.

Element	Slurry Atomisation % m/v	Certificate Value % m/v	Recovery (slurry/cert) %
Al	0.692 ± 0.022	0.855 ± 0.019	81
Fe	0.685 ± 0.021	0.759 ± 0.045	90
Ca	0.184 ± 0.002	0.204 ± 0.006	90
	$\mu g\ g^{-1}$	$\mu g\ g^{-1}$	
Ti	344 ± 3	454 ± 17	76
Mg (ion)	304 ± 2	383 ± 8	79
Mg (atom)	366 ± 2	383 ± 8	96
Mn	12.1 ± 0.9	12.4 ± 1	100
Cu	6.1 ± 0.4	6.28 ± 0.3	97
Sr	99.6 ± 5.0	(102)	98
V	11.0 ± 0.2	(14)	79
Zn	10.2 ± 0.1	11.89 ± 0.78	86
Co	3.1 ± 0.1	2.29 ± 0.17	133
Ni	7.0 ± 0.5	6.10 ± 0.27	114
Cr	12.5 ± 1.6	(11)	113

( ) = uncertified values.

TABLE 48

Determination of major, minor and trace elements in NBS 1632(a) by
ICP - AES slurry atomisation using double pass spray chamber.

Element	Slurry Atomisation % m/v	Certificate Value % m/v	Recovery (slurry/cert) %
Al	2.56 ± 0.04	(3.1)	87
Fe	1.03 ± 0.01	1.11 ± 0.02	93
Ca	0.254 ± 0.001	0.230 ± 0.01	110
Ti	0.161 ± 0.001	(0.18)	89
	$\mu g \ g^{-1}$	$\mu g \ g^{-1}$	
Mg (ion)	877 ± 12	600 - 1300*	
Mg (atom)	1060 ± 1	600 - 1300*	
Mn	29.3 ± 0.4	28.2 ± 2	104
Cu	16.3 ± 0.1	16.5 ± 1	99
Sr	94.5 ± 1.0	(88)	107
V	39.8 ± 0.7	44 ± 3	90
Zn	26.0 ± 0.6	28 ± 2	93
Co	9.3 ± 0.5	(6.8)	137
Ni	18.5 ± 1.0	19.4 ± 1	95
Cr	33.0 ± 0.5	34.4 ± 1.5	96

* = Values reported by Gladney (201)

( ) = Values not certified.

TABLE 49

Determination of major, minor and trace elements in NBS 1635 by ICP - AES Slurry Atomisation using double pass spray chamber.

Element	Slurry Atomisation % m/v	Certificate Value % m/v	Recovery (slurry/cert) %
Al	0.240 ± 0.001	(0.32)	75
Fe	0.177 ± 0.016	0.239 ± 0.005	74
Ca	0.395 ± 0.001	0.560 ± 0.02*	71
	$\mu g\ g^{-1}$	$\mu g\ g^{-1}$	
Ti	158 ± 5	(200)	79
Mg (ion)	575 ± 7	980*	59
Mg (atom)	658 ± 22	980*	67
Mn	14.3 ± 0.5	21.± 1.5	67
Cu	3.1 ± 0.5	3.6 ± 0.3	86
Sr	105 ± 1.5	140*	75
V	3.2 ± 0.1	5.2 ± 0.5	62
Zn	4.0 ± 0.7	4.7 ± 0.5	86
Co	1.1 ± 0.4	(0.65)	169
Ni	3.0 ± 1.8	1.74 ± 0.1	172
Cr	6.5 ± 0.4	2.5 ± 0.3	260

( ) = Values not certified.

* = Values reported by Gladney (201).

TABLE 50

Determination of major, minor and trace elements in SARM 20 coal by
ICP - AES slurry atomisation using a double pass spray chamber.

Element	Slurry Atomisation % m/v	Certificate Value % m/v	Recovery (slurry/cert) %
Al_2O_3	9.33 ± 0.18	11.27 (11.16-11.73)	83
Fe_2O_3	0.981 ± 0.009	1.17 (1.15 - 1.19)	84
CaO	1.588 ± 0.041	1.87 (1.85 - 1.89)	85
TiO_2	0.540 ± 0.003	0.63 (0.61 - 0.65)	86
MgO (ion)	0.33 ± 0.001	0.43 (0.41 - 0.45)	77
Mg (atom)	0.39 ± 0.39	0.43 (0.41 - 0.45)	92
	$\mu g\ g^{-1}$	$\mu g\ g^{-1}$	
Mn	70.2 ± 0.4	80 (77 - 82)	88
Cu	16.4 ± 0.3	18 (15 - 19)	93
Sr	314 ± 0.1	330 ± (318 - 336)	95
V	42.3 ± 0.1	47 ± (45 - 50)	90
Zn	15.9 ± 1.1	17 ± (14 - 18)	94
Co	16.3 ± 0.1	8.3 ± (76 - 90)	196
Ni	226 ± 0.1	25 (23 - 26)	91
Cr	64.2 ± 1.3	[67]	

[ ] = Value not certified.

TABLE 51

Determination of major, minor and trace elements in SARM 19 coal by ICP - AES slurry atomisation using a double pass spray chamber.

Element	Slurry Atomisation % m/v	Certificate Value % m/v	Recovery (slurry/cert) %
Al_2O_3	6.93 ± 0.59	8.01 (7.86 - 8.15)	87
Fe_2O_3	1.49 ± 0.10	1.75 (1.73 - 1.76)	85
CaO	1.19 ± 0.08	1.39 (1.37 - 1.41)	86
TiO_2	0.295 ± 0.019	0.341 (0.324 - 0.356)	87
MgO (ion)	0.165 ± 0.013	0.20 (0.20 - 0.22)	82
MgO (atom)	0.214 ± 0.017	0.20 (0.20 - 0.22)	107
	$\mu g\ g^{-1}$	$\mu g\ g^{-1}$	
Mn	123 ± 7	157 ± (143 - 168)	78
Cu	11.3 ± 0.8	13 (11 - 14)	87
Sr	116 ± 8.0	126 (125 - 141)	92
V	29.6 ± 2.0	35 (33 - 37)	85
Zn	12.9 ± 0.5	12 (12 - 16)	100
Co	8.0 ± 0.1	5.6 (5 - 6.6)	143
Ni	13.9 ± 2.7	16 (13 - 20)	87
Cr	45.3 ± 2.3	50 (47 - 58)	91

TABLE 52

Determination of major, minor and trace elements in SARM 18 coal by ICP – AES slurry atomisation.

Element	Slurry Atomisation % m/v	Certificate Value % m/v	Recovery (slurry/cert) %
Al_2O_3	2.44 $\pm$ 0.009	2.57 (2.54 – 2.61)	95
Fe_2O_3	0.248 $\pm$ 0.002	0.29 (0.28 – 0.29)	86
CaO	0.145 $\pm$ 0.001	0.18 (0.17 – 0.19)	81
TiO_2	0.090 $\pm$ 0.001	0.144 (0.111 – 0.116)	79
MgO (ion)	0.088 $\pm$ 0.001	0.11 (0.10 – 0.11)	80
MgO (atom)	0.112 $\pm$ 0.001	0.11 (0.10 – 0.11)	101
	$\mu g\ g^{-1}$	$\mu g\ g^{-1}$	
Mn	19.3 $\pm$ 0.2	22 (21 – 23)	83
Cu	4.5 $\pm$ 0.9	5.9 (5.2 – 6.4)	77
Sr	41.7 $\pm$ 0.9	44 (42 – 45)	95
V	17.8 $\pm$ 0.5	23 (21 – 25)	78
Zn	6.1 $\pm$ 0.6	5.5 (5.2 – 6.8)	107
Co	5.7 $\pm$ 0.2	6.7 (5.5 – 7.2)	85
Ni	8.1 $\pm$ 0.4	10.8 (10.1 – 11.5)	75
Cr	13.3 $\pm$ 0.5	16 (14 – 18)	83

TABLE 53

Determination of major, minor amd trace elements in BCR 40 by ICP - AES slurry atomisation using a double pass spray chamber.

Element	Slurry Atomisation % m/v	Certificate Value % m/v	Recovery (slurry/cert) %
Al	1.526 + 0.024	-	-
Fe	0.879 + 0.008	-	-
Ca	0.168 + 0.003	-	-
Ti	0.080 + 0.002	-	-
Mg (ion)	0.115 + 0.002	-	-
Mg (atom)	0.118 + 0.005	-	-
	$\mu g\ g^{-1}$	$\mu g\ g^{-1}$	
Mn	124 + 1.0	139 + 5	90
Cu	28.2 + 1.1	-	-
Sr	41.8 + 1.0	-	-
V	47.0 + 0.6	-	-
Zn	20.9 + 1.4	30.2 + 2	70
Co	7.7 + 0.1	-	-
Ni	21.0 + 0.5	25.4 + 1.7	80
Cr	24.7 + 1.7	31.2 + 2.0	77

TABLE 54

Determination of major, minor and trace elements in BCR 181 by ICP – AES slurry atomisation using a double pass spray chamber.

Element	Slurry Atomisation % m/v	Certificate Value % m/v	Recovery (slurry/cert) %
Al	0.171 ± 0.023	-	-
Fe	0.267 ± 0.017	-	-
Ca	0.009 ± 0.001	-	-
	$\mu g\ g^{-1}$	$\mu g\ g^{-1}$	
Ti	81 ± 9	-	-
Mg (ion)	28.9 ± 5.8	-	-
Mg (atom)	48.2 ± 2.9	-	-
Mn	2.2 ± 0.5	-	-
Cu	9.3 ± 0.3	-	-
Sr	6.4 ± 0.2	-	-
V	8.2 ± 0.1	12.0 ± 0.4	68
Zn	5.5 ± 1.2	8.4 ± 0.6	66
Co	1.0 ± 0.1	-	-
Ni	3.4 ± 0.3	-	-
Cr	4.1 ± 0.8	-	-

TABLE 55

Determination of major, minor and trace elements in BCR 182 by ICP - AES slurry atomisation using a double pass spray chamber.

Element	Slurry Atomisation % m/v	Certificate Value % m/v	Recovery (slurry/cert) %
Al	1.16 ± 0.02	-	-
Fe	0.599 ± 0.003	-	-
Ca	0.166 ± 0.003	-	-
Ti	0.050 ± 0.001	-	-
Mg (ion)	0.092 ± 0.002	-	-
Mg (atom)	0.099 ± 0.001	-	-
	$\mu g\ g^{-1}$	$\mu g\ g^{-1}$	
Mn	157 ± 2.8	195 ± 6	81
Cu	9.4 ± 0.6	-	-
Sr	28.9 ± 0.2	-	-
V	19.2 ± 0.1	24.3 ± 1	79
Zn	22.9 ± 1.0	33.3 ± 1.5	70 .
Co	6.5 ± 0.5	-	-
Ni	19.9 ± 1.3	-	-
Cr	18.7 ± 1.8	-	-

TABLE 56

Operating conditions for ARL 3520 ICP at East Midland Regional laboratory (EMRL).

Power / kW	1.4
Gas flows / $lmin^{-1}$	
Coolant	14
Auxilary	0.9
Injector	0.9
Injector central diameter / mm	1.8
Viewing height / mm	16
Nebuliser type	Ebdon (V - Groove)
Torch	Fassel

Examination of the particle size analysis (Figure 45) shows that 94.7% of the coal is smaller than 7.9 μm. The results for NBS 1632(a) see Table 48, again are in excellent agreement with the certificate value, despite the particle size not being completely under 8 μm see (Figure 46). However the results for 1635 (Table 49) are disappointing considering that 100% of the particle size is below 13 μm (Figure 47).

The results for SARM 20, 19 and 18 all show excellent agreement with the certified values, (Tables 50-52) which is attributed to the particle size of the three coals existing 100% below 7.9 μm for SARM 20 and 19 (Figures 48 and 49) while for SARM 18 Figure 50, 99.9% of the particle size is less than 7.9 μm.

The results for the BCR reference coals was disappointing which is partly due to the lack of information on these coals. The low recoveries for BCR 40 Table 53 can be attributed to the large particle size of this coal as shown in Figure 51. Tables 54 and 55 show the results for BCR 181 and 182, whilst Figures 52 and 53 show the corresponding particle size analysis. When the results for BCR 181 and 182 are compared with those values achieved using the same system with the modified ARL spray chamber (Table 26) reasonable agreement is achieved, showing a similar trend. However the recovery for aluminium in all coals show a similarly low trend which can be attributed to the inability to obtain complete atomisation.

It was thought that the recoveries for the coals could be improved by the use of a 3 mm injector, but unfortunately during initial optimisation experiments with a 3 mm injector, the instrumentation developed a fault, which caused the curtailment of the experiments.

FIGURE 45

By weight particle size distribution of coal NBS SRM 1632(b)

MEAN PARTICLE SIZE / μm
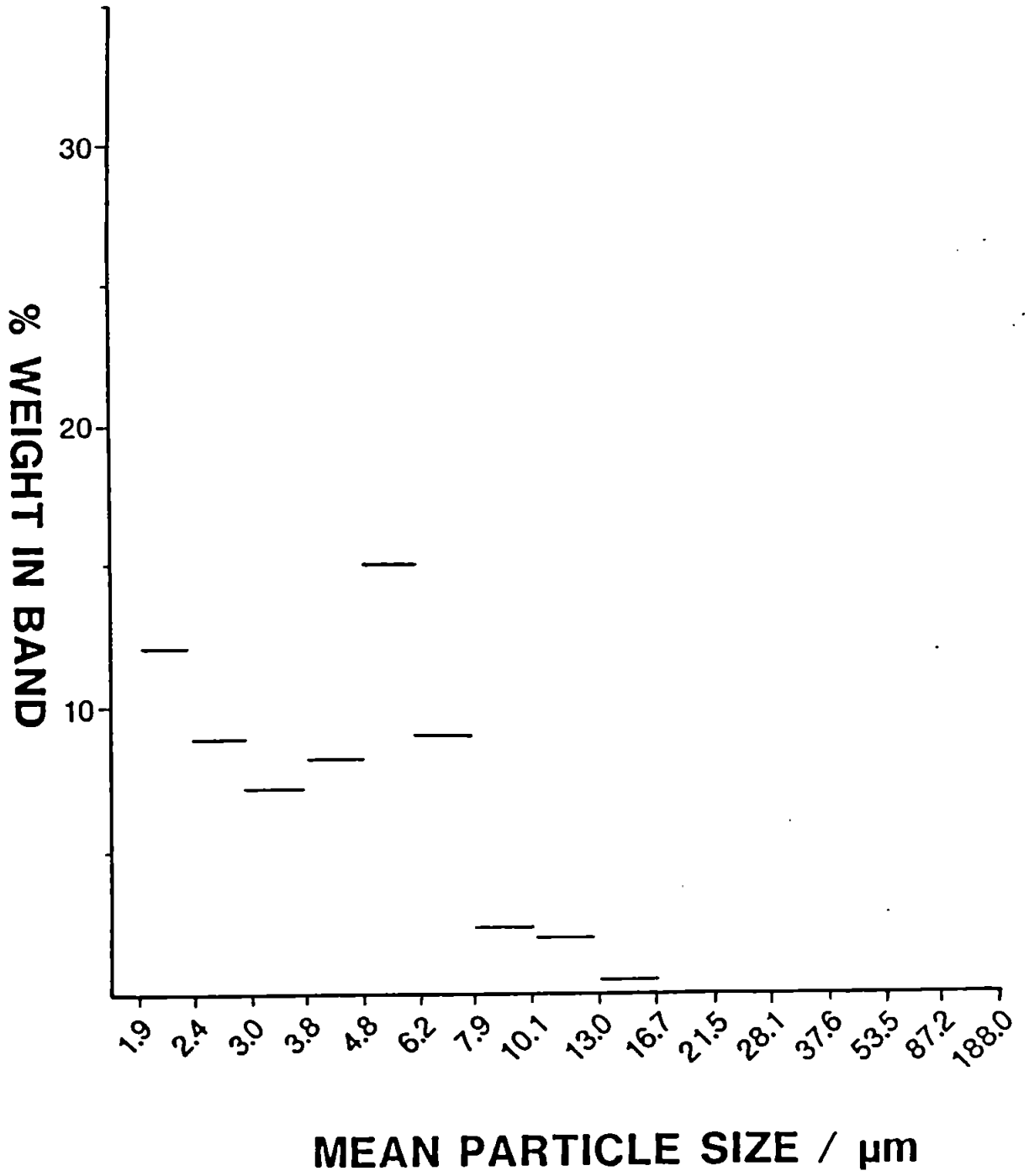
FIGURE 46

By weight particle size distribution of coal NBS SRM 1632(a)
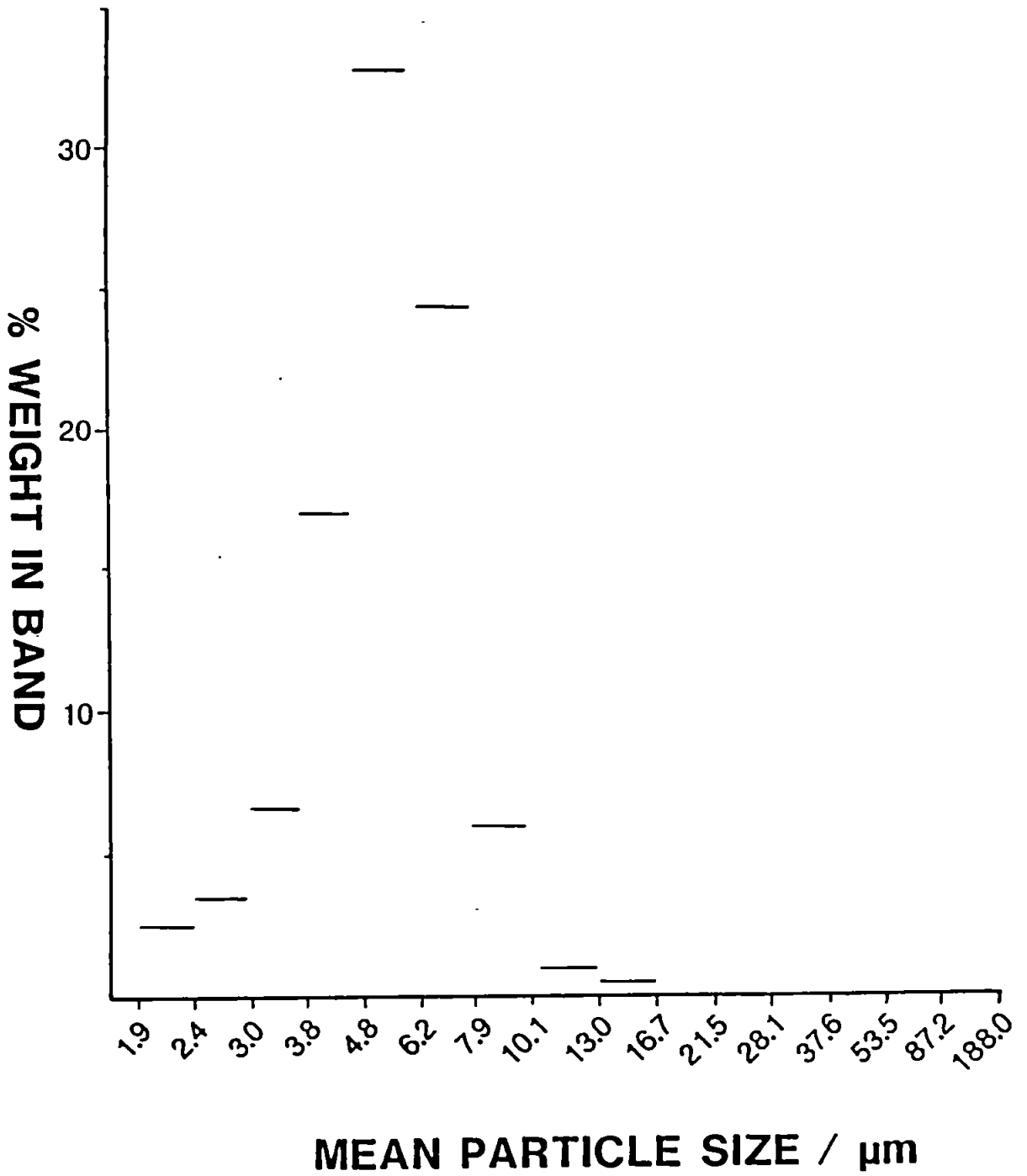
FIGURE 47

By weight particle size distribution of coal NBS SRM 1635

- 169 -
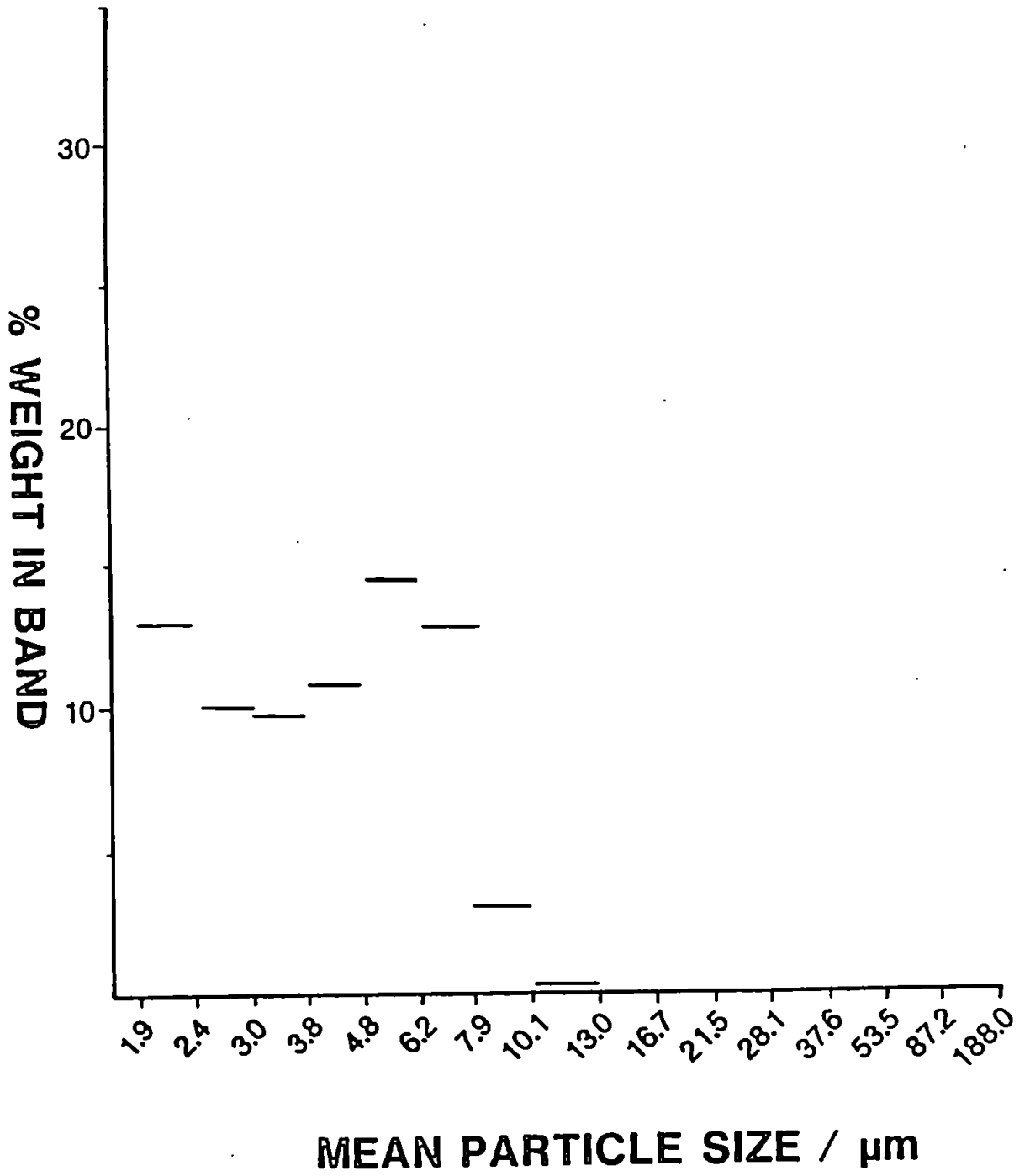
FIGURE 48

By weight particle size distribution of coal SA 20

- 170 -
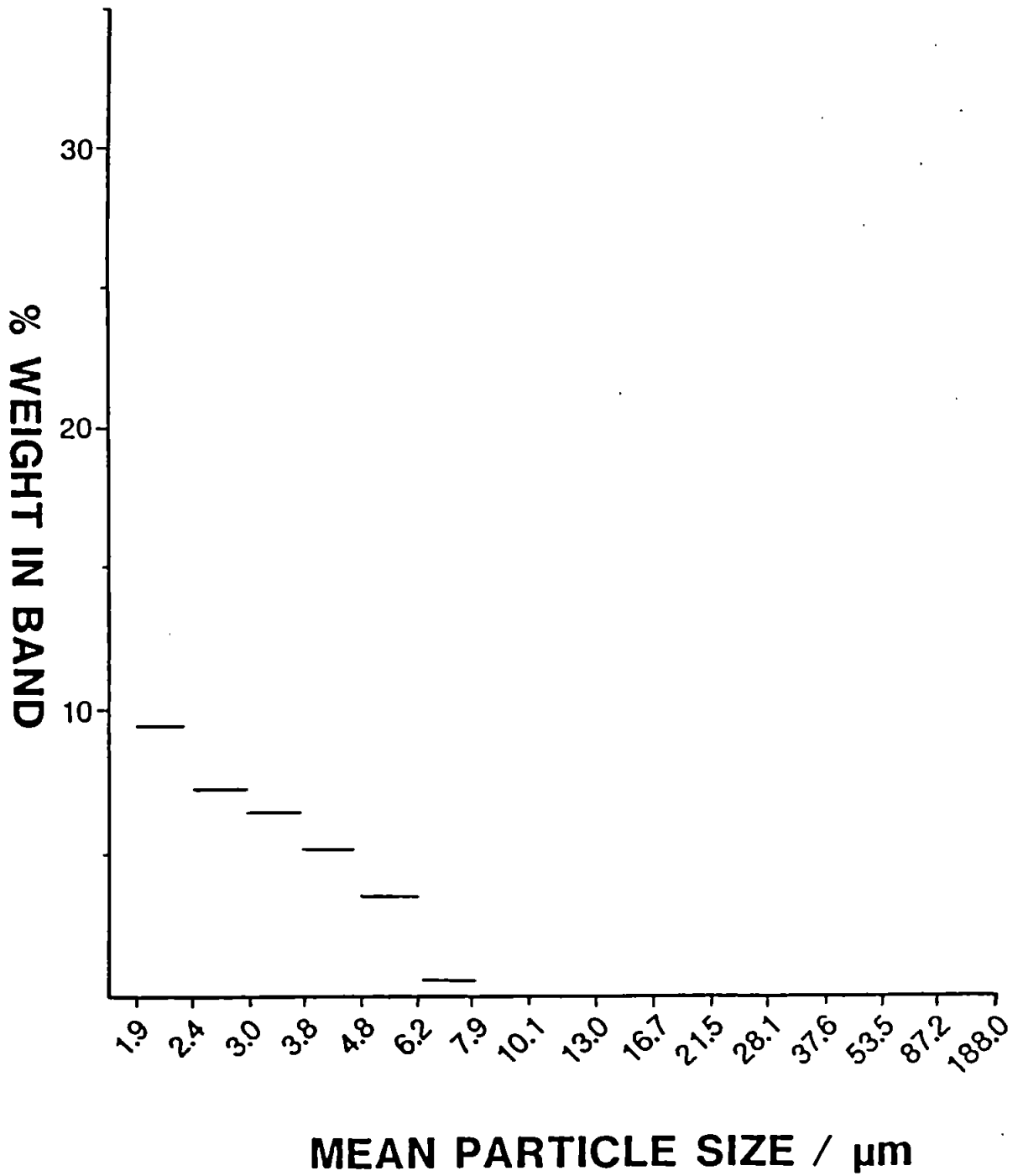
FIGURE 49

By weight particle size distribution of coal SA 19
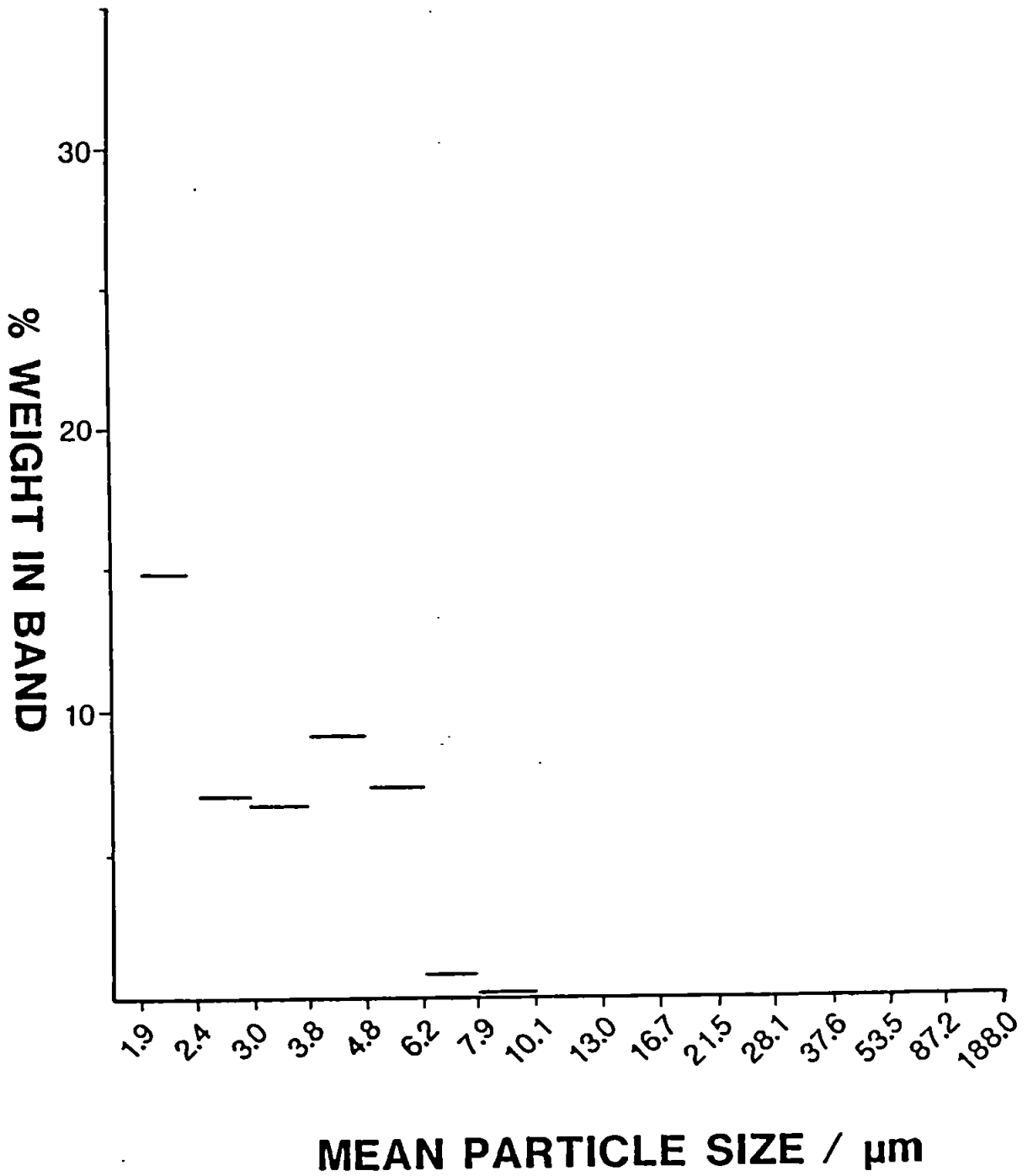
FIGURE 50

By weight particle size distribution of coal SA 18

MEAN PARTICLE SIZE / μm
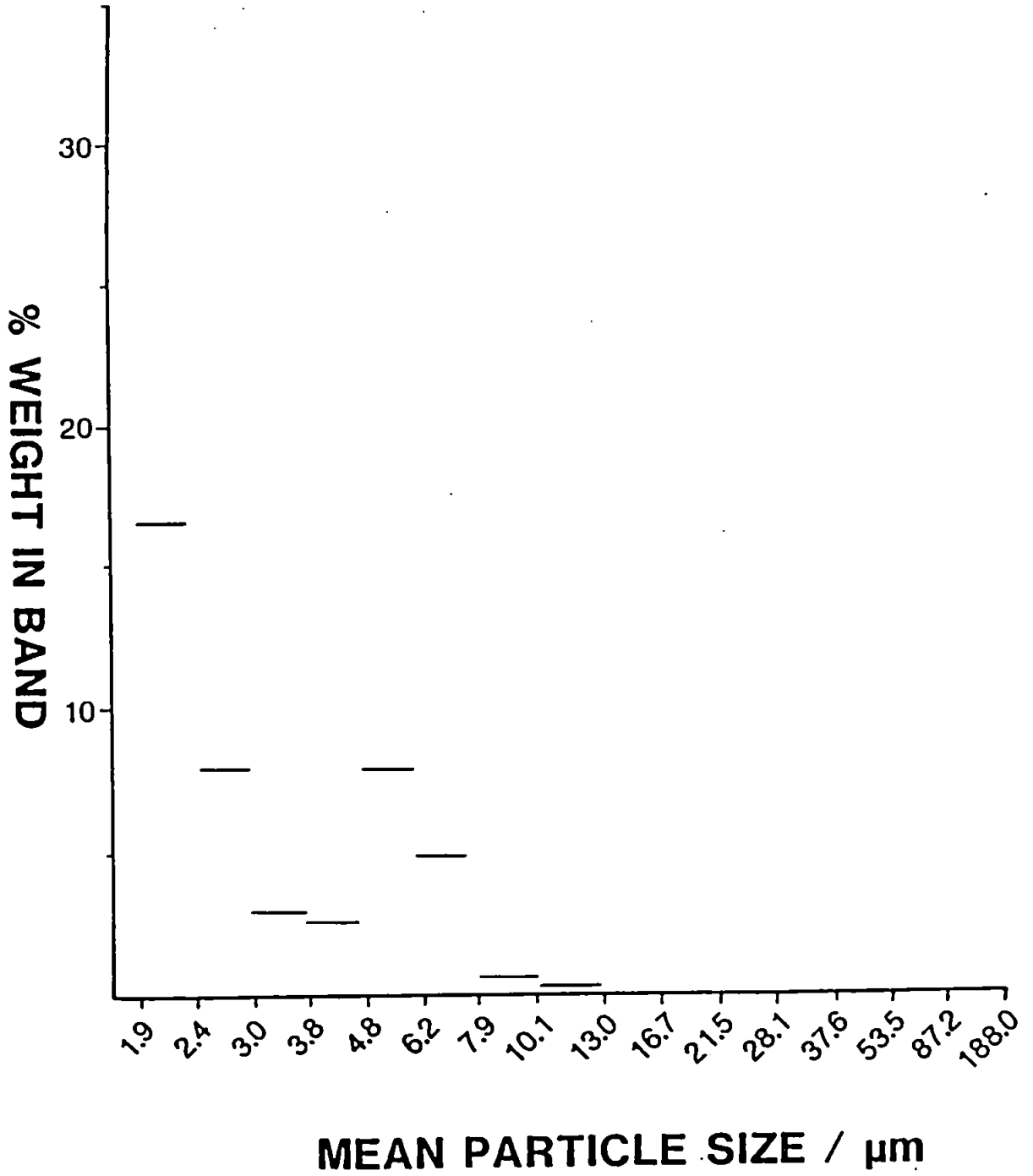
FIGURE 51

By weight particle size distribution of coal BCR 40

MEAN PARTICLE SIZE / µm
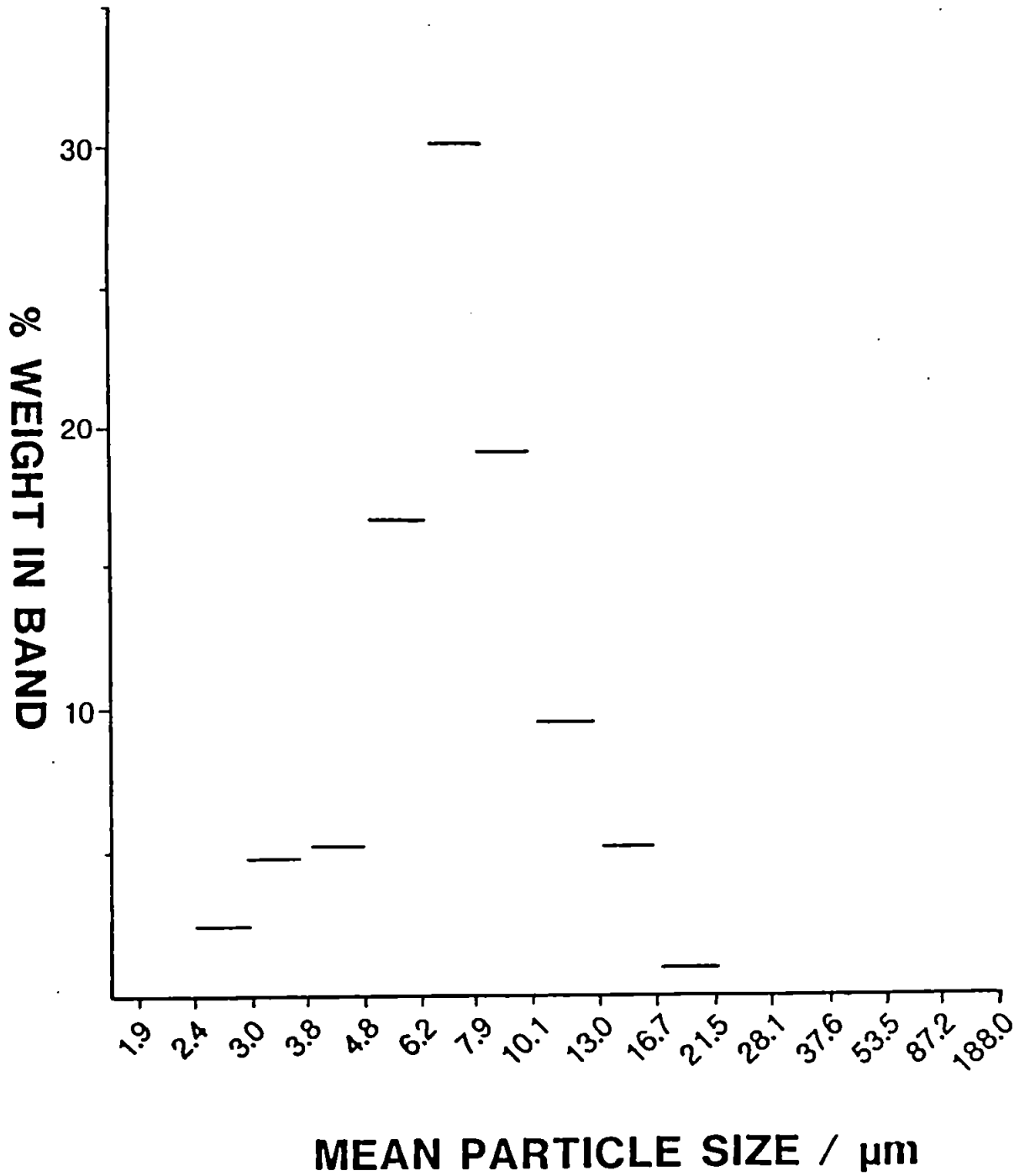
FIGURE 52

By weight particle size distribution of coal BCR 181
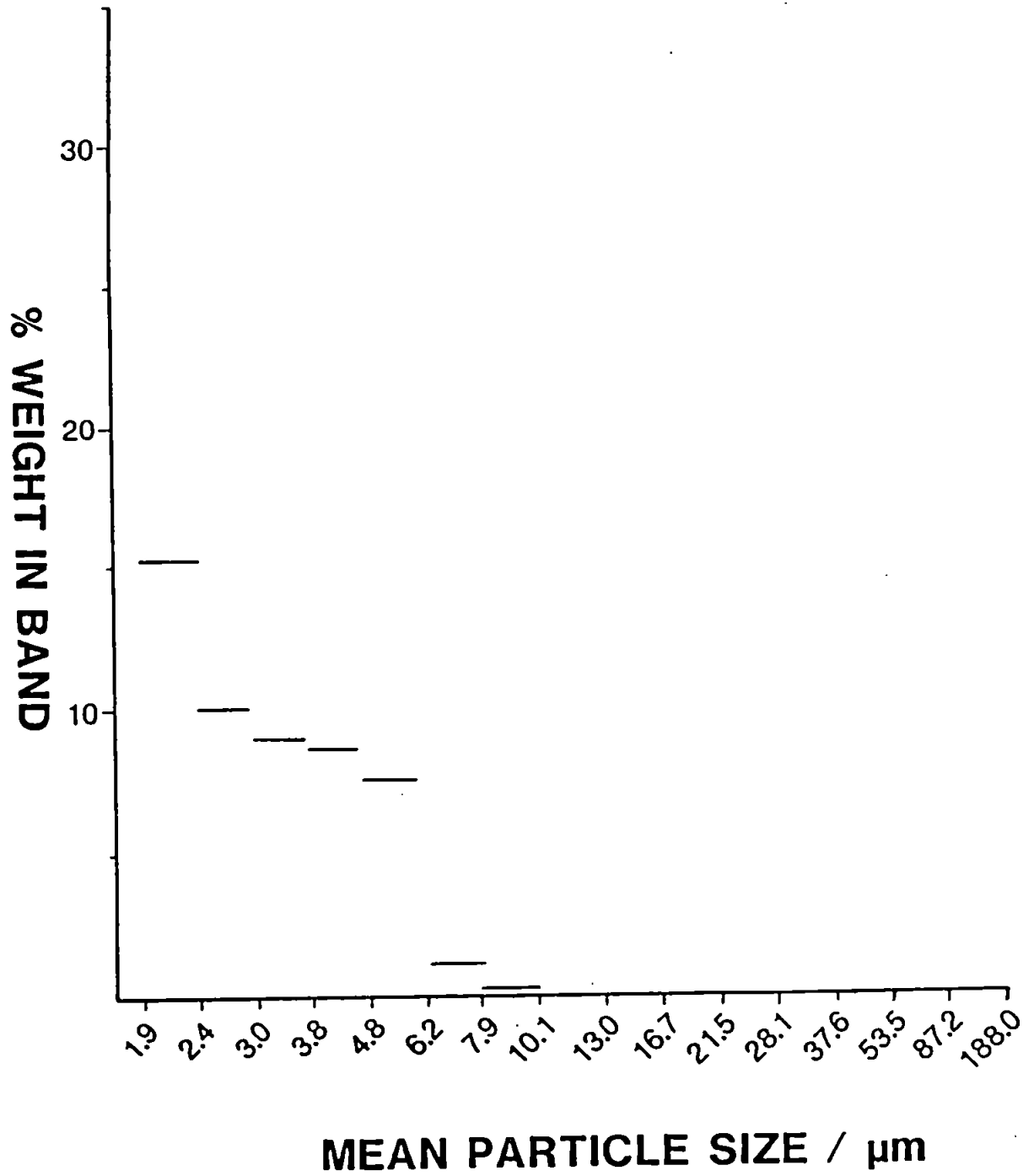
FIGURE 53

By weight particle size distribution of coal BCR 182
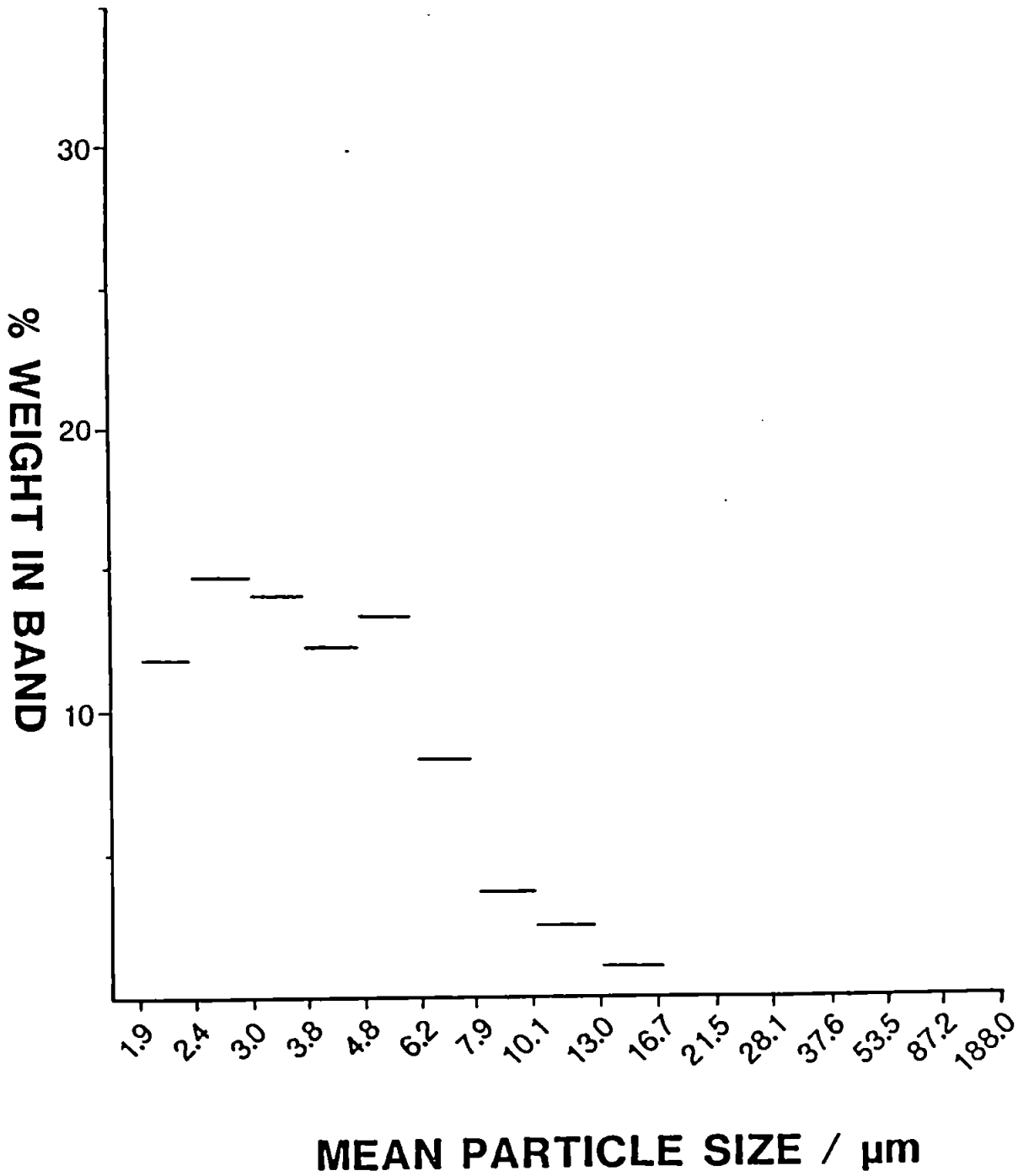
6.12 SUMMARY

The parameters that govern slurry atomisation have been identified as the particle size of the slurry, injector gas flow rate, and spray chamber design. Successful slurry atomisation using ICP-AES has been achieved using a number of certified reference coals with minimal modification to existing instrumentation. Low flow rates were found preferable when using the ARL single pass spray chamber but the injector flow rate had to be increased when the double pass spray chamber was used. The atomisation efficiences for elements determined in coal slurries using a double pass spray chamber were slightly lower in comparison to similar elements analysed when a modified ARL chamber was used. This was attributed to the exclusion of large particles with the double pass spray chamber, whereas these particles reached the plasma when the modified ARL chamber was used. The favoured configuration was that of the modified ARL spray chamber with reduced flow rates using the 1.8 mm i.d. injector. The use of the modified ARL chamber in comparison to the double pass chamber led to shorter residence times, therefore allowing shorter sample washout, times enabling faster analysis of the samples.

Simplex optimisation was used to derive optimum conditions for the determination of aluminium in coals. The critical parameters were found to be power, observation height and injector gas flow rate. The simplex procedure identified two local optima which suggested that within the plasma, there were two regions most suited for the atomisation of aluminium. These regions are either low in the plasma below the NAZ with its high energy, or high up in the plasma where increased residence time would also lead to the destruction of molecular aluminium species.

The slurry atomisation technique has been shown to be viable for various elements and requires only simple aqueous calibration with minimal modification to existing instrumentation. Sulphur was not determined owing to its presence in the surfactant, but if Aerosol OT was substituted with Triton X100 or similar surfactant, it would enable the rapid determination of sulphur in coal with minimal sample preparation.

CHAPTER 7

THE ANALYSIS OF COAL BY SLURRY ATOMISATION USING INDUCTIVELY

COUPLED PLASMA MASS SPECTROMETRY

7.1 INTRODUCTION

The concept of extracting ions formed by a plasma for elemental analysis by mass

spectrometry (MS) was pioneered by Gray (213). The original work used a d.c. capillary

arc plasma (CAP) from which a small fraction of the produced ions was extracted through a

sample orifice into a vacuum system containing an electrostatic ion lens, quadruple mass

analyser and electron multiplier. This technique demonstrated the necessary sensitivity for

the rapid trace element analysis of nebulised solutions with isotope ratio capabilities.

However the d.c. arc plasma source used suffered from inter-element and matrix effects due

to the low temperature of the plasma. Houk et al. (214) have extended the principle so as

to include the inductively coupled plasma (ICP) originally designed for atomic emission, as

an ionisation source. They concluded that the "ICP-MS approach should be less susceptible

to interelement interference effect than CAP-MS because of the superior sample injection

vaporisation, atomisation capabilities and higher electron number density of the ICP".

The coupling of the ICP to MS has evolved as a successful technique for the determination

of trace elements in a wide variety of samples with great rapidity. The rare earth elements

are difficult to determine by ICP-AES due to their inherently complex optical spectra,

however in ICP-MS this problem does not arise and these elements can more readily be

determined. The majority of elements can be determined by ICP-MS, thus allowing the use

of one technique in their determination as opposed to several previous techniques. The

original ICP-MS systems were designed for solution introduction, but the ICP can accept a

variety of sample introduction systems, as long as the sample can be introduced in the

injector gas flow. The most common method of sample introduction into the ICP-MS is by pneumatic nebulisation of solutions, but any method of sample introduction suitable for ICP-AES would be, in principle, suitable for ICP-MS.

Clearly advantages would be gained if the sample could be directly introduced into the ICP-MS as a slurry. Disadvantages of sample solution nebulisation include dissolution procedures which are time consuming, complex, error prone, hazardous and may result in loss of volatile analytes. More significantly in the use of ICP-MS, certain dissolution techniques such as fusions may result in an increased dissolved solid content of the sample which may lead to blockage of either the nebuliser or sample cone by which ions are extracted into the mass spectrometer. Use of acids such as perchloric and hydrofluroic are potentially hazardous whilst the use of hydrochloric may cause problems owing to polyatomic ion interferences arising from the acid matrix. The use of slurry nebulisation as a means of sample introduction into various analytical techniques including ICP-AES, would seem to be a viable and advantageous technique and one which is applicable to ICP-MS. Recent work (39) has shown that slurries of soils and catalysts can successfully be introduced into the ICP-MS and aqueous solutions used for calibration . Conventional instrumentation was used without modification.

The purpose of this work was to investigate the possibilities of introducing powdered coal suspensions by slurry nebulisation for direct coal analysis by ICP-MS with aqueous calibration. No previous attempt has been reported of slurry nebulisation of coal into an ICP-MS and preliminary investigations were performed to eludicate the applicability of this technique for the rapid analysis of coal. As coal is a notoriously difficult matrix to being into solution, the elimination of the dissolution step would be highly desirable, as this would greatly reduce the costly and time-consuming sample preparation stage, thereby allowing multi-element and multi-isotopic data to be acquired for the determination of major, minor and trace elements in coal.

7.2 EXPERIMENTAL

7.2.1 Instrumentation

The ICP-MS results were obtained using a commercially available instrument, the VG Plasmaquad (VG Isotopes, Ion Path, Road Three, Winsford, Cheshire, UK). Full instrument specification and typical operating conditions are given in Table 57, whilst Figure 54 illustrates a schematic diagram of the instrumentation. Typical instrument settings are given in Table 58 and Figure 55 shows the plasma sampling interface.

The original small quadrupole filter described by Gray (213) is replaced in this instrument by a large, high resolution quadrupole filter with its associated circuitry (215). This quadruple, the VG 12-12, is similar to that described by Brubaker (216) in which a set of short rods are included prior to the main analyser rods. Their function is to provide a delayed d.c. ramp, which is fed through coupling capacitors from the main a.c. rod supply, but without the d.c. component. This reduces the fringe field at the end of the main analysing rods, allowing the entering ions to traverse the rod with a lower velocity. Thus the residence time of the ions in the quadrupole field is increased, thereby allowing a more efficient filtering process to be achieved.

7.2.2 Chemicals and Reagents

Eight reference coals were analysed: Bituminous coal (NBS SRM 1632(b), National Bureau of Standards, Washington, DC, USA), sub-bituminous coal (NBS SRM 1635) high-volatile low rank bituminous coal (SARM 18, SA Bureau of Standards, P/Bag X191, Pretoria 0001, SA), low rank sub-bituminous (SARM 19), low rank sub-bituminous (SARM 20), coking coal (BCR No. 181, Community Bureau of Reference, Brussels), steam coal (BCR No. 182) and coal (BCR No. 40).

All reagents were of AnalaR or Spectrasol quality and all solutions were prepared with deionised, distilled water.

TABLE 57

Instrumental details and generating conditions for the inductively coupled

plasma mass spectrometer (ICP - MS).

Instrument: Plasmaquad (VG Isotopes, UK).

Plasma System
R.f. generator   27.12 MH$_2$ 0 - 1500 W RMS carrier wave power
                           (Henry Radio, California, USA).

Torch system   VG design plasmatherm type 3 turn water cooled coil
                           and quartz torch of the Fassel dimensions.

Gas Controls   A mass flow controller (Tylan) modulates the
                           incoming Ar supply for the carrier gas, whilst the
                           auxiliary and plasma gas flows are regulated by two
                           precision rotameters.

Nebuliser   Ebdon high solids Kel-F nebuliser (P.S. Analytical,
                           Arthur House, Orpington, Kent, UK). pumped at
                           1.5 cm^3 min^{-1}.

Spray Chamber   VG design, Scott double pass type water cooled
                           spray chamber constructed from glass.

Ion Sampling
Sampling cone   Nickel coated Nicone (appeture 1.0 mm).
Skimmer cone   Nickel coated Nicone (appeture 0.7 mm).
Vacuum System   3 Stage System.

                           Expansion stage pumped by a rotary EIM/18 (Edwards
                           High vacuum ltd, Crawley, Sussex, UK) pump, 20
                           m^3 hr^{-1} to working pressure of 2 mbar.

                           Intermediate stage, Balzars 200 diffusion pump,
                           2000 lmin$^-$ working pressure of 10^{-4} mbar.

                           Analyser stage, Balzars, Diffset 063 diffusion
                           pump, 180 lmin^{-1} working pressure of 2.5 x 10^{-6} mbar.

                           Both diffusion pumps backed by a E2M/18 rotary pump.

Pressure detectors   Pirani PRM 10 and PRL 10 detect pressure in expansion
                           and intermediate stage respectively. Penning
                           gauge detector used for analyser stage. All three
                           detectors operated by Edwards 1108 Controller.

Multi Channel   VG Masslab 12-12 quadrapole ananlyser, mass range
                           1-300 Analyser a.m.u. Resolution >2M. Fitted with
                           Channeltron ion counting electron multiplier.

Multi Channel   VG MCA 100 Mh 4096 channels, 2 x 10^9 counts per
                           channel.
Analyser
Data System
System   IBM PC/XT fitted with 8087 maths co-processor. 640
                           Kbyte RAM, 10 Mbytes head disc, 360 Klyte floppy
                           discs. Sigma dazlercard for graphics fitter with
                           7210 graphical processor.

FIGURE 54

Schematic diagram of inductively coupled mass spectrometer instrumentation
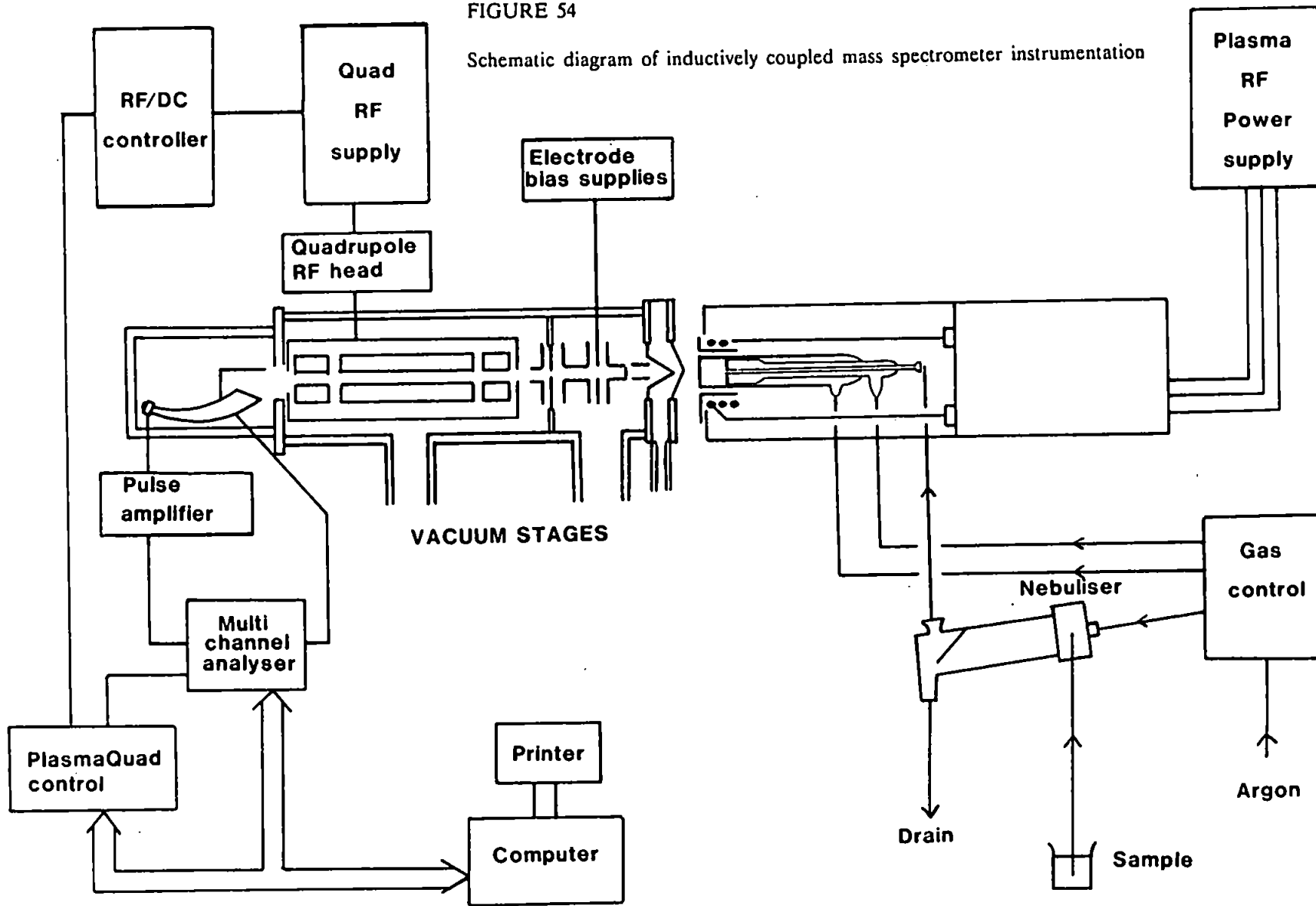
TABLE 58

Typical instrument settings for inductively coupled plasma mass spectrometer.

Forward r.f. power/W	1300
Gas flow rates/lmin^{-1}	
Coolant	13.00
Auxiliary	0.7
Nebuliser	0.73
Nebuliser pressure p.s.i.	35
Ion lens settings	Optimised for resolution, mass — calibration and counts over the mass range of interest.

FIGURE 55

Diagram illustrating the plasma sampling interface
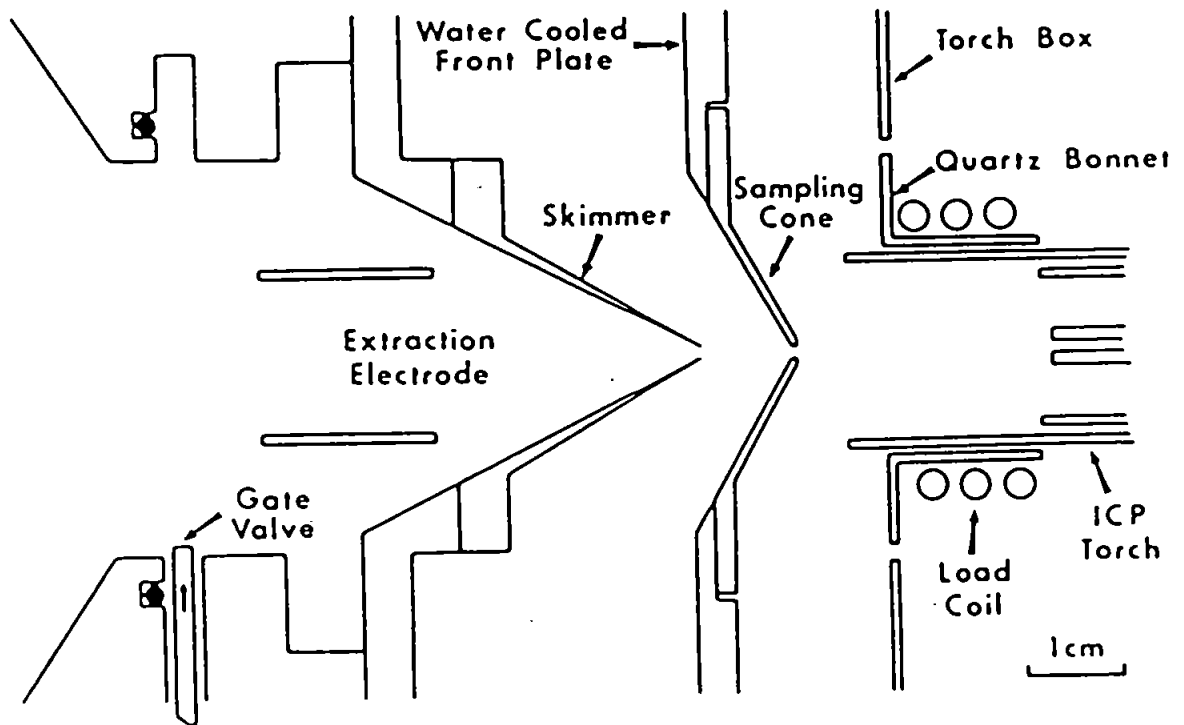
7.2.3 Slurry preparation

Coal slurries were prepared as previously described in section 5.5.1. Aerosol OT was used as a surfactant in all slurry preparations at a concentration of 0.1% m/v so as to stabilise the suspension. Particle size analysis by laser diffraction was performed on six of the reference coals.

In order to prevent any cone blockage, dilutions were made of the original slurries so for analysis of minor/trace levels slurries of 0.2 g per 100 ml were produced and for the major elements, slurries were prepared at 0.002 g per 100 ml. At these levels no cone blockage effects were observed over extensive running periods of the instrumentation.

7.3   RESULTS AND DISCUSSIONS

The particle size analysis data for the 8 coals is shown in Figures 56 - 60. A range of particle size is shown. For NBS 1635 100% of the particles are below 1.9 μm, illustrating the success of the grinding technique, but for NBS 1632(b) (Figure 56) particles as large as 37 μm remained suggesting that the grinding technique was not as efficient for this coal. The remaining coals exhibit a particle size below 10-13 μm region.

Initial investigations were performed on the introduction of slurries into the ICP-MS using a De Galan high solids nebuliser and cyclone spray chamber as fitted in the standard instrument. During all analysis indium (Mass 115) was used as an internal standard. Preliminary investigations were performed on a semi-quantitive basis for certain coals as this enabled a rapid scan of the mass range allowing the identification and quantification of relative peak intensities, thus providing an indication of relative concentration. Having established suitable plasma operating conditions, the eight certified reference material coals were analysed using the scan details described in Table 59. The results obtained were extremely encouraging and despite initial problems associated with nebuliser blockage, the

FIGURE 56

By weight particle size distribution of coal NBS SRM 1632(b)
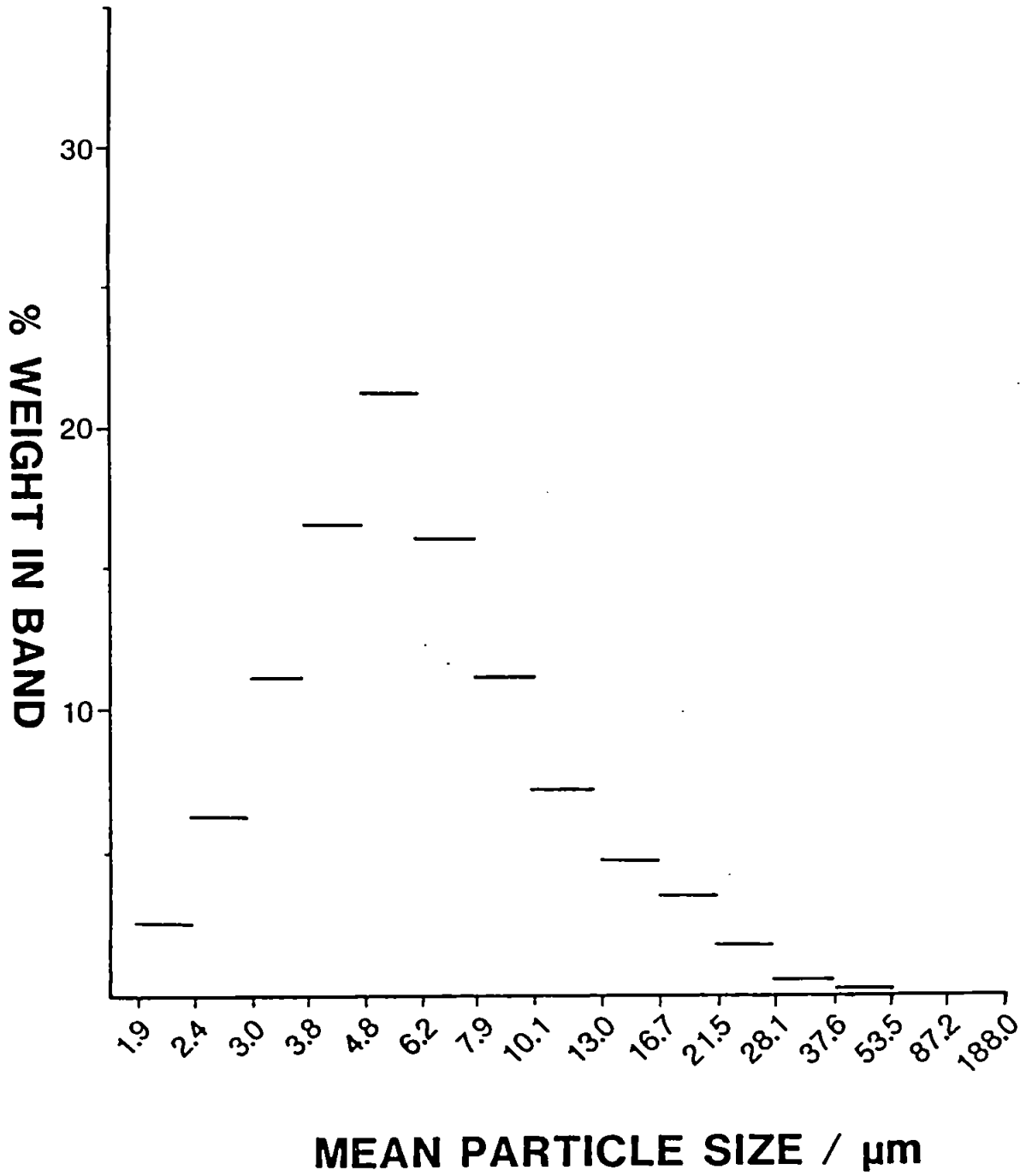
FIGURE 57

By weight particle size distribution of coal SA 18

MEAN PARTICLE SIZE / μm
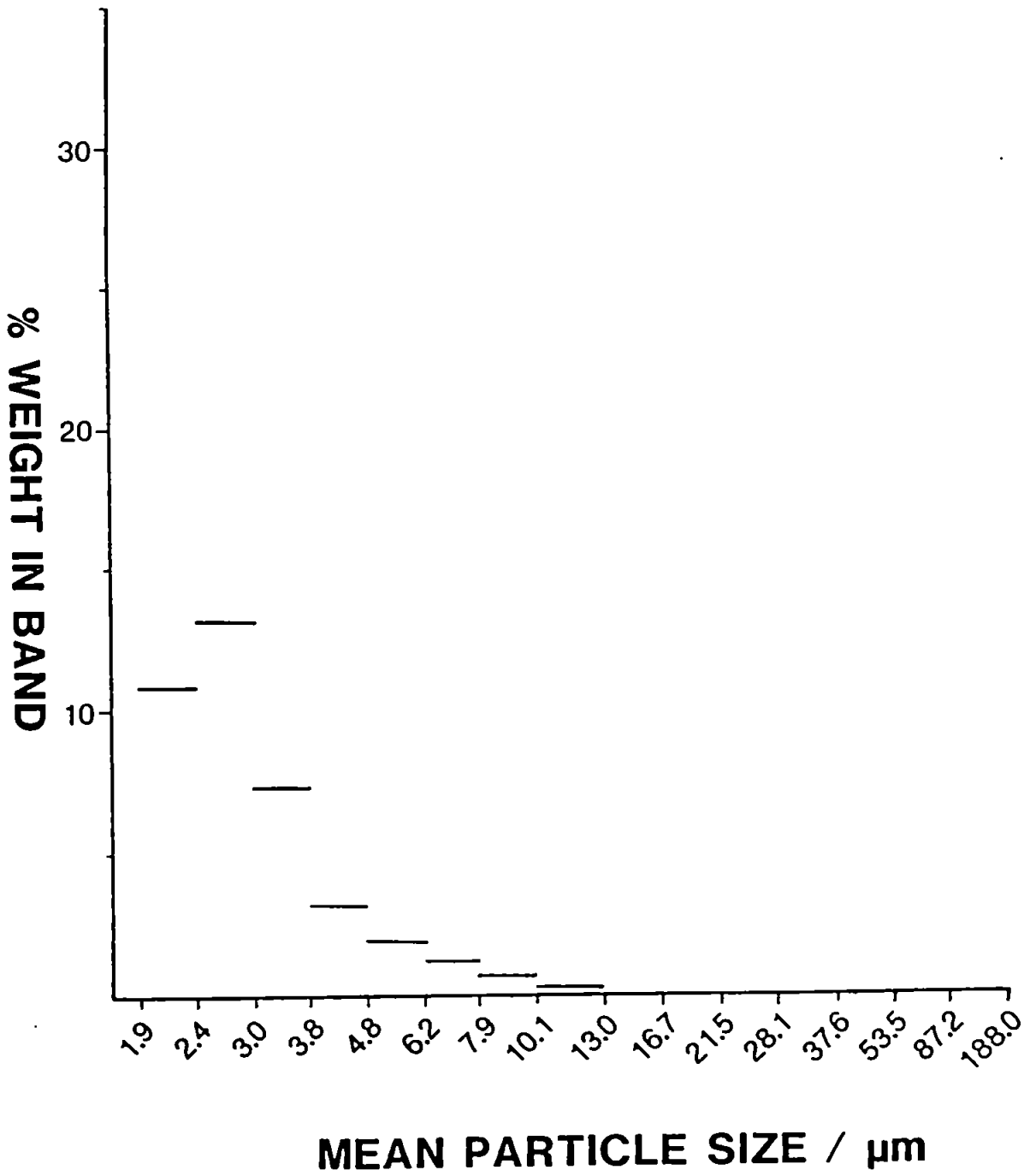
FIGURE 58

By weight particle size distribution of coal SA 20

MEAN PARTICLE SIZE / μm
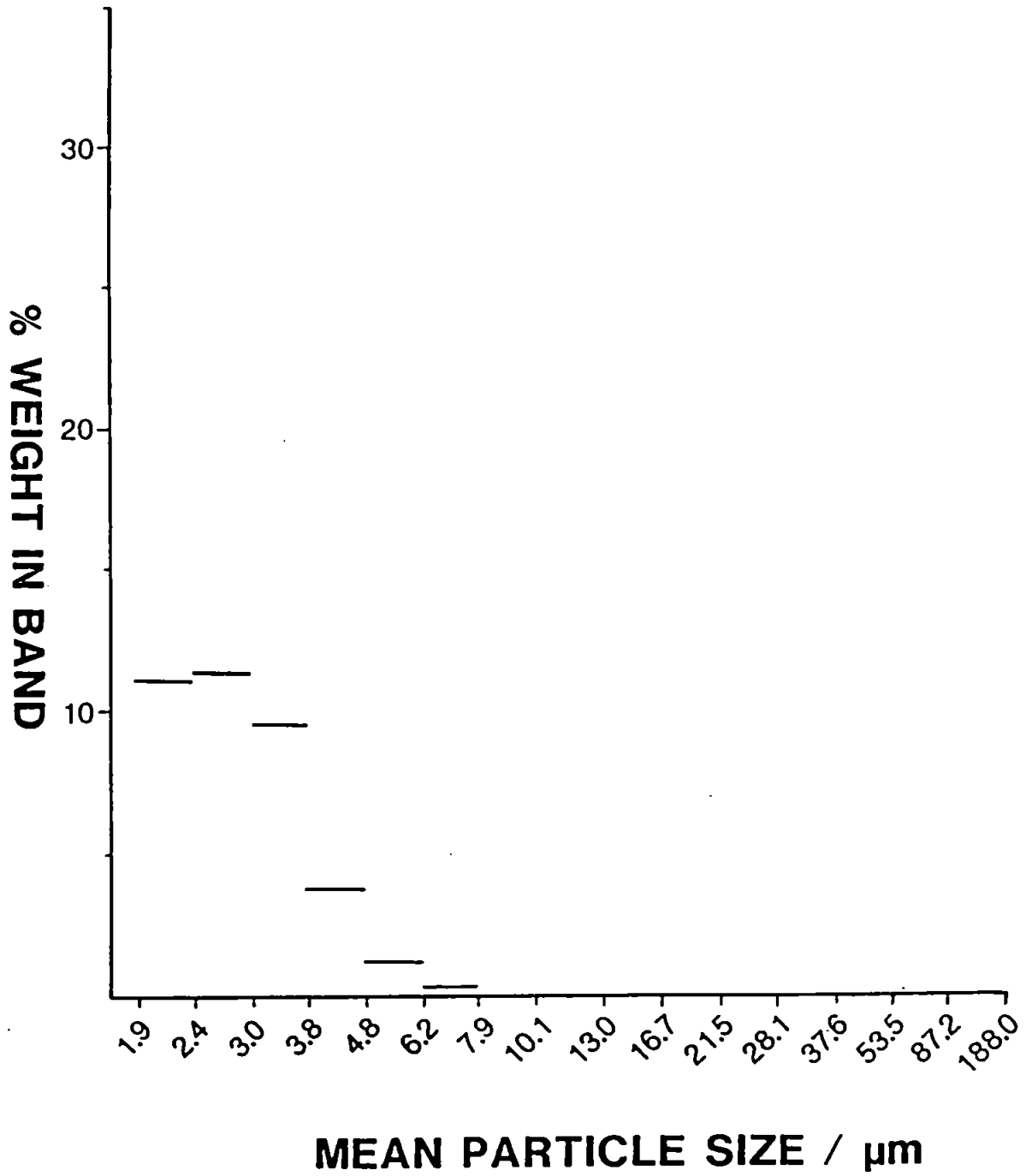
FIGURE 59

By weight particle size distribution of coal BCR 181
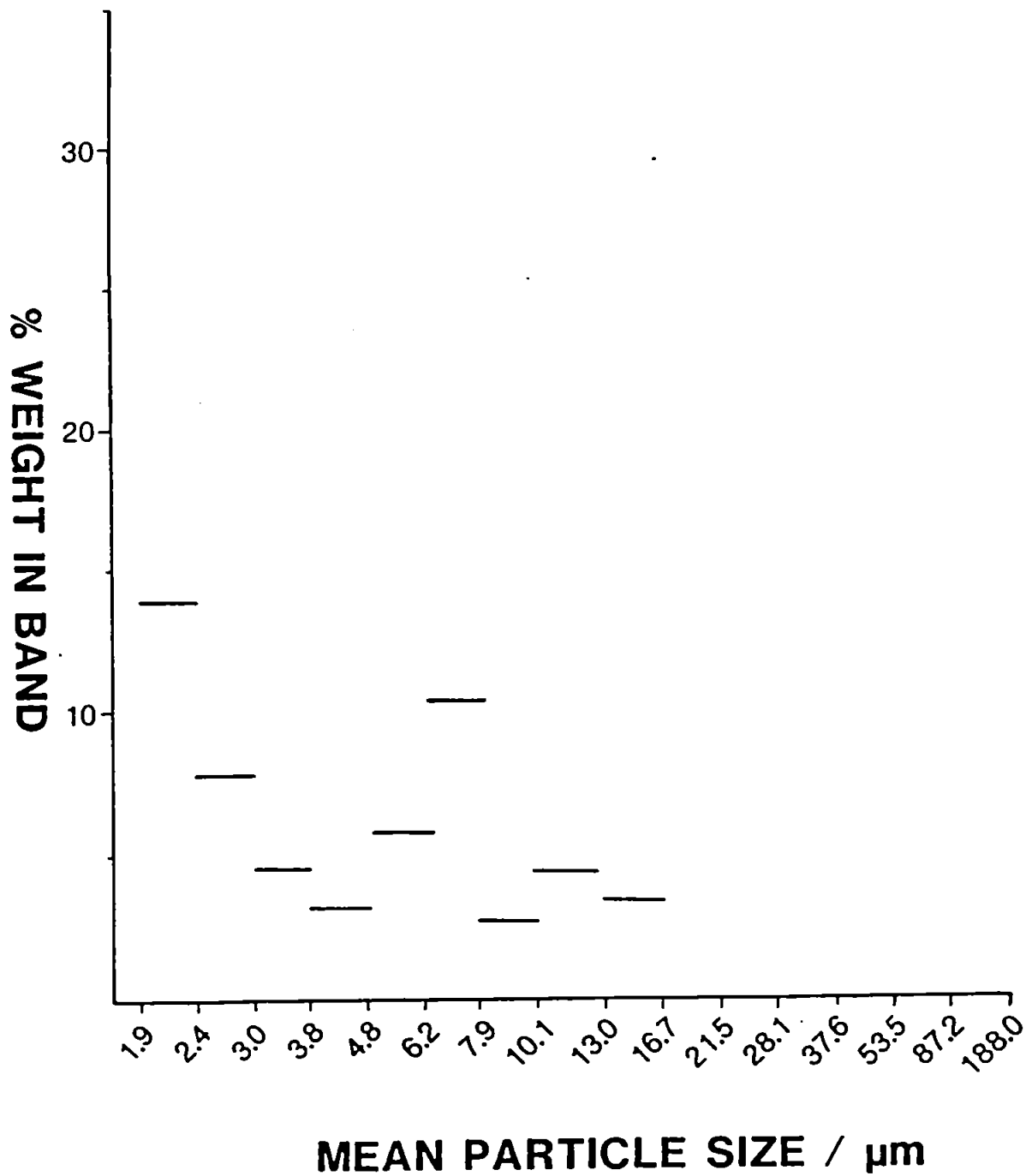
FIGURE 60

By weight particle size distribution of coal BCR 182
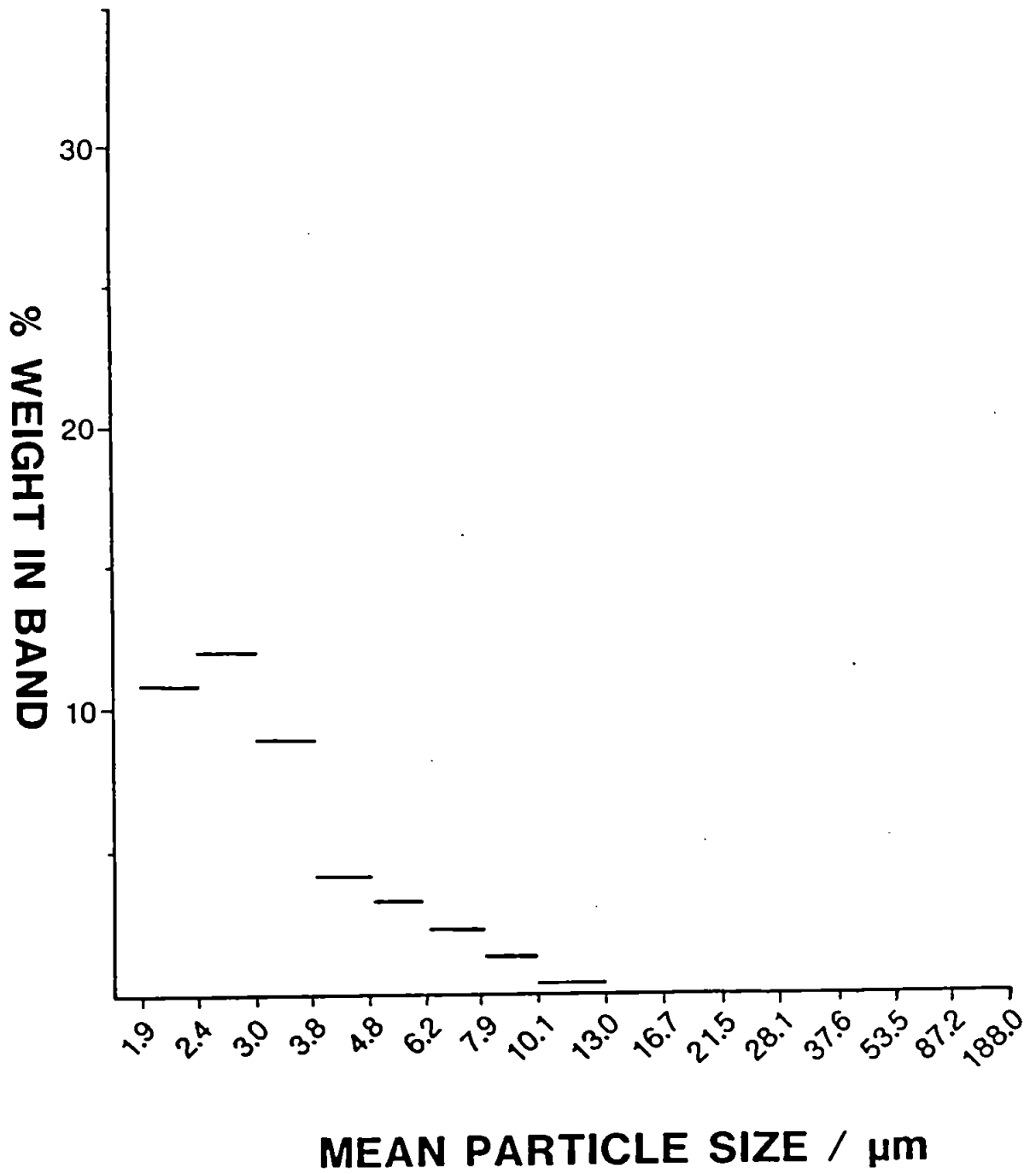
TABLE 59

Scan details of the mass spectrometer.

Mass range /u	4-255
Sweeps	120
Channels	2096
Dwell time /μs	250
Total run time/s	61
Internal Standard (100ng g^{-1})	^{115}In

results showed good agreement with the certified values. However problems did arise with the cyclone nebuliser, which under the operating conditions resulted in an unstable plasma owing to the formation of water droplets at the base of the injector.

The cyclone spray chamber was replaced by a Scott type double pass spray chamber, retaining the De Galan nebuliser and the analysis was repeated using similar plasma and scan conditions as previously described. Over fifty elements were determined for each coal, and where possible, the values from the analysis were compared directly to certificate values with reasonable agreement. The plasma was observed to be more stable during this analysis, as water was not entering the injector tube. Information on the major elements was not possible owing to the oversaturation of the channeltron detector, clearly even a 0.2 g per 100 ml was too concentrated. Although this concentration is suited for minor and trace level determination, the major constituants, often present in percentage level, saturated the detector. This problem was alleviated in later analysis by the preparation of 0.002 g per 100 ml slurries for the determination of the major elements in reference coals. The repeatability using the De Galan nebuliser and double pass spray chamber was checked to determine the with-in run precision by performing six analyses of SARM 18 reference coal. From the results the relative standard deviation was calculated and at first inspection this seemed to be poor with only a few elements better than 10% RSD. These disappointing values can be attributed to the proximity of the measurements to the elemental detection limit which results in low counts with a small variation in a small number yielding a high relative standard deviation. Also the method of collection of data in ICP-MS is dependent upon ion counting over a period and a long dwell time would significantly reduce the RSD's. Plasma stability was further assisted by the water cooling of the spray chamber, which would eliminate any variation in water vapour loading of the plasma and which could lead to a cooling of the plasma.

The De Galan nebuliser was replaced with another Babington type V-groove, the Ebdon nebuliser, whilst the Scott double pass spray chamber was retained. The analysis was repeated for all coals and the results obtained show good agreement with the certified values. Later it was shown that the internal standard indium has similarities in properties and chemistry to that of aluminium and when indium was removed from the calculation, it was discovered that the results bore better agreement with the certified values, see Tables 60-67. The elements listed in these tables were chosen as certificate information exists for them. However all information resulting from the analysis is not recorded here owing to the excessive quantity of the data.

Comparison of the results obtained by slurry atomisation and the certificate values exhibits excellent agreement with the majority of elements falling within or close to the range specified by the certificate value for SARM 18, Table 60. The reported value for aluminium is extremely low for all analyses as the results shown here have been corrected for the removal of the indium as the internal standard, which showed similar anomalies to aluminium. If however the results obtained for aluminium using indium as an internal standard are evaluated (Table 68) it is possible to see that the results have been improved, but they show a similar low trend as observed in ICP-AES and DCP-AES. A theory has been suggested so as to explain the low recoveries of aluminium by suggesting that the refractory aluminium oxide is incompletely atomised by the plasma (217) and also that the unatomised particles might be larger in slurry atomisation in comparison to solution nebulisation. However, NBS SRM 1635 exhibits 100% of coal particles are below 1.9 μm and the aluminium recovery is still low typically 75%.

The agreement between the ICP-MS results and the certificate value was generally good. Good agreement existed for copper in SARM 18, 19, 20 and NBS 1635 (Tables 60 - 62 and 64), but for NBS 1632(b) Table 63, the ICP-MS value is high. The zinc values are higher than the certified value for all coals except for BCR 182, Table 66. There are polyatomic

TABLE 60

Determination of major, minor and trace elements in reference coal SARM 18 by slurry atomisation ICP – MS.

Element	Slurry Nebulisation $\mu g\ g^{-1}$	Certificate Value $\mu g\ g^{-1}$	Range
Li	14.30	11.00	–
Be	3.70	4.10	3.9-4.5
Mg	654	660	600-660
Al	4247	13595	13440-13800
Ti	569	628	664-694
V	16.90	23.00	21-25
Cr	16.10	16.00	14-18
Mn	23.40	22.00	21-23
Fe	2095	2030	1960-2030
Co	6.70	6.70	5.5-7.2
Ni	10.10	10.80	9-13
Cu	7.50	5.90	5.2-6.4
Zn	8.70	5.50	5.2-6.8
Ga	11.80	(8)	–
Ge	8.20	(8)	–
As	0.74	–	–
Se	2.70	–	–
Rb	8.10	8.10	6.7-9.5
Sr	39.50	44.00	42-45
Y	20.90	(12)	–
Nb	8.70	(6)	–
Mo	0.86	(1)	–
Cd	9.80	–	–
Sn	1.20	(1)	–
Sb	0.60	(0.30)	–
Cs	1.10	(1)	–
Ba	74.50	78.00	71-82
La	9.40	–	–
Ce	22.30	22.00	21-24
Sm	2.10	2.00	1.9-2.2
Eu	0.36	(0.30)	–
Tb	0.45	(0.30)	–
Yb	3.90	–	–
Pb	6.00	(5)	–
Th	6.10	3.40	3.0-4.3
U	3.40	1.50	1.5-2.0

( ) = indicated values only and not certified.

TABLE 61

Determination of major, minor and trace elements in reference

coal SARM 19 by slurry atomisation ICP - MS.

Element	Slurry Nebulisation $\mu g \ g^{-1}$	Certificate Value $\mu g \ g^{-1}$	Range
Li	44.90	(37)	-
Be	3.10	2.80	2.3-3.1
Mg	1146	1200	1200-1230
Al	3855	42370	41580-43110
Ti	1631	2043	1940-2132
V	30.20	35.00	33-37
Cr	54.90	50.00	47-58
Mn	167.30	157.00	143-168
Fe	11647	12250	12100-12300
Co	6.50	5.60	5.0-6.6
Ni	17.50	16.00	13-20
Cu	13.80	13.00	11-14
Zn	23.60	12.00	12-16
Ga	37.60	14.00	13-15
Ge	21.80	13.00	10-14
As	7.50	7.00	6-8
Se	6.90	(1)	-
Rb	7.80	9.0	8-10
Sr	109.20	126.00	125-141
Y	33.80	20.00	-
Nb	10.20	10.00	-
Mo	1.90	2.00	-
Cd	19.00	-	-
Sn	2.20	(3)	-
Sb	0.36	(0.30)	-
Cs	1.20	1.40	1.3-2.0
Ba	263.00	304.00	295-318
La	23.50	27.00	26-29
Ce	52.40	56.00	51-59
Sm	3.90	4.90	4.2-5.0
Eu	0.80	(0.70)	-
Tb	0.70	(0.70)	-
Yb	6.00	(2)	-
Pb	18.50	20.00	17-23
Th	14.70	12.00	11-14
U	7.50	5.00	3-6

TABLE 62

Determination of major, minor and trace elements in reference

coal SARM 20 by slurry atomisation by ICP - MS.

Element	Slurry Nebulisation $\mu g\ g^{-1}$	Certificate Value $\mu g\ g^{-1}$	Range
Li	115.00	(90)	-
Be	3.20	2.50	2.1-3.0
Mg	2300.00	2580.00	2460-2700
Al	4768	59610	59040-62050
Ti	2837.00	3780.00	3660-3900
V	43.40	47	45-50
Cr	75.60	(67)	-
Mn	92.00	80.00	77-82
Fe	8544.00	8409	8266-8553
Co	9.90	8.30	7.6-9.0
Ni	26.30	25	23-26
Cu	21.00	18.00	15-19
Zn	33.60	17.00	14-18
Ga	45.20	16.00	15-18
Ge	8.20	-	-
As	6.00	4.70	4.6-6.0
Se	5.40	0.80	0.7-1.0
Rb	8.4	10.0	9-14
Sr	291.00	330.00	318-338
Y	44.30	29.00	23-30
Nb	16.30	(16)	-
Mo	1.30	-	-
Cd	19.30	-	-
Sn	3.50	(4)	-
Sb	0.50	(0.4)	-
Cs	2.00	(2)	-
Ba	328.90	372	363-384
La	40.70	43.00	40-57
Ce	83.60	87.00	73-88
Sm	5.80	6.30	5.9-6.6
Eu	1.20	(1)	-
Tb	1.10	(0.90)	-
Yb	7.80	(2)	-
Pb	25.00	26.00	20-29
Th	22.00	18.00	16-20
U	8.60	4.00	3-5

( ) = indicated values only and not certified.

TABLE 63

Determination of major, minor and trace elements in reference coal
NBS 1632(b) by slurry atomisation ICP - MS.

Element	Slurry Nebulisation $\mu g\ g^{-1}$	Certificate Value $\mu g\ g^{-1}$
Li	11.50	(10)
Be	0.70	-
Mg	368	383 ± 8
Al	3455	8550 ± 190
Ti	312	454 ± 17
V	9.10	(14)
Cr	13.10	(11)
Mn	13.20	12.40 ± 1.0
Fe	5982	7590 ± 450
Co	2.50	29 ± 0.17
Ni	12.30	6.10 ± 0.27
Cu	5.80	6.28 ± 0.3
Zn	12.80	11.89 ± 0.79
Ga	6.30	
Ge	5.90	-
As	3.80	3.72 ± 0.09
Se	5.40	1.29 ± 0.11
Rb	4.30	5.05 ± 0.11
Sr	86.60	(102)
Y	9.20	-
Nb	1.80	-
Mo	0.90	(0.90)
Cd	3.70	0.0573 ± 0.0027
Sn	0.60	
Sb	0.40	(0.24)
Cs	0.50	(0.44)
Ba	56.70	67.50 ± 2.1
La	3.50	(5.1)
Ce	7.70	(9)
Sm	0.90	(0.87)
Eu	0.30	(0.17)
Tb	0.30	-
Yb	1.50	-
Pb	3.50	3.67 ± 0.26
Th	2.80	1.34 ± 0.036
U	1.00	0.436 ± 0.012

( ) = indicated values only and not certified.

TABLE 64

Determination of major, minor and trace elements in reference coal
NBS 1635 by slurry atomisation ICP – MS.

Element	Slurry Nebulisation $\mu g\ g^{-1}$	Certificate Value $\mu g\ g^{-1}$
Li	2.60	–
Be	0.50	–
Mg	818	–
Al	1946	(3200)
Ti	205	(200)
V	3.80	5.20 + 0.5
Cr	6.70	2.50 + 0.3
Mn	21.40	21.40 + 1.5
Fe	2206	2390 + 5.0
Co	1.30	0.65
Ni	4.90	1.74 + 0.1
Cu	3.60	3.60 + 0.3
Zn	8.80	4.70 + 0.5
Ga	7.90	(1.05)
Ge	2.50	–
As	0.60	0.42 + 0.15
Se	4.00	0.90 + 0.3
Rb	0.70	
Sr	110	–
Y	12.20	–
Nb	0.90	–
Mo	0.50	–
Cd	10.60	0.03 + 0.01
Sn	0.20	
Sb	0.20	(0.14)
Cs	0.08	–
Ba	74.80	–
La	2.20	–
Ce	4.20	(3.6)
Sm	0.50	–
Eu	0.15	(0.06)
Tb	0.17	–
Yb	–	–
Pb	2.10	1.90 + 0.2
Th	3.30	0.62 + 0.04
U	1.40	0.24 + 0.02

( ) = indicated values only and not certified.

TABLE 65

Determination of major, minor and trace elements in reference coal

BCR 181 by slurry atomisation ICP - MS.

Element	Slurry Nebulisation $\mu g \ g^{-1}$	Certificate Value $\mu g \ g^{-1}$
Li	3.10	-
Be	0.60	-
Mg	61.00	-
Al	1423	-
Ti	89.00	-
V	8.70	12.00 ± 0.4
Cr	7.50	
Mn	3.00	-
Fe	2747	-
Co	4.20	-
Ni	7.00	-
Cu	10.80	-
Zn	6.90	8.40 ± 0.6
Ga	2.20	
Ge	6.60	-
As	22.10	27.70 ± 1.2
Se	3.90	
Rb	0.50	-
Sr	5.20	-
Y	3.90	-
Nb	0.40	-
Mo	0.90	-
Cd	1.00	0.05 ± 0.003
Sn	-	
Sb	0.50	-
Cs	0.05	-
Ba	7.00	-
La	1.10	-
Ce	2.60	-
Sm	0.30	-
Eu	0.09	-
Tb	0.08	-
Yb	-	-
Pb	3.90	2.59 ± 0.16
Th	0.80	-
U	0.50	-

TABLE 66

Determination of major, minor and trace elements in reference coal
BCR 182 by slurry atomisation ICP - MS.

Element	Slurry Nebulisation $\mu g\ g^{-1}$	Certificate Value $\mu g\ g^{-1}$
Li	19.6	-
V	22.7	24.30 + 1.0
Mn	210	195.00 + 6.0
Zn	30	33.30 + 1.5
Se	4	-
Cd	3.0	0.06 + 0.004

TABLE 67

Determination of major, minor and trace elements in reference coal
BCR No 40 by slurry atomisation ICP - MS.

Element	Slurry Nebulisation $\mu g\ g^{-1}$	Certificate Value $\mu g\ g^{-1}$
Cr	33.40	31.30 + 2.0
Mn	156	139 + 5.0
Co	8.30	7.80 + 0.6
Ni	27.00	-
Zn	40.80	30.20 + 1.9
As	11.50	13.20 + 1.1
Cd	3.50	0.11 + 0.02
Pb	23.10	24.20 + 1.7

TABLE 68

Determination of aluminium in 5 reference coals by ICP – MS slurry atomisation using indium as an internal standard.

	Slurry Atomisation $\mu g\ g^{-1}$ Al	Certificate Value $\mu g\ g^{-1}$ Al	Range
SARM 18	15800	13595	13440-13800
SARM 19	38488	42370	41580-43110
SARM 20	50550	59610	59040-62050
NBS 1632(b)	6034	8550 $\pm$ 19	-
NBS 1635	2436	(3200)	-

( ) = indicated value only and not certified.

interferences at 64 ($^{32}SO_2^+$) and 66 ($^{34}SO_2^+$) which overlap the isotopes of Zn. Thus isotopes of zinc were not determined and zinc 68 used but the abundance is relatively low at only 18.5%, thus explaining the poor accuracy of the determinations.

The determination of arsenic in all 8 coals was successful with reported values corresponding with the certified value for SARM 19, 20, NBS 1632(b), whilst the values for NBS 1635, BCR 181 and BCR 40 showed extremely close agreement to the 95% confidence limit. Normally the determination of arsenic is problematic by ICP-MS as reported by several workers (218) owing to the polyatomic interference of $^{75}ArCl^+$ upon the determination of ^{75}As. Munro et al. (218) showed that this interference became more pronounced with increasing concentration of chlorine e.g. HCl acid. The successful determination of arsenic in these coals can be attributed to the freedom from the $^{75}ArCl^+$ interference due to low chlorine content of these particular coals.

The determination of selenium proved disappointing. There are six isotopes of Se some of which suffer polyatomic interferences. The most abundant isotope is found at ^{80}Se but this suffers interfence from $^{40}Ar_2^+$ as reported by several workers (214, 215, 219). The second most abundant isotope ^{78}Se suffers interference from $^{40}Ar\ ^{38}Ar^+$, whilst $^{40}Ar\ ^{37}Cl^+$ interferes upon ^{77}Se. However the ^{82}Se isotope which was used for the analysis is free from such interference, but the values obtained were higher than the reported certified values which can be attributed to the low abundance of this particular isotope and the extremely low value of selenium present in the certified coals.

The determination of rubidium, strontium, niobium and molybdenum 85, 88, 89, 93 and 98 u respectively shows good agreement with the certificate values, with excellent agreement for molybdenum in SARM 18, 19, and NBS 1632(b) see Tables 60, 61 and 63. The abundance of all these isotopes are high with the exception of Mo whose abundance is 24.0% and excellent values achieved can be attributed to the low detection limit of the ICP-MS for Mo.

Cadmium determination proved disappointing in all coals owing to the low abundance of the ^{111}Cd isotope used and the extremely low values of cadmium in the slurries. However excellent agreement exists for the determination of tin at 120 u for SARM 18, 19 and 20, Tables 60-62. There are 10 naturally occurring isotopes of tin and ^{120}Sn was chosen as it has the highest natural abundance (33%). The values of antimony were slightly higher than those reported in the certificate but these values were uncertified.

Excellent values were obtained in reference coals SARM 18, 19, 20 and NBS 1632(b) for cesium as shown in Tables 60-63 using the ^{133}Cs isotope which is 100% naturally abundant. For the same coals, barium showed slightly low recoveries, the exception being SARM 18, whilst lanthanum whose ^{139}La isotope showed 99.9% abundance, showed reasonable agreement with the latter three coals, see Tables 61-63.

Elements from the lanthanides, which included Ce, Sm, Eu and Tb, showed excellent agreement with the certified coals as shown in Tables 60-63. These elements are difficult to determine by ICP-AES owing to their relatively complex spectra, however the inherently simple spectra of ICP-MS allows the successful determination of such elements. Ytterbium exhibits slightly high results in this study which can attributed to contamination from previous work on the instrument on the lanthanides. The same is true for thorium and uranium,, which show elevated values for coals SARM 18, 19, 20, NBS 1632(b) and 1635, see Table 60-64. Once again this is attributed to contamination of the instrumentation from previous analysis on ores which contained significant levels of Th and U.

Despite certain anomalies, there was in general excellent agreement with results obtained by slurry atomisation and certificate values. This agreement shown graphically in Figures (61 - 63) which illustrate log-log plots of results obtained by slurry atomisation, compared to certificate values. The resulting gradient is 1.0 which indicates excellent agreement between reported and observed values.

FIGURE 61

Logarithmic plots of concentration of given elements against concentration for the certified material SA 18 by slurry atomisation ICP-MS.
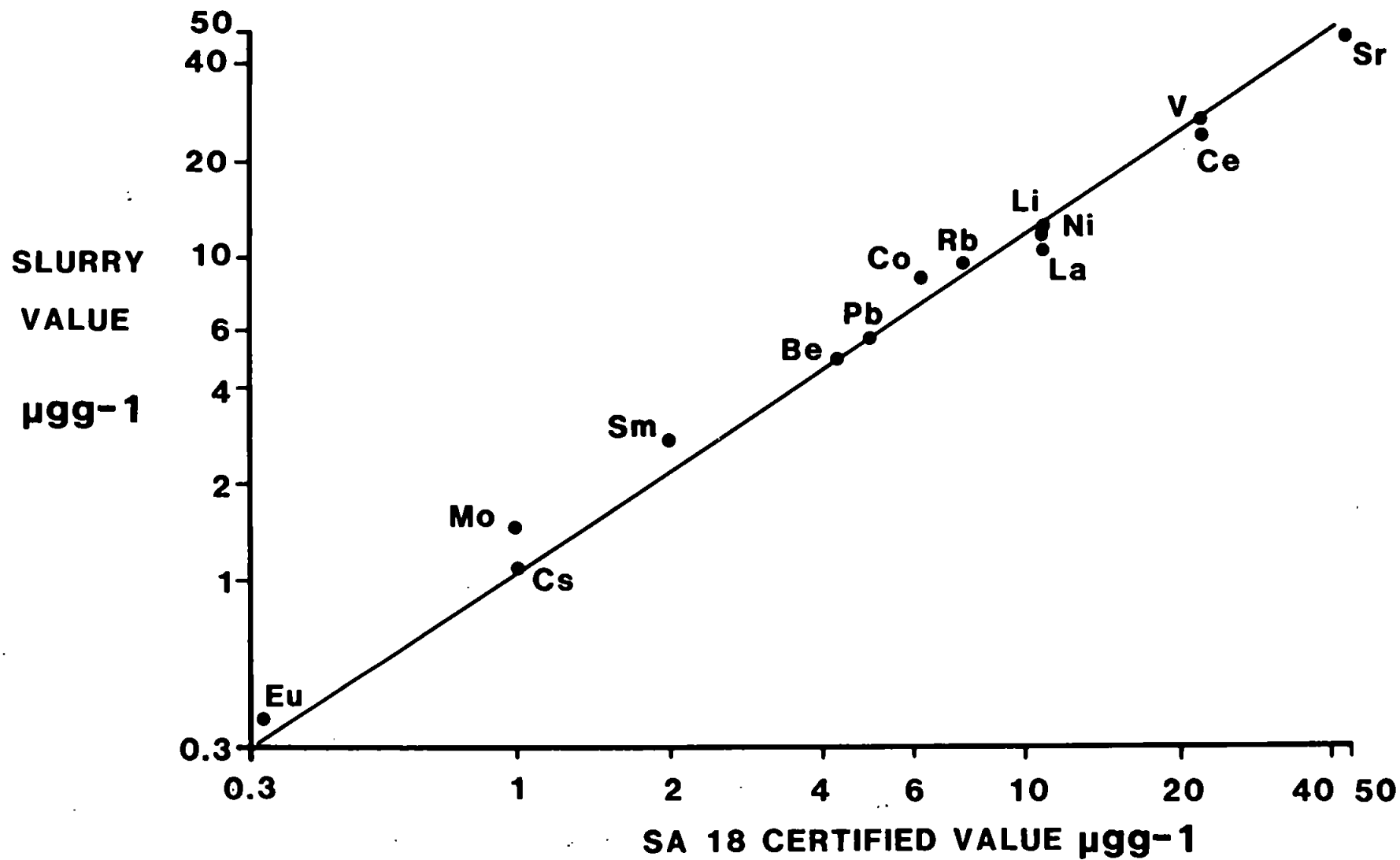
FIGURE 62

Logarithmic plots of concentration of given elements against concentration for the certified material SA 19 by slurry atomisation ICP-MS.
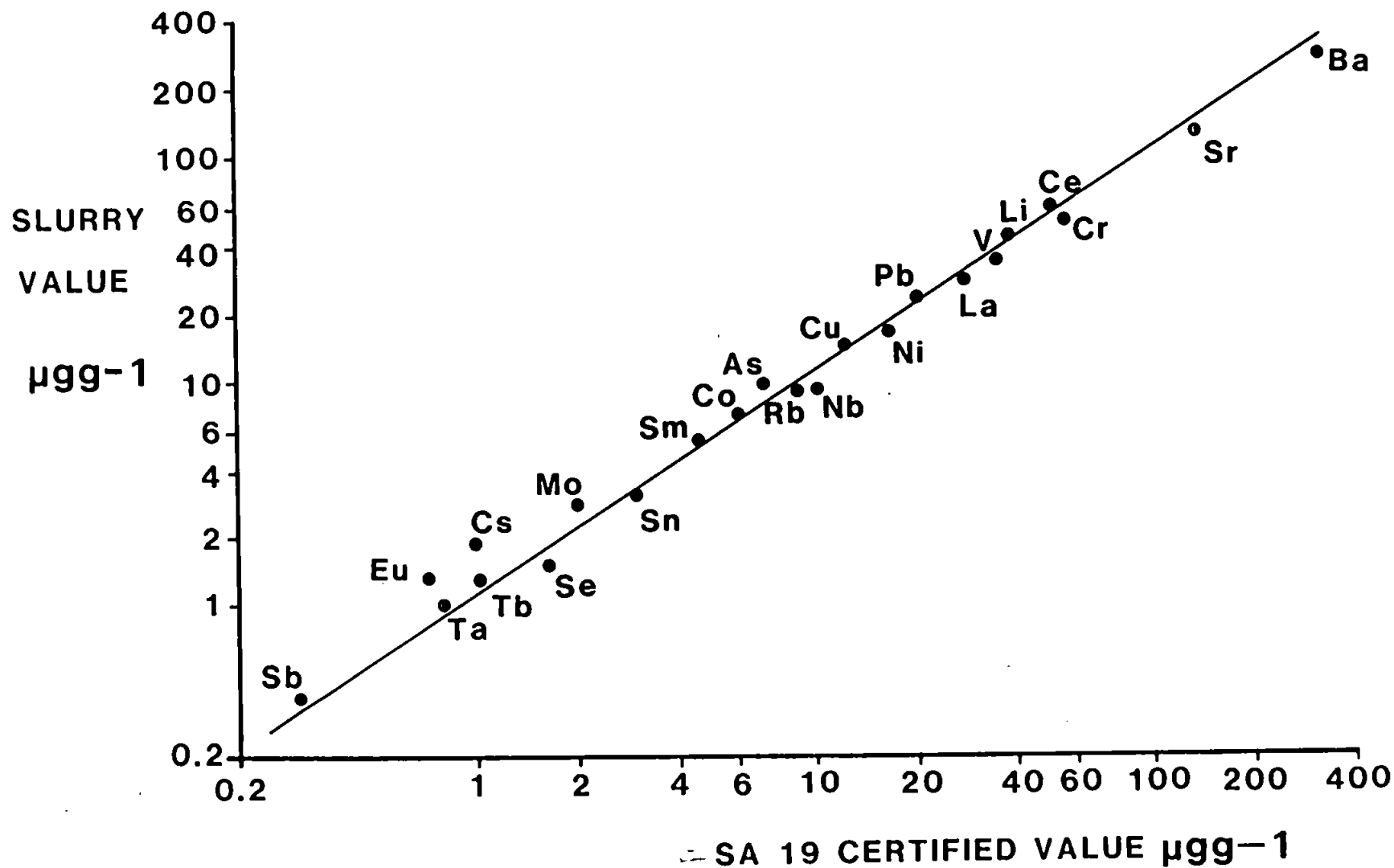
FIGURE 63

Logarithmic Plots of concentration of given elements against .   .:   concentration for the certified
material SA 20 by slurry atomisation ICP-MS.
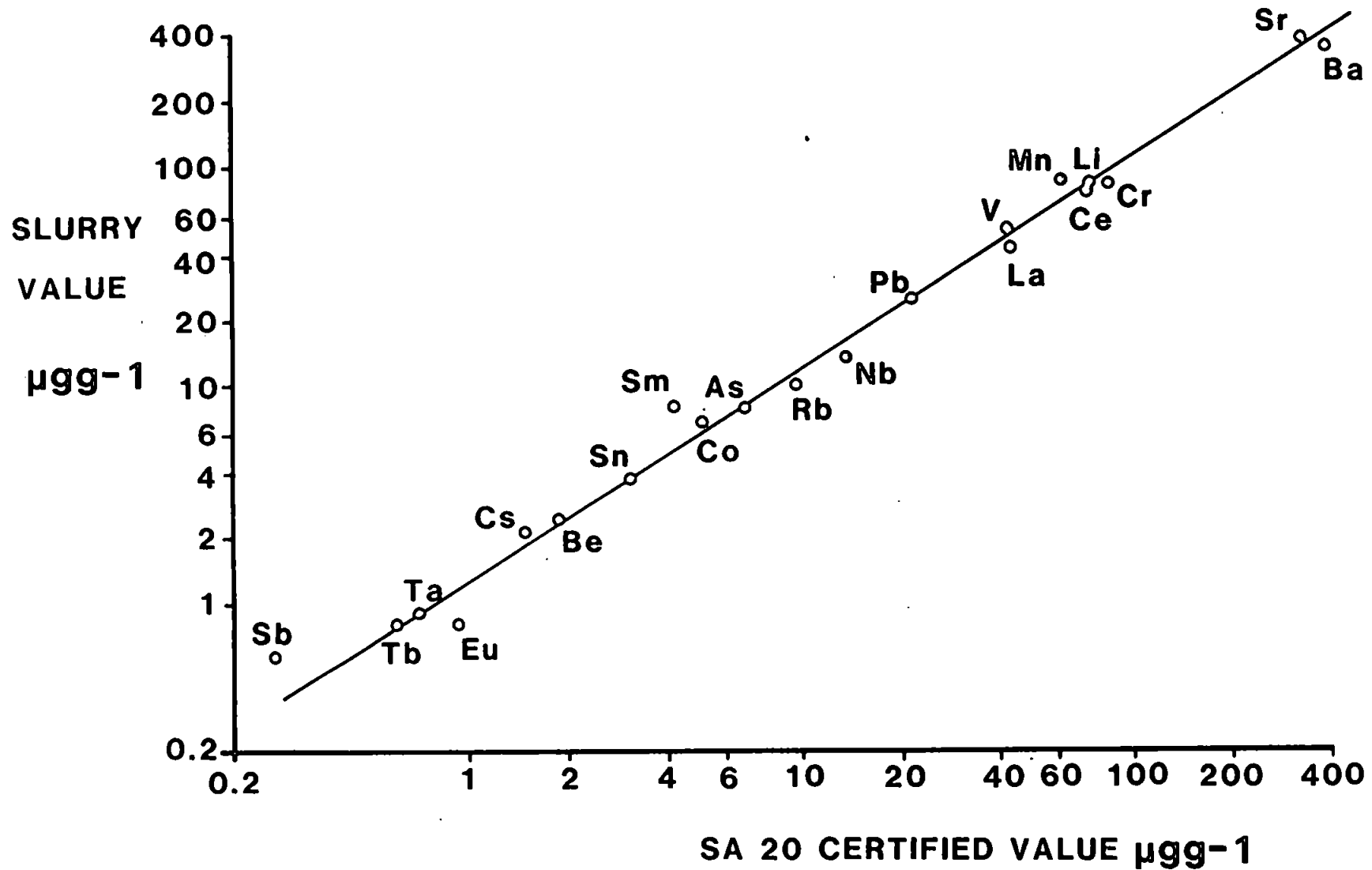
7.3.1 Laser Ablation of Zirconia grinding spheres

From the hafnium values reported in Table 69, it can be seen that there exists a large discrepancy between the levels found using ICP-MS and the certified values. This suggest that contamination has occurred during either the sample preparation or analysis stage. The most likely source of contamination within the sample preparation stage is from the zirconia grinding elements. Hafnium is found naturally together with zirconium in ores such as zircon ($ZrSiO_4$) albeit in small concentrations, typically 2%. However in certain alvite ores, the levels of hafnium exceed that of zirconium.

Investigative work was performed to ascertain the content of the zirconia spheres used as grinding elements. In Section 6.10 a Na_2O_2 fusion provided information on the contents of the spheres. However owing to the complex spectra of the lanthanides, hafnium was not determined by ICP-AES. As previously stated, ICP-MS is well suited for the determinations of the lanthanides therefore laser ablation ICP-MS was the technique used in the determination of hafnium and other elements in the zirconia spheres.

Laser ablation offers a convenient method for the direct introduction of a large variety of solid samples into the ICP. The sample is vaporised : by a brief pulse of laser radiation, and the resulting vaporisation plume is carried into the ICP where ion formation occurs preceding mass spectrometric analysis. The main advantage of this method is the ability to handle non-conducting as well as conducting samples by direct vaporisation of the material. In addition the small sample area examined by the focused laser beam allows spatial analysis which was not previously available by standard macroanalytical techniques.

TABLE 69

Semi-quantitative determination of hafnium in reference coals by laser ablation ICP - MS.

	Slurry Atomisation $\mu g \ g^{-1}$	Certificate Value $\mu g \ g^{-1}$	Range
SARM 18	82	1.7	1.7-1.9
SARM 19	170	5.4	4.7-6.1
SARM 20	228	4.8	4.1-5.1
NBS 1632(b)	21	(0.43)	-
NBS 1635	102	(0.29)	-

( ) = not certified values.

A Nd: YAG laser beam was focussed onto the surface of the zirconia sphere held in an ablation cell, by means of a microscope. The resulting millisecond pulse of energy from the laser produced a small mass of vaporised sample in the nanogram region. This ablated material was then swept into the plasma in a stream of argon carrier gas, where it was subsequently ionised and analysed by the mass spectrometer.

7.3.2 Results and Discussion

The reported results for the analysis of the zirconia grinding elements are on a semi-quantitative basis and therefore only provide an indicative value for the elements present, see Table 70. Figure 64 illustrates the spectrum for this analysis over the mass range 2 - 240 u. Figures 65, 66 and 67 show more detailed spectra in a specific part of the spectrum as shown in 67. The reported values for the analysis of zirconia spheres as shown in Table 70 show extremely high concentration of certain elements. The values of hafnium are extremely high. From Figure 64, the intensities of the peak match those of zirconium. The most intense peak corresponds to the ^{180}Hf isotope peak which is the most abundant hafnium isotope at 35%. The remaining peaks of ^{179}Hf, ^{178}Hf, ^{177}Hf and ^{176}Hf are present in the same proportion as their natural abundances i.e. 13.8%, 27.2%, 18.6% and 5.2% respectively. However the hafnium levels in Table 70 exceed those of zirconium which emphasise the importance of handling the data with caution. A possible explanation for the elevated hafnium values is attributed to the possible presence of a dimeric zirconium, but on examination of Figures 68 and 69 of levels of Zi and Hf in coal, it seems likely from the isotopic structure that the signal is due to hafnium.

On examination of the ratios of hafnium to zirconium which vary between 1.5%, 2.5% and 2.6% respectively for coals SARM 18, 19 and 20 illustrates that the hafnium is present in coal in similar quantities to its natural abundance of 2% (220). On examination of the results from the raw data for levels of zirconia and hafnium in the same coals after grinding,

TABLE 70

Semi-quantitative analysis of zirconia spheres by laser ablation ICP-MS

<u>SEMI—QUANTITATIVE ANALYSIS REPORT</u>
Internal Standard used :Zr   Mass :   96
SAMPLE IDENTITY :zr2
****** = No response calibration

ELEM	MASS	CONC (ppm)	ELEM	MASS	CONC (ppm)
Li	7	12.285561	Be	9	28.478384
B	11	58.126400	Na	23	5254.2224
Mg	24	4607.5002	Al	27	4628.3147
P	31	205223.08	Sc	45	454.62355
Ti	46	4123.0100	Ti	48	2913.1704
V	51	80.299925	Cr	52	87.053467
Mn	55	56.049776	Fe	57	3247.4443
Co	59	8.8712357	Ni	60	221.43674
Cu	63	78.430094	Cu	65	138.98892
Zn	66	348.21656	Zn	68	872.75507
Ga	69	86.380876	Ge	72	130.49951
As	75	121.71067	Se	77	107.90070
Br	81	263.33717	Se	82	184.42677
Rb	85	10.550088	Sr	88	14.890188
Y	89	2798.9974	Nb	93	22.488844
Zr	96	28000.000	Mo	98	11.465855
Ru	101	11.558029	Rh	103	1.0768321
Pd	108	384.84689	Ag	109	29.615265
Cd	111	65.662438	In	115	6.1808562
Sn	120	131.77620	Sb	121	32.030900
I	127	9.2087970	Te	128	5.2292662
Cs	133	5.2660230	Ba	138	69.804913
La	139	87.913309	Ce	140	232.64667
Pr	141	26.790943	Nd	146	124.83165
Sm	152	61.439849	Eu	153	14.013859
Gd	158	168.63061	Tb	159	42.373328
Dy	163	531.03748	Ho	165	172.44944
Er	166	769.05705	Tm	169	158.60144
Yb	172	1390.1282	Lu	175	290.77121
Hf	178	53860.267	Ta	181	11.149181
W	182	10.608061	Re	187	1.7389535
Os	189	31.275403	Ir	193	9.1539460
Pt	195	28.780331	Au	197	13.407002
Hg	202	13.254680	Tl	205	1.7219651
Pb	208	48.526609	Bi	209	1.5249290
Th	232	1184.8625	U	238	2199.1088

FIGURE 64

Mass spectrum (40-240 u) of laser ablated zirconia grinding elements
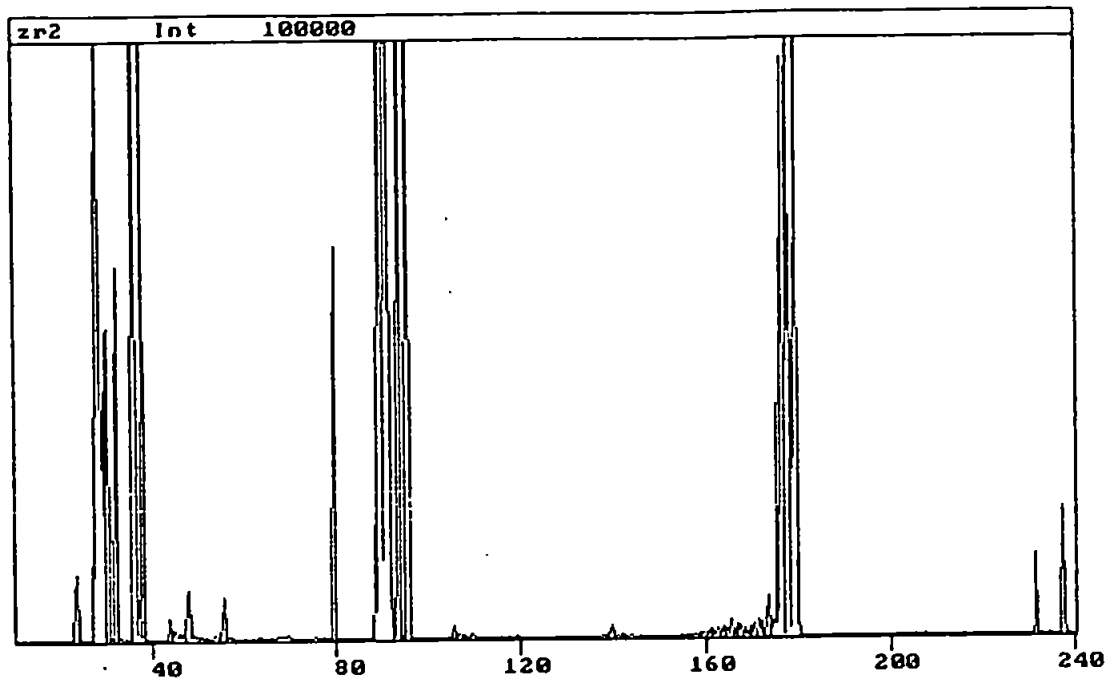
FIGURE 65

Mass spectrum (205-250 u) of laser ablated zirconia grinding elements
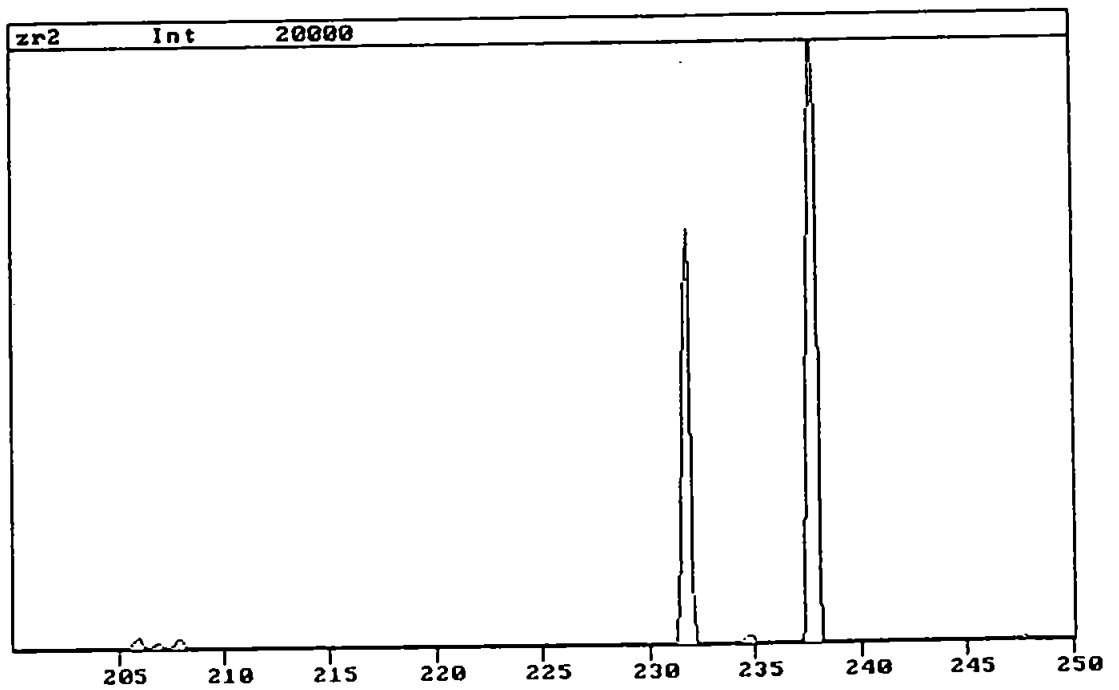
FIGURE 66

Mass spectrum (10-60 u) of laser ablated zirconia grinding elements
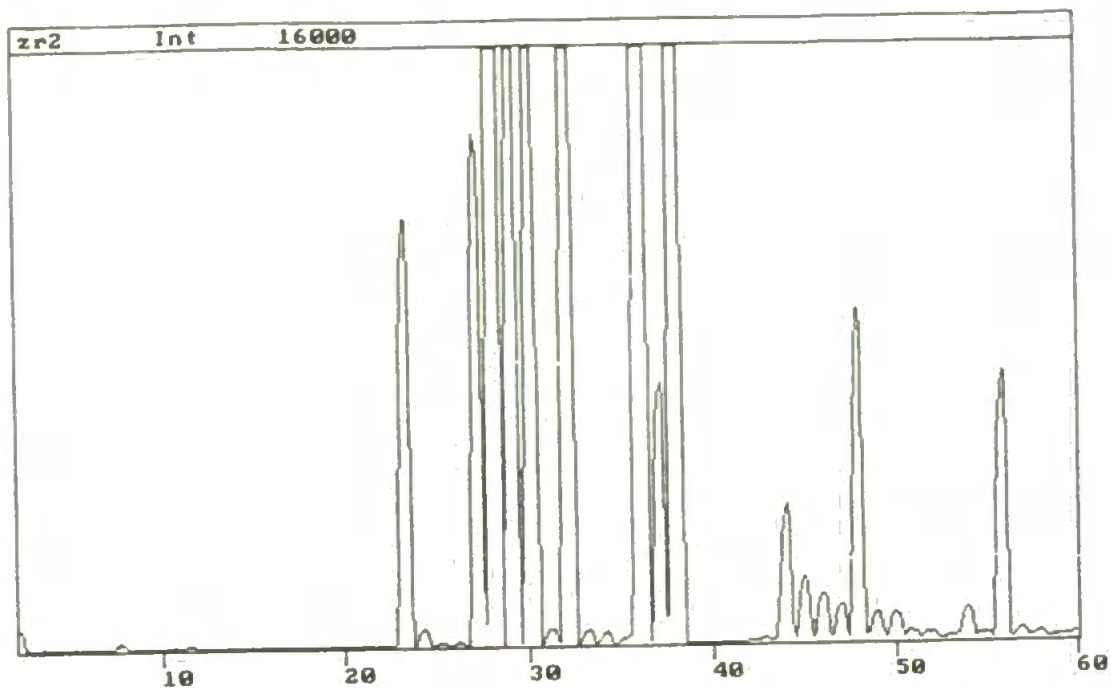
FIGURE 67

Mass spectrum (140-190 u) of laser ablated zirconia grinding elements
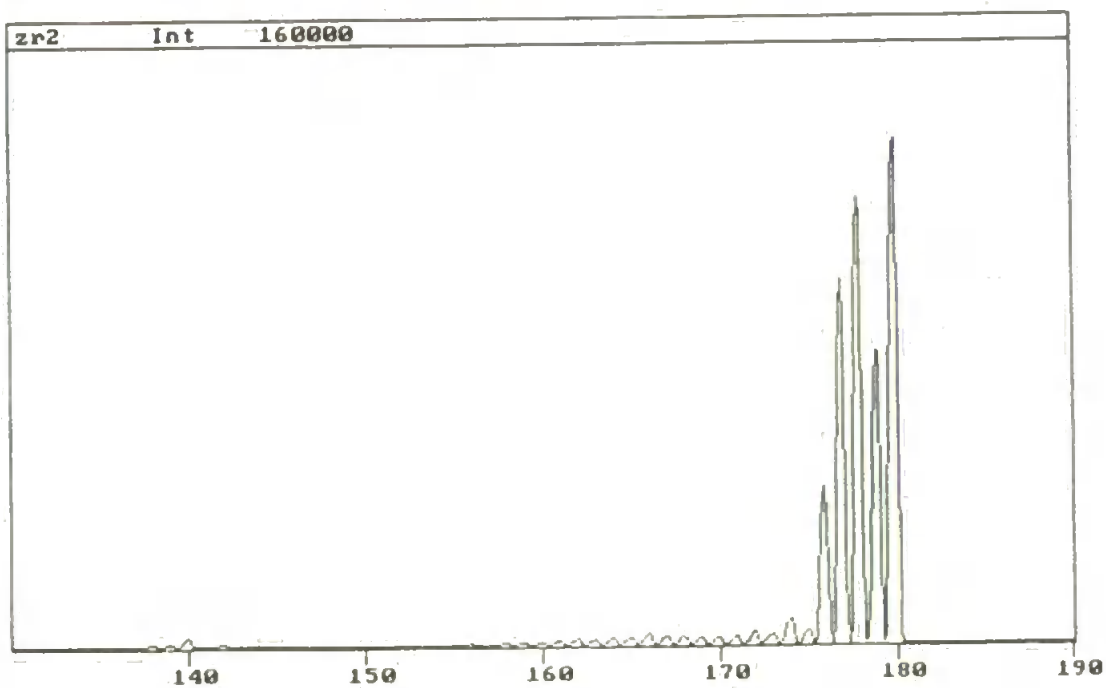
FIGURE 68

Mass spectrum (88-100 u) showing zirconia in NBS 1635 coal standard

Zirconium in NBS 1635 coal standard
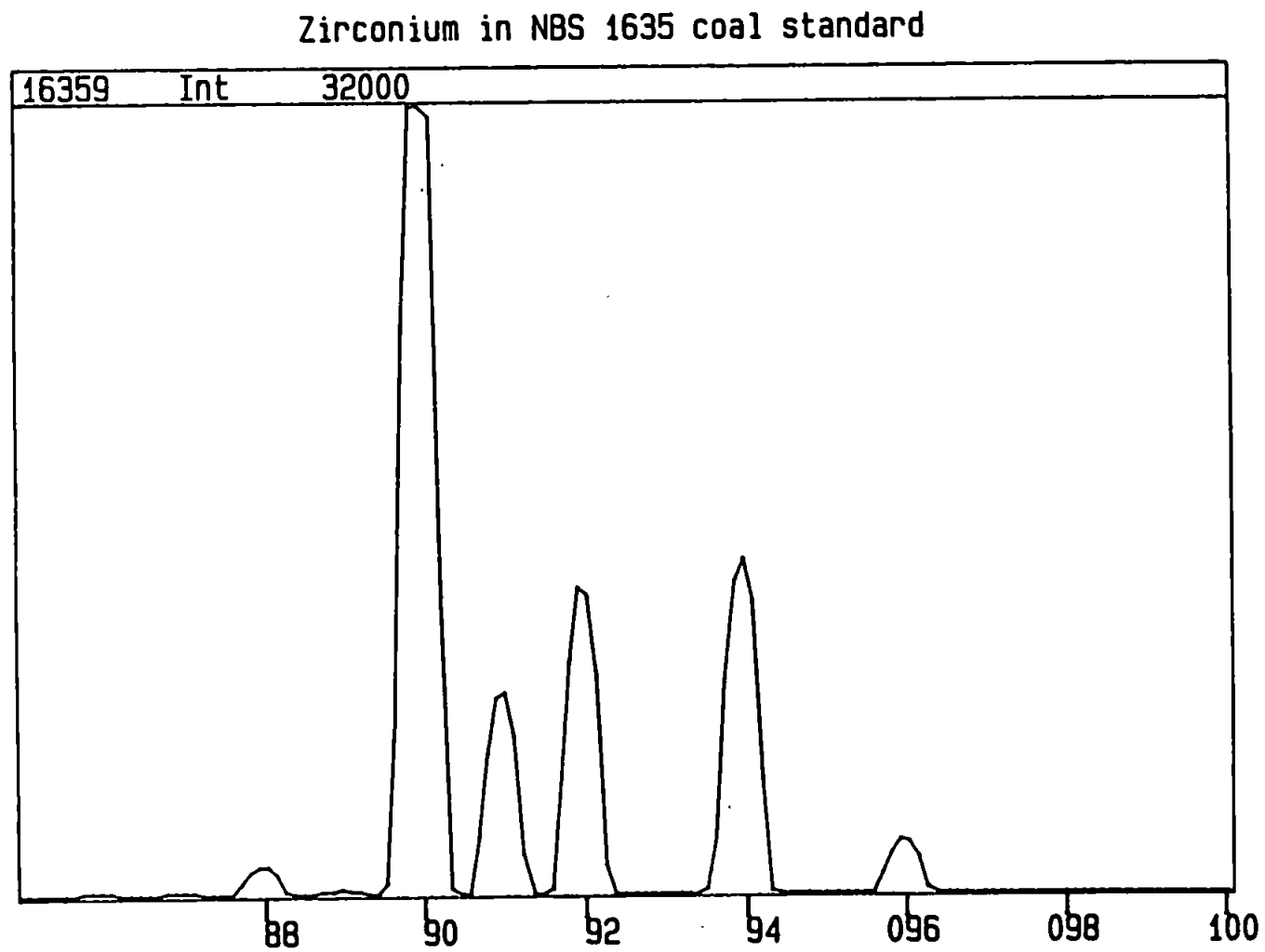
FIGURE 69

Mass spectrum (172-190 u) showing hafnium in NBS 1635 coal standard

Hafnium in NBS 1635 standard coal
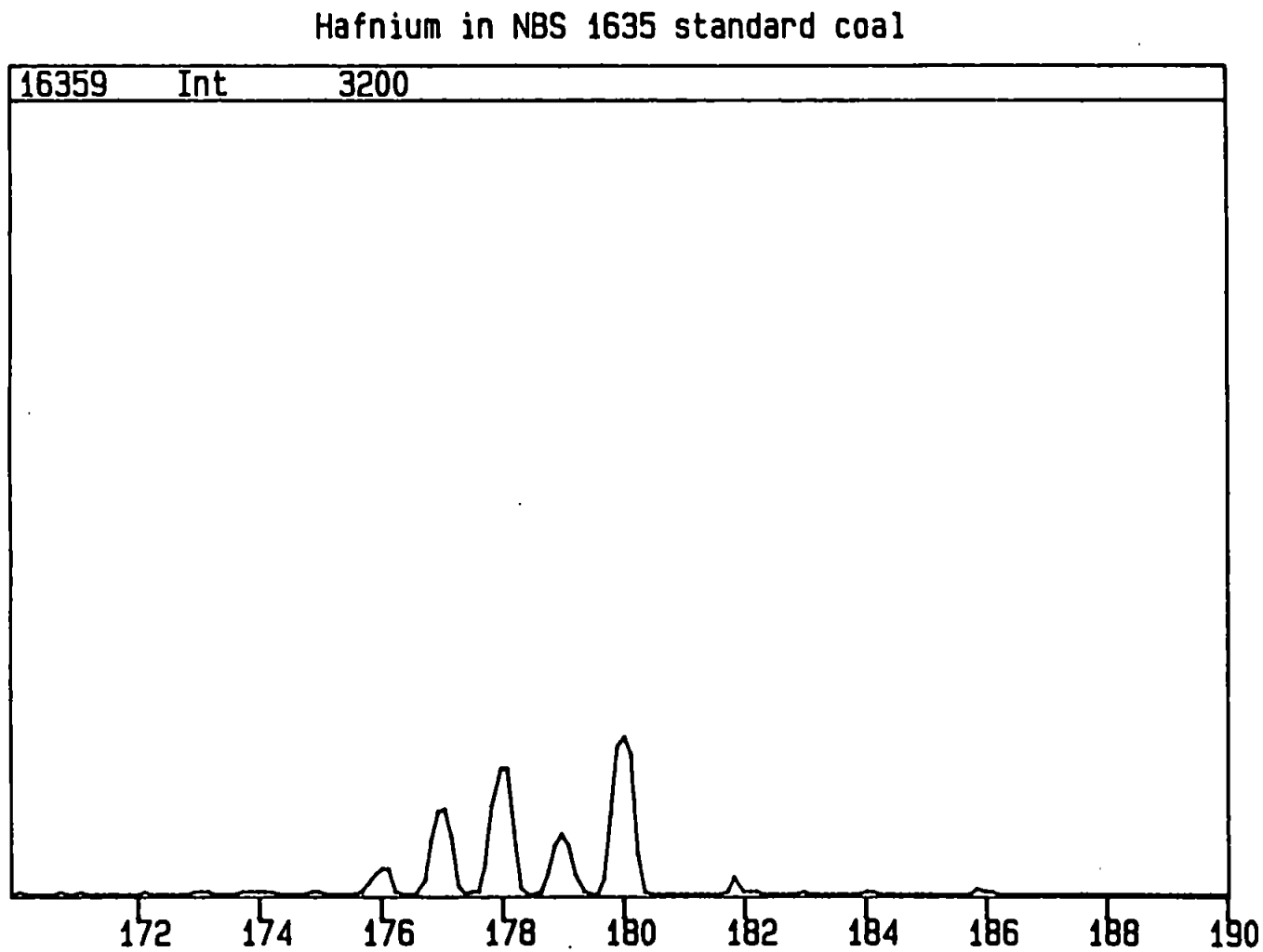
the values of both elements have increased due to contamination from the grinding elements but the ratio of hafnium to zirconia remains unchanged i.e. 1.5%, 1.5% and 1.6% for SARM 18, 19 and 20 respectively.

Recent investigations (221) of the possible contamination from the zirconia spheres has showed that the contribution to the blank after 11 hours grinding equates to 4% hafnium to zirconia which is similar to the natural abundance of hafnium in zirconia. This illustrates that there is no preferential 'leaching out' of the hafnium during the grinding procedure.

However the semi-quantitative results shown in Table 70 indicate that in the determination of zirconia spheres, there exists a larger quantity of hafnium than zirconium. This seems unlikely and illustrates the care which must be taken when handling semi-quantitative data.

7.4 CONCLUSION

These results for the analysis of solid coal samples by slurry atomisation ICP-MS have shown encouraging results and highlight the potential for this method of sample introduction with the ICP-MS.

The results obtained for a variety of reference coal material showed in most cases, extremely good agreement with the certificate values, with the exception to aluminium which showed a consistently low bias. The results are particularly encouraging for certain coals, as the particle size were not below 10 μm. This can be explained by the successful atomisation of the coal matrix.

Cone blockages were not observed using either 0.2% and 0.002% slurries during the period of analysis. The powerful analytical tool of ICP-MS offers rapid analysis of sample with minimal sample pretreatment and aqueous calibration.

The anomalous results using laser ablation ICP-MS highlight the problems experienced by several workers which were attributed to the inhomogeneity problems because of the very small sample being vaporised. It is extremely unlikely that the zirconia spheres contain more hafnium than zirconium, therefore care must be shown when analysing the data. The coal samples have clearly been contaminated with zirconium from the zirconia grinding elements and with this is associated some hafnium which is naturally found with zirconium, and this explains the elevated levels of hafnium found in the coal slurries. If Zr and Hf were important analytes alternative grinding materials such as tungsten carbide would be preferable.

CHAPTER 8

THE EFFECT OF SLURRY CONCENTRATION ON EXCITATION, IONISATION AND ROTATIONAL TEMPERATURES AND ELECTRON DENSITY IN THE ICP

8.1 INTRODUCTION

The ICP has and continues to enjoy widespread use as an emission source in the analysis of many elements. However, fundamental plasma mechanisms are not clearly understood. In order to elucidate plasma mechanisms thus allowing enhancement of analytical performance and comparison of several ICP systems, a variety of diagnostic techniques may be applied. These include the measurement of excitation temperature (T_{exc}), ionisation temperature (T_{ion}), rotational temperature (T_{rot}) and electron density (n_e) all of which provide information in the investigation of plasma processes and have been used by many workers. The potential of slurry atomisation in furthering the development of these studies has yet to be investigated for the ICP.

Recently Ramsey and Thompson (222), studied matrix effects using solution samples in the ICP. They concluded that losses in analyte sensitivity observed could be attributed to cooling of the plasma by the matrix, and that the cooling was related to the energy required for the dissociation and ionisation of the matrix.

The significance of this in slurry atomisation is apparent. As yet the effect of various slurry concentrations upon the plasma still remains unclear and it may be that the energy required in slurry analysis to dissociate and analyse the solid matrix might be analytically significant, especially at high (10-15% m/v) slurry concentration with refractory materials. Thus a study

- 217 -

of the effects of slurry concentration upon plasma cooling was required and this has been obtained by measurement of the various physical properties of the plasma during slurry atomisation.

8.2 CONCEPT OF TEMPERATURE

To distinguish between different kinds of temperature, it must be realised that a particular method gives information about one kind of temperature only, the gas temperature, the electron temperature, the excitation temperature or the ionisation temperature. In order to ascertain whether local thermal equilibrium is established or not, various methods involving different definitions of temperature must be used and coincidence of the temperature values imply that thermal equilibrium prevails.

The conditions in an atomic gas can be characterised by four different kinds of temperature previously mentioned, namely:

1. The electron temperature, which is determined by the kinetic energy of the electrons.
2. The gas temperature, which is determined by the kinetic energy of the neutral atoms.
3. The excitation temperature, which describes the population of the various energy levels.
4. The ionisation temperature which governs the various ionisation states.

For molecular gases, temperatures assigned to dissociation equilibria and to the rotational and vibrational states of the molecule should be added. Furthermore the electron density is important and of interest because the free electron is one of the most likely courses of analyte excitation and ionisation (223).

In this work, various parameters have been measured which include, T_{exc}, T_{ion}, n_e and T_{rot} according to the method used for their measurement as reported by several workers including Boumans (224), Kornblum and De Galan (225), Griem (226) and Boumans (227),

Griem, being important in the measurement and determination of n_e. For a system in thermodynamic equilibrium, the temperature values obtained would be numerically equal to one another. However for the inductively coupled plasma, the discharge is spatially inhomogeneous and is thus characterised by concentration and temperature gradients that give rise to convective and diffusional transport of species, and thus we do not observe thermal equilibrium.

By definition all emission sources deviate from LTE. It is often useful to consider emission sources using a concept termed partial LTE (pLTE). For an analyte system in pLTE, Saha equilibrium exists between excited levels and the ion ground level. The neutral ground level, however, is not in Saha equilibrium with these levels owing to local radiative energy losses. This effect of radiative loss upsets the delicate balance between the neutral ground level on the one hand and atomic excited levels and the ion ground level on the other. Raaijmakers et al. (228) outlined two methods to describe the pLTE regime. For spectrochemical work, they described pLTE by using two temperatures; the excitation temperature (T_{exc}) which described the excitation equilibrium between excited levels and the ionisation temperature (T_{ion}) which describes the ionisation equilibrium between the atom and ion ground levels. For a plasma in LTE both these temperatures and the neutral ground state temperature are equal to the electron temperature. However for a plasma in pLTE, T_{exc} is not equal to T_{ion}. Alternatively, in plasma physical work the system is described by either the electron density (n_e) or electron temperature (T_e) and an additional parameter, b_1, which takes into account the over-populated ($b_1 > 1$, ionising plasmas) or under-populated ($b_1 < 1$, recombining plasma) ground level.

Convention, however, assumes the plasma to exist in discrete volumes, each of which attain local thermodynamic equilibrium. The theoretical considerations concerning these measurements are given below.

8.2.1 Excitation Temperature

Observation of spectral line intensities leads primarily to the temperature of excitation. The intensity ratio or the two line method, which is considered here assumes that the population of atoms, ions or molecules of the thermometric species at the different energy level follows a Boltzmann distribution, i.e. derived for a system in local thermal equilibrium (LTE).

The absolute intensity I of an atom line involved in the transition from an upper level q to a lower level p is given by the expression: (224).

$$I_{qp} = \frac{d}{4\pi} A_{qp} \, n_{aq} \, h\nu_{qp} \qquad (8.1)$$

where

d = depth of source (cm)

A_{qp} = Transition probability (s^{-1})

n_{aq} = density of neutral atoms in level q (number per cm^3)

h = Planck constant (Joules s^{-1})

ν_{qp} = Frequency of the spectral line emitted in the transistion q - p (s^{-1}).

For atoms

$$n_{aq} = n_a \frac{g_q}{Z_a} \exp(-E/kT) \qquad (8.2)$$

Substituting (8.2) into (8.1) and omitting the subscript a since it is a generalization,

$$I_{qp} = \frac{d}{4\pi} A_{qp} \, h\nu_{qp} \, n \, \frac{g_n \exp(-E/kT)}{Z} \qquad (8.3)$$

The equation for temperature measurement according to the two-line procedure is derived from (8.3). If the lines are labelled a and b and the subscripts p and q designating lower and upper levels are omitted for clarity, then

$$\frac{I_a}{I_b} = \frac{(gA)_a}{(gA)_b} \frac{v_a}{v_b} \exp\left[-(E_a - E_b)/kT\right] \tag{8.4}$$

Both lines should belong either to the spectrum emitted by the neutral atom or to the spectrum emitted by the ion of the element.

The practical form of equation 8.2 can be expressed as

$$n_{aq} = n_a \frac{g_q}{Z_a} 10^{-5040 \, V_q/T} \tag{8.5}$$

where V_q = excitation potential (eV)

Rearranging (8.4) and re-numbering (8.5), the following practical equation is obtained.

$$T = \frac{5040(V_a - V_b)}{\log(gA)_a / (gA)_b - \log\lambda_a / \lambda_b - \log I_a / I_b} \tag{8.6}$$

where V is the excitation potential (eV), A the relative transition probability, g the statistical weight, the wavelength (m) and I the relative intensity. Subscripts a and b refer to the two lines respectively.

The accuracy and precision of the temperature measurements can be improved by using a thermometric species which possesses a high ionisation potential, thereby preventing a reduction in the temperature of the plasma on introduction of the thermometric species. Also the difference in V_a and V_b should be large together with the ratio $(gA)_a/(gA)_b$ thereby avoiding the use of extreme values for I_a/I_b. Bridges and Kornblith (229), have published values for oscillator strengths (gf) for Fe I with accuracies to $\pm$ 10% which can be converted into transition probability A_{qp} by the use of equation (8.7).

$$A_{qp} = \frac{6.6702 \times 10^{15}}{\lambda^2} \; \frac{g_p}{g_q} \; f_{pq} \tag{8.7}$$

where wavelength is expressed in Angstrom units.

8.2.2 Ionisation Temperature

At equilibrium the ratio of any atomic excited state population state (nj) and any ionic excited state population (nk^+) is given by the Saha equation: (225).

$$\frac{nk^+}{nj} = \left(\frac{2\pi M_e kT}{h^2}\right)^{3/2} \frac{2Zk^+}{Zi} \frac{1}{n_e} \exp(-E_{ion}/kT_{ion}) \tag{8.8}$$

where M_e = mass of the electron (9.11×10^{-31} kg)

k = Boltzman constant (1.38×10^{-23} J K^{-1})

h = Planck constant (6.62×10^{-34} J S^{-1})

T_{ion} = ionisation temperature K

Zk^+ and Zi = partition functions of ion and atom

n_e = electron density (m^{-3})

E_{ion} = ionisation potential (eV)

Equation (8.8) can be used to derive the ionisation temperature (T_{ion}) if for the electron density, n_e, some value is known or chosen. It is evident from the equation that the concentration of the two species in consecutive ionisation stages is inversely proportional to the electron density n_e.

The determination of T_{ion} can be performed by measuring the relative intensities of atom and ion lines of a particular thermometric species, determination of n_e and inserting these values into equation 8.8.

8.2.3 Electron Density

The electron number density is commonly determined by the measurement of the Stark half-width ($\Delta\lambda S\frac{1}{2}$) of the Balmer series lines of H, in particular the H_β 486.133 nm line.

Stark broadening is caused by the action of charged particles i.e. ions and electrons. Two theories exist for each kind of particle, to describe the experimental line profile. The broadening by ions is well described by the quasi-static approximation, which owing to the linearity of the Stark effect, is proportional to the two-thirds power of the ion density, which is equal to the electron density. Broadening by electrons, conversely, is calculated with the impact approximation, resulting in contributions that are proportional to the product of electron density and a logarithmic factor that decreases with increasing electron density. The component in a power law for the electron impact for H lines is below 1, therefore the combined width due to ion and electron broadening approach the two thirds power of the electron density. This relation of n_e to $\Delta\lambda S\frac{1}{2}$ is described by Griem (226) by the relationship:

$$n_e = C(n_e, T)\ \Delta\lambda S^{3/2} \tag{8.9}$$

where $\Delta\lambda$ S is the full Stark half width and $C(n_e, T)$ is a weak function of both electron density and temperature. The values of the coefficients $C(n_e, T)$ have been tabulated (226) and were obtained by graphical interpolation of profiles for several hydrogen and helium lines. An accuracy of + 5% for the determination of n_e using the H_β broadened line can be achieved and no assumptions are necessary as to the existence of LTE.

8.2.4 Rotational temperature

Very often, the rotational temperature T_{rot} is assumed to be of the same magnitude as the kinetic temperature T_{kin} because of the low energies involved in the rotational process. Thus for a transition $J' - J''$, a rotational line intensity can be calculated (227)

$$I = Dv^4 S \exp(-Er/kT_{rot})$$ (8.10)

where coefficient D contains the rotational partition function, the statistical weight $(2J' + 1)$ and universal constants, S is the oscillator strength and Er the rotational energy.

In this work, the effect of increasing coal slurry concentration upon T_{exc}, T_{ion}, n_e and T_{rot} was investigated. No spatially resolved information was collected and the results were obtained using the instrument operating conditions found optimal for slurry atomisation.

8.3 EXPERIMENTAL

8.3.1 Excitation temperatures

A set of coal slurries were prepared as described in section (5.5.1) to cover a range of concentration including 5%, 10%, 15%, 20%, 25% and 30% m/v coal. The thermometric species used was iron, the choice of which was governed by the concentration of the element in the coal. The lines used in the determination of T_{exc} are shown in Table 71. Bridges and Kornblinth (229) provided tabulations of oscillator strengths (log gf) which were converted to gA values by the use of equation (8.7). The results obtained are shown in

TABLE 71

Fe (I) emission lines used in determination of excitation temperature.

Fe (I) wavelength /nm	Transition Probability statistical weight g A (x 10^8 sec^{-1})	Excitation potential /eV
371.993	1.79	3.33
372.762	1.45	4.28
373.486	9.76	4.17
373.713	1.29	3.36
374.826	4.64	3.41
374.948	7.02	4.22

Table 72 which shows there is little or no cooling of the plasma at high slurry concentration as regards T_{exc}. The values of T_{exc} were evaluated from the intensities of the various line pairs using the computer program (Appendix I). The results obtained shows average values of T_{exc} of 4500 K.

8.3.2 Ionisation temperature

The ionisation temperature T_{ion} was determined by measuring the relative intensities of the Mg (I) 280.270 nm and Mg (II) 285.213 nm lines using the slurries and the technique described above. The ionisation temperature was calculated with the aid of a computer program (Appendix II) from equation 8.8 substituting a value for n_e from the H_β measurements (see Section 8.4.3). Magnesium was chosen as the thermometric species as the concentration of zinc which is a species recommended by Boumans (224), was too low in the slurry. The results obtained are shown in Figure 70 which indicate an average value for T_{ion} in the region of 5850 K with no significant variation with slurry concentration.

8.3.3 Electron Density

The electron density, n_e was determined by measuring the Stark half-width ($\Delta \lambda S \frac{1}{2}$), of the broadened H_β Balmer line at 486.133 nm. This was accomplished by slowly scanning the H_β line (0.01 nm s^{-1}), using entrance slits on the monochromator of 25 μm. The determined half-width is not entirely due to stark broadening, but includes broadening contributions by the Doppler effect and the instrument. The contributions from Doppler and instrumental broadening were calculated by scanning the Ti (I) 487.014 nm line. The Doppler component was calculated using equation 8.11 (225), assuming a temperature of 6000K.

$$\Delta \lambda D = 7.16 \times 10^{-7} (T/M)^{1/2} \lambda^\circ \qquad (8.11)$$

TABLE 72

Variation of excitation temperature /κ. with slurry concentration, using different line pairs.

Line pairs/nm	SLURRY CONCENTRATION					
	5%	10%	15%	20%	25%	30%
371.993/372.762	4093	3918	3890	4065	4080	3875
371.993/373.486	4561	4213	4213	4132	4572	3928
371.993/374.948	4532	4338	4315	4309	3949	4026
371.993/374.826	6623	7032	5232	4324	2478	2872
372.762/373.486	2247	2510	2410	3594	2192	3496
372.762/374.948	1727	1652	1625	2254	7669	2532
372.762/374.826	3945	3755	3795	4041	4356	4013
372.762/373.713	4058	3907	3950	4137	3893	4191
373.486/374.826	4407	4032	4124	4112	5048	4097
373.486/373.713	4535	4213	4310	4220	4332	4302
374.948/374.826	4385	4169	4237	4308	4214	4205
374.948/373.713	4506	4344	4416	4408	3757	4403

FIGURE 70

Variation of ionisation temperature with slurry concentration
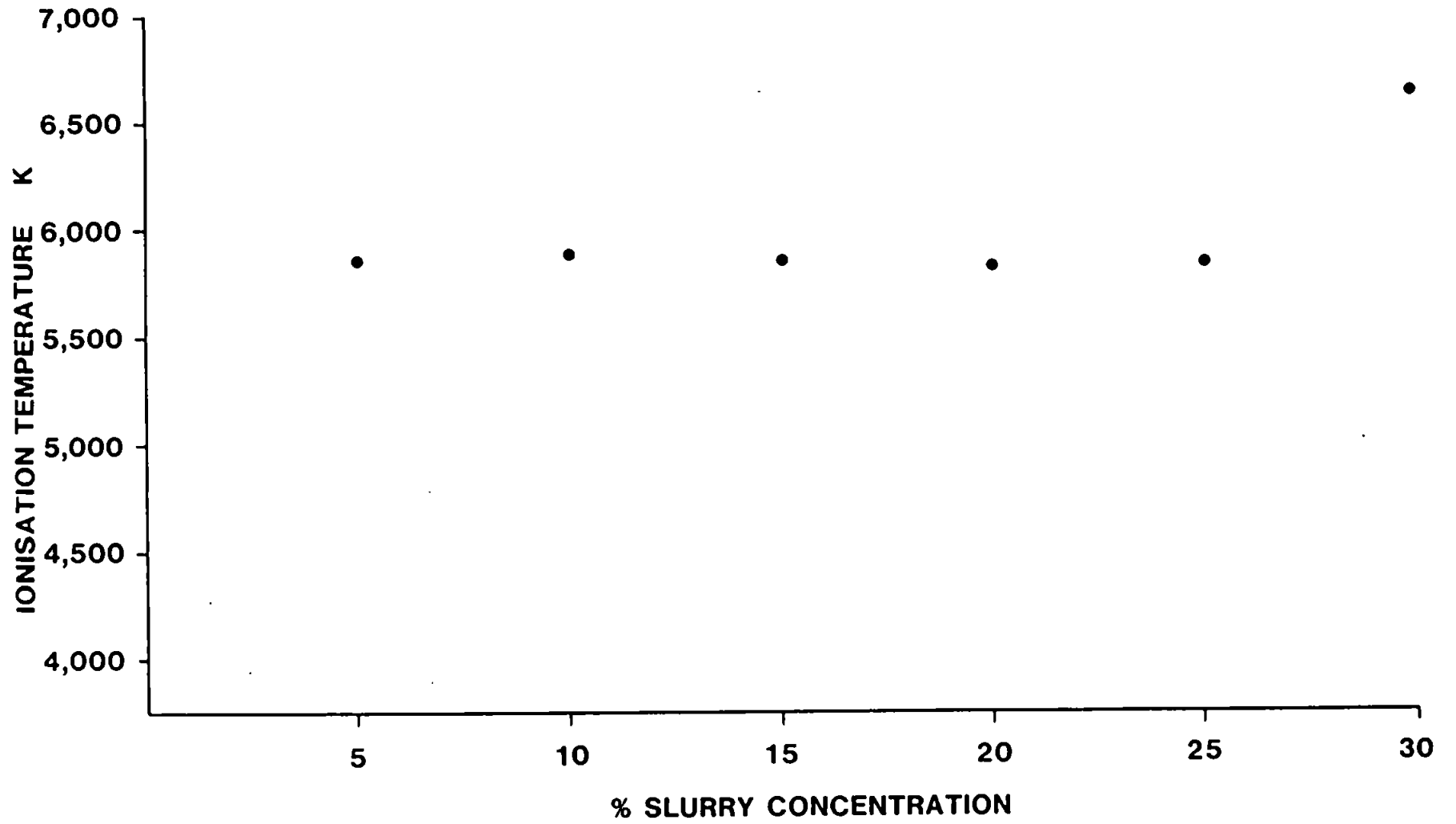
where $\Delta \lambda_D$ is the Doppler half-width, T the temperature, M the mass number of the species used (Ti = 47.9) and λ° the spectral wavelength of the species used. The Doppler half-width was calculated to be 0.0039 nm. The instrumental broadening $\Delta \lambda_{inst}$ was determined using equation 8.12, (223).

$$\Delta \lambda_{inst} = \left[(\Delta \lambda_{\frac{1}{2}} \text{ measured at } 487.014)^2 - (\Delta \lambda D)^2 \right]^{\frac{1}{2}} \qquad (8.12)$$

The instrumental broadening was calculated to be 0.0426 nm. The stark half-width, $\Delta \lambda S$ was then obtained by the subtraction of the Doppler and instrumental components from the measured half width of the H_β Balmer line. The electron densities over the range of 10^{20} - 10^{22} m^{-3} Table 73 were interpolated from the values of $C(n_e, T)$ at 5000 K for electron densities of 10^{20} m^{-3}, 10^{21} m^{-3} and 10^{22} m^{-3} published by Griem (227). The electron density was calculated by converting the stark half-width $\Delta \lambda S_{\frac{1}{2}}$ into Angstrom units, selecting the closest value of $C(n_e, 5000)$ to the value of $S_{\frac{1}{2}}$ from Table 73 and then inserting the values of $C(n_e, T)$ and $\Delta \lambda S_{\frac{1}{2}}$ into equation 8.9. The procedure was simplified by use of a computer program (Appendix III).

The results obtained (Figure 71) showed no variation with slurry concentration but the value for n_e of 9.74×10^{19} m^{-3} was lower than reported by other workers (230), who recorded values for n_e between 0.9×10^{21} to 4.5×10^{21} m^{-3}.

8.3.4 Rotational temperature

The rotational temperature can be determined using the (o-o) band of the $A^2 + - X^2$ transition system for the OH spectrum at 306.4 nm. Line assignments were taken from Dieke and Crosswhite (231) and Boumans (227) using the (0-0) band (Figure 72) the Q_1 branch was selected for all intensity measurements as they were satisfactorily resolved. The relationship between line intensity and energy is given in the form of log $(I \lambda / A)$ where I is the intensity, in the wavelength of the various branches and A the transition probabilities

TABLE 73

Interpolated values for n_e, $C(n_e, T)$ and $\Delta \lambda\, S_{\frac{1}{2}}$ (226)

n_e/m^{-3}	$C(n_e, 5000k)$	$\Delta\ S_{\frac{1}{2}}\ \overset{o}{A}$
1.0×10^{20}	3.84×10^{20}	0.408
2.0×10^{20}	3.83×10^{20}	0.648
3.0×10^{20}	3.81×10^{20}	0.853
4.0×10^{20}	3.80×10^{20}	1.035
5.0×10^{20}	3.78×10^{20}	1.205
6.0×10^{20}	3.76×10^{20}	1.366
7.0×10^{20}	3.74×10^{20}	1.519
8.0×10^{20}	3.72×10^{20}	1.666
9.0×10^{20}	3.70×10^{20}	1.809
1.0×10^{21}	3.68×10^{20}	1.947
2.0×10^{21}	3.66×10^{20}	3.102
3.0×10^{21}	3.64×10^{20}	4.080
4.0×10^{21}	3.61×10^{20}	4.970
5.0×10^{21}	3.59×10^{20}	5.789
6.0×10^{21}	3.56×10^{20}	6.574
7.0×10^{21}	3.53×10^{20}	7.326
8.0×10^{21}	3.50×10^{20}	8.054
9.0×10^{21}	3.47×10^{20}	8.762
1.0×10^{22}	3.44×10^{20}	9.454

FIGURE 71

Variation of electron number density with slurry concentration
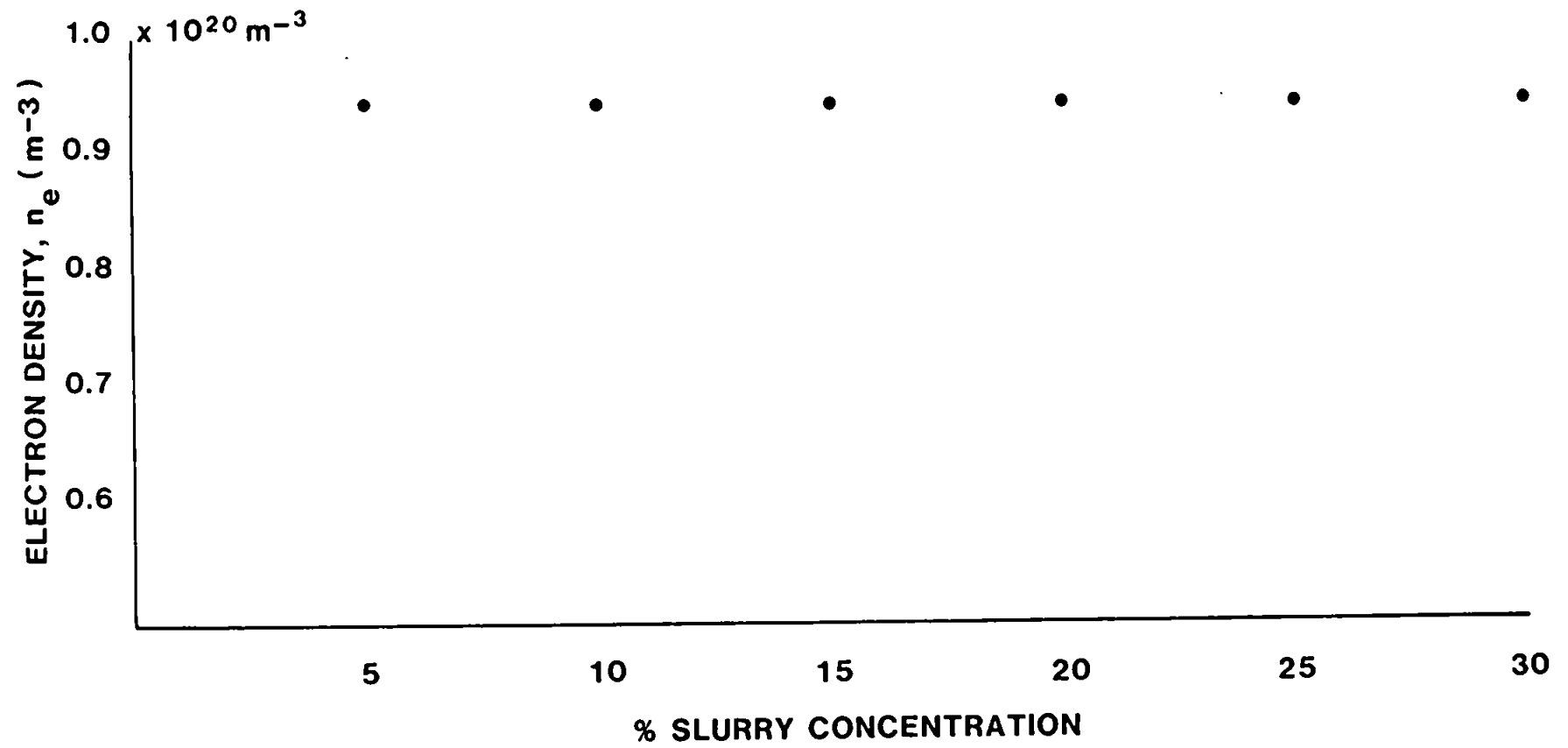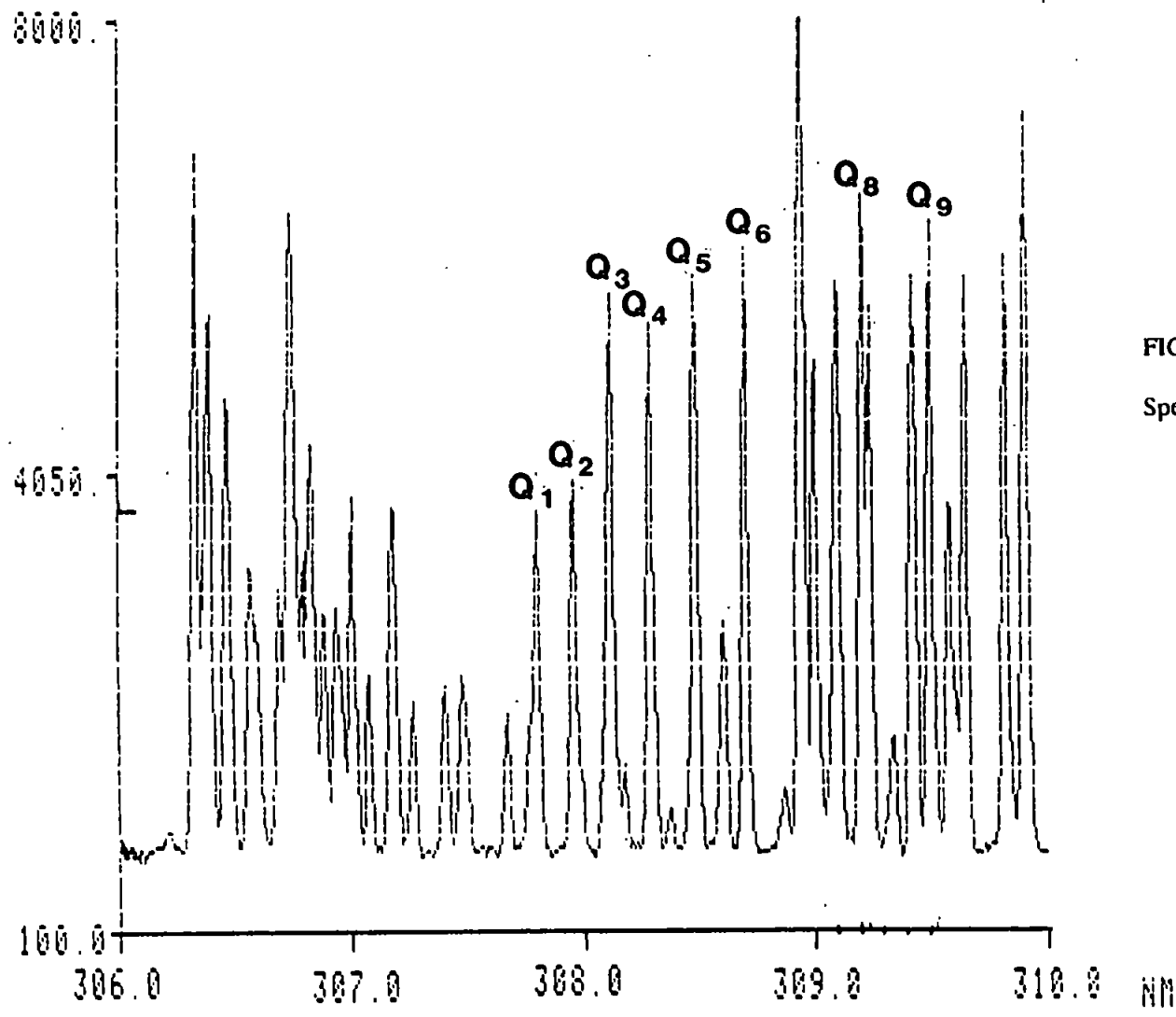
FIGURE 72

Spectral scan of the (0-0) band of OH

against E. The values for line assignments, wavelengths, transition probabilities and energies are given in Table 74. The OH spectrum was scanned between 306 nm and 310 nm for each slurry and the results recorded using the printer from which the intensity was measured for each assigned Q branch. A graphical plot of log $(I\lambda/A)$ against E resulted in a straight line, thus allowing the deduction of the rotational temperature from the slope - 0.625/T. Figures 73 - 78 illustrate these plots whilst the rotational temperature for various slurries are reported in Table 75. The average OH-T_{rot} was 2645K which is slightly higher than found by other workers. Hasegawa and Winefordner (232) reported values of 2000K for T_{rot} obtained from OH measurements, compared to 4000K obtained from N_2 - T_{rot} measurements for the same plasma.

8.4 DISCUSSION

The values obtained for T_{exc} (4500 K), T_{ion} (5850 K), n_e (0.97 x 10^{20} m^{-3}) and T_{rot} (2645 K) shows reasonable agreement with those obtained by other workers. Excitation temperature have been reported to vary between 4000 - 7000 K (233) depending on the energy level of the lines of the thermometric species and position within the plasma. For this study, the temperature measurement are made in the location of the plasma which gave the best solution/slurry response and was typically 10-20 mm above the load coil. Ionisation temperatures, T_{ion} have been calculated at between 6000 and 7000 K (223, 233) which agrees with the value of 5850 K when experimental error is taken into account. Electron density has been reported to vary between 1 x 10^{20} - 4.5 x 10^{21} m^{-3} (230, 234) and the T_{rot} have been reported in the range of between 2,000 - 5,000 K (232, 235). The rotational temperature is generally considered to be comparable to the kinetic temperature and is therefore significant when considering the dissociation of solid matrices.

Most significantly, it can be seen that the plasma is not in LTE owing to the variation in the various calculated values for the temperature of the plasma. Once the lack of LTE is established it becomes difficult to attempt to elucidate excitation measurements as diagnostic

TABLE 74

Values for assignment, wavelengths, energies and transition probabilities for the Q_1, branch of the OH (0-0) band. (226)

k	/nm	E/cm^{-1}	$A/10^8 \ s^{-1}$
1	307.844	32,475	0.0
2	307.995	32,543	17.0
4	308.328	32,779	33.7
5	308.520	32,948	42.2
6	308.734	33,150	50.6
8	309.239	33,652	67.5
9	309.534	33,952	75.8

TABLE 75

Effect of slurry concentration upon rotational temperature.

Slurry Concentration/ % m/v	Rotational Temperature/ K
0	3472
5	2498
10	2907
15	2500
20	2717
25	2604

FIGURE 73

Plot of line intensity against energy when nebulising water into the plasma

FIGURE 74

Plot of line intensity against energy when nebulising 5% slurry into the plasma

FIGURE 75

Plot of line intensity against energy when nebulising 10% slurry into the plasma
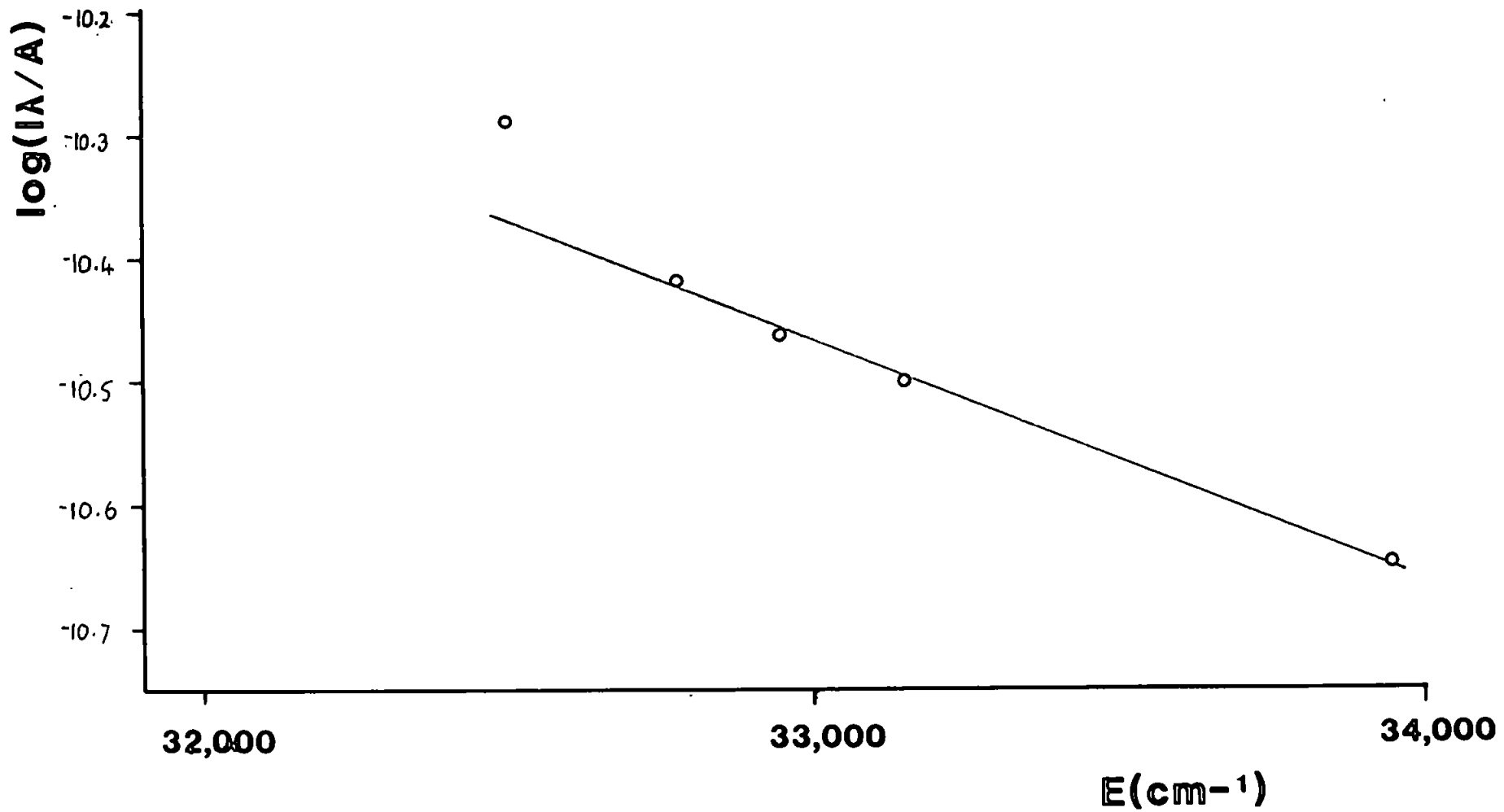
FIGURE 76

Plot of line intensity against energy when nebulising 15% slurry into the plasma
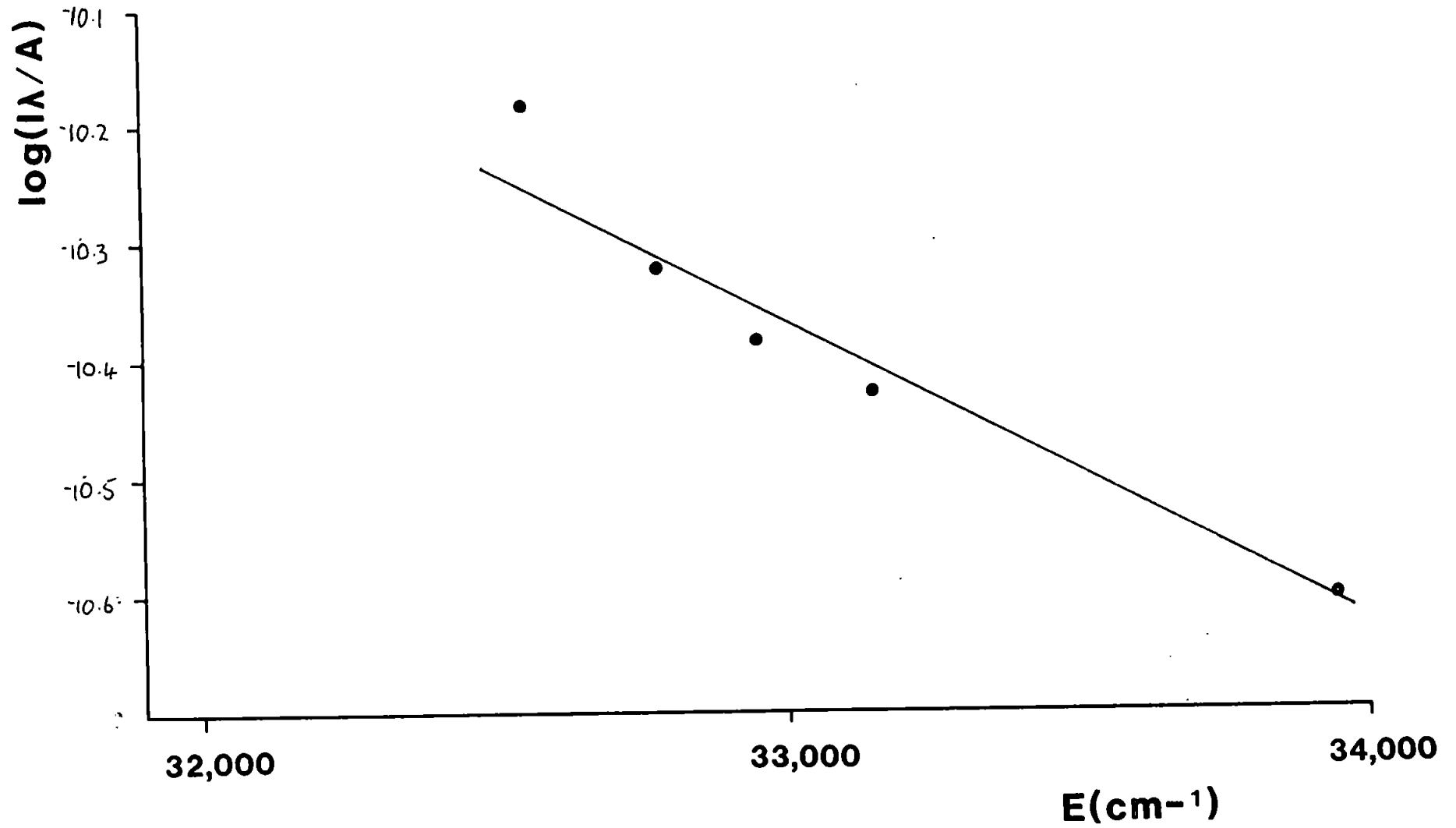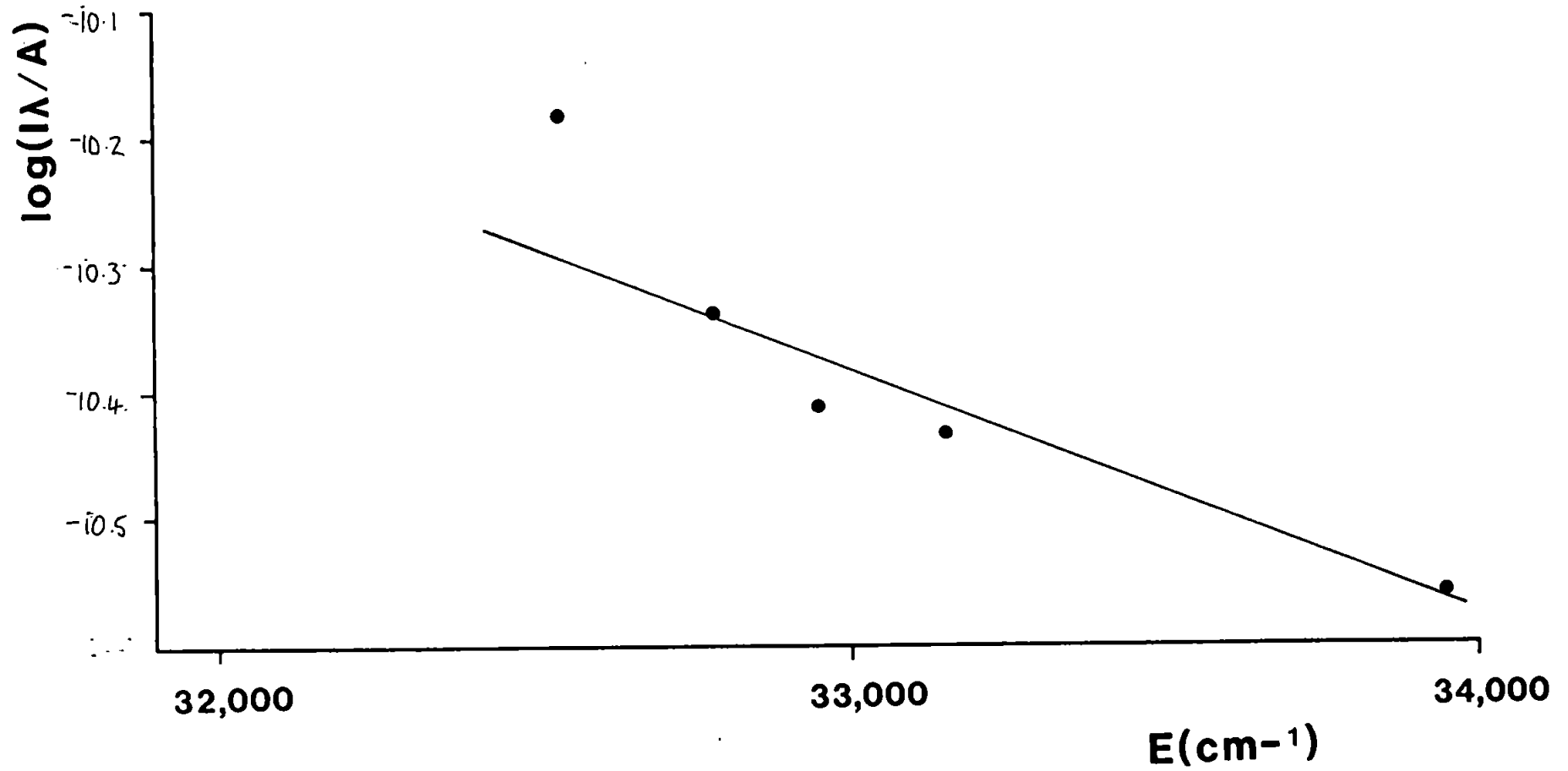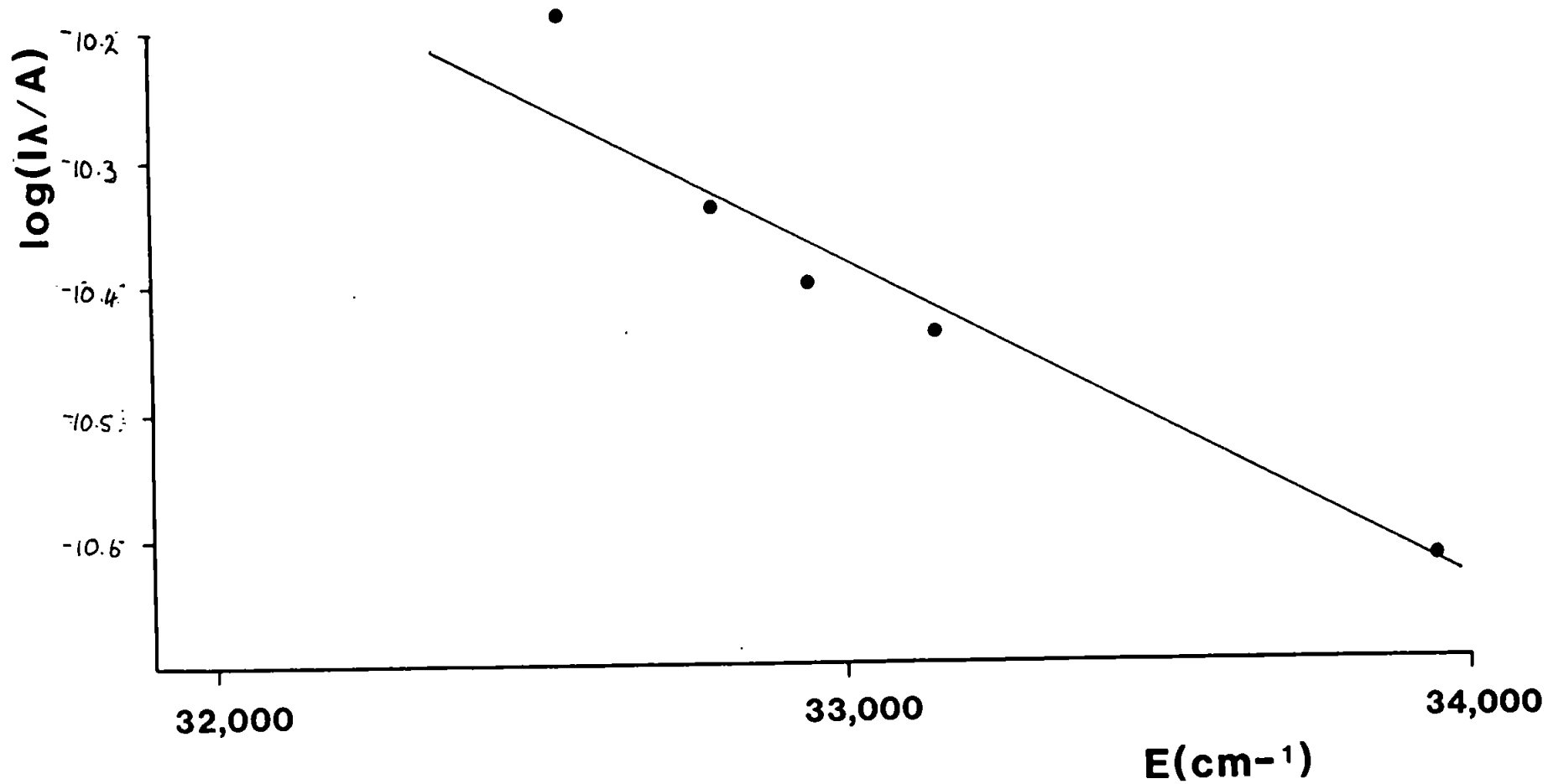
FIGURE 77

Plot of line intensity against energy when nebulising 20% slurry into the plasma
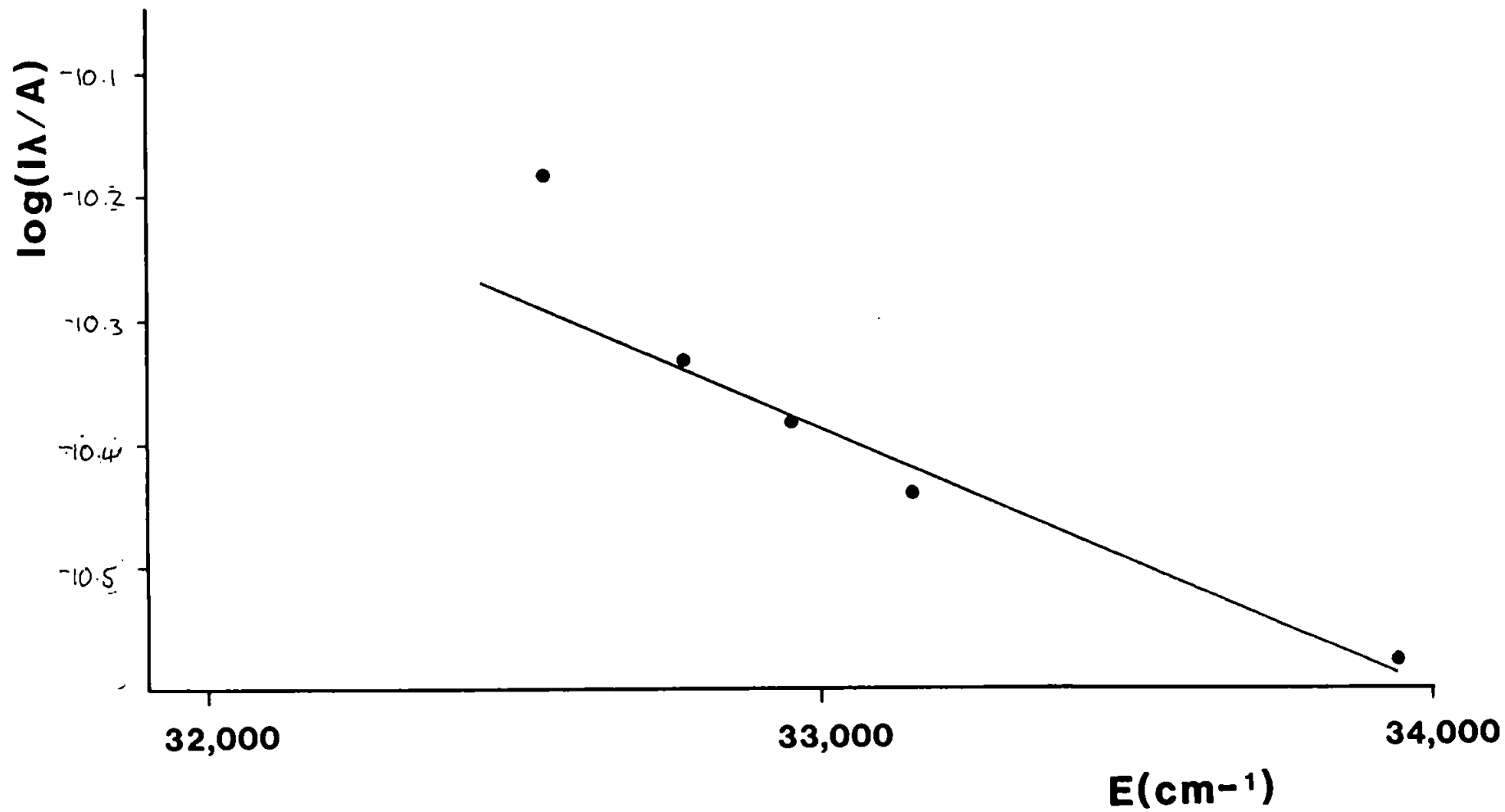
FIGURE 78

Plot of line intensity against energy when nebulising 25% slurry into the plasma
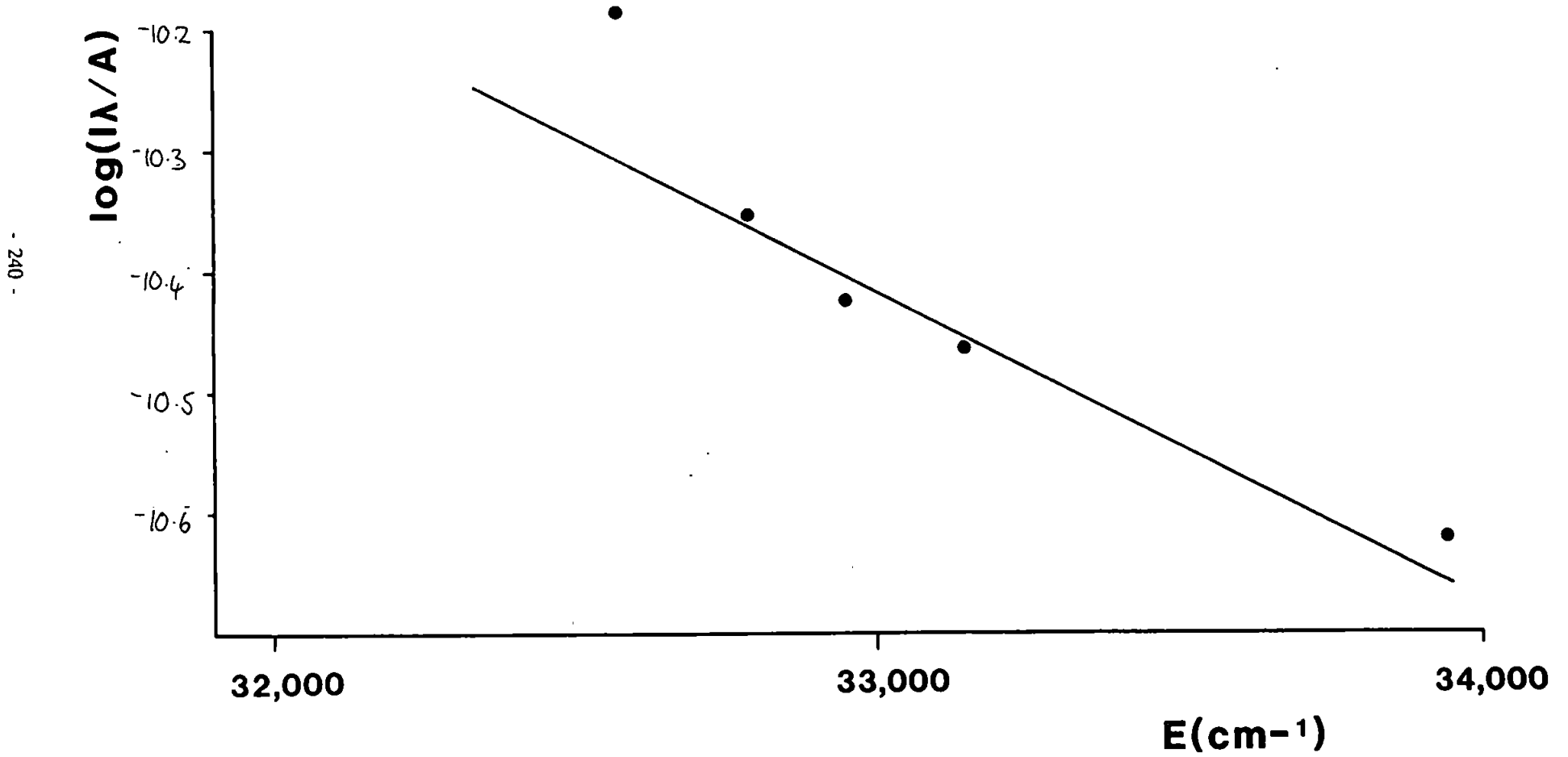
measurements assume that LTE exists. This results in temperatures and electron densities which become difficult to interpret owing to the lack of LTE. There exists two approaches to circumvent this difficulty. The first involves characterising the plasma so that the extent from LTE is known.

The most surprising observation is the uniformity of the various temperatures against slurry concentration, the exception being the excitation temperature which decreased slightly with increasing slurry concentration, depending upon the thermometric pair used. This is in contradiction to recent work (198) performed on the effect of slurry concentration in the DCP which reported that the values of T_{exc} and n_e reduced with increasing slurry concentration. This could be explained by the fact that the ICP has a higher electron density than the DCP and is thus able to tolerate higher slurry loadings, but the comparative values of n_e for the ICP and DCP, show that the DCP had a higher value of n_e 3 x 10^{21} m^{-3} cf 0.97 x 10^{20} m^{-3}.

A plot of SBR for Fe at 374.948nm against slurry concentration is shown in Figure 79. One might expect this plot to be linear, but it loses its linearity towards high concentration. This might possibly be explained by a cooling process within the plasma, caused by the increased loading upon the excitation source thus resulting in a decrease in dissociation and ionisation energies resulting in lower emission. However from the various temperature measurements this is seen not to be the case as there is little or no variation of temperature with increasing slurry concentration.

Therefore in order to elucidate the loss of linearity, a mass transport experiment was performed so as to ascertain the amount of sample reaching the plasma for a 5% and 30% m/v slurry. Each slurry was introduced in the conventional manner and the slurry aerosol was collected in the injector top by impaction onto U tubes filled with silica gel (236). The U tubes were then weighed to constant weight and thus the weight of sample collected was

FIGURE 79
GRAPH OF SBR FOR THE 374.948nm IRON LINE
AGAINST SLURRY CONCENTRATION
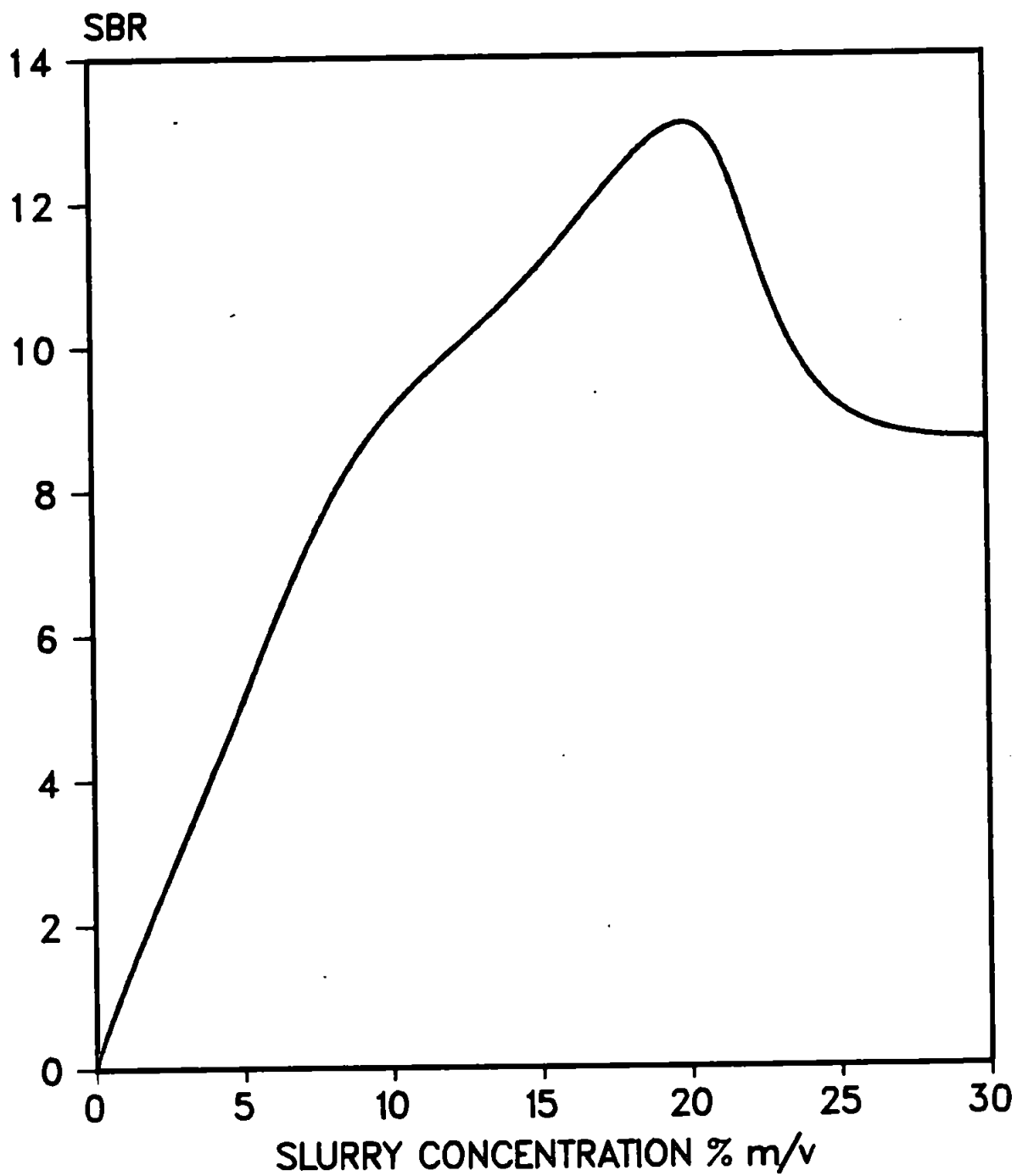
determined. The weight of coal collected after 10 mins of aspiration of the 5% slurry was 0.0703 g whilst 0.0503 g was collected over the same period for the 30% m/v slurry. Clearly it can be seen that this would result in loss of linearity and may be attributed to increased viscosity of the slurry. This problem could be alleviated by the use of internal standards. Slurry concentrations < 10% m/v showed no deviation from linearity and thus it might be concluded, that with the sample introduction system at present, coal slurries up to 10% m/v can be pumped, with no significant loss in emission signal. No cooling of the plasma was evident as reported by Ramsey and Thompson (222). However it is evident that transport effects pay a significant role in slurry atomisation when concentrations exceed that of 10% m/v and below this value these effects are not observed.

8.5 SUMMARY

The values for excitation temperatures, ionisation temperature, electron density and rotational temperature found within a range of coal slurries were 4500 K, 5850 K, 0.97 x 10^{20} m^{-3} and 2645 K respectively. No significant reduction was recorded for these parameters, with exception to T_{exc} which showed a slight decrease depending on the thermometric species chosen. However problems were encountered with the introduction of high concentration slurries owing to viscosity effects which caused pumping problems. These problems could be alleviated if samples below 10% m/v concentration were used.

CHAPTER 9

CONCLUSION AND SUGGESTIONS FOR FUTURE WORK

9.1 CONCLUSION

The work previously described has illustrated the successful analysis of whole powdered coal by slurry atomisation and the determination of a wide range of elements using several analytical techniques.

Owing to the low levels of toxic elements such as arsenic, selenium, cadmium and antimony in coal, electrothermal atomisation atomic absorption spectroscopy (ETA-AAS) was the chosen technique as it offered sufficiently low detection limits. The problem of volatility of the analytes preventing efficient matrix destruction was overcome by the use of matrix modifiers e.g. nickel nitrate which prevented the early loss of analyte, by forming a more thermally stable compound.

During the arsenic determination nickel arsenide was formed thus allowing the retention of the analyte, which would otherwise be lost during the ashing stage until the atomisation stage. Sample destruction and pyrolysis was aided by the addition of magnesium nitrate, or ashing aid to the slurry. However despite these precautions problems were encountered from an interference which had been previously reported by Riley (153) and was attributed to a broadened aluminium-line spectral interference. Despite careful control of the atomisation program, the arsenic signal could not be completely separated from that of aluminium, this resulted in positive errors. However the problem was alleviated by the use of Smith-Hieftje background correction, which successfully corrected for the presence of a structural background. Arsenic was successfully determined in various coal slurries with a limit of detection of 0.03 μgg^{-1} using a 10% m/v slurry.

Similarly the determination of selenium was hindered by a structured background interference from iron. The use of the 204.0 nm line proved unsuccessful owing to insufficient sensitivity and the problem of structured interferences was alleviated by the use of the Smith-Hieftje background correction along with the introduction of air ashing. The latter allowed oxidation of the iron until the background could be corrected. The formation of nickel selenide prevented the early loss of the analyte and this together with the use of Smith-Hieftje background correction allowed the successful determination of selenium with a detection limit of 0.05 μgg^{-1} using a 15% m/v coal slurry.

Conversely, in the determination of cadmium, there was no difference in the results obtained by continuum source or Smith-Hieftje background correction as no problem arose from structured interference. Such interference cannot be corrected by conventional continuum-source background correction systems, which by definition assumes that the background is unstructured across the band pass of the spectrometer. The cadmium results showed good agreement with the certificate values. Ash-atomise plots showed that cadmium was not lost until 500°C and the degree of vaporisation has been reported as being dependant on what form the cadmium metal is found (192). However for routine analysis the addition of ammonium phosphate as matrix modifier (193) might prove preferential and should eliminate any loss of cadmium, regardless of its form. The 217.6 nm line used in conjunction with Smith-Hieftje background correction yielded the best results for antimony determinations. Interference problems from iron prevented analysis of antimony of the alternative wavelengths and although the interference was less evident at the 217.6 nm line, the determination of antimony in 1632 (a) was unsuccessful owing to either high ash content of this bituminous coal, higher iron levels in comparison to 1635 or errors in this indicative rather than certified value.

Although ETA-AAS is sensitive it is a slow technique. More rapid techniques are offered by both direct current plasma and inductively coupled plasma atomic emission spectroscopy for multi-element analysis. Both are regarded as solution based techniques but recently they have been demonstrated to be excellent sources of excitation when using slurry atomisation.

The particle size of materials can be reduced using a simple grinding technique. The resulting slurries are made up to volume and stirred magnetically, prior to analysis. Major, minor and trace elements were successfully determined by DCP-AES and were found to be in excellent agreement with the certificate values. The majority of particles were below 16 μm and this is in agreement with McCurdy (37) who stated that particles as large as 23 μm reached the plasma. These initial results show the DCP to be an excellent excitation source for coal analysis and illustrate that a precision, often better than 2%, can be achieved using aqueous calibration with minimal sample preparation.

A comprehensive study of various parameters involved in slurry atomisation ICP-AES was investigated. The technique is an attractive one, offering a high temperature source, long linear working range and low detection limits in the ngg^{-1} region. Various designs of spray chamber were investigated which included an ARL modified chamber, a single pass and double pass spray chamber, to elucidate the optimum system for the introduction of slurries. The optimal system was found to be the ARL chamber which was modified by removing the baffle to eliminate any obstruction, in conjunction with a 1.8 mm i.d. injector tube. Simplex optimisation was found to be valuable in the investigation of ICP operating parameters and this procedure enabled the successful determination of various major, minor and trace elements in coal by slurry atomisation using reduced injector flow rates.

Problems arising from the low atomisation efficiences of aluminium were investigated using slurry atomisation and the simplex optimisation procedure. Using the simplex method in the study of the operating parameters under operator control, the height of observation and

injector flow rate were found to be the most critical parameters in the instrumental optimisation. The simplex identified a high injector flow rate and low observation height as optimal conditions for complete aluminium recovery, whilst a univariate search suggested a higher observation height and flow rate as also practical for the complete recovery for aluminium, though a second sub-optimal condition at low carrier gas flow rate was identified. Using the conditions identified by the simplex successful analysis of coal was undertaken with recoveries for aluminium ranging between 97% and 120%.

Owing to elevated levels of certain elements, analysis of the zirconia grinding elements was undertaken to establish their composition using a sodium peroxide fusion and using ICP-AES for the determination. Percentage levels of nickel and aluminium were found, whilst smaller amounts of iron, titanium and boron were detected.

Subsequent analysis of coals at British Coal laboratories using a ARL 3520 and a commercially available spray chamber proved successful, once modifications were undertaken to the spray chamber. The majority of the coals had their particle size less than 16 μm after grinding of the coal using the bottle and bead method. Calibration was achieved using aqueous standards and the instrument was operated using similar conditions to those normally used in routine analysis of aqueous coal digests. Hence the method of slurry atomisation illustrated the ease with which it can be adapted to existing instrumentation with minor modifications and enables the rapid determination of elements with decreased sample preparation.

Inductively coupled plasma mass spectrometry (ICP-MS) is a recent technique which has enabled the rapid determinations of many elements in the pg ml^{-1} level. The ICP is an excellent source for ionisation and conventionally the sample has been introduced into the ICP as a solution. Recent work with the introduction of coal slurries into ICP-AES has shown the plasma to be an efficient source for sample matrix destruction and excitation and

hence it seemed timely for the evaluation of the introduction of coal slurries into ICP-MS. The results from this initial work showed the versatility of the technique in the determination of major, minor and trace levels and owing to the sensitivity of the technique either 0.2% or 0.002% slurries were used depending upon the concentration of the element of interest in the slurry. A comprehensive analysis for each sample was completed in under two minutes, which highlighted the speed at which elemental information was obtained. Semi-quantative analysis of the zirconia grinding elements by laser ablation ICP-MS gave some indication of the content of the grinding spheres.

One advantage of slurry atomisation is that sample preparation time is reduced over conventional solution analysis, however certain matrices require long grinding times using the bottle and bead method. For rapid particle size reduction, or for determination of hafnium or zirconium, alternative grinding techniques should be investigated such as a ball mill which uses tungsten carbide grinding elements.

Previous work with solutions has shown that cooling of the plasma is observed as the matrix loading is increased (222). This has serious implications with respect to slurry atomisation. To elucidate the effect of slurry concentration upon the plasma various diagnostic techniques are available and in this work, the measurement of T_{exc}, T_{ion}, T_{rot} and n_e were made whilst introducing various concentrations of the coal matrix. No significant reduction in these parameters with increasing slurry concentration was observed. However a plot of SBR for Fe at 374.948 against slurry concentration was only linear as high as 10% m/v and a mass transport evaluation would suggest the problem as one arising from viscosity.

This work has shown that ETA-AAS, DCP-AES, ICP-AES and ICP-MS have all successfully been used in the determinations of major, minor and trace elements using slurry atomisation. This procedure has been developed and applied to each technique and calibration was achieved by the use of aqueous calibration with minimal modification to instrumentation.

9.2 FUTURE WORK

Further improvements and understanding of slurry atomisation are still required including the elucidation of mechanisms which occur within the plasma. In Chapter 8, various diagnostic tools were used in preliminary studies in an attempt to elucidate plasma mechanisms by the introduction of slurries into the ICP. Models which result from such measurements may be applied to the inductively coupled plasma and direct current plasma in order to predict the atomisation/excitation behaviour of coal slurries. Comparison of the kinetic temperature with values for T_{exc}, T_{ion} and n_e could test the theory of reductive pyrolysis as the first stage of atomisation and that slurry atomisation and excitation mechanisms are discrete processes, where as solution atomisation and excitation may be more closely linked.

The analysis of post plasma trapped material by a variety of techniques including electron microscopy, X-ray diffraction, thermal analysis and infra red spectroscopy would indicate the changes experienced by the coal particles as they pass through the plasma. This information would help elucidate slurry mechanisms within the plasma.

Recent work by Barnes has suggested that running an air plasma results in a higher kinetic gas temperature. This could be investigated by the introduction of oxygen into the plasma and with this increased kinetic gas temperature an improvement in the atomisation efficiency might result. Depending on its success, other molecular gases could also be introduced into the plasma and the effects upon coal slurry atomisation observed.

The introduction of larger particles could be facilitated by the use of larger injector tubes. However these wide bore injectors are unable to 'puncture' the plasma due to the unsteady fireball which spins as a result of the tangential entry of the outer gas flows. The use of a laminar flow torch would reduce the instability, thus allowing the use of a wider injector and thus introduction of larger particles into the plasma.

One of the main advantages of slurry atomisation over conventional solution analysis is its rapidity owing to the elimination of time-consuming digestion steps. In order to further shorten the time of analysis of slurry atomisation, investigation into various other grinding procedures are required, which would allow the efficient reduction of particle size in a shorter period than at present.

In order to make slurry atomisation more efficient, various techniques such as computer aided tomography would allow the prediction of correct plasma operating and observation conditions for analytical applications. This method could investigate the effect that slurry particles introduction has upon the plasma. The information gathered using a diode array detector would enable the identifications of temperature gradients and thus the information could be applicable to slurry atomisation using DCP-AES, ICP-AES and ICP-MS.

As with any technique, the desire for lower limits of detection and use of smaller sample volumes would be beneficial in slurry atomisation. Lower limits of detection are possible in ICP-AES when hydride generation is used, as this eliminates the nebuliser and its associated limitations. However a nebuliser is a prerequisite for slurry atomisation, and thus in order to achieve lower limits of detection, so improvements are required in the delivery system of the nebulizer, so as to reduce the noise associated with the pump. The problem of smaller sample volumes has initiated the discrete introduction of samples into the ICP, where upon the transient signal is integrated from start to finish. To date various techniques for the introduction of discrete samples exist including electrothermal vaporisation, laser ablation and direct insertion of sample via a graphite rod. However it is envisaged that flow injection analysis would enable the injection of a small volume of slurry (typically 100-500 μl) into the ICP, thus resulting in a transient signal from a minimum sample volume.

Finally the investigation and comprehension of the problem of reduced atomisation efficiencies with aluminium is required. This could be achieved by performing several simplex optimisation studies, each using new starting condition, in order to identify the correct optima.

Currently the understanding of slurry atomisation is such that the analysis of several matrices is possible. In order to attain higher efficiency and sensitivity of this technique, investigations into the mechanism of sample dissociation and analyte excitation are required.

REFERENCES

1. Nadkarni, R.A., Anal. Chem., 1980, 52, 929.

2. Schultz, H., Hattman, E.A. and Bocher, W.B., in Babu S.P., Ed "Trace Elements in Fuel", Am. Chem. Soc., 1975.

3. Goldschmidt, V.M., Ind. Eng. Chem., 1935, 27, 1100.

4. CSO, Annual Abstracts of Statistics, HMSO, 1987, No. 123.

5. Pollock, E.N., in Babu S.P., Ed "Trace Elements in Fuel", Am. Chem. Soc., 1975.

6. Nichols, C.L. and D'Auria, J.M., Analyst, 1981, 106, 874.

7. Gladney, E.S., Gordon, G.E. and Zoller, W.H., J. Environ. Sci. Health., 1978, A13, 481.

8. Churey, D.J., Gutenman, W.H., Kabata-Pendias, A. and Lisk, D.J., J. Argric. Food Chem., 1979, 27, 910.

9. Coles, D.G., Ragaini, R.C., Ondov, J.M., Fisher, G.L., Silberman, D. and Prentice, B.A., Environ. Sci. Technol., 1979, 13, 455.

10. Pearce, W.C., PhD Thesis, (Sheffield Polytechnic), CNAA, 1984.

11. Spielholtz, G.I. and Diehl, H., Talanta, 1966, 13, 991.

12. Bernas, B., Anal. Chem., 1968, 40, 1683.

13. Hartstein, A.M., Freedman, R.W. and Platter, D.W., Anal. Chem., 1973, 45, 611.

14. British Standards Institution, BS1016, "Analysis and testing of coal and coke", British Standards Institution, 2 Park Street, London, W1A 2BS, 1942.

15. Jenkins, R., Gould, R.W., Gedcke, D., "Quantitative X-Ray Spectrometry", Marcel Deker Inc., New York, 1981.

16. Rousseau, R.M., X-Ray Spectrom., 1984, 13, 115.

17. Rousseau, R.M., X-Ray Spectrom., 1984, 13, 121.

18. Jensen, B.B., Marcussen, J.N. and Pind, N., Anal Chim. Acta., 1985, 167, 305.

19. Willis, J.P., Book of abstracts of 24th Coll. Spectrosc. Int., Garmisch - Partenkirchen, FRG, 1985, 4, 668.

20. Jackson, P.F.S. and Whitehead, J., Analyst, 1966, 91, 418.

21. Ure, A.M. and Bacon, J.R., Analyst, 1978, 103, 807.

22. Guidoboni, R.J., Anal. Chem., 1973, 45, 1275.

23. Koppenaal, D.W., Lett, R.G., Brown, F.R. and Manahan, S.E., Anal. Chem., 1980, 52, 44.

24. Slates, R.V., Dupont Report, DP-1421, N.T.I.S., 1976, pp 21.

25. Kessler, T., Sharkey, A.G. and Friedel, R.A., Report No USBM-TPR-42, US Bureau of Mines, Pittsburgh, 1971, 15 pp.

26. Kessler, T., Sharkey, A.G. and Friedel, R.A., Report No RI-7714, US Bureau of Mines, Pittsburgh, 1973, 8 pp.

27. Bacon, J.R. and Ure, A.M., Analyst, 1984, 109, 1229.

28. Ruch, R.R., Cahill, R.A., Frost, J.K., Camp, L.R., and Gluskoter, H.J., J. Radioanal. Nucl. Chem., 1977, 38, 415.

29. Pringle, T.G., Landsberger, S., Davidson, W.F. and Jervis, R.E., J. Radioanal. Nucl. Chem., 1985, 90, 363.

30. Bellido, L.F. and Arezzo, B de C., J. Radioanal. Nucl. Chem., 1986, 100, 21.

31. Greenfield, S., Jones, I.L. and Berry, C.T., Analyst, 1964, 89, 713.

32. Wendt, R.H. and Fassel, V.A., Anal. Chem., 1965, 37, 920.

33. Pearce, W.C., Thornewill, D. and Marston, J.H., Analyst, 1985, 110, 625.

34. Ebdon, L. and Wilkinson, J.R., J. Anal. At. Spectrom., 1987, 2, 39.

35. Ebdon, L. and Wilkinson, J.R., J. Anal. At. Spectrom., 1987, 2, 325.

36. Decker, R.J., Spectrochim. Acta., 1980, 35B, 19.

37. McCurdy, D.L., Wichman, M.D. and Fry, R.C., Appl. Spectrosc., 1985, 39, 984.

38. Date, A.R. and Gray, A.L., Spectrochim. Acta., 1985, 40B, 115.

39. Williams, J.G., Gray, A.L., Norman, P. and Ebdon, L., J. Anal. At. Spectrom., 1987, 2, 469.

40. Gilbert, P.J., Anal. Chem., 1962, 34, 1025.

41. Langmyhr, F.J., Analyst, 1979, 104, 993.

42. Fagioli, F., Landi, S., Locatelli, C. and Bighi, C., Anal. Lett. 1983, 16, 275.

43. Faioli, F. and Landi, S., Anal. Lett., 1983, 16, 1435.

44. Willis, J.B., Anal. Chem., 1975, 47, 1752.

45. Fuller, C.W., Analyst, 1976, 101, 961.

46. Fuller, C.W., Hutton, R.C. and Preston, B., Analyst, 106, 913.

47. Mohamed, N. and Fry, R.C., Anal. Chem., 1981, 53, 450.

48. Fry, R.C. and Denton, M.B., Anal. Chem., 1977, 49, 1413.

49.   O'Reilly, J.E. and Hale, M.A., Anal. Lett., 1977, 10, 1095.

50.   O'Reilly, J.E. and Hicks, D.G., Anal. Chem., 1979, 51, 1905.

51.   Mohamed, N., McCurdy, D.L., Wichman, M.D., Fry, R.C. and O'Reilly, J.E., Appl. Spectrosc., 1985, 39, 979.

52.   Headridge, J.B., Spectrochim. Acta., 1980, 35B, 785.

53.   Langmhyr, F.J., Fresenius Z Anal. Chem., 1985, 322, 654.

54.   Fuller, C.W. and Thompson, I., Analyst, 1977, 102, 141.

55.   Ebdon, L. and Pearce, W.C., Analyst, 1982, 107, 942.

56.   Langmyhr, F.J. and Aadalen, V., Anal. Chim. Acta., 1980, 115, 365.

57.   Ebdon, L. and Parry, H.G.M., J. Anal. At. Spectrom., 1987, 2, 131.

58.   Ebdon, L. and Parry, H.G.M., J. Anal. At. Spectrom., (Jan. 1987) in the press.

59.   Hinds, M.W., Jackson, K.W., Newman, A.P., Analyst, 1985, 110, 947.

60.   Stephen, S.C., Littlejohn, D. and Ottaway, J.M., Analyst, 1985, 110, 1147.

61.   Ebdon, L. and Lechotycki, A., Microchem. J., 1986, 34, 340.

62.   Ebdon, L. and Lechotycki, A., Microchem. J., 1987, 36, 207.

63.   Mackey, J.R. and Murphy, W.J., Chem. Letts., 1984, 8, 1275.

64.   Spiers, G.A., Dudas, M.J. and Hodgins, L.W., Clay&Clay minerals., 1983, 5, 31.

65.   Watson, A.E. and Moore, G.L., S. Afr. J. Chem., 1984, 37, 81.

66.   Mason, J.L., Anal. Chem., 1963, 35, 874.

67.   Knouf, S.E., ICP Information Newslt., 1985, 11, 256.

68.   Nohe, J.D., ICP Information Newslt., 1985, 11, 7.

69.   Mohamed, N., Brown, R.M. and Fry, R.C., Appl. Spectrosc., 1981, 35, 153.

70.   Sparkes, S.T., and Ebdon, L., Anal. Proc., 1986, 23, 410.

71.   Walsh, A., Spectrochim. Acta., 1955, 7, 1087.

72.   L'vov, B.V., Spectrochim. Acta., 1984, 39B, 149.

73.   Kirkbright, G.F., Analyst, 1971, 96, 609.

74.   Greenfield, S., Hieftje, G.M., Omenetto, N., Scheeline, A. and Slavin, W., Anal. Chim. Acta., 1986, 180, 69.

75.   Koirtyohann, S.R., Spectrochim. Acta., 1980, 35B, 663.

76. L'vov, B.V., Inz. Fiz Zh., 1959, 2, 44.

77. L'vov, B.V., Spectrochim. Acta., 1984, 39B, 159.

78. L'vov, B.V., "Atomic Absorption Spectrochemical Analysis", Adam Hilger, London, 1970.

79. Ottaway, J.M., At. Spectrosc., 1982, 3, 89.

80. Regan, J.G.T. and Warren, J., At. Absorpt. Newslt., 1978, 17, 89.

81. Guevremount, R., Anal. Chem., 1980, 52, 1574.

82. Hinderberger, F.J., Kaiser, M.K. and Koirtyohann, S.R., At. Spectrosco., 1981, 2, 1.

83. Kantor, T. and Bezur, L., J. Anal. At. Spectrom., 1986, 1, 9.

84. Egila, J., Littlejohn, D., Ottaway, J.M. and Xiao - Quan, S., J. Anal. At. Spectrom., 1987, 2, 293.

85. L'vov, B.V., Spectrochim. Acta., 1978, 33B, 153.

86. Slavin, W. and Manning, D.C., Anal. Chem., 1979. 51, 261.

87. Slavin, W. and Manning, D.C., Spectrochim. Acta., 1980, 35B, 701.

88. L'vov, B.V. and Pelieva, L.A., Zh. Anal. Khim., 1978, 33, 1225.

89. Manning, D.C., Slavin, W. and Myers, S., Anal. Chem., 1979, 51, 2375.

90. Giri, S.K., Littlejohn, D. and Ottaway, J.M., Analyst, 1982, 107, 1095.

91. Frech, W. and Jonsson, S., Spectrochim. Acta., 1982, 37B, 1021.

92. Chakrabarti, C.L., Hamed, C.C., Wan, W.C., Li, P.C., Bertels, D.C. Goregoire, and Lee, S., Anal. Chem., 1980, 52, 167.

93. Slavin, W. and Manning, D.C., Spectrochim. Acta., 1982, 37B, 955.

94. Sturgeon, R.E., Fresenius, Z., Anal. Chem., 1986, 324, 807.

95. Koirtyohann, S.R. and Pickett, E.E., Anal. Chem., 1965, 37, 601.

96. de Loos-Vollebregt, M.T.C., de Galan, L., Prog. Anal. Atom. Spectrosc., 1985, 8, 47.

97. Smith Jr, S.B. and Hieftje, G.M., Appl. Spectrosc., 1983, 37, 419.

98. Littlejohn, D., Duncan, I.S., Hendry, J.B.M., Marshall, J. and Ottaway, J.M., Spectrochim. Acta., 1985, 40B, 1677.

99. Sharp, B.L., Selected Annual Reviews of the Analytical Sciences, 1976, Vo. 4, Chemical Society, London.

100. Reed, T.B., J. Appl. Phys., 1961, 32, 821.

101. Ebdon, L., Mowthrope, D.J. and Cave, M.R., Anal. Chim. Acta., 1980, 115, 171.

102. Scott, R.H., Fassel, V.A., Kniseley, R.N. and Nixon, D.E., Anal. Chem., 1974, 46, 75.

103. Browner, R.F. and Boorn, A.W., Anal. Chem., 1984, 56, A786.

104. Thompson, M., Goulter, J.E. and Sieper, F., Analyst, 1981, 106, 32.

105. Carr, J.W. and Horlick, G., Spectrochim. Acta., 1982, 37B, 1.

106. Ohls, K. and Sommer, D., Fresenius, Z., Anal. Chem., 1979, 296, 241.

107. Blakemore, W.M., Casey, P.H. and Collie, W.R., Anal. Chem., 1984. 1984, 56, 1376.

108. Cope, M.J., Kirkbright, G.F. and Burr, P.M., Analyst, 1982, 107, 611.

109. Carbi, G., Cavalli, P., Achilli, M., Rossi, G. and Omeneto, N., At. Spectrosc., 1982, 3, 81.

110. Hull, D.R. and Horlick, G., Spectrochim. Acta., 1984, 39B, 843.

111. Long, S.E., Snook, R.D. and Browner, R.F., Spectrochim. Acta., 1985, 40B, 553.

112. Matusiewicz, H. and Barnes, R.M., Anal. Chem., 1985, 57, 406.

113. Salin, E.D. and Horlick, G., Anal. Chem., 1979, 51, 2284.

114. Sommer, D. and Ohls, K., Fresenius, Z., Anal. Chem., 1980, 304, 97.

115. McLeod, C.W., Clarke, P.A. and Mowthrope, D.J., Spectrochim. Acta., 1986, 41B, 63.

116. Monasterois, C.V., Jones, A.M. and Salin, E.D., Anal. Chem., 1986, 58, 780.

117. Dagnall, R.M., Smith, D.J., West, T.S. and Greenfield, S., Anal. Chim. Acta., 1971, 54, 397.

118. Ng, K.G., Zerezghi, M. and Caruso, J.A., Anal. Chem., 1984, 56, 417.

119. Scott, R.H., Spectrochim. Acta., 1978, 33B, 123.

120. Gray, A.R., PhD Thesis, (Plymouth Polytechnic), CNAA, 1985.

121. Wilkinson, J.R., PhD Thesis, (Plymouth Polytechnic), CNAA, 1981.

122. Norman, P., PhD Thesis (Plymouth Polytechnic), CNAA, 1987.

123. Foulkes, M.E., Anal. Proc., in the press.

124. Wirz, P., Gross, M., Ganz, S. and Scharmann, A., Spectrochim. Acta., 1983, 38B, 1217.

125. Gray, A.L., Spectrochim. Acta., 1985, 40B, 1525.

126. Houk, R.S., Anal. Chem., 1986, 58, 97A.

127. Gray, A.L., Analyst, 1985, 110, 551.

128. Gray, A.L. and Date, A.R., Analyst, 1983, 108, 1033.

129. Jiang, S.J. and Houk, R.S., Anal. Chem., 1986, 58, 1739.

130. Jiang, S.J. and Houk, R.S., Spectrochim. Acta., 1987, 42B, 93.

131. Boomer, D.W., Powell, M., Sing, R.L.A. and Salin, E.D., Anal. Chem., 1986, 58, 975.

132. Case, A.E., J. Inst. Brewing., 1938, 14, 362.

133. Sandhu, S.S., Analyst, 1981, 106, 311.

134. Maher, W.A., Analyst, 1983, 108, 939.

135. British Standards Institute, B.S. 1016, "Methods for Analysis and Testing of Coal and Coke, Part 10; Arsenic in Coal and Coke". British Standards Institution, 2 Park Street, London, W1A 2BS, 1977.

136. Bassett, J., Analyst, 1963, 88, 238.

137. Nakahara, T., Anal. Chim. Acta., 1981, 131, 73.

138. Goulden, P.D., Anthony, D.H. and Austen, K.D., Anal. Chem., 1981, 53, 2027.

139. Smith, A.E., Analyst, 1975, 100, 300.

140. Smith, R.G., Van Loon, J.C., Knechtel, J.R., Fraser, J.L., Pitts, A.E. and Hodges, A.E., Anal. Chim. Acta., 1977, 93, 61.

141. Chakraborti, D., DeJonghe, W. and Adams, F., Anal. Chim. Acta., 1980, 119, 331.

142. Walsh, P.R., Fashing, J.L. and Duce, R.A., Anal. Chem., 1976, 48, 1014.

143. Yamamoto, Y., Kumamaru, T., Hayashi, Y., Kanke, M. and Matsui, A., Talanta, 1972, 19, 1633.

144. Ohta, K. and Suzuki, M., Talanta, 1978, 25, 160.

145. Hudnick, V. and Gromiscek, S., Anal. Chim. Acta., 1984, 157, 135.

146. Reichel, W. and Bleakley, B.G., Anal. Chem., 1974, 46, 59.

147. Holak, W., Anal. Chem., 1969, 41, 1712.

148. Godden, R.G. and Thomerson, D.R., Analyst, 1980, 105, 1137.

149. Chu, R.C., Barron, G.P. and Baumgarner, P.A.W., Anal. Chem., 1972, 44, 1476.

150. Fernandez, F.J. and Manning, D.C., At. Absorp. Newsl., 1971, 10, 86.

151. Wilkinson, J.R., Ebdon, L. and Jackson, K.W., Anal. Proc., 1982, 19, 305.

152. Ebdon, L. and Wilkinson, J.R., Anal. Chim. Acta., 1987, 194, 177.

153. Riley, K.W., At. Spectrosc., 1982, 3, 120.

154. Ebdon, L., "An Introduction to Atomic Absorption Spectroscopy - a Self-Teaching Approach", Heyden, London, 1982.

155. Smith, S., Schleicher, R.G. and Hieftje, G.M., paper no. 442 presented at the 33rd Pittsburgh Conference on Analytical Chemistry and Applied Spectroscopy, Atlantic City, NJ, March, 1982.

156. Raptis, S.E., Kaiser, G. and Tolg, G., Fresenius, Z., Anal. Chem., 1983, 316, 105.

157. Verlinden, M., Deelstra, H. and Adriaenssens, E., Talanta, 1981, 28, 637.

158. Thompson, D.D. and Allen, R.J., At. Spectrosc., 1981, 2, 53.

159. Ishizaki, M., Talanta, 1978, 25, 167.

160. Germaai, M.S., Grokmen, I., Sigleo, A.C., Kowalczyk, G.S., Olmez, I., Small, A.M., Anderson, D.L., Failey, M.P., Gulovali, M.C., Choquette, C.E., Lepel, E.A., Gordon, G.E. and Zoller, W.H., Anal. Chem., 1980, 52, 240.

161. Greenberg, R.R., Anal. Chem., 1979, 51, 2004.

162. Vijan, P.N. and Wood, G.R., Talanta, 1976, 23, 89.

163. Nakahara, R.A., Anal. Chim. Acta., 1982, 135, 363.

164. Agterdenbos, J., van Eltern, J.T., Bax, D. and Ter Heege, J.P., Spectrochim. Acta., 1986, 41B, 303.

165. Pierce, F.D. and Brown, H.R., Anal. Chem., 1976, 48, 693.

166. Aggett, J. and Aspell, A.C., Analyst, 1976, 101, 341.

167. Kirkbright, G.F. and Taddia, M., Anal. Chim. Acta., 1978, 100, 145.

168. Thompson, M., Pahlavanpour, B., Walton, S.J. and Kirkbright, G.F., Analyst, 1978, 103, 705.

169. Kirkbright, G.F., Hsiao-Chuan, S. and Snook, R.D., At. Spectrosc., 1980, 1, 85.

170. Martin, T.D., Kopp, J.F. and Ediger, R.D., At. Absorpt. Newsl., 1975, 14, 109.

171. Ediger, R.D., At. Absorpt. Newsl., 1975, 14, 127.

172. Alfthan, G. and Kumpalainen, J., Anal. Chim. Acta., 1982, 140, 222.

173. Brown, A.A., Ottaway, J.M. and Fell, G.S., Anal. Proc., 1982, 19, 321.

174. Oster, O. and Preewelz, W., Clin. Chim. Acta., 1982, 124, 277.

175. Carnrick, G.R., Manning, D.C. and Slavin, W., Analyst, 1983, 108, 1297.

176. Saeed, K., Thomassen, Y. and Langmyhr, F.J., Anal., Chim. Acta, 1979, 110, 285.

177. Alexander, J., Saeed, K. and Thomassen, Y., Anal. Chim. Acta., 1980, 120, 377.

178. Ping, L., Lei, W., Matsumoto, K. and Fuwa, K., Analytical Sciencies, 1985, 1, 257.

179. Manning, D.C., At. Absorpt. Newsl., 1978, 17, 167.

180. Welz, B., Schlemmer, G and Vollkopf, U., Spectrochim. Acta., 1984, 39B, 501.

181. Han-Wen, S., Xiao-Quan, S. Zhe-Ming, N., Talanta, 1982, 29, 589.

182. Jablonski, W.A. and Watson, C.A., Analyst, 1970, 95, 131.

183. Thompson, M., Pahlavanpour, B., Walton, S.J. and Kirkbright, G.F., Analyst, 1978, 103, 568.

184. Pahlavanpour, B., Thompson, M. and Thorne, L., Analyst, 1980, 105, 756.

185. Haynes, B.W., At. Absorp. Newsl., 1979, 18, 46.

186. Hamner, R.M., Lechak, D.L., Greenberg, P., At. Absorp. Newsl.,1976, 15, 122.

187. Atomic Absorption Methods Manual Vol. 2, Flameless Operation, Instrumentation Laboratory Inc., 1975.

188. Koizumi, H., Anal. Chem., 1978, 50, 1101.

189. Slavin, W. and Carnrick, G.R., At. Spectrosc., 1986, 7, 9.

190. Niskavaara, H., Virtasalo, J. and Lajunen, H.J., Spectrochim. Acta., 1985, 40B, 1219.

191. Fernandez, F.J. and Giddings, R., At. Spectrosc., 1982, 3, 61.

192. Sturgeon, R.E., Chakrabarti, C.L. and Langford, C.H., Anal. Chem., 1976, 48, 1792.

193. Allen, T., "Particle Size Measurement", 3rd edition, Chapman and Hall Ltd., London, 1981.

194. Decker, R.J., Spectrochim Acta., 1980, 35B, 19.

195. Nygaard, D.D. and Gilbert, T.R., Appl. Spectrosc., 1981, 35, 52.

196. Eastwood, D., Henrick, M.S. and Miller, M.H., Spectrochim. Acta., 1982, 37B, 293.

197. Miller, M.H., Eastwood, D. and Hendrick, M.S., Spectrochim. Acta., 1984, 39B, 13.

198. Sparkes, S.T., PhD. Thesis (Plymouth Polytechnic), CNAA, 1986.

199. Norman, P., Private Communication, Jan., 1986.

200. Sparkes, S.T. and Ebdon, L., Anal. Proc., 1986, 23, 410.

201. Gladney, E.S., Anal. Chim. Acta., 1980, 118, 385.

202. De Oliveira, E., McLearn, J.W. and Berman, S.S., Anal. Chem., 1983, 55, 2047.

203. McCurdy, D.L. and Fry, R.C., Anal. Chem., 1986, 58, 3126.

204. Thompson, M. and Walsh, J.N., "A Handbook of Inductively Coupled Plasma Spectrometry", Blackie, Glasgow, 1983.

205. Ebdon, L. and Cave, M.R., Analyst, 1982, 107, 172.

206. Spendly, W., Hext, G.R. and Himsworth, F.R., Technometrics, 1962, 4, 441.

207. Nelder, J.A. and Mead, R., Compt. J., 1965, 7, 308.

208. Yarbro, L. and Deming, S.N., Anal. Chim. Acta., 1974, 73, 391.

209. Cave, M.R., PhD Thesis, (Sheffield Polytechnic), CNAA, 1980.

210. Norman, P., Plymouth Polytechnic, unpublished work, 1985.

211. McCurdy, D.L. and Fry, R.C., Anal. Chem., 1986, 58, 3126.

212. Ambrose, A.J., Personal Communication, Aug., 1987.

213. Gray, A.L., Analyst, 1975, 100, 289.

214. Houk, R.S., Fassel, V.A., Flesch, G.D., Svec, H.J., Gray, A.L. and Taylor, C.E., Anal. Chem., 1980, 52, 2283.

215. Date, A.R. and Gray, A.L., Analyst, 1981, 106, 1255.

216. Brubaker, W.M., Adv. Mass Spectrom., 1968, 4, 293.

217. Monnig, C.A. and Koirtyohann, S.R., Anal. Chem., 1985, 57, 2533.

218. Munro, S., Ebdon, L. and McWeeny, D.J., J. Anal. Atomic Spectrom., 1986, 1, 211.

219. Date, A.R. and Gray, A.L., Spectrochim. Acta., 1983, 38B, 29.

220. Greenwood, N.N. and Earnshaw, A., "Chemistry of the Elements", Pergamon Press, Oxford, 1984.

221. Foulkes, M.E., private communication, Sept., 1987.

222. Ramsey, M.H. and Thompson, M., J. Anal. At. Spectrom., 1986, 1, 185.

223. Alder, J.F., Bombelka, R.M. and Kirkbright, G.F., Spectrochim. Acta., 1980, 35B, 163.

224. Boumans, P.W.J.M., "Theory of Spectrochemical Excitation", Hilger & Watts Ltd., Plenum Press, New York, 1966.

225. Kornblum, G.R. and de Galan, L., Spectrochim. Acta., 1977, 32B, 71.

226. Griem, H.R., "Plasma Spectroscopy", McGraw-Hill, New York, 1964.

227. Boumans, P.W.J.M. "Inductively Coupled Plasma Emission Spectroscopy" Part 2, Applications and Fundamentals, John W Wiley & Sons, New York, 1987.

228. Raaijmakers, I.J.M., Boumans, P.W.J.M., van der Sijde, B. and Schram, D.C., Spectrochim. Acta., 1983, 38B, 697.

229. Bridges, J.M. and Kornblith, R.L.J., Astrophys., 1974, 192, 793.

230. Walters, P.E., Gunter, W.H. and Zeeman, P.B., Spectrochim. Acta., 1986, 41B, 133.

231. Dieke, G.H. and Crosswhite, H.M., J. Quant. Spectrosc. Radiat. Transfer, 1962, 2, 97.

232. Haawgawa, T. and Winefordner, J.D., Spectrochim. Acta., 1987, 42B, 637.

233. Furuta, N., Spectrochim. Acta., 1985, 40B, 1013.

234. Hasegawa, T. and Winefordner, J.D., Spectrochim. Acta., 1987, 42B, 773.

235. Kornblum, G.R. and de Galan, L., Spectrochim. Acta., 1974, 29B, 249.

236. Cave, M.R., PhD Thesis, (Sheffield Polytechnic), CNAA, 1980.

APPENDIX I

Computer program to calculate excitation temperature

```
10REM ION TEMPERATURE
20MODE 0
30DIM T(21),D(21),A(21)
40INPUT "Ionization potential ";V
50INPUT "Temperature guess     ";T
60INPUT "Electron density      ";E
70INPUT "Ion line intensity    ";N
80INPUT "Atom line intensity   ";M
90PRINT
100 P=(E/M)*N
110L=LOG(P)-49.9289:T(1)=T
120FOR I=1 TO 20
130A(I)=L-1.5*LOG(T(I))+11605*V/T(I)
140D(I)=1.5/T(I)-11605*V/(T(I)^2)
150T(I+1)=T(I)-A(I)/D(I)
160NEXT I
170PRINT "Ionization temperature =";T(21):PRINT:PRINT "Continue  Y/N"
180A$=GET$:IF A$="Y" THEN CLS:GOTO 70
190 CHAIN "MENU"
```

APPENDIX II

Computer program to calculate ionisation temperature

```
5 MODE 0
10REM TEMPERATURE MEASUREMENTS
20DIM WAVE(10),POT(10),GF(10),IN(10),GA(10)
25 PRINT "Check data at the end of program":STOP
30READ N
40FOR I=1 TO N:READ WAVE(I),POT(I),GF(I),IN(I)
45 VDU2
50PRINT 1,WAVE(I),POT(I),GF(I),IN(I):NEXT I
60INPUT "WAVELENGTHS NUMBERS FOR A AND B";A,B
70FOR I=1 TO N:GA(I)=((6.6702*10^15)*10^GF(I))/WAVE(I)^2:NEXT I
80TEMP=(5040*(POT(A)-POT(B))/(LOG(GA(A)/GA(B))-LOG(WAVE(A)/WAVE(B))-LOG(IN(A)
/IN(B))))
85 PRINT "TEMPERATURE=";TEMP
87 PRINT:GOTO 60
90 DATA 7
100DATA 3719.93,3.3321,-.43,25610
110DATA 3727.62,4.2833,-.52,1250
120DATA 3734.86,4.1777,.31,11500
140DATA 3749.48,4.2205,.17,7855
150DATA 3748.26,3.4170,-1.01,4861
160DATA 3737.13,3.3683,-0.57,14064
170 DATA 3722.56,3.4170,-1.28,2919
200 CHAIN "MENU"
```

APPENDIX III

Computer program to calculate electron density

```
10REM CALCULATION OF ELECTRON DENSITY
20 MODE 0
30AM=47.9:WL=4.87014E-7:T=5000
40INPUT "Enter half width of Titanium 487.014 nm line";C
50INPUT "Enter measured half width of H-beta 416.133 nm line";B
60REM DOPPLER BROADENING
70D=(7.16E-7*WL)*(T/AM)^.5
80REM INSTRUMENTAL BROADENING
90I=(C^2-D^2)^.5
100X=B
110V=(B^2-I^2)^.5
120PRINT "Doppler half width at ";T;" K is ";V
130S=(X^2-V^2)^.5
140PRINT "Stark half width = ";S
150PRINT:INPUT "Enter coefficient C(Ne,T) from tables (eg 3.66E+35) ";K
160E=K*S^1.5
170PRINT:PRINT "Electron density = ";E
180PRINT
190PRINT "Continue    Y/N";:A$=GET$
200IF A$="Y" THEN 20
210 CHAIN "MENU"
```

MEETINGS OF THE ROYAL SOCIETY OF CHEMISTRY

i Annual Chemical Congress, 25th - 28th March, 1985, University of St Andrews.

ii Joint Analytical Division and the Atomic Spectroscopy Group meeting, October, 1985, "Sample Introduction and the ICP", University of Bristol.

iii Analytical Division meeting, 16th and 17th April, 1986, "Research and Development Topics in Analytical Chemistry", UCL, London.

iv Analytical Division joint meeting, "SAC 86 International Conference and Exhibition on Analytical Chemistry" together with "Third Biennial National Atomic Spectroscopy Symposium", 20th - 26th July, 1986, University of Bristol.

v Atomic Spectroscopy Group AGM, 16th December 1986, "Combination Techniques in Analytical Atomic Spectroscopy", Imperial College, London.

vi Analytical Division Meeting, 8th and 9th July, 1987, "Research and Development Topics in Analytical Chemistry", University of Strathclyde.

vii Analytical Spectroscopy Group Meeting, 3rd and 4th September, 1987, "New Perspectives in Atomic Spectroscopy", Plymouth Polytechnic.

LECTURES AND ASSOCIATED STUDIES

i   RSC meeting, 28th October, 1983, Plymouth Polytechnic, Prof J P Riley, "Analytical Chemistry Applied to Marine Pollution Problems".

ii   RSC lecture, 17th February, 1984, Plymouth Polytechnic, Prof J N Miller, "Hunting the Snark - Recent Developments in Ultra Sensitive Molecular Spectroscopy".

iii   RSC lecture, 16th November, 1984, Plymouth Polytechnic, Dr D Woodcock, "Fungicides and the Environment".

iv   Departmental Colloquium, 8th February, 1985, Plymouth Polytechnic, Dr C Corfield, "Gas Cromatography - Mass Spectrometry, Useful Applications of a Technique Come of Age".

v   RSC lecture, 15th March, 1985, Plymouth Polytechnic, Dr P S Liss, "The Role of the Oceans in the Chemistry of the Atmosphere".

vi   Departmental Colloquium, 10th September, 1985, Plymouth Polytechnic, Dr J M Harnly, "Recent Developments in Analytical Atomic Spectroscopy".

vii   RSC lecture, 1st November 1985, Plymouth Polytechnic, Dr T E Hunt, "Trace Element Speciation in Aquatic Systems".

viii RSC lecture, 7th February, 1986, Plymouth Polytechnic, Prof A F Fell, "Snapshot Chromatography-Biomedical Applications of New Technology in HPLC".

ix   RSC lecture, 7th March, 1986, Plymouth Polytechnic, Dr P Campion, "The Chemistry of PWR and AGR Nuclear Power Reactor Coolant".

x   RSC lecture, 23rd January, 1987, Exeter University, Prof J N Miller, "Illumination in chemical analysis".

xi   RSC lecture, 13th November, 1987, Plymouth Polytechnic, Dr A Howard, "Speciation".

PRESENTATIONS AND PUBLICATIONS

Resulting from the work reported in this thesis the following papers have been presented and published.

(a) Presentations

1. "Direct analysis of powdered whole coal without sample dissolution by ETA-AAS". Paper presented at the Third Biennial National Atomic Spectroscopy Symposium, Unviersity of Bristol, July 1986.

2. Coal analysis by Analytical Atomic Spectroscopy Without Sample Dissolution". Poster presentation at Research and Development Topics in Analytical Chemistry meeting, University of Strathclyde, July, 1987.

3. "The Use of Slurries in Analytical Atomic Spectrometry". Paper presented at Atomic Spectroscopy Group and Western Region conference on "New perspectives in Atomic Spectroscopy", Plymouth Polytechnic, September, 1987.

(b) Publications

1. Ebdon, L. and Parry, H.G.M.,
    "Direct Atomic Spectrometric Analysis by Slurry Atomisation. Part 2.
    Elimination of Interferences in the Determination of Arsenic in Whole Coal by
    Electrothermal Atomisation Atomic Absorption Spectrometry".
    J. Anal. At. Spectrom., 1987, 2, 131.

2. Ebdon, L. and Parry,H.G.M.,
    "Direct Atomic Spectrometric Analysis by Slurry Atomisation. Part 5.
    Determination of Selenium in Coal by Electrothermal Atomisation Atomic
    Absorption Spectrometry.
    J. Anal. At. Spectrom., 1988 In the Press.

3. Parry, H.G.M. and Ebdon, L.
    "Coal Analysis by Analytical Atomic Spectrometry (ICP-AES and ICP-MS)
    without Sample Dissolution".
    Anal. Proc., 1988 In the Press.